GENETIC STUDIES ON HOST AND PATHOGEN TO INFORM PHYTOPHTHORA BLIGHT RESISTANCE BREEDING

A Dissertation

Presented to the Faculty of the Graduate School

of Cornell University

In Partial Fulfillment of the Requirements for the Degree of

Doctor of Philosophy

by

Gregory Martin Vogel

Dec 2020

GENETIC STUDIES ON HOST AND PATHOGEN TO INFORM PHYTOPHTHORA BLIGHT RESISTANCE BREEDING

Gregory Martin Vogel, Ph. D.

Cornell University 2020

Phytophthora blight, caused by the oomycete pathogen *Phytophthora capsici*, is a devastating disease of various vegetable crops, including squash (*Cucurbita pepo*) and pepper (*Capsicum annuum*). Options for host resistance to Phytophthora blight vary dramatically between these two crops. In squash, no sources of complete resistance have been described, although variation for quantitative disease resistance exists in both commercial and unadapted germplasm. In pepper, on the other hand, landraces demonstrating complete or near-complete disease resistance have been identified and used in breeding. However, varieties with durable resistance to diverse pathogen isolates have not been developed. In order to contribute to genetic solutions for disease control in these two crops, genetic variation in squash associated with quantitative disease resistance as well as genetic variation in *P. capsici* associated with virulence on distinct pepper genotypes were characterized. In squash, two quantitative trait locus (QTL) mapping approaches were used in a zucchini × gray zucchini population, resulting in the discovery of six QTL, representing the first reported for Phytophthora blight resistance in *C. pepo*. In order to identify genetic variants in *P. capsici* associated with virulence on pepper, a collection of 252 pathogen isolates, predominantly from vegetable production regions of New York state, was genotyped at over 100,000 single-nucleotide polymorphism (SNP) loci using genotyping-by-sequencing. The utility of this isolate collection as a genetic resource was

demonstrated by the successful identification of SNPs associated with mating type and sensitivity to the fungicide mefenoxam via a genome-wide association study (GWAS). Inoculation of 117 genetically distinct isolates onto a panel of 16 pepper accessions revealed a significant effect of inter-species genotype-genotype interactions on disease outcomes. However, the only SNP associated with virulence in a GWAS demonstrated an effect that was consistent across pepper genotypes, suggesting that genes involved in host-specific virulence may be of smaller effect and more challenging to map. The results of these genetic experiments – conducted on both pathogen and host – are expected to inform efforts to breed vegetable crops with durable Phytophthora blight resistance.

BIOGRAPHICAL SKETCH

Greg was born in Washington, D.C. in 1991. Growing up in Silver Spring, MD, his interest in plants began as a fascination with vegetable gardening, and in particular, growing different varieties of tomatoes. A formative experience working on an organic vegetable farm after he graduated high school cemented his decision to study agriculture. Greg attended the University of Wisconsin-Madison and graduated in 2013 with a Bachelor of Science in Agronomy and a Certificate in Global Health. While in college, he worked in a carrot, beet, and onion breeding program led by Dr. Irwin Goldman, whose mentorship and passion for vegetable genetics led Greg to decide to pursue a graduate education in plant breeding. After working as an instructor of English as a Second Language, and then as a technician in the Floral and Nursery Plants Research Unit of the USDA Agricultural Research Service, Greg began his graduate career at Cornell University in 2015. He rotated in different labs his first year before beginning his dissertation research focused on disease resistance in vegetable crops as a co-advisee of Dr. Michael Gore and Dr. Christine Smart.

ACKNOWLEDGEMENTS

First, I thank my advisors Dr. Christine Smart and Dr. Michael Gore for their support during my graduate career. I have been inspired by Chris' passion for outreach and extension, and she ensured that I received a thorough, well-rounded training in her lab, where I was able to spend time doing everything from driving tractors to learning how to use a confocal laser-scanning microscope. I am incredibly grateful for her providing me with the opportunities and resources that allowed me to pursue my scientific interests. I am also extremely thankful to Mike for his willingness to accept me as a member of his lab. The generous attention and thoughtful feedback that I received from Mike allowed me to succeed as a graduate student and become a better scientist. I would also like to thank the members of my committee, Dr. Michael Mazourek and Dr. Philipp Messer. Michael supported my training and career development as if I were his own student, and I am extremely grateful to him for providing me with opportunities to teach in his class and conduct disease trials for his breeding program. Philipp's helpful input and advice on my projects were a highlight of my committee meetings and I very much appreciated his invitation to participate in his journal club for two semesters.

I would also like to thank several other people who supported me in my professional development. Dr. Steve Reiners extended to me an opportunity to organize a session at the Empire State Producers Expo, which was one of the most rewarding experiences I had as a graduate student. I am grateful to Elizabeth Buck in Cornell Cooperate Extension for providing me with an opportunity to lead an extension workshop in her region. I also thank Dr. Martha Mutschler-Chu for her mentorship when I rotated my first year, as well as Mutschler lab members Darlene DeJong, Stella Zitter, and John Smeda.

The research in this dissertation would not have been possible without the contributions of many people, including Mariami Bekauri, Ali Cala, Maryn Carlson, Colin Day, Amara Dunn, Kimberly D'Arcangelo, Garrett Giles, Taylere Hermann, Christopher Hernandez, Dan Ilut, Nicholas Kaczmar, Nicholas King, Rachel Kreis, Mary Kreitinger, Kyle LaPlant, Karen Luong, Charlotte Mineo, Kelly Robbins, Ryokei Tanaka, and Di Wu. I also need to thank undergraduate interns Andrew Aldcroft, Santiago Tijaro Bulla, Jessica Helwig, Rafael Estrada, Ella Reeves, and Carolina Puentes Silva, both for the work they did and for their enthusiasm and passion that made the lab such an enjoyable place to work in the summer. I am particularly grateful to Holly Lange for her support and friendship. I also owe thanks to many members of the administrative and facilities staff at Cornell Agri-Tech, including Kate Keagle, Holly King, Kundan Moktan, and Chris Olmstead, as well as Fitzgerald drivers Gary and Larry for transporting me safely to and from Geneva every day for five years. Finally, I would like to thank all the current and former graduate students and postdocs of the Smart and Gore labs whom I have had the pleasure to work with and learn from, and the students, staff, and faculty at Cornell Agri-Tech who have helped me feel part of such a welcoming community.

Finally, I would like to thank my parents for their endless and unconditional support and my wife Carolina, not only for moving to Ithaca from El Salvador in the middle of January, nor for spending weekends collecting squash leaf punches with me, but for her love and kindness that have made this experience possible.

TABLE OF CONTENTS

LIST OF FIGURES

LIST OF TABLES

LIST OF ABBREVIATIONS

ANOVA: Analysis of variance

AUDPC: Area under the disease progress curve

AVR: Avirulence

BLUE: Best linear unbiased estimator

BSA: Bulk segregant analysis

BSA-Seq: Bulk segregant analysis with whole genome resequencing

CI: Credible interval

CRN: Crinkling and necrosis

DNA: Deoxyribonucleic acid

DPI: Days post inoculation

FDR: False discovery rate

FST: Fixation index

GBLUP: Genomic best linear unbiased prediction

GBS: Genotyping-by-sequencing

GRM: Genomic relationship matrix

GWAS: Genome-wide association study

HSD: Honestly significant difference

IBS: Identity by state

KASP: Kompetetive allele specific polymerase chain reaction

LD: Linkage disequilibrium

LG: Linkage group

LOD: Logarithm of odds

LS: Least squares

MAF: Minor allele frequency

MAS: Marker-assisted selection

MLR: Multiple linear regression

MQM: Multiple quantitative trait locus mapping

NJ: Neighbor joining

NMRIL: New Mexico recombinant inbred line

NPGS: National Plant Germplasm System

PC: Principal component

PCA: Principal component analysis

PCR: Polymerase chain reaction

QTL: Quantitative trait locus/loci

R: Resistance

RAN: Random

rAUDPC: Relative area under the disease progress curve

RG: Relative growth

RNA: Ribonucleic acid

RES: Resistant

RIL: Recombinant inbred line

rRNA: Ribosomal ribonucleic acid

RXLR: Argenine-any amino acid-Leucine-Argenine

SNP: Single nucleotide polymorphism

SUS: Susceptible

CHAPTER 1

A COMBINED BSA-SEQ AND LINKAGE MAPPING APPROACH IDENTIFIES GENOMIC REGIONS ASSOCIATED WITH PHYTOPHTHORA ROOT AND CROWN ROT RESISTANCE IN SQUASH[1]

ABSTRACT

Phytophthora root and crown rot, caused by the soilborne oomycete pathogen *Phytophthora capsici*, leads to severe yield losses in squash (*Cucurbita pepo*). To identify quantitative trait loci (QTL) involved in resistance to this disease, we crossed a partially resistant squash breeding line with a susceptible zucchini cultivar and evaluated over 13,000 F_2 seedlings in a greenhouse screen. Bulked segregant analysis with whole genome resequencing (BSA-Seq) resulted in the identification of five genomic regions – on chromosomes 4, 5, 8, 12, and 16 – featuring significant allele frequency differentiation between susceptible and resistant bulks in each of two independent replicates. In addition, we conducted linkage mapping using a population of 176 F_3 families derived from individually genotyped F_2 individuals. Variation in disease severity among these families was best explained by a four-QTL model, comprising the same loci identified via BSA-Seq on chromosomes 4, 5, and 8 as well as an additional locus on chromosome 19, for a combined total of six QTL identified between both methods. Loci, whether those identified by BSA-Seq or linkage mapping, were of small to moderate effect, collectively accounting for 28-35% and individually for 2-10% of the phenotypic variance explained. However, a multiple linear regression model using one marker in each BSA-Seq QTL could predict $F_{2:3}$ disease severity with only a slight drop in cross-validation accuracy compared

[1] Vogel, G., LaPlant, K.E., Mazourek, M., Gore, M.A., and Smart, C.D. A combined BSA-Seq and linkage mapping approach identifies genomic regions associated with Phytophthora root and crown rot resistance in squash. Theoretical and Applied Genetics. *In revision*.

to genomic prediction models using genome-wide markers. These results suggest that marker-assisted selection could be a suitable approach for improving Phytophthora crown and root rot resistance in squash.

INTRODUCTION

Squash and pumpkin (*Cucurbita pepo, C. maxima,* and *C. moschata*) are important crops grown for fruit that can be consumed either immature (e.g. summer squash) or mature (e.g. winter squash and pumpkin), as well as used decoratively (e.g. pumpkin and gourds). One of the major diseases affecting their production in the United States, which was valued at over $380 million in 2018 (United States Department of Agriculture 2019), is Phytophthora root and crown rot, caused by the soilborne oomycete *Phytophthora capsici*. Phytophthora root and crown rot causes lesions on roots and lower stems, leading to damping off in young seedlings and reduced vigor or death in older plants (Hausbeck and Lamour 2004). Disease management strategies are mostly limited to cultural practices meant to improve drainage, prevent splashing of infested soil, and reduce water movement within a field, in addition to the use of fungicides (Granke et al. 2012). However, the efficacy of several chemical active ingredients has been threatened by the emergence of fungicide insensitivity in pathogen populations (Lamour and Hausbeck 2000; Parra and Ristaino 2001; Dunn et al. 2010; Jackson et al. 2012). Host resistance is greatly desired by growers but has not been identified in appreciable levels in commercial cultivars.

To date, no sources of complete Phytophthora root and crown rot resistance have been described in squash, although germplasm screens in *C. pepo* (Padley et al. 2008) and *C. moschata* (Chavez et al. 2011) revealed a range of resistance levels among accessions of both species. In *C. pepo*, the most economically valuable of the three major domesticated squash

species (Lust and Paris 2016), cultivars of *C. pepo* ssp. *pepo* (e.g. zucchini and pumpkin) are slightly less susceptible than cultivars of *C. pepo* ssp. *ovifera* (e.g. crookneck summer squash and acorn squash), but these differences are too small to provide economically relevant levels of disease control (Camp et al. 2009; Meyer and Hausbeck 2012; Krasnow et al. 2017).

Little is known about Phytophthora root and crown rot resistance in wild *Cucurbita* species, which have played an important role in breeding for resistance to other diseases of squash (Rhodes 1964; Menezes et al. 2015; Holdsworth et al. 2016), although a *C. moschata* breeding line with introgressions from *C. lundelliana* and *C. okeechobeenesis* subsp. *okeechobeenesis* showed resistance to several Florida isolates of *P. capsici* (Padley et al. 2009). In crosses with different breeding lines representing distinct sources of resistance, segregation ratios suggest that resistance is genetically complex and controlled by multiple genes (Padley et al. 2009; Michael et al. 2019).

Selection for Phytophthora root and crown rot resistance is typically performed in controlled environments at the seedling stage (Padley et al. 2009; LaPlant et al. 2020). Nevertheless, predictable levels of disease pressure are often difficult to obtain, as the extent and rate of symptom development are highly influenced by the choice of pathogen isolate and inoculation method as well as the environmental conditions in the greenhouse and age of plants at the time of inoculation (Lee et al. 2001; Tian and Babadoost 2004; Enzenbacher and Hausbeck 2012). Higher than expected disease severity in a selection screen may leave little genetic variation remaining among the survivors in a breeding population and result in the death of plants possessing desirable resistance alleles. Knowledge of the quantitative trait loci (QTL) conferring Phytophthora root and crown rot resistance would enable marker-assisted selection (MAS), eliminating or reducing the number of generations in which plants would need to be

inoculated in a resistance breeding program**.** While QTL conferring Phytophthora root and crown rot resistance have been reported recently in *C. moschata* (Ramos et al. 2020), to our knowledge none have been identified in *C. pepo*.

The combination of bulked segregant analysis with whole genome resequencing (BSA-Seq), first shown in yeast to be capable of detecting QTL of both major and minor effect (Ehrenreich et al. 2010; Wenger et al. 2010), has since become a popular method for mapping QTL in crop species (Takagi et al. 2013; Yang et al. 2013; Lu et al. 2014; Illa-Berenguer et al. 2015). Compared to traditional linkage mapping, where progeny are individually genotyped and phenotyped, BSA requires the preparation of fewer samples for genotyping and allows for more efficient phenotyping, as only individuals representing the phenotypic extremes of a population need to be identified (Michelmore et al. 1991). The choice of whole genome resequencing as the genotyping strategy in BSA provides an effective way to estimate genome-wide allele frequencies in bulks (via allele-specific read counts) without the need for prior marker development (Ehrenreich et al. 2010; Magwene et al. 2011; Takagi et al. 2013). BSA-Seq, however, features several disadvantages compared to traditional QTL mapping, such as the inability to estimate allelic effect sizes or to test for QTL by QTL interactions (i.e. epistasis).

In this study, we used a combination of BSA-Seq and traditional linkage mapping to discover QTL conferring resistance to Phytophthora root and crown rot in a biparental zucchini (*C. pepo*) population. Using a cross between a susceptible zucchini cultivar and a Cornell breeding line with intermediate resistance to Phytophthora root and crown rot, but poor fit as a zucchini or summer squash cultivar due to its growth habit and fruit shape (LaPlant et al. 2020), our goal was to identify QTL that can be directly used in MAS for introgressing disease resistance loci into genetic backgrounds representing more widely grown squash types. By

synthesizing results from the two QTL mapping methods, we were able to estimate allelic effect sizes, generate lists of candidate genes in QTL regions, and test the predictive ability of QTL in independent datasets from those used for their detection.

MATERIALS AND METHODS

Development of mapping population. A replicated greenhouse experiment evaluating germplasm from the Cornell squash breeding program for Phytophthora root and crown rot resistance resulted in the identification of one $F_{4:5}$ family, Pc-NY21, with superior resistance compared to the other entries in the trial (LaPlant et al. 2020). This family was selected from a cross between Romulus, a Cornell zucchini cultivar, and PI 615089 from the National Plant Germplasm System, a white vegetable marrow accession with partial Phytophthora resistance. Eight individual F_5 progeny from Pc-NY21, which were descended from the same F_4 plant, were crossed with 'Dunja F_1' (Enza Zaden), a susceptible zucchini variety, and an equal number of individuals from the eight F_1 families were then intermated to generate an F_2 mapping population.

Selection of bulks and sequencing of DNA pools. Two separate sets of F_2 individuals (Rep 1 and Rep 2) were evaluated for root and crown rot resistance in a greenhouse at Cornell AgriTech in Geneva, NY, in the fall of 2017. For each set, 6,912 seeds were sown in 72-cell trays (for a total of 96 trays) and inoculated with a zoospore suspension of *P. capsici* when the plants had two fully expanded true leaves (17-18 days after sowing). New York *P. capsici* isolate 0664-1 (Dunn et al. 2010) was used for inoculations and inoculum was prepared as in LaPlant et al. (2020). Inoculum was diluted to a concentration of $1x10^4$ zoospores/mL and sprayed over the tops of trays using a diaphragm pump backpack sprayer at a rate so as to deliver an intended total of 144 mL per tray, for a target of 20,000 zoospores (2 mL) inoculated onto each seedling.

A random (RAN), susceptible (SUS), and resistant (RES) tissue bulk were selected in each replicate. In order to target 15% of the population to include in each bulk, as has been shown in simulations to maximize QTL detection power and resolution (Magwene et al. 2011; Takagi et al. 2013), approximately 11 plants were sampled from each 72-cell tray. Plants for the RAN bulks were randomly sampled within 3 days prior to inoculation. Plants for the SUS bulks were sampled 4-5 days after inoculation, a point when early disease symptoms were beginning to appear in the population but before plants were completely killed. Plants sampled for the SUS bulks were visually identified as those within their respective trays featuring the greatest degree of wilt, stem necrosis, and sporulation on stem lesions. Plants for the RES bulks were sampled 7-10 days after inoculation and were identified as the plants that featured the least degree of wilt and leaf chlorosis in their respective trays. In trays where the most phenotypically extreme 11 plants were difficult to distinguish, as few as 6 or as many as 16 plants were sampled for the SUS and RES bulks. Tissue was sampled from all selected plants by taking a 3 mm hole punch from a newly emerging leaf. Tubes containing tissue samples were flash frozen in liquid nitrogen, stored at -80° C, and then lyophilized for 48 h prior to DNA extraction.

To minimize the heterogeneity of the DNA contributed by each individual to its pool, tissue samples from each tray were bulked separately for a total of 96 tubes per bulk (RAN, SUS, or RES). After extracting DNA from samples representing within-tray bulks, equimolar volumes of DNA from the 96 samples were then combined for a final DNA pool representing selections from all trays. This strategy was elected as a compromise between performing a separate DNA extraction for every individual plant sample and bulking >1,000 leaf punches prior to DNA extraction. DNA extractions were performed using the DNeasy 96 plant kit (Qiagen, Valencia, CA, USA), with the following modifications to maximize the purity and integrity of DNA from

diseased plant samples: the volumes of buffers AP1, P3, and AW1 were doubled; the -20° C incubation was extended from 20 to 60 m; and an additional wash step was performed with 800 µl molecular-grade ethanol. The DNA concentration of each sample was measured using a Qubit fluorometer (Thermo Fisher Scientific, Waltham, MA, USA) prior to pooling.

The six DNA pools (RAN, SUS, and RES for each of the two replicates) and parental DNA samples were submitted to the Cornell University Biotechnology Resource Center for library preparation and sequencing. To represent the resistant parent, DNA was extracted from the F_4 progenitor of Pc-NY21. PCR-free libraries were created by mechanically shearing DNA samples and ligating adapters, using reagents equivalent to those in the TruSeq library preparation kit (Illumina, San Diego, California). For several DNA pools, two separate libraries were created, resulting in technical replicates. Library yields were determined using digital droplet PCR. Libraries were then pooled and sequenced on either 1 or 2 lanes, depending on the library, of an Illumina NextSeq500 generating paired-end 150 bp reads. Due to a technical error during library preparation, reads for Rep 1 RAN were unusable and therefore not included in any analyses.

BSA-Seq data analysis. Raw reads were filtered and trimmed from both ends using fastp v 0.20.0 (Chen et al. 2018) with default parameters, except the arguments *--correction* and *--trim_poly_g* were enabled to correct bases in overlapped regions and remove polyG strings in read tails. Trimmed reads were then aligned to the *C. pepo* reference genome (v 4.1; Montero-Pau et al. 2018) with bwa v 0.7.17 (Li and Durbin 2009) using the MEM algorithm and default parameters. Resulting bam files were sorted and indexed with samtools and variants were called using the bcftools *mpileup* and *call* commands (Li et al. 2009). The minimum alignment mapping quality was set to 20 and the consensus-caller method was used. The resulting VCF file

was filtered with VCFtools version 0.1.17 (Danecek et al. 2011) to remove indels and SNPs with more than 2 alleles. Reference and alternate allele counts for every SNP in each pool were then extracted from the filtered VCF file using a custom python script, and imported into R (R Core Team 2019) for filtering.

SNPs with a total read depth lower than the 5th percentile or higher than the 95th percentile of the read depth distribution across all SNPs were removed, as were SNPs with a minor allele frequency (calculated using allele counts in each pool) <0.10. Unanchored SNPs (i.e. those on scaffold Cp4.1LG00) were also removed. Parental genotypes with fewer than 6 reads were set to missing, and only SNPs where the parents were homozygous for opposite alleles were retained. Parental genotypes were then used to recode alleles from reference/alternate coding to Dunja-derived/Pc-NY21 derived. Allele counts in samples representing technical sequencing replicates of the same DNA pool were summed at this point. Further filtering was then performed within each pool, by setting to missing any sites with an allele frequency <0.10 or >0.90 or with a read depth lower than the 10th percentile for that pool. These missing sites were not included for calculation of allele frequencies nor for any statistical test involving that pool.

For visualization of allele frequencies, allele frequency means for each pool were estimated in 500 Kb sliding windows with a 100 Kb increment. To test for deviations in allele frequencies between SUS and RES pools, the software program MULTIPOOL (v 0.10.2; Edwards and Gifford 2012), which estimates pool allele frequencies using a dynamic Bayesian network, was used. The argument –mode was set to *contrast*. We set 1,056 as the number of individuals contributing DNA to each pool (-n) and 125,636 as the length, in base pairs, of a centimorgan in squash (-c), which was estimated by dividing the mean of the lengths of three

published genetic maps (Esteras et al. 2012; Holdsworth et al. 2016; Montero-Pau et al. 2017) by the estimated *C. pepo* genome size of 283 Mb (Montero-Pau et al. 2018). MULTIPOOL was also used to test for allele frequency deviations between Rep 1 SUS and Rep 2 SUS as well as Rep 1 RES and Rep 2 RES in order to generate a null distribution of LOD scores reflecting the comparison between two independent bulks of plants selected in the same direction.

Phenotyping of $F_{2:3}$ population. One hundred eighty-seven F_2 plants were self-pollinated to generate $F_{2:3}$ families. These F_2 plants represented two different cohorts of individuals: a 'random' cohort of 169 plants started from remnant seed and a 'selected' cohort comprising 18 survivors from the BSA-Seq screen. In order to collect seed from infected plants from the BSA-Seq screen, 42 seedlings (18 in Rep 1 and 24 in Rep 2) that appeared healthy at 14-15 days post inoculation were treated with mefenoxam (Ridomil Gold EC; Syngenta AG, Basel, Switzerland) and transplanted to 3-gal pots. Eighteen of these 42 plants survived and produced viable seed after self-pollination.

The 187 $F_{2:3}$ families, in addition to parental and F_1 checks, were evaluated for Phytophthora root and crown rot resistance as seedlings in the greenhouse. An $F_{5:6}$ family derived from one selfed F_5 Pc-NY21 individual was included to represent the resistant parent. Experimental units consisted of 12 adjacent cells in a 72-cell tray and were arranged in a randomized complete block design with three replications. Three of the 187 families were only included in two blocks due to limited seed. Inoculum was prepared as in the BSA-Seq screen, except plants were inoculated by pipetting a suspension of 10,000 zoospores to the potting soil surface adjacent to each plant.

Plots were rated for incidence of mortality at several days post inoculation (dpi) (3, 5, 7, 10, and 12 dpi for Rep 1; 3, 4, 5, 6, 7, and 10 dpi for Reps 2 and 3). Seedlings were declared

dead when they either had all wilted leaves, had only one or fewer non-chlorotic leaves, or were completely prostrate due to stem lesions. The relative Area Under the Disease Progress Curve (rAUDPC; Fry 1978) was then calculated for each plot according to the following formula:

$$rAUDPC = \frac{1}{100 \times (t_n - t_1)} \sum_{i=1}^{n-1} \frac{y_i + y_{i+1}}{2} \times (t_{i+1} - t_i) \quad (1)$$

where y_i is the mortality rating as a percentage at the ith observation, t_i is the time point in days at the ith observation, and n is the total number of observations. The relative AUDPC was used to normalize AUDPC values between blocks as they were rated for different numbers of days.

Ratings for any plot with fewer than 6 germinated plants were set to missing. The following mixed linear model was then fit using the R package lme4 (Bates et al. 2007) in order to estimate best linear unbiased estimators (BLUEs) for the effect of each family on rAUDPC:

$$y_{ij} = \mu + \gamma_i + b_j + e_{ij} \quad (2)$$

In this model, y_{ij} are raw phenotypic observations, μ is the grand mean, γ_i is the fixed effect for the ith family, $b_j \sim iidN(0, \sigma_b^2)$ is a random effect for the *j*th block (i.e. replication), and $e_{ij} \sim iidN(0, \sigma_e^2)$ is the residual effect. Separate models were also fit using mortality ratings at 3, 5, 7, and 10 dpi as the response variables. In order to calculate line-mean heritability (H^2; Holland et al. 2003), a similar model was fit, except family was included as a random instead of fixed effect. The following formula was then used:

$$H^2 = \frac{\sigma_g^2}{\sigma_g^2 + \frac{\sigma_e^2}{r}} \quad (3)$$

where σ_g^2 is the genotype variance, σ_e^2 is the error variance, and r is the harmonic mean of the number of replications per family without missing data.

Genotyping of F2 individuals and genetic map construction. Newly emerged leaves were sampled from the F_2 parents of the $F_{2:3}$ mapping population and desiccated using silica gel

(Millipore Sigma, Burlington, MA). Total genomic DNA was then isolated using the DNeasy Plant Mini Kit (Qiagen, Valencia, CA, USA) following manufacturer's directions, except DNA was eluted into ultrapure water instead of Buffer AE. DNA samples were obtained from a total of 188 F_2 progeny (19 'selected' and 169 'random), as well as the two parents of the population, with the F_4 progenitor of Pc-NY21 sampled to represent the resistant parent. DNA samples were sent to the University of Wisconsin-Madison Biotechnology Center for preparation of genotyping-by-sequencing (GBS) libraries digested with *Ape*KI (Elshire et al. 2011), a restriction enzyme that has previously been shown effective for GBS variant discovery and genotyping in *C. pepo* (Holdsworth et al. 2016). Libraries were then paired-end sequenced on an Illumina NovaSeq6000 with a target output of two million reads per sample.

Genotypes were called using GBS-SNP-CROP (Melo et al. 2016), a variant calling pipeline designed to run with paired-end reads. As part of this pipeline, reads were demultiplexed, trimmed using Trimmomatic (v 0.39; Bolger et al. 2014), and aligned to the squash reference genome (Montero-Pau et al. 2018) using BWA-mem (Li and Durbin 2009). Variants were called using the default parameters in GBS-SNP-CROP, except the arguments -altStrength, -mnAlleleRatio, -mnAvgDepth, and -mxAvgDepth were set to 0.9, 0.15, 7, and 150, respectively. These parameters were chosen in order to enrich for variants with allele frequencies as expected in an F_2 population (altStrength), avoid undercalling of heterozygotes (mnAlleleRatio), and avoid spurious variants (mnAvgDepth) or variants in regions with alignment issues (mxAvgDepth), taking into account the read depth distributions in our dataset. Genotype calls were then converted to a dosage matrix and imported into R for filtering.

Unanchored SNPs were removed, as were SNPs that did not meet the following criteria: minor allele frequency (MAF) >0.1, call rate >0.9, and read depth between 15 and 90. Three

individuals with over 40% missing data were removed as well. SNPs were then removed that were not homozygous for opposite alleles in the parents or that failed a chi-squared goodness of fit test ($p < 0.01$) for 1:2:1 AA:AB:BB segregation among the F_2 progeny. In order to identify potential errors during DNA extraction or library preparation, pairwise genotype concordance was calculated among all pairs of samples. Four pairs of samples were found to have >99% identical genotype calls. For each pair, the sample with the least missing data was retained for genetic map construction and the phenotypic records for those retained samples were set to missing. Finally, markers were pruned by identifying sequences of consecutive SNPs with identical genotype calls on all non-missing individuals and retaining the marker with the least missing data. Genotypes were then re-coded as "A/B/H" for genetic map construction.

The R package R/qtl (Broman et al. 2003) was used to estimate recombination fractions between all pairs of markers in order to build a genetic map. Linkage group assignments were based on the physical coordinates of markers on the reference genome, except for six markers which displayed high recombination fractions with all markers on their respective linkage groups and were manually re-located to the correct linkage group. The MSTMap algorithm (Wu et al. 2008) was then used to re-order markers within each linkage group, using the R package ASMap (Taylor and Butler 2017). Recombination fractions were converted into map distances using the Kosambi map function.

Linkage mapping and validation of BSA-Seq QTL. A multiple QTL mapping (MQM) procedure was performed in R/qtl (Broman and Sen 2009) using the 176 $F_{2:3}$ families with genotype and phenotype data that passed filtering. First, conditional genotype probabilities were calculated at 1 cM positions across the genetic map using the *calc.genoprob* function. The genotyping error rate was set to 0.001, reflecting the average proportion of discordant genotype

calls among the four pairs of erroneously duplicated samples. In order to estimate penalties for the inclusion of terms in model selection, rAUDPC values were permuted 1,000 times relative to genotypes and a two-dimensional QTL scan using Haley-Knott regression (Haley and Knott 1992) was performed using the *scantwo* function. Penalties at α=.05 were derived from the resulting null distribution of LOD scores using the *calc.penalties* function, and the best fitting QTL model was identified with the forward/backward stepwise search algorithm implemented in the *stepwiseQTL* function, again using Haley-Knott regression. The function *bayesint* was used to calculate 90% Bayesian credible intervals for QTL locations, with the ends of the intervals extended to marker positions so as to convert genetic markers to physical coordinates on the reference genome.

The *fitqtl* function, which performs a likelihood ratio test after dropping one QTL from the model at a time, was used to calculate LOD scores and p-values for each QTL, as well as estimate their effect sizes and proportion of phenotypic variance explained. Two QTL models were fit, one containing the loci detected via BSA-Seq and one containing those identified from multiple QTL mapping using the $F_{2:3}$ phenotypes. The QTL detected via BSA-Seq were placed on the genetic map by identifying, for each QTL, the GBS marker nearest the midpoint of the MULTIPOOL LOD peaks from Reps 1 and 2. For plotting QTL effects and estimating QTL allele frequencies in the two F_2 cohorts, missing GBS genotypes were imputed using the Viterbi algorithm as implemented in the *argmax.geno* function. Significant differences between rAUDPC means for $F_{2:3}$ families with differing QTL marker alleles were determined using Tukey's honestly significant difference test at α=.05 using the function *HSD.test* in the R package agricolae (Mendiburu and Simon 2015).

Synteny with *C. moschata*. To assess if QTL in *C. pepo* were syntenic with those

reported by Ramos et al. (2020) in *C. moschata*, we followed the approach used in the 'SyntenyViewer' module of the Cucurbit Genomics Database (Zheng et al. 2019) in order to identify and visualize regions of synteny between the genomes of the two species. Briefly, the *C. pepo* (Montero-Pau et al. 2018) and *C. moschata* (Sun et al. 2017) protein sequences were aligned against each other using blastp (Camacho et al. 2009) and synteny blocks were identified from the resulting alignments using MCScanX (Wang et al. 2012). The R package circlize (Gu et al. 2014) was then used to visualize syntenic relationships.

Candidate gene identification. QTL regions, which we defined as the union of BSA-Seq and MQM credible intervals, were cross-referenced with the squash reference gff file (Montero-Pau et al. 2018) using bedtools v 2.28 (Quinlan and Hall 2010) in order to generate a list of genes annotated in QTL regions. SnpEff v 4.3T Cingolani et al. 2012) was then used to annotate variants between Pc-NY21 and Dunja for their putative functional impact on these genes. The whole genome resequencing genotype calls from BSA-Seq were used for variant annotation. These genotype calls were filtered on read depth and minor allele count frequency as for the BSA-Seq analysis, except, in order to prevent the removal of potential causative variants, indels were retained, low read-depth sites were not set to missing, and variants that were heterozygous in one parent were not removed. Variants where the minor allele was not called in at least 5 samples, including parents and pools, were removed. Genes in QTL regions were also evaluated for their homology with melon (*Cucumis melo*) genes shown to be differentially expressed following inoculation with *P. capsici*, as reported by Wang et al. (2020). Homologues were defined as reciprocal best hits on the basis of e-value after using blastp (Camacho et al. 2009) to align the complete sets of melon (v 3.6.1; Garcia-Mas et al. 2012) and squash (Montero-Pau et al. 2018) protein sequences against each other.

Prediction models. A cross-validation approach was used to assess the ability of different linear models, featuring markers either genome-wide or only in QTL regions, to predict rAUDPC estimates among $F_{2:3}$ families. Four models were compared: a multiple regression model in which the allele dosages at the GBS markers tagging each BSA-Seq QTL were treated as fixed effects (QTL MLR); a genomic best linear unbiased prediction model (GBLUP), where genome-wide markers were used to model the covariance between families with a genomic relationship matrix; a GBLUP plus QTL model (GBLUP+QTL) where, in addition to the genomic relationship matrix, QTL marker allele dosages were included as fixed effects; and a whole-genome regression Bayesian approach (BayesB; Meuwissen et al. 2001), in which marker effects are assigned a prior distribution where a portion equal zero and the rest have a scaled-*t* distribution. The QTL MLR model was fit using the lme4 R package (Bates et al. 2007), the two GBLUP models using R package rrBLUP (Endelman 2011), and the BayesB model using R package BGLR (Perez and Gustavo de los Campos 2014). The genotype data used in models, whether genome-wide or only at the five QTL markers, were from the genetic map-imputed GBS SNP set.

For cross-validation, the data were partitioned randomly into two subsets: a training set used to fit a given model, comprising 80% of the individuals, and a test set used for assessing prediction accuracy, comprising 20% of the individuals. The same partitions were used for all five models, to enable direct comparison, and this was replicated 50 times. In each cross-validation partition, prediction accuracy was estimated by taking the Pearson's correlation coefficient between the observed values and estimated breeding values of the test individuals, as predicted by the training-set model.

Data availability. Whole genome resequencing reads used in BSA-Seq and genotyping-

by-sequencing reads used in linkage mapping have been deposited in the National Center of Biotechnology Information Sequence Read Archive (SRA) under BioProject accession number PRJNA662576. Files containing allele counts used in BSA-Seq, genotype and phenotype data used in linkage mapping, and annotated variant calls used for candidate gene identification are available at CyVerse (https://datacommons.cyverse.org/browse/iplant/home/shared/GoreLab/dataFromPubs/Vogel_SquashQTL_2020). All scripts used for data analysis are available on Github (http://github.com/gmv23/Pcap-QTL-Mapping).

RESULTS

BSA-Seq. DNA pools were sequenced from two independent replicates of resistant, susceptible, and random (Rep 2 only) bulks selected from phenotypic screens featuring >6,500 F_2 squash seedlings each. A total of 192 Gb of sequencing reads were generated from the five DNA pools and the parents of the population (Table 1.1). After aligning reads to the squash reference genome and identifying variants, between 182,311-186,020 SNPs were retained in each pool after filtering. These SNPs featured a median read depth of 9-10 in the parents, 57-70 in SUS and RES pools, and 24 in the Rep 2 RAN pool (Table 1.1). While the majority of the genome featured dense marker coverage, several regions contained few or no SNPs, including regions >1 Mb in size on chromosomes 7, 13, 14, 16, and 20 (Figure S1.1; Figure S1.2).

Table 1.1: Sequencing statistics for BSA-Seq samples.

Sample[a]	Raw reads (Gb)	Raw reads (X)[b]	Filtered reads (Gb)	Filtered reads (X)[b]	Aligned reads (Gb)[c]	Aligned reads (X)[bc]	Median SNP read depth
Dunja	4.34	16	3.82	14	2.59	10	10
PcNY-21	4.15	16	3.59	14	2.30	9	9
Rep 1 SUS	50.40	191	43.63	166	26.57	101	64
Rep 1 RES	35.55	135	28.12	107	18.12	69	57
Rep 2 SUS	39.90	151	34.82	132	22.79	87	68
Rep 2 RES	43.08	163	38.28	145	25.22	96	70
Rep 2 RAN	14.58	55	12.10	46	7.71	29	24

[a] SUS=susceptible pool, RES=resistant pool, RAN=random pool

[b] Genome coverage (X) was calculated by dividing total the base pairs represented in samples by the *C. pepo* reference genome size of 263,500,452 bp.

[c] Only aligned reads with a mapping quality >20 are counted.

Allele frequencies at individual SNPs fluctuated, with the median standard deviation of SNP allele frequencies binned in 500 Kb windows ranging from 0.07 in Rep 2 RES, the pool with the highest read depth, to 0.11 in Rep 2 RAN, the pool with the lowest read depth. Averaging individual values in 500 Kb sliding windows enabled easier visualization of allele frequencies, showing that for the majority of the genome, RES, SUS, and RAN pools featured little differentiation (Figure S1.1; Figure S1.2).

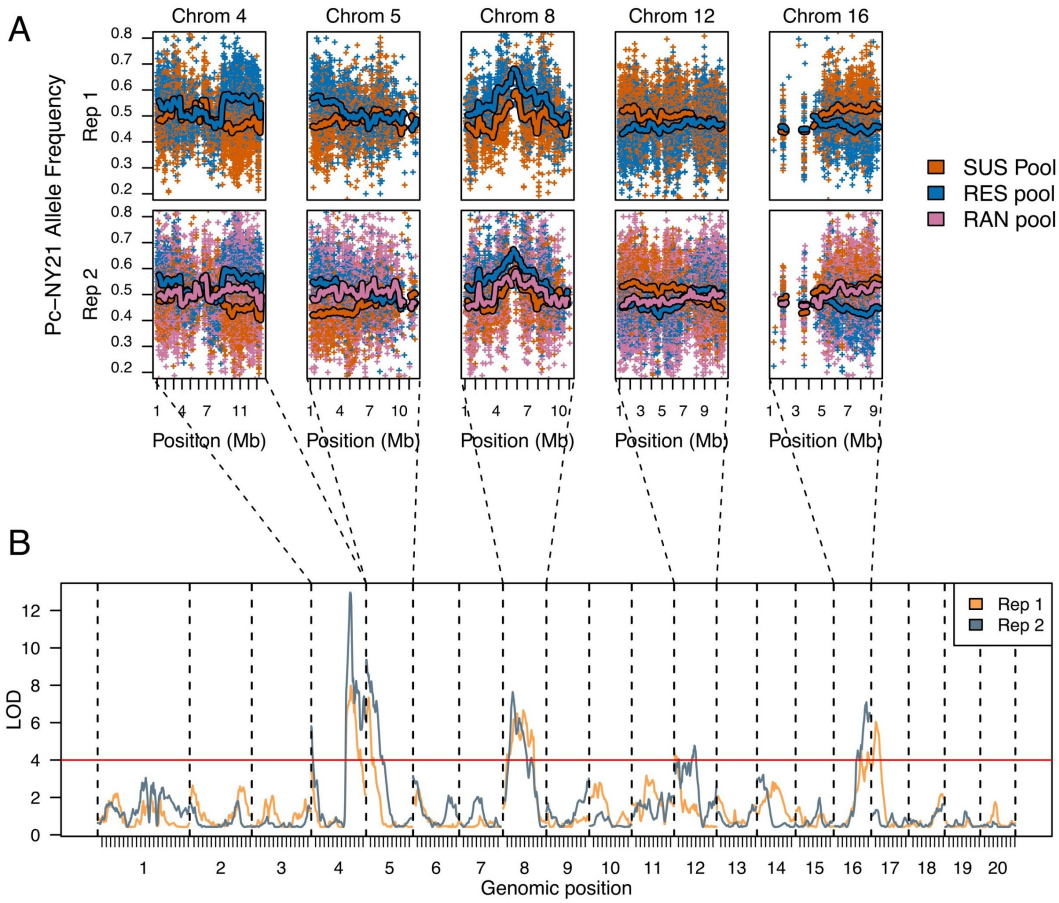

Figure 1.1: A) Pc-NY21 allele frequencies in susceptible (SUS), resistant (RES), and random (RAN) (Rep2 only) pools for all chromosomes that feature a region surpassing a MULTIPOOL LOD score of 4 in both reps. Plus signs are individual SNP allele frequencies and lines are smoothed means calculated in 500 Kb sliding windows with a 100 Kb increment. For ease of

visualization, only a random subset of 25% of SNPs are shown. Smoothed means were not calculated in any window featuring fewer than 30 SNPs. B) Genome-wide LOD scores from MULTIPOOL testing for allele frequency deviations between susceptible and resistant pools for Reps 1 and 2 of BSA-Seq.

We used the program MULTIPOOL to test for differences in allele frequencies between pools and determine 90% credible intervals for QTL positions. A null test between replicates for both RES and SUS pools resulted in a maximum LOD score of 2.59, and we decided to use a conservative LOD score threshold of 4 for QTL detection. Five genomic regions, on chromosomes 4, 5, 8, 12, and 16, featured LOD scores >4 in both Reps 1 and 2 after testing for differences between RES and SUS pools (Table 1.2; Figure 1.1). Two additional regions, on chromosome 17 and the beginning of chromosome 4, surpassed the LOD score threshold in only one of two reps, and were therefore not considered for further analysis. In the QTL regions on chromosomes 4, 5, and 8, the RES pool featured a higher frequency of the Pc-NY21 allele compared to the SUS pool, whereas the opposite was true in the chromosome 12 and 16 regions, indicating that the allele conferring resistance in each of these two regions was inherited from susceptible parent Dunja. In all five QTL regions, the RAN pool in Rep 2 displayed allele frequency values intermediate between those of the RES and SUS pools. Segregation distortion was evident in the chromosome 8 QTL, where RES, SUS, and RAN pools all showed enrichment for the Pc-NY21 allele, although this deviation was greater in the RES compared to the SUS pool.

Table 1.2: BSA-Seq QTL mapping results.

Chromosome	Max LOD[ab]	Max LOD Position (Mb) (90% CI)[ab]	Max allele frequency difference[bc]	Max allele frequency difference position (Mb)[bc]
Cp4.1LG04	7.98 / 12.96	9.16 (8.3-10.38) / 9.04 (8.7-9.36)	0.13 / 0.17	9.25 / 9.05
Cp4.1LG05	7.34 / 9.36	0.6 (0.18-1.68) / 0.05 (0.04-2.47)	0.12 / 0.13	0.65 / 2.55
Cp4.1LG08	6.66 / 7.64	4.7 (1.95-6.72) / 2.25 (1.84-5.18)	0.12 / 0.13	3.15 / 2.55
Cp4.1LG12	4.4 / 4.77	0.06 (0.06-6.9) / 4.71 (0.36-7.38)	-0.09 / -0.09	0.25 / 4.95
Cp4.1LG16	4.6 / 7.09	6.36 (4-8.22) / 7.57 (5.84-8.26)	-0.10 / -0.12	7.95 / 7.45

[a] Maximum LOD scores, positions, and 90% credible intervals (CIs) determined using MULTIPOOL.

[b] Values for Reps 1 and 2 are separated by a "/."

[c] Maximum smoothed allele frequency difference, calculated as mean resistant pool allele frequency – mean susceptible pool allele frequency in 500 Kb sliding windows with a 100 Kb increment.

The maximum smoothed allele frequency difference between RES and SUS pools was modest in all cases, ranging from 0.09 on chromosome 12 (averaging across reps) to 0.15 on chromosome 4 (Table 1.2). For the QTL on chromosomes 4 and 5, which featured the highest LOD scores, 90% credible intervals ranged from 0.66 to 2.43 Mb in size, and the location of LOD peaks were consistent between reps, displaying a difference of 0.12 Mb on chromosome 4 and 0.55 Mb on chromosome 5. The QTL on chromosomes 8, 12, and 16, on the other hand, had larger credible intervals ranging from 2.41 Mb to 7.01 Mb in size, and showed little consistency in the location of QTL peaks between reps, varying in the case of the chromosome 12 QTL by as much as 4.65 Mb, almost half the length of the chromosome.

Validation of BSA-SEQ results and linkage mapping with $F_{2:3}$ families. One hundred eighty-seven F_2 plants – comprising 18 survivors of the BSA-Seq screen ('selected' plants) and 169 plants grown from remnant seed ('random' plants) – were individually genotyped with genotyping-by-sequencing and selfed to generate an $F_{2:3}$ mapping population. In a greenhouse experiment, the family-mean heritabilities among $F_{2:3}$ families for mortality at 3,5,7, and 10 dpi ranged from 0.40-0.76, with heritability increasing with dpi (Table S1.1). A summary statistic incorporating ratings at all time points, rAUDPC, featured a higher heritability (0.77) compared to mortality at any individual time point, and was therefore used for all future analyses. The distribution of BLUEs for rAUDPC among $F_{2:3}$ families appeared slightly non-normal, with a long left (i.e. resistant) tail (Figure 1.2A). Transgressive segregation was observed, with two families displaying rAUDPC estimates lower than Pc-NY21 and 33 families displaying rAUDPC estimates higher than Dunja. Lower rAUDPC estimates were observed among $F_{2:3}$ families derived from 'selected' plants, which featured a median of 60.69, compared to $F_{2:3}$ families from 'random' plants, which featured a median rAUDPC estimate of 74.18 (Table S1.1; Figure 1.2B).

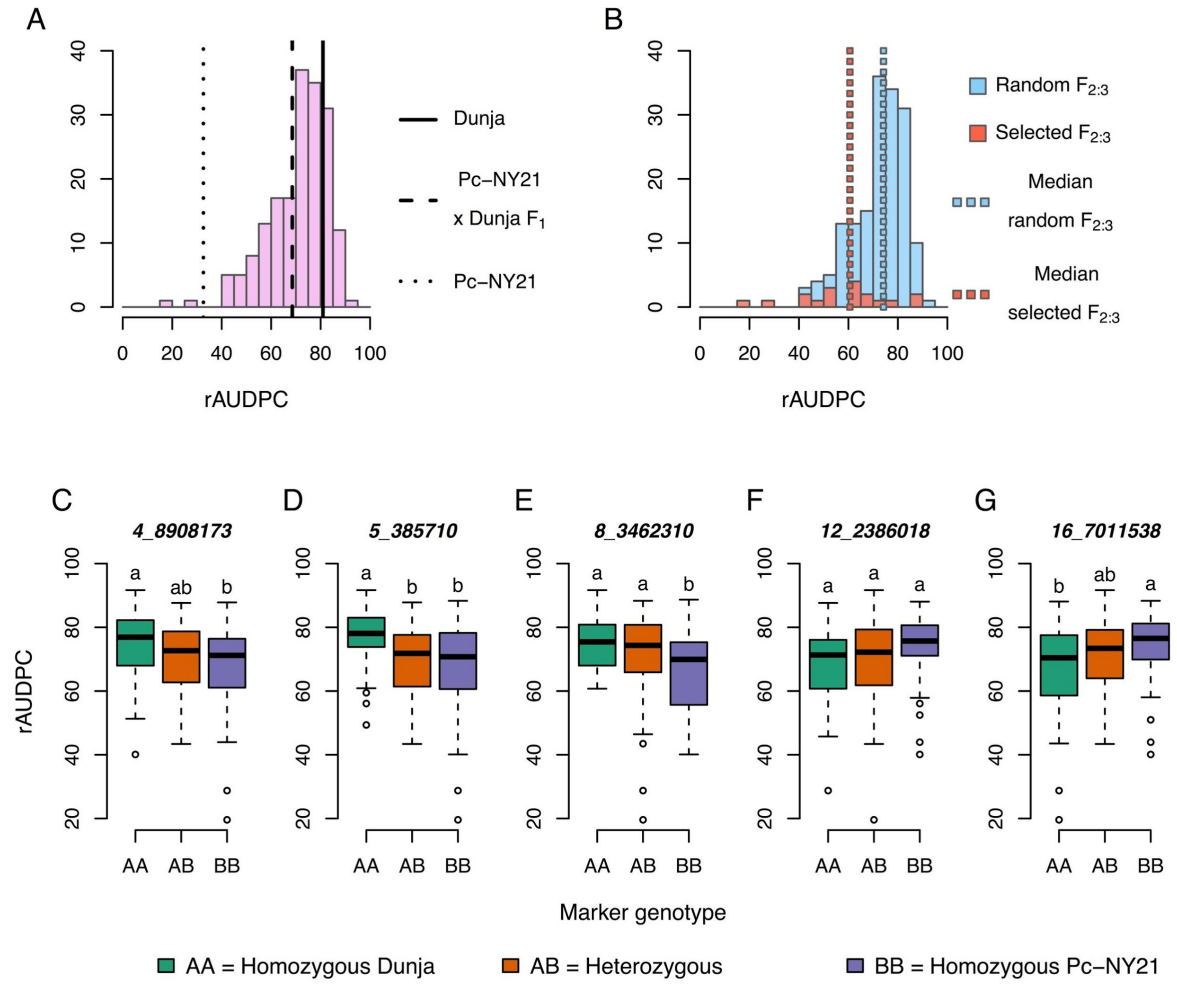

Figure 1.2: Distributions of best linear unbiased estimates of relative Area Under the Disease Progress Curve (rAUDPC) for 187 $F_{2:3}$ families. A) Histogram of $F_{2:3}$ rAUDPC estimates with lines representing estimates for the parents and F_1 generation B) Overlapping histograms for $F_{2:3}$ families derived from 169 'random' F_2 individuals grown from remnant seed (blue) and 18 'selected' F_2 individuals that survived the BSA-Seq screen. C-G) rAUDPC estimates for $F_{2:3}$ families vs their F_2 parent's genotype at each of five SNP markers tagging QTL detected via BSA-Seq. Values are shown for 176 $F_{2:3}$ families with both phenotype and genotype data.

A genetic map was constructed from 605 GBS-derived SNPs that were called on 181 F_2 individuals with high-quality genotype data. The map was 2,023.38 cM in length and consisted of 20 linkage groups corresponding to the 20 chromosomes of *C. pepo* (Figure S1.3). Linkage groups featured between 7-76 markers and ranged in length from 43.50-193.55 cM. Genetic marker positions were largely correlated with physical marker positions on the reference genome, except for 6 markers that mapped to the wrong linkage group and two genomic regions – covering approximately 8 Mb on the beginning of chromosome 4 and 1 Mb on the end of chromosome 17 – where the genetic marker order was inverted in relation to the physical marker order (Figure S1.4).

The GBS markers nearest the BSA-Seq QTL locations, which ranged from 1-196 Kb away from the midpoint of the LOD peaks from BSA-Seq Reps 1 and 2, were identified (Table S1.2). For all 5 of these QTL markers, the frequency of the resistant allele, as determined by BSA-Seq, was enriched in the 'selected' compared to the 'random' $F_{2:3}$ families, with the magnitude of the allele frequency difference (0.19) greatest for the QTL on chromosome 4 and smallest (0.04) for the chromosome 16 QTL. rAUDPC means were significantly different among $F_{2:3}$ families with different marker genotypes for the QTL on chromosomes 4, 5, 8, and 16, although not for the chromosome 12 QTL (Figure 1.2C-G). Consistent with the BSA-Seq results, the Pc-NY21 allele was associated with lower rAUDPC estimates at the chromosome 4, 5, and 8 QTL markers, and associated with higher rAUDPC estimates at the QTL markers on chromosomes 12 and 16. A multiple regression model fit with the 5 markers tagging BSA-Seq QTL explained 27.82% of the variance in rAUDPC estimates among $F_{2:3}$ families, with individual QTL explaining between 1.92-9.82% of the phenotypic variation (Table 1.3). Additive allelic effects on rAUDPC ranged in absolute value from 1.93 for the chromosome 12 QTL to

4.98 for the QTL on chromosome 5, and dominance deviations, as a percentage of the additive effect, varied from 30-115%, indicating a mixture of partially dominant and dominant gene actions.

The genetic map and $F_{2:3}$ phenotypic data were also used to discover QTL *de novo* using a multiple QTL mapping approach. The best fitting model, explaining 35.18% of the phenotypic variance, was found to contain four non-interacting QTL, consisting of the same loci identified via BSA-Seq on chromosomes 4, 5, and 8, in addition to a locus on chromosome 19 where the resistant allele was contributed by Dunja (Table 1.4; Figure S1.5). MQM and BSA-Seq credible intervals overlapped for the three QTL identified via both approaches, except for the chromosome 4 QTL, where the BSA-Seq Rep 2 and MQM credible intervals were disjoint (Figure 1.3). For the QTL on chromosomes 5 and 8, the most likely QTL positions as determined by MQM were very close to the GBS markers tagging BSA-Seq QTL, differing by 0.48 cM on chromosome 8 and falling on the same marker on chromosome 5. In the case of the chromosome 4 QTL, however, the MQM position and the BSA-Seq QTL marker were 9.08 cM apart.

Table 1.3: Effect sizes of BSA-Seq QTL in $F_{2:3}$ population.

Chromosome	Position of QTL-tagging GBS marker (Mb)[a]	Position of QTL-tagging GBS marker (cM)[a]	LOD	Proportion variance explained (%)	F test p-value	a[b]	d[c]
4	8.91	84.16	2.98	5.85	1.61×10^{-3}	-4.1	1.21
5	0.39	1.71	4.87	9.82	2.70×10^{-5}	-4.98	-3.39
8	3.46	44.48	3.12	6.13	1.22×10^{-3}	-4.02	-1.99
12	2.39	24.94	1.17	2.25	0.08	1.93	-2.22
16	7.01	49.84	1.00	1.92	0.12	2.05	1.60

[a] Genotyping-by-sequencing (GBS) markers representing BSA-Seq QTL were those nearest the midpoint of MULTIPOOL LOD peaks from BSA-Seq Reps 1 and 2.

[b] a=additive effect of Pc-NY21 allele on rAUDPC.

[c] d=dominance effect of Pc-NY21 allele.

Table 1.4: Multiple QTL mapping results and effect sizes.

Chromosome	Position (Mb) (90% CI[a])	Position (cM) (90% CI)	LOD	Proportion variation explained (%)	F test p-value	a[c]	d[d]
4	8.07 (0-0.02;8.07-8.5)[b]	75.08 (69.98-81.23)	5.54	10.12	5.51×10^{-6}	-5.28	2.5
5	0.39 (0.10-1.02)	1.71 (0.00-8.02)	5.33	9.69	8.85×10^{-6}	-4.94	-3.33
8	3.46 (1.26-3.94)	44.00 (14.06-50.14)	3.98	7.11	1.68×10^{-4}	-4.63	1.13
19	3.3 (2.73-3.56)	35.20 (32.60-37.96)	4.66	8.41	3.76×10^{-5}	2.26	-6.52

[a] CI=credible interval.

[b] Chromosome 4 credible interval disjoint due to discrepancy in marker orders between reference genome and genetic map.

[c] a=additive effect of Pc-NY21 allele on rAUDPC.

[d] d=dominance effect of Pc-NY21 allele.

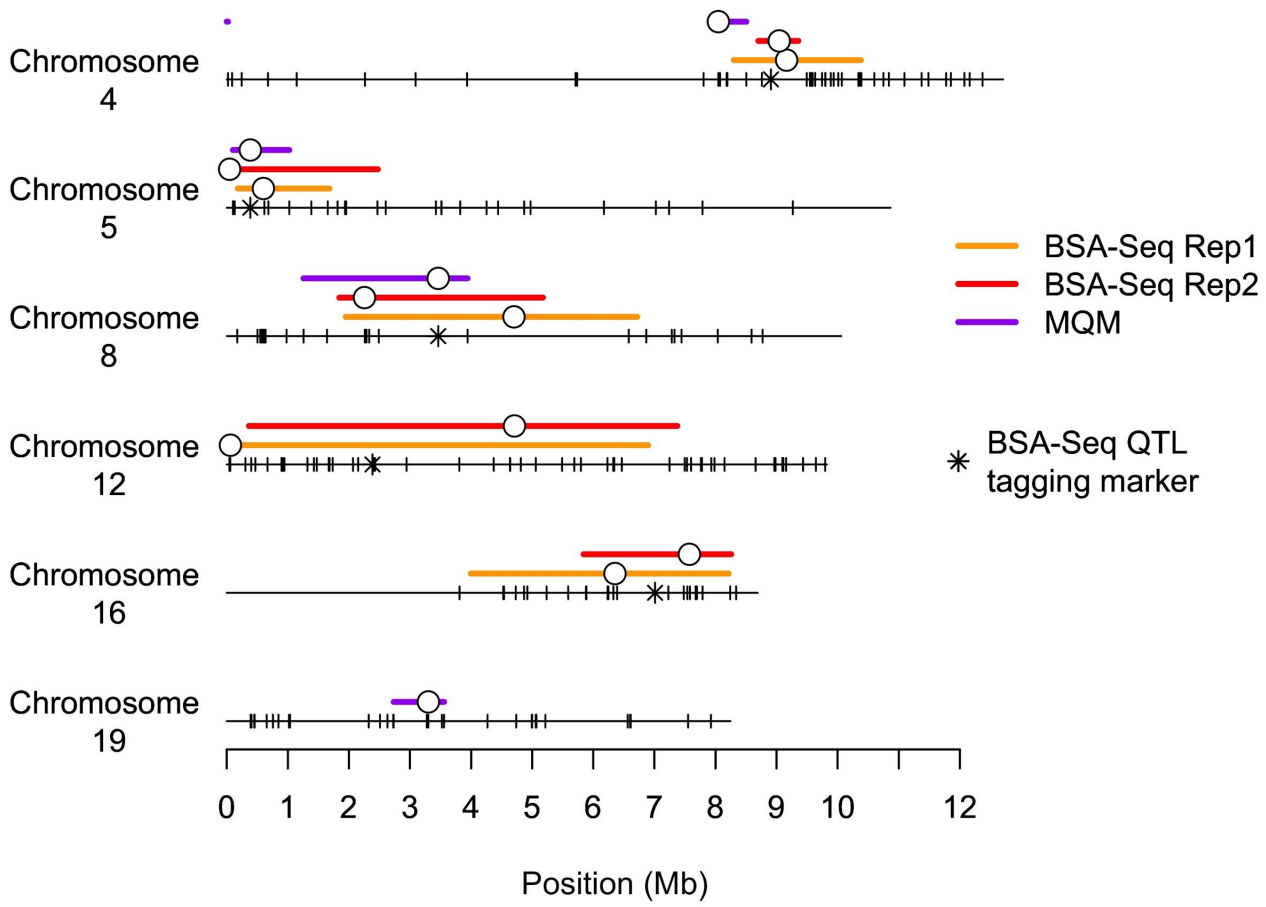

Figure 1.3: Most likely QTL positions (open circles) and credible intervals (bars) for QTL detected via BSA-Seq Reps 1 and 2 and multiple QTL mapping (MQM). Tick marks represent SNPs discovered by genotyping-by-sequencing (GBS) and used for genetic map construction. BSA-Seq QTL tagging markers were identified as those closest to the midpoint of QTL locations from Reps 1 and 2 of BSA-Seq.

Table 1.5: Candidate gene counts in QTL regions.

Chromosome	QTL region (Mb)[a]	Number genes	Number genes, moderate effect variant[b]	Number genes, high effect variant[b]	Number genes, DE melon homolog[c]	Number genes, DE melon homolog and moderate/high effect
4	0-0.02; 8.07-10.38	365	234	46	99	63
5	0.04-2.47	425	205	33	127	63
8	1.25-6.72	666	444	104	175	115
12	0.06-7.38	815	415	65	234	127
16	4.00-8.26	694	404	85	217	144
19	2.73-3.56	85	32	5	23	11

[a] QTL region defined as union of BSA-Seq and multiple QTL mapping credible intervals.

[b] Functional effects of variants (moderate or high) determined by SnpEff.

[c] DE=differentially expressed in Wang et al. (2020); homologs between squash and melon defined as reciprocal best hits following reciprocal blastp alignments.

Candidate gene identification. QTL regions were defined conservatively as the union of BSA and MQM credible intervals for the purposes of candidate gene identification. Excluding the chromosome 19 QTL, which was only identified via MQM and therefore featured a much narrower credible interval, QTL regions contained between 365-815 annotated genes (Table 1.5). In each QTL region, between 280-548 of these genes featured variants that were polymorphic between Dunja and PcNY-21 and had a functional effect predicted to be moderate (e.g. missense mutation or in-frame insertion/deletion) or high (e.g. nonsense mutation or frameshift insertion/deletion). Of the genes with a predicted moderate or high-effect variant, 63-144 in each QTL region featured homologs in melon that were differentially expressed post inoculation with *P. capsici*. Several of these had annotations potentially related to disease resistance, including three receptor-like protein kinases on chromosomes 4, 5, and 12 (Cp4.1LG04g11730, Cp4.1LG08g07850, and Cp4.1LG12g09630, respectively) and a nucleotide-binding site Toll/interleukin-1 receptor (TIR-NB) protein on chromosome 5 (Cp4.1LG05g03340).

Prediction models. In order to assess the practical value of the QTL discovered via BSA-Seq, a multiple linear regression model containing QTL markers was compared to three genomic prediction models using genome-wide markers for their ability to predict $F_{2:3}$ rAUDPC estimates. The median prediction accuracy of the QTL MLR model, as determined by cross-validation, was found to be moderate (0.43), although it was slightly outperformed by all three genomic prediction models (Figure 1.4). The GBLUP and Bayes-B models performed similarly (median prediction accuracies of 0.51 and 0.50, respectively). Incorporating fixed QTL marker effects into the GBLUP model, in the case of the GBLUP+QTL model, only provided a slight benefit, resulting in a median prediction accuracy of 0.54.

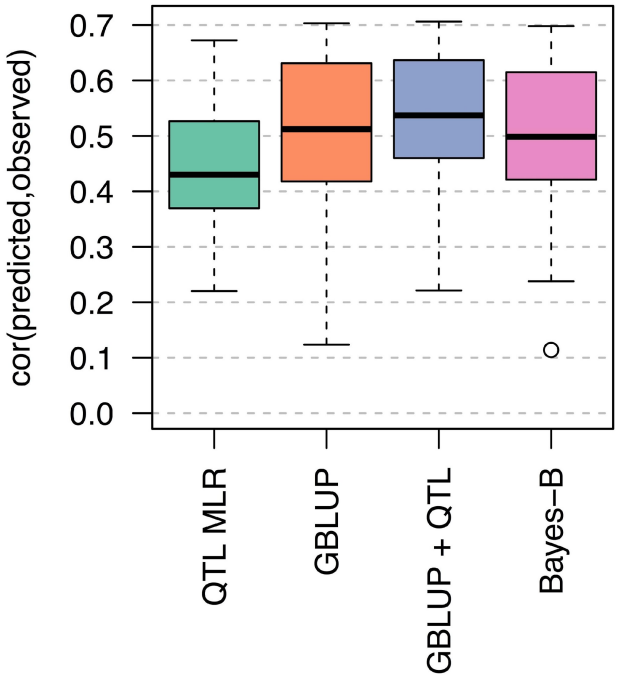

Figure 1.4: Cross-validation prediction accuracies for four models predicting $F_{2:3}$ rAUDPC. QTL MLR: multiple linear regression model with allele dosages at five SNP markers tagging BSA-Seq QTL. GBLUP: Genomic best linear unbiased prediction model using 605 genome-wide SNPs. GBLUP+QTL: GBLUP model with five SNP markers tagging BSA-Seq QTL as fixed effects. Bayes-B: Bayes-B model using 605 genome-wide SNPs.

DISCUSSION

As *P. capsici* continues to spread to previously un-infested farms, often via contaminated surface water sources that may flood or inadvertently be used for irrigation (Gevens et al. 2007; Jones et al. 2014), host resistance is becoming increasingly important for the sustainable management of Phytophthora root and crown rot. Little is known, however, about the genetic basis of resistance in *C. pepo*, the squash species that includes economically important

market classes such as zucchini, summer squash, and carving pumpkins. In this study, we identified a total of six genomic regions associated with variation for Phytophthora root and crown rot resistance in a biparental *C. pepo* population. Our approach, where we genotyped both individual progeny as well as bulked samples representing phenotypic extremes, also enabled us to compare the power, resolution, and practicality of two alternate strategies for discovering QTL.

Many aspects influence the QTL detection power and mapping resolution of BSA-Seq experiments. These include factors associated with the genetic architecture of the trait, such as the effect sizes, gene action, and degree of linkage between causative loci, in addition to technical considerations controlled by the experimenter, namely the size of the mapping population, size of selected bulks, and depth of sequencing coverage (Ehrenreich et al. 2010; Magwene et al. 2011; Takagi et al. 2013; Pool 2016). Generally, in a QTL mapping experiment, an increase in population size results in greater statistical power to detect QTL and more precise localization of QTL, since more recombination events are captured among the individuals in the population. However, with BSA-Seq, the gains in power and resolution conferred by an increase in population size are dependent on the choice of bulk size and sequencing coverage (Magwene et al. 2011; Pool 2016). Analytical results and simulations show that increasing the bulk proportion up to approximately 15-20% of the population size should provide an increase in power by reducing variation in allele frequencies due to random sampling (Magwene et al. 2011; Takagi et al. 2013). However, with larger population sizes, an adequate reduction in sampling variance may be achieved with lower bulk proportions (Pool 2016). Furthermore, since bulk allele frequencies are not measured directly, but are instead estimated from a sub-sample of randomly drawn sequencing reads, larger bulks may not be advantageous without corresponding

increases in sequencing depth (Magwene et al. 2011; Pool 2016)

The mapping population we evaluated in this experiment, consisting of approximately 7,000 plants per rep, was large compared to most BSA-Seq experiments in plants, although several other researchers have evaluated plant populations in the range of 10,000 or even 100,000 individuals (Yang et al. 2013; Haase et al. 2015; Yuan et al. 2016). Following recommendations in the literature (Magwene et al. 2011; Takagi et al. 2013), we aimed to include 15% of the total population, or approximately 1,000 individuals, in each RAN, SUS, and RES bulk. Our realized sequencing depth of 24-70 (Table 1.1), however, meant that the number of reads sampled at a given site on average captured fewer than 0.5% of the approximately 2,000 distinct chromosomes represented in bulks. Consequently, variation from sequencing noise likely represented a much greater source of error in our experiment than variation from sampling individuals for bulks. Given our population size and level of sequencing depth, it may therefore have been advantageous to have selected smaller bulks, thereby applying a higher selection intensity and driving a higher divergence in allele frequency between RES and SUS bulks.

Nevertheless, we were able to overcome some of the limitations imposed by shallow sequencing and low allele frequency differentiation by using a statistical method, MULTIPOOL, that considers information from all markers on a chromosome simultaneously in order to identify the positions of QTL (Edwards and Gifford 2012). Compared to other methods for QTL mapping with BSA-Seq data, MULTIPOOL results in a low rate of false negatives and false positives even at low levels of sequencing coverage (Duitama et al. 2014; Huang et al. 2020). The two methods most popular in the plant breeding literature – QTL-Seq (Takagi et al. 2013) and the G' test (Magwene et al. 2011), both based on sliding window-smoothed statistics – perform well in many scenarios but improperly control for multiple testing, leading to poor detection of QTL in

low read depth situations (Huang et al. 2020). While the authors of MULTIPOOL do not suggest a LOD threshold for declaring a QTL significant, we were able to determine an appropriate cut-off by assessing a null distribution of LOD scores from inter-rep comparisons of bulks selected in the same direction. Our use of multiple replicates, which are not typical in BSA-Seq experiments but common in conceptually similar 'evolve & resequence' experiments (Long et al. 2015), also granted us greater confidence in the five QTL that were discovered, as they represented regions featuring significant differentiation between two independent selections of RES and SUS bulks.

Multiple QTL mapping with 176 $F_{2:3}$ families resulted in the identification of a similar set of QTL compared to BSA-Seq. Both methods agreed in the identification of three regions – on chromosomes 4, 5, and 8 – where the resistant allele was inherited from resistant parent Pc-NY21. However, the two methods identified distinct loci where the allele associated with resistance was inherited from Dunja, possibly due to the lower effect sizes of these QTL. Multiple QTL mapping credible intervals were considerably narrower than the credible intervals determined by MULTIPOOL from the BSA-Seq data (Figure 1.3), although this is likely explained by the fact that MQM credible intervals, as estimated in R/qtl, do not account for uncertainty in the positions of other identified QTL and are therefore overly liberal (Broman and Sen 2009). Indeed, credible intervals for these same loci as identified in R/qtl via a single QTL interval mapping scan, as opposed to MQM, were similar in size to those identified via BSA-Seq (data not shown). For the loci on chromosomes 5 and 8, the most likely QTL position determined by MQM was remarkably close to the midpoint of the QTL positions identified by Reps 1 and 2 of BSA-Seq, differing by 62 kb on chromosome 5 and 16 kb on chromosome 8 (Figure 1.3). This was not the case, however, with the chromosome 4 QTL, where MQM determined the most

likely QTL position to be over 1 Mb from the midpoint of the BSA-Seq positions. Of the 20 chromosomes, chromosome 4 also featured the greatest discrepancy in terms of marker order on the genetic and physical maps, with markers on the first 8 Mb of the chromosome inverted on the genetic map compared to their coordinates in the reference genome sequence (Figure S1.4). This discordance, which could either reflect a mis-assembly in the reference genome or a true inversion in the parents of our population, likely was the reason for the poor estimation of the QTL position by MULTIPOOL, as markers showing no signal in terms of allele frequency differentiation were incorrectly assumed to be tightly linked with markers featuring high signal. Several artifacts of this discrepancy between the physical and genetic maps can be seen in our results: the quite sudden allele frequency differentiation between RES and SUS pools between 8-9 Mb on chromosome 4, which appears much more abruptly compared to the onset of other QTL we identified, as well as the appearance of a second, spurious LOD peak at the beginning of the chromosome, which actually surpassed our significance threshold in Rep 2. In this case, an approach using small reference-based sliding windows, such as QTL-Seq, may have resulted in a more accurate determination of the chromosome 4 QTL position compared to a model-based method liked MULTIPOOL that considers all markers on a chromosome at once.

Overall, the two approaches – BSA-Seq using a large population of F_2 individuals and linkage mapping with a modestly sized population of $F_{2:3}$ families – performed similarly in terms of mapping power, resolution, and localization of QTL. Other considerations, however, may influence the decision by a researcher to choose one of these methods over the other. Genotyping of individual progeny, as required in linkage mapping, allows for the estimation of QTL effect sizes and the testing of QTL x QTL interaction effects, both of which are not possible with BSA-Seq. Individual genotyping also enables a researcher to use a single genotype dataset to map

multiple traits, also impossible with BSA-Seq given that the individuals that contribute to the sequenced DNA pools are selected based on their values for one particular phenotype. On the other hand, BSA-Seq is easily scaled up to larger population sizes, making it a more powerful approach for trait mapping in early generations like an F_2 or BC_1. This is especially relevant in squash, since plants require manual self-pollination and take up considerable space in a field or greenhouse, making the generation of inbred lines highly resource-intensive.

Between the two QTL mapping approaches used in this experiment, a total of six QTL were identified, suggesting an oligogenic genetic architecture for Phytophthora root and crown rot resistance in squash. Each QTL was of small to moderate effect, with the largest-effect QTL we identified, those on chromosomes 4 and 5, individually accounting for only 9-10% of the phenotypic variance explained among $F_{2:3}$ families in the MQM model. Furthermore, models including the five QTL discovered via BSA-Seq or the four discovered via MQM only explained a modest proportion of the phenotypic variance: 28 and 35%, respectively. Considering the relatively high broad-sense heritability for rAUDPC in the $F_{2:3}$ population (0.77), it seems likely that we lacked the statistical power to detect additional small-effect loci contributing to variation among $F_{2:3}$ families. Based on these results, Phytophthora root and crown resistance may have a more polygenic genetic architecture in squash compared to pepper (*Capsicum annuum*), where the genetics of resistance have been much better characterized. Crosses with different resistant pepper accessions have consistently identified, in addition to small and moderate-effect loci, a major QTL accounts for over 50% of the phenotypic variance explained in many populations (Thabuis et al. 2003; Thabuis et al. 2004;; Mallard et al. 2013; Liu et al. 2014). It remains unknown if such large-effect resistance genes exist in *Cucurbita* germplasm. In addition, mapping experiments in pepper using diverse isolates of *P. capsici* have shown that minor

resistance QTL often have isolate-specific effects (Ogundiwin et al. 2004; Truong et al. 2011; Rehrig et al. 2014; Siddique et al. 2019). Although a sibling line of the resistant parent in our cross expressed a consistent resistance response when inoculated with diverse *P. capsici* isolates (LaPlant et al. 2020), it is possible that separate genes from those discovered in this experiment are involved in resistance to different isolates.

Despite the wide range of crops susceptible to Phytophthora root and crown rot (Granke et al. 2012), relatively little research has been conducted on the genetic basis of resistance in species beside pepper. Recently, however, Ramos et al. (2020) reported the identification of three resistance QTL in *C. moschata*, two of which featured resistance alleles inherited from the susceptible butternut parent of their cross. Interestingly, we found that the regions comprising the QTL identified by Ramos et al. on *C. moschata* chromosomes 11 and 14 contained blocks of shared synteny with the *C. pepo* QTL regions we identified on chromosomes 4 and 8, respectively (Figure S1.6). While these results are suggestive of a possible common evolutionary origin for the casual resistance genes at these loci, it also possible that QTL from the two species shared regions of synteny due to chance, especially when considering the fact that a substantial portion of the *C. pepo* genome (8%) was contained within the six QTL we identified. Because Ramos et al. used a BSA-Seq strategy combined with further selective genotyping for marker validation, QTL effect sizes were not reported, making additional comparisons between QTL from the two experiments difficult.

Unfortunately, the successful identification of candidate genes in our experiment was made difficult by the high degree of statistical uncertainty in QTL positions, as the intersections of credible intervals from BSA-Seq and MQM generally spanned several Mb and comprised hundreds of genes (Figure 1.3; Table 1.5). Furthermore, unlike qualitative disease resistance,

which is typically conferred by proteins belonging to a small number of well-characterized gene families (Kourelis and van der Hoom 2018), quantitative disease resistance in plants is mediated by a wide variety of genes with diverse functions (Nelson et al. 2018). In squash, Phytophthora root and crown rot resistance is associated with a reduction in pathogen infection of vascular tissue (Krasnow et al. 2017), similar to in pepper, where the secretion of root exudates and the formation of callose and cell well appositions appear to prevent the colonization of *P. capsici* beyond the outermost layers of the cortex in resistant roots and stems (Kim and Kim 2009; Dunn and Smart 2015; Piccini et al. 2019). The genes that confer these defense responses are unknown and may have various functions, such as those related to pathogen recognition, signaling, or the production of antimicrobial molecules. Therefore, we found functional annotations relatively uninformative for the identification of candidate genes in QTL intervals. However, we were able to identify a reduced number of higher-confidence candidate genes – between 63-144 per QTL region – that were segregating for variants of moderate or high effect in our population and that featured a homolog in melon that was differentially expressed post inoculation with *P. capsici*. Additional sources of information, such as transcriptomic data on the parents of our population, may be able to further prioritize candidate genes in QTL intervals.

The results from this experiment are promising for the implementation of MAS for Phytophthora root and crown rot resistance in squash. Although QTL effect sizes were small, we showed that prediction models using just five markers – one for each QTL detected via BSA-seq – could predict the resistance levels of $F_{2:3}$ families with a drop in prediction accuracy of only 0.07-0.08 compared to whole genome prediction models that did not fit QTL effects (Figure 1.4). While this difference is not negligible, genotyping progeny at five markers instead of several hundred may be easier to implement in a breeding program and could translate to meaningful

cost savings. Nevertheless, further research is still necessary to test the effects of these QTL in different populations and environments. It should be noted that both parents of our cross belonged to *C. pepo* ssp. *pepo*, the more resistant (Camp et al. 2009; Meyer and Hausbeck 2012; Krasnow et al. 2017) of the two independently domesticated subspecies of *C. pepo* (Decker 1988; Sanjur et al. 2002) and were therefore both likely fixed for the resistant alleles at additional, unknown loci that are presumably polymorphic between *C. pepo* ssp. *pepo* and ssp. *ovifera*. Efforts to introgress resistance from Pc-NY21 into *C. pepo* ssp. *ovifera* cultivars via MAS may not be successful without accounting for these loci. Furthermore, it is important to mention that neither of the parents of our mapping population were fully inbred lines, since they were chosen more for their utility in breeding rather than their suitability for QTL mapping. By only using informative markers that were homozygous in the parents, we were able to map the genomic positions of QTL that were polymorphic between Dunja and Pc-NY21. If the parent carrying the resistant allele for a given QTL was actually heterozygous at that locus, however, these markers would be uninformative for MAS, as they would be unable to differentiate between the resistant and susceptible haplotypes from the donor parent of the resistant allele. We suspect, however, that this is not the case for the major QTL we identified on chromosomes 4, 5, and 8, given the low proportion of heterozygous markers in PcNY-21 in these regions (data not shown).

In conclusion, we discovered a total of six genomic regions associated with Phytophthora root and crown rot resistance in a biparental squash population. Three featured resistant alleles inherited from the resistant parent of our cross and were identified independently via both BSA-Seq and linkage mapping; the other three featured resistant alleles inherited from the susceptible parent of the cross and were each identified via only one of the two methods. Despite the small

to moderate effect sizes of these QTL, we believe that markers in these regions can be used to accelerate disease resistance breeding in various market classes of squash. Our mapping resolution was too low to conclusively identify strong candidates for genes conferring resistance in QTL regions. Nevertheless, these results represent an early step toward uncovering the genetic and molecular mechanisms underlying Phytophthora root and crown rot resistance in squash.

ACKNOWLEDGEMENTS

We are grateful for technical assistance from Andrew Aldcroft, Mariami Bekauri, Colin Day, Garrett Giles, Holly Lange, Nicholas King, Carolina Puentes Silva, and Carolina Vogel, as well as statistical advice from Chris Hernandez and Ryokei Tanaka. We would also like to thank Jeff Glaubitz, Peter Schweitzer, and Jing Wu from the Cornell Institute of Biotechnology for consultation regarding library preparation for whole genome sequencing; Mainor Najera, Fernando Villalta Mata, and Andrés Villalta Pereira from VillaPlants for provision of seed increase services; and Mary Kreitinger for assistance in obtaining permits for shipping of seed, tissue, and supplies. Funding for this project was provided by the Cucurbit Coordinated Agricultural Project (CucCAP; USDA National Institute of Food and Agriculture Specialty Crop Research Initiative Grant No. 2015-51181-24285) and the New York State Department of Agriculture and Markets.

REFERENCES

Bates D, Mächler M, Bolker B, Walker S (2015) Fitting linear mixed-effects models using lme4. J Stat Softw 67:1–48

Bolger AM, Lohse M, Usadel B (2014) Trimmomatic: a flexible trimmer for Illumina sequence data. Bioinformatics 30:2114–2120

Broman KW, Sen Ś (2009) Fit and exploration of multiple-QTL models. In: Broman KW, Sen S (eds) A Guide to QTL Mapping with R/qtl. Springer, New York, NY, pp 241–282

Broman KW, Wu H, Sen Ś, Churchill GA (2003) R/qtl: QTL mapping in experimental crosses. Bioinformatics 19:889–890

Camacho C, Coulouris G, Avagyan V, Ma N, Papadopoulos J, Bealer K, Madden TL (2009) BLAST+: architecture and applications. BMC Bioinformatics 10:421

Camp AR, Lange HW, Reiners S, Dillard HR, Smart CD (2009) Tolerance of summer and winter squash lines to Phytophthora blight, 2008. Plant Disease Management Reports 3:V022

Chavez DJ, Kabelka EA, Chaparro JX (2011) Screening of *Cucurbita moschata* Duchesne germplasm for crown rot resistance to Floridian isolates of *Phytophthora capsici* Leonian. HortScience 46:536–540

Chen S, Zhou Y, Chen Y, Gu J (2018) fastp: an ultra-fast all-in-one FASTQ preprocessor. Bioinformatics 34:i884–i890

Cingolani P, Platts A, Wang LL, Coon M, Nguyen T, Wang L, Land SJ, Lu X, Ruden DM (2012) A program for annotating and predicting the effects of single nucleotide polymorphisms, SnpEff. Fly 6:80–92

Danecek P, Auton A, Abecasis G, Albers CA, Banks E, DePristo MA, Handsaker RE, Lunter G,

Marth GT, Sherry ST, McVean G, Durbin R (2011) The variant call format and VCFtools. Bioinformatics 27:2156–2158

Decker DS (1988) Origin(s), evolution, and systematics of *Cucurbita pepo* (Cucurbitaceae). Econ Bot 42:4–15

Dunn AR, Milgroom MG, Meitz JC, McLeod A, Fry WE, McGrath MT, Dillard HR, Smart CD (2010) Population structure and resistance to mefenoxam of *Phytophthora capsici* in New York State. Plant Dis 94:1461–1468

Dunn AR, Smart CD (2015) Interactions of *Phytophthora capsici* with resistant and susceptible pepper roots and stems. Phytopathology 105:1355–1361

Edwards MD, Gifford DK (2012) High-resolution genetic mapping with pooled sequencing. BMC Bioinformatics 13:S8

Elshire RJ, Glaubitz JC, Sun Q, Poland JA, Kawamoto K, Buckler ES, Mitchell SE (2011) A robust, simple genotyping-by-sequencing (GBS) approach for high diversity species. PLoS ONE 6:e19379

Endelman JB (2011) Ridge regression and other kernels for genomic selection with R Package rrBLUP. Plant Genome 4:250–255

Enzenbacher TB, Hausbeck MK (2012) An evaluation of cucurbits for susceptibility to Cucurbitaceous and Solanaceous *Phytophthora capsici* isolates. Plant Dis 96:1404–1414

Esteras C, Gómez P, Monforte AJ, Blanca J, Vicente-Dólera N, Roig C, Nuez F, Picó B (2012) High-throughput SNP genotyping in *Cucurbita pepo* for map construction and quantitative trait loci mapping. BMC Genomics 13:80

Fry WE (1978) Quantification of general resistance of potato cultivars and fungicide effects for integrated control of potato late blight. Phytopathology 68:1650

Garcia-Mas J, Benjak A, Sanseverino W, et al (2012) The genome of melon (*Cucumis melo* L.). Proc Natl Acad Sci USA 109:11872–11877

Gevens AJ, Donahoo RS, Lamour KH, Hausbeck MK (2007) Characterization of *Phytophthora capsici* from Michigan surface irrigation water. Phytopathology 97:421–428.

Granke LL, Quesada-Ocampo L, Lamour K, Hausbeck MK (2012) Advances in research on *Phytophthora capsici* on vegetable crops in the United States. Plant Dis 96:1588–1600

Gu Z, Gu L, Eils R, Schlesner M, Brors B (2014) *circlize* implements and enhances circular visualization in R. Bioinformatics 30:2811–2812

Haley CS, Knott SA (1992) A simple regression method for mapping quantitative trait loci in line crosses using flanking markers. Heredity 69:315–324

Hausbeck MK, Lamour KH (2004) *Phytophthora capsici* on vegetable crops: research progress and management challenges. Plant Dis 88:1292–1303

Holdsworth WL, LaPlant KE, Bell DC, Jahn MM, Mazourek M (2016) Cultivar-based introgression mapping reveals wild species-derived Pm-0, the major powdery mildew resistance locus in squash. PLoS ONE 11:e0167715

Holland JB, Nyquist WE, Cervantes-Martínez CT (2003) Estimating and interpreting heritability for plant breeding: an update. In: Plant Breeding Reviews. John Wiley & Sons, Ltd, pp 9–112

Huang L, Tang W, Bu S, Wu W (2020) BRM: a statistical method for QTL mapping based on bulked segregant analysis by deep sequencing. Bioinformatics 36:2150–2156

Illa-Berenguer E, Van Houten J, Huang Z, van der Knaap E (2015) Rapid and reliable identification of tomato fruit weight and locule number loci by QTL-seq. Theor Appl Genet 128:1329–1342

Jackson KL, Yin J, Ji P (2012) Sensitivity of *Phytophthora capsici* on vegetable crops in Georgia to mandipropamid, dimethomorph, and cyazofamid. Plant Dis 96:1337–1342

Jones LA, Worobo RW, Smart CD (2014) Plant-pathogenic oomycetes, *Escherichia coli* strains, and *Salmonella* spp. frequently found in surface water used for irrigation of fruit and vegetable crops in New York State. Appl Environ Microbiol 80:4814–4820

Kim S-G, Kim Y-H (2009) Histological and cytological changes associated with susceptible and resistant responses of chili pepper root and stem to *Phytophthora capsici* infection. Plant Pathol J 25:113–120

Kourelis J, van der Hoorn RAL (2018) Defended to the nines: 25 years of resistance gene cloning identifies nine mechanisms for R protein function. Plant Cell 30:285–299

LaPlant KE, Vogel G, Reeves E, Smart CD, Mazourek M (2020) Performance and resistance to phytophthora crown and root rot in squash lines. HortTechnology 1:1–11 https://doi.org/10.21273/HORTTECH04636-20

Lamour KH, Hausbeck MK (2000) Mefenoxam insensitivity and the sexual stage of *Phytophthora capsici* in Michigan cucurbit fields. Phytopathology 90:396–400

Lee BK, Kim BS, Chang SW, Hwang BK (2001) Aggressiveness to pumpkin cultivars of isolates of *Phytophthora capsici* from pumpkin and pepper. Plant Dis 85:497–500

Li H, Durbin R (2009) Fast and accurate short read alignment with Burrows–Wheeler transform. Bioinformatics 25:1754–1760

Li H, Handsaker B, Wysoker A, et al (2009) The Sequence Alignment/Map format and SAMtools. Bioinformatics 25:2078–2079

Liu W-Y, Kang J-H, Jeong H-S, Choi H-J, Yang H-B, Kim K-T, Choi D, Choi GJ, Jahn M, Kang B-C (2014) Combined use of bulked segregant analysis and microarrays reveals

SNP markers pinpointing a major QTL for resistance to *Phytophthora capsici* in pepper. Theor Appl Genet 127:2503–2513

Long A, Liti G, Luptak A, Tenaillon O (2015) Elucidating the molecular architecture of adaptation via evolve and resequence experiments. Nat Rev Genet 16:567–582

Lust TA, Paris HS (2016) Italian horticultural and culinary records of summer squash (*Cucurbita pepo*, Cucurbitaceae) and emergence of the zucchini in 19th-century Milan. Ann Bot 118:53–69

Magwene PM, Willis JH, Kelly JK (2011) The statistics of bulk segregant analysis using next generation sequencing. PLoS Comput Biol 7:e1002255

Mallard S, Cantet M, Massire A, Bachellez A, Ewert S, Lefebvre V (2013) A key QTL cluster is conserved among accessions and exhibits broad-spectrum resistance to *Phytophthora capsici*: a valuable locus for pepper breeding. Mol Breed 32:349–364

Melo ATO, Bartaula R, Hale I (2016) GBS-SNP-CROP: a reference-optional pipeline for SNP discovery and plant germplasm characterization using variable length, paired-end genotyping-by-sequencing data. BMC Bioinformatics 17:29

Mendiburu FD, Simon R (2015) Agricolae - Ten years of an open source statistical tool for experiments in breeding, agriculture and biology. PeerJ PrePrints

Menezes CB, Maluf WR, Faria MV, Azevedo SM, Resende JT, Figueira AR, Gomes LA (2015) Inheritance of resistance to papaya ringspot virus-watermelon strain (PRSV-W) in "Whitaker" summer squash line. Crop Breeding and Applied Biotechnology 15:203–209

Meuwissen THE, Hayes BJ, Goddard ME (2001) Prediction of total genetic value using genome-wide dense marker maps. Genetics 157:1819–1829

Michael VN, Fu Y, Meru G (2019) Inheritance of resistance to phytophthora crown rot in

Cucurbita pepo. HortScience 54:1156–1158

Michelmore RW, Paran I, Kesseli RV (1991) Identification of markers linked to disease-resistance genes by bulked segregant analysis: a rapid method to detect markers in specific genomic regions by using segregating populations. Proc Natl Acad Sci USA 88:9828–9832

Montero-Pau J, Blanca J, Bombarely A, Ziarsolo P, Esteras C, Martí-Gomez C, Ferriol M, Gómez P, Jamilena M, Mueller L, Picó B, Cañizares J (2018) De novo assembly of the zucchini genome reveals a whole-genome duplication associated with the origin of the *Cucurbita* genus. Plant Biotechnol J 16:1161–1171

Montero-Pau J, Blanca J, Esteras C, Martínez-Pérez EM, Gómez P, Monforte AJ, Cañizares J, Picó B. (2017) An SNP-based saturated genetic map and QTL analysis of fruit-related traits in zucchini using genotyping-by-sequencing. BMC Genomics 18:94

Nelson R, Wiesner-Hanks T, Wisser R, Balint-Kurti P (2018) Navigating complexity to breed disease-resistant crops. Nat Rev Genet 19:21–33

Ogundiwin EA, Berke TF, Massoudi M, Black LL, Huestis G, Choi D, Lee S, Prince JP (2005) Construction of 2 intraspecific linkage maps and identification of resistance QTLs for *Phytophthora capsici* root-rot and foliar-blight diseases of pepper (*Capsicum annuum* L.). Genome 48:698–711

Padley LD, Kabelka EA, Roberts PD (2009) Inheritance of resistance to crown rot caused by *Phytophthora capsici* in *Cucurbita*. HortScience 44:211–213

Padley LD, Kabelka EA, Roberts PD, French R (2008) Evaluation of *Cucurbita pepo* accessions for crown rot resistance to isolates of *Phytophthora capsici*. HortScience 43:1996–1999

Parra G, Ristaino JB (2001) Resistance to mefenoxam and metalaxyl among field isolates of

Phytophthora capsici causing Phytophthora blight of bell pepper. Plant Dis 85:1069–1075

Pérez P, Campos G de los (2014) Genome-wide regression and prediction with the BGLR statistical package. Genetics 198:483–495

Piccini C, Parrotta L, Faleri C, Romi M, Del Duca S, Cai G (2019) Histomolecular responses in susceptible and resistant phenotypes of *Capsicum annuum* L. infected with *Phytophthora capsici*. Sci Hortic 244:122–133

Pool JE (2016) Genetic mapping by bulk segregant analysis in *Drosophila*: experimental design and simulation-based inference. Genetics 204:1295–1306

Quinlan AR, Hall IM (2010) BEDTools: a flexible suite of utilities for comparing genomic features. Bioinformatics 26:841–842

R Core Team (2019) R: A langauge and environment for statistical computing. Vienna, Austria

Ramos A, Fu Y, Michael V, Meru G (2020) QTL-seq for identification of loci associated with resistance to Phytophthora crown rot in squash. Sci Rep 10:5326

Rehrig WZ, Ashrafi H, Hill T, Prince J, Van Deynze A (2014) CaDMR1 cosegregates with QTL Pc5.1 for resistance to *Phytophthora capsici* in pepper (*Capsicum annuum*). Plant Genome 7:1-12

Rhodes AM (1964) Inheritance of powdery mildew resistance in the genus *Cucurbita*. Plant Dis Rep 48:54–55

Sanjur OI, Piperno DR, Andres TC, Wessel-Beaver L (2002) Phylogenetic relationships among domesticated and wild species of *Cucurbita* (Cucurbitaceae) inferred from a mitochondrial gene: implications for crop plant evolution and areas of origin. Proc Natl Acad Sci USA 99:535–540

Siddique MI, Lee H-Y, Ro N-Y, Han K, Venkatesh J, Solomon AM, Patil AS, Changkwian AC, Kwon J-K, Kang B-C (2019) Identifying candidate genes for *Phytophthora capsici* resistance in pepper (*Capsicum annuum*) via genotyping-by-sequencing-based QTL mapping and genome-wide association study. Sci Rep 9:9962

Sun H, Wu S, Zhang G, et al (2017) Karyotype stability and unbiased fractionation in the paleo-allotetraploid *Cucurbita* genomes. Mol Plant 10:1293–1306.

Takagi H, Abe A, Yoshida K, et al (2013) QTL-seq: rapid mapping of quantitative trait loci in rice by whole genome resequencing of DNA from two bulked populations. Plant J 74:174–183

Taylor J, Butler D (2017) R package ASMap: efficient genetic linkage map construction and diagnosis. J Stat Soft 79:1-29

Thabuis A, Palloix A, Pflieger S, Daubéze A-M, Caranta C, Lefebvre V (2003) Comparative mapping of *Phytophthora* resistance loci in pepper germplasm: evidence for conserved resistance loci across Solanaceae and for a large genetic diversity. Theor Appl Genet 106:1473–1485

Thabuis A, Palloix A, Servin B, Daubéze AM, Signoret P, Hospital F, Lefebvre V (2004) Marker-assisted introgression of 4 *Phytophthora capsici* resistance QTL alleles into a bell pepper line: validation of additive and epistatic effects. Mol Breed 14:9–20

Tian D, Babadoost M (2004) Host range of *Phytophthora capsici* from pumpkin and pathogenicity of isolates. Plant Dis 88:485–489

Truong HTH, Kim KT, Kim DW, Kim S, Chae Y, Park JH, Oh DG, Cho MC (2012) Identification of isolate-specific resistance QTLs to phytophthora root rot using an intraspecific recombinant inbred line population of pepper (*Capsicum annuum*). Plant

Pathol 61:48–56

United States Department of Agriculture (2019) Vegetables and melons. In: Agricultural Statistics 2019. United States Government Printing Office, Washington, D.C.

Wang Y, Tang H, Debarry JD, et al (2012) MCScanX: a toolkit for detection and evolutionary analysis of gene synteny and collinearity. Nucleic Acids Res 40:e49

Wang P, Wu H, Zhao G, He Y, Kong W, Zhang J, Liu S, Liu M, Hu K, Liu L, Xu Y, Xu Z (2020) Transcriptome analysis clarified genes involved in resistance to *Phytophthora capsici* in melon. PLoS ONE 15:e0227284

Wu Y, Bhat PR, Close TJ, Lonardi S (2008) Efficient and accurate construction of genetic linkage maps from the minimum spanning tree of a graph. PLoS Genet 4:e1000212

Zheng Y, Wu S, Bai Y, et al (2019) Cucurbit Genomics Database (CuGenDB): a central portal for comparative and functional genomics of cucurbit crops. Nucleic Acids Res 47:D1128–D1136

SUPPLEMENTARY MATERIAL

Table S1.1: Broad-sense heritabilities (H^2), parental and F_1 estimates, and medians of 'random' and 'selected' cohorts of $F_{2:3}$ families for five traits.

Trait[a]	H^2	Dunja	PcNY-21	Dunja x PcNY-21 F_1	Median, 'random' $F_{2:3}$ families	Median, 'selected' $F_{2:3}$ families
dpi3	0.4	16.67	0	25	19.44	12.31
dpi5	0.66	74.07	13.89	54.17	63.64	45.04
dpi7	0.72	94.44	41.67	75	83.33	61.25
dpi10	0.76	100	55.56	91.67	97.22	86.11
rAUDPC	0.77	80.95	32.61	68.54	74.18	60.59

[a] dpi3, dpi5, dpi7, dpi10 = plot mortality at 3, 5, 7, and 10 days post inoculation, respectively. rAUDPC = relative Area Under the Disease Progress Curve.

Table S1.2: Positions of SNP markers tagging BSA-Seq QTL and their PcNY-21 allele frequencies in 'random' and 'selected' F_2 cohorts.

Chromosome	Position (bp)	Distance from BSA mean LOD peak (bp)	PcNY-21 allele frequency, 'random' $F_{2:3}$ families	PcNY-21 allele frequency, 'selected' $F_{2:3}$ families
4	8908173	195977	0.47	0.66
5	385710	62160	0.51	0.63
8	3462310	15990	0.53	0.71
12	2386018	968	0.54	0.42
16	7011538	47288	0.46	0.42

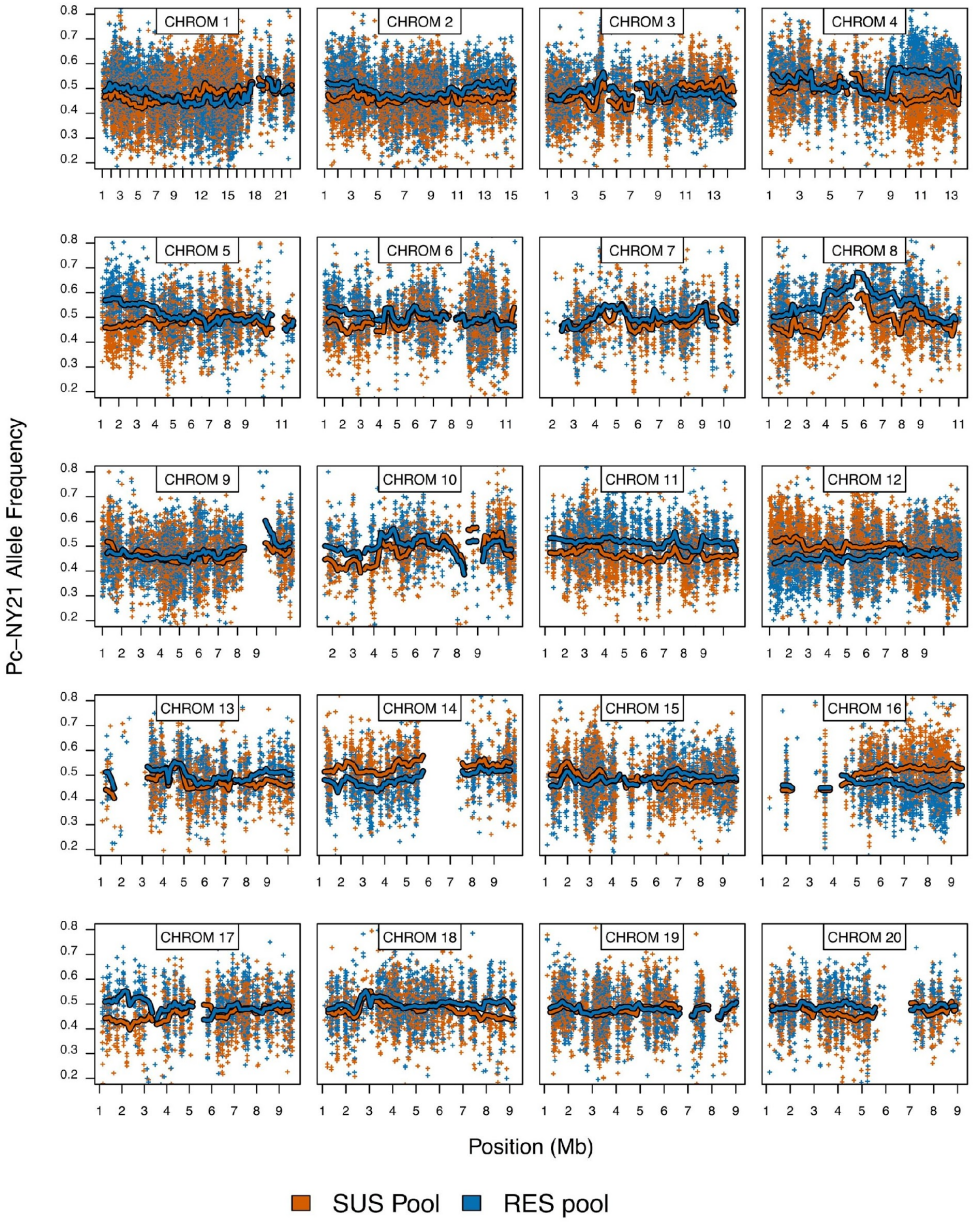

Figure S1.1: Pc-NY21 allele frequencies in Rep 1 susceptible (SUS) and resistant (RES) pools across all 20 chromosomes. Plus signs are individual SNP allele frequencies and lines are smoothed means calculated in 500 Kb sliding windows with a 100 Kb increment. For simplicity of visualization, only a random subset of 25% of SNPs are shown. Smoothed means are not calculated in any window featuring fewer than 30 SNPs.

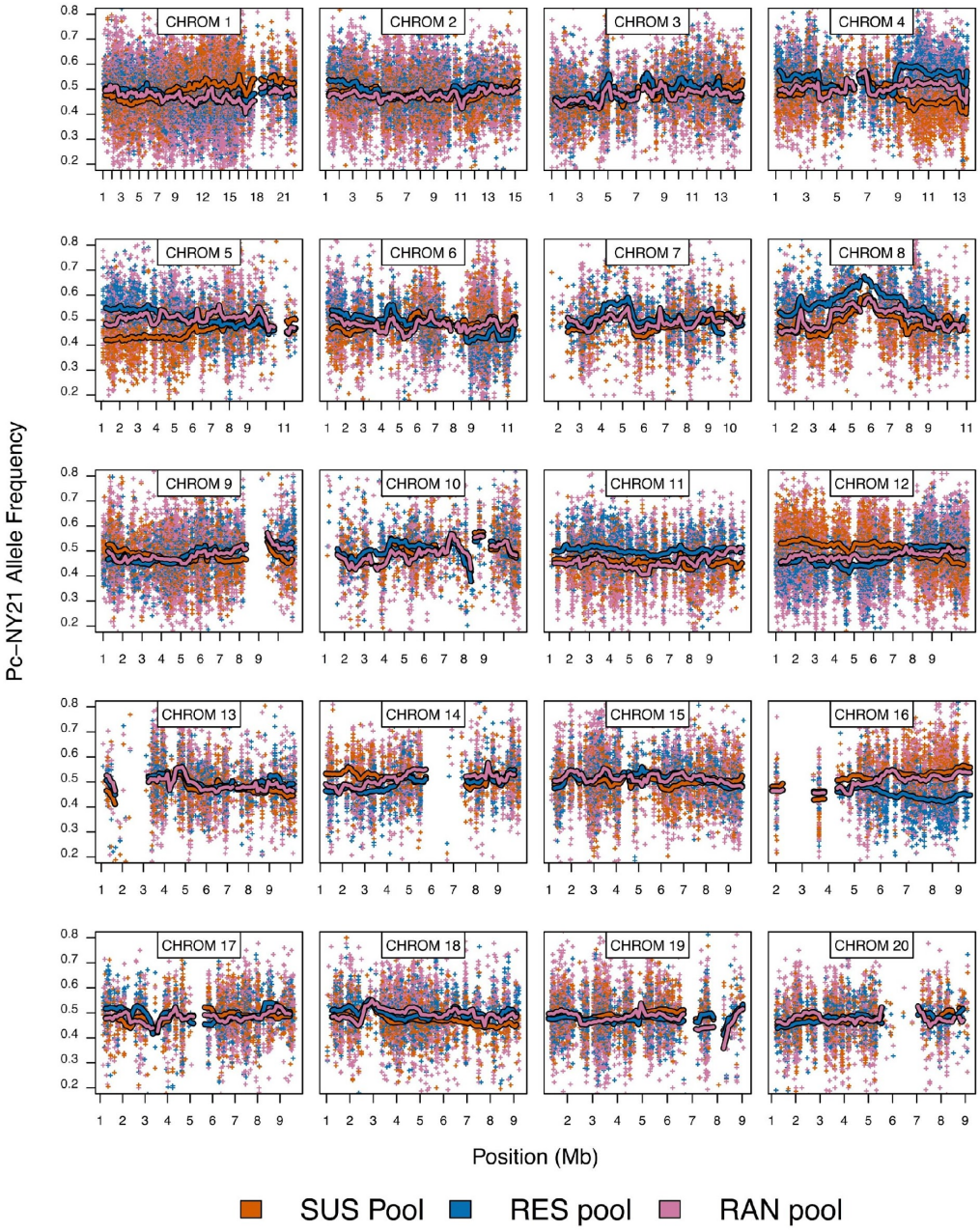

Figure S1.2: Pc-NY21 allele frequencies in Rep 2 susceptible (SUS), resistant (RES), and random (RAN) pools across all 20 chromosomes. Plus signs are individual SNP allele frequencies and lines are smoothed means calculated in 500 Kb sliding windows with a 100 Kb increment. For simplicity of visualization, only a random subset of 25% of SNPs are shown. Smoothed means are not calculated in any window featuring fewer than 30 SNPs.

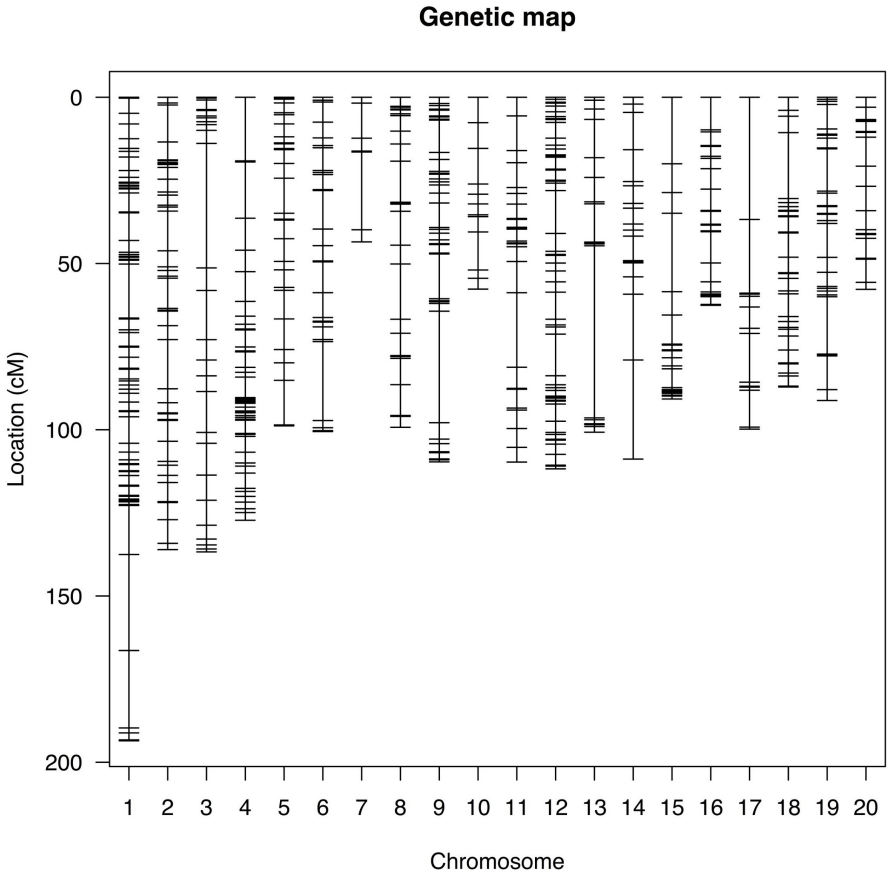

Figure S1.3: Position of 605 SNP markers on 20 linkage groups of a genetic map created using 181 F_2 individuals.

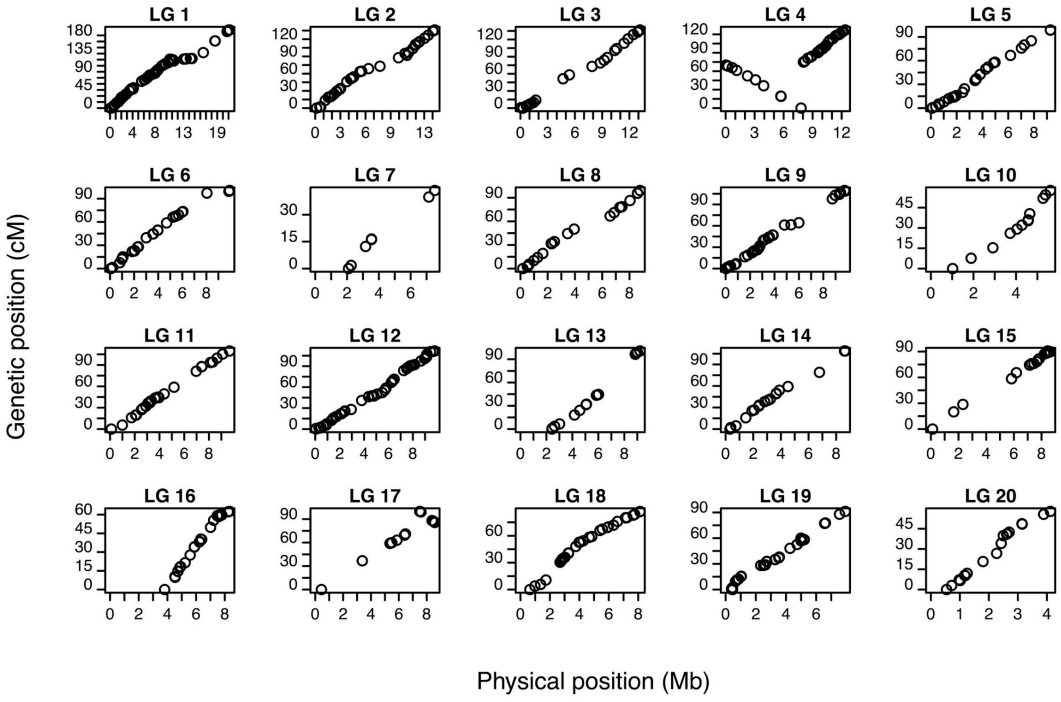

Figure S1.4: Physical position (Mb) vs genetic position (cM) of 605 SNP markers placed on the genetic map. Markers assigned to a different linkage group on the genetic map compared to their location in the reference genome are not shown.

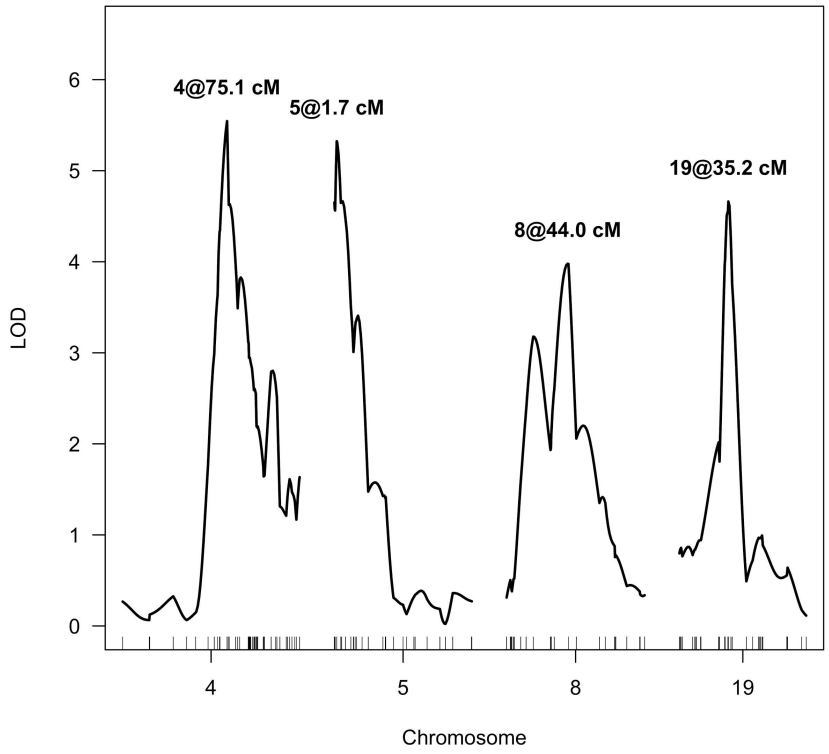

Figure S1.5: Multiple QTL mapping LOD scores using rAUDPC estimates for 176 $F_{2:3}$ families and a genetic map with 605 SNPs called on their F_2 parents. Only linkage groups where a QTL was identified are shown.

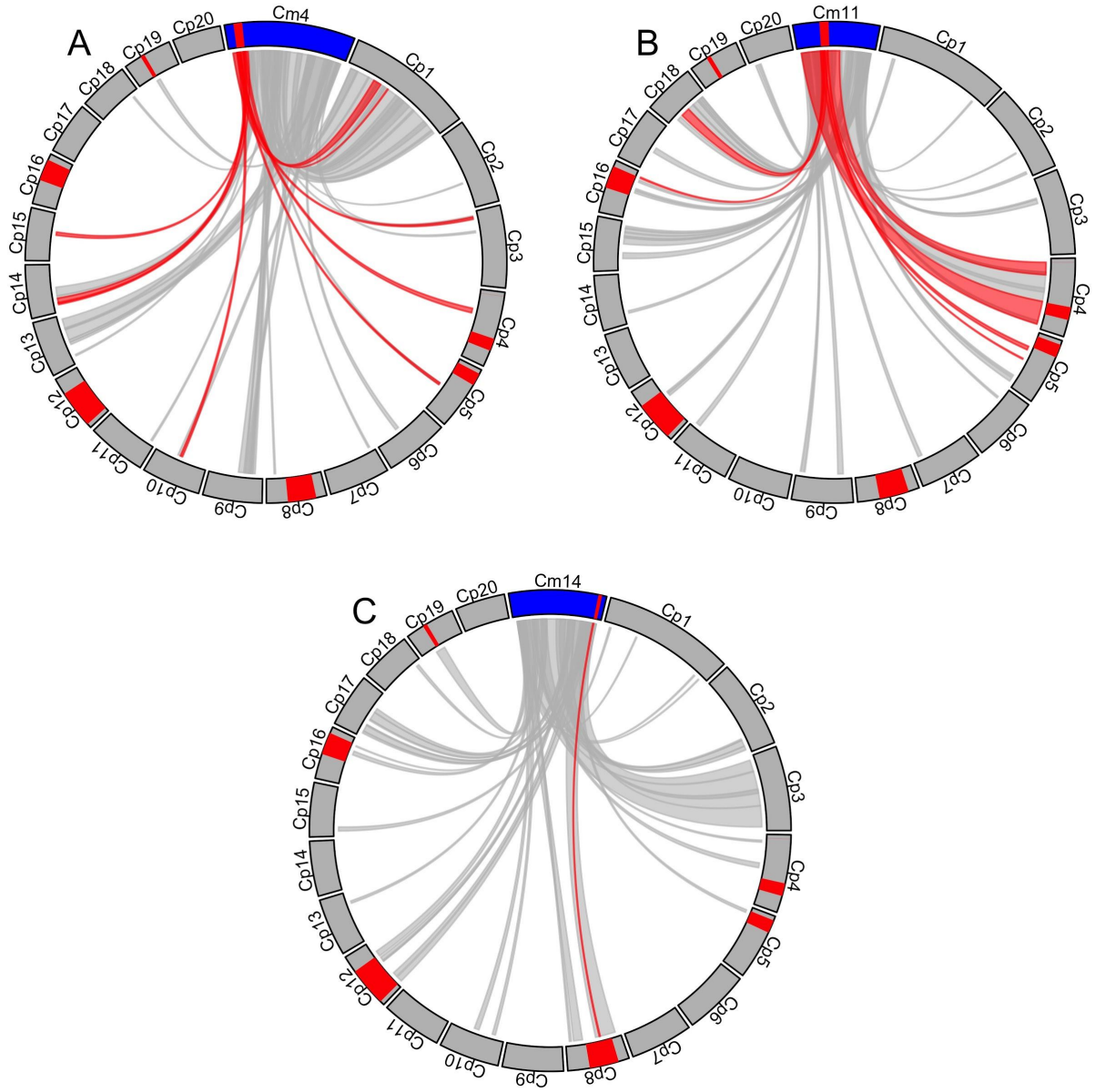

Figure S1.6. Syntenic blocks shared between *C. moschata* chromosomes 4, 11, and 14 (A-C, respectively) and *C. pepo*. QTL regions identified in *C. moschata* by Ramos et al. (2020) and in *C. pepo* in this publication are colored in red. Chords between syntenic blocks where the *C. moschata* counterpart overlaps a QTL are colored in red. Only syntenic blocks with a score >400 as reported by MCScanX are shown.

CHAPTER 2

GENOME-WIDE ASSOCIATION STUDY IN NEW YORK *PHYTOPHTHORA CAPSICI* ISOLATES REVEALS LOCI INVOLVED IN MATING TYPE AND MEFENOXAM SENSITIVITY[2]

ABSTRACT

Phytophthora capsici is a soilborne oomycete plant pathogen that causes severe vegetable crop losses in New York (NY) State and worldwide. This pathogen is difficult to manage, in part due to its production of long-lasting sexual spores and its tendency to quickly evolve fungicide resistance. We single-nucleotide polymorphism (SNP) genotyped 252 *P. capsici* isolates, predominantly from NY, in order to conduct a genome-wide association study for mating type and mefenoxam sensitivity. The population structure and extent of chromosomal copy number variation in this collection of isolates were also characterized. Population structure analyses showed isolates largely clustered by the field site where they were collected, with values of F_{ST} between pairs of fields ranging from 0.10 to 0.31. Thirty-three isolates were putative aneuploids, demonstrating evidence for having up to four linkage groups present in more than two copies, and an additional two isolates appeared to be genome-wide triploids. Mating type was mapped to a region on scaffold 4, consistent with previous findings, and mefenoxam sensitivity was associated with several SNP markers at a novel locus on scaffold 62. We identified several candidate genes for mefenoxam sensitivity, including a homolog of yeast ribosome synthesis factor Rrp5, but failed to locate near the scaffold 62 locus any subunits of RNA Polymerase I,

[2] Vogel, G., Gore, M.A., and Smart, C.D. 2020. Genome-wide association study in New York *Phytophthora capsici* isolates reveals loci involved in mating type and mefenoxam sensitivity. Phytopathology. https://doi.org/10.1094/PHYTO-04-20-0112-FI.

the hypothesized target site of phenylamide fungicides in oomycetes. This work expands our knowledge of the population biology of *P. capsici* and provides a foundation for functional validation of candidate genes associated with epidemiologically important phenotypes.

INTRODUCTION

Phytophthora capsici is a soilborne oomycete plant pathogen that causes a disease known as Phytophthora blight on several economically important vegetable crops, including pepper, squash, and pumpkin. Phytophthora blight results in serious crop losses via both root and crown rot, which can lead to sudden irreversible wilting of the plant, and fruit rot, which manifests as rapidly expanding sunken lesions featuring a distinctive white sporulation (Granke et al. 2012). Vegetable growers have found *P. capsici* highly difficult to control for several reasons: it produces spores that can remain dormant in the soil for many years (Lamour and Hausbeck 2003, Carlson et al. 2017), rapidly reproduces asexually under suitable environmental conditions (Hausbeck and Lamour 2004), and tends to quickly evolve insensitivity to once effective fungicides (Parra and Ristaino 2001; Kousik and Keinath 2008).

Previous population genetic surveys of *P. capsici* isolates, both in Michigan (Lamour and Hausbeck 2001) and New York (NY; Dunn et al. 2010), have shown that different agricultural fields feature distinct, sexually recombining pathogen populations with limited gene flow between them. These results are consistent with the biology of *P. capsici*. Asexual sporangia and zoospores, both short-lived structures that cannot survive desiccation, are limited in their ability to spread quickly, as they are dispersed in water but not wind (Schlub 1983; Bowers et al. 1990; Granke et al. 2009). Sexual oospores, on the other hand, possess thick walls that allow them to survive harsh environmental conditions. Oospores can overwinter in temperate climates and

remain viable in the soil for years (Bowers et al. 1990; Lamour and Hausbeck 2003; Babadoost and Pavon 2013; Carlson et al. 2017).

As a heterothallic species, *P. capsici* only reproduces sexually when isolates of opposite mating type are in contact (Erwin and Ribeiro 1998). The mating types of *Phytophthora* species, referred to as A1 and A2, do not signify the production of particular sex organs, as isolates of either mating type are hermaphroditic and thus capable of producing both antheridia and oogonia, the male and female reproductive organs, respectively (Ashby 1929; Judelson 1997). Rather, each mating type secretes a specific hormone (α_1 or α_2) that induces sexual reproduction in isolates of the opposite mating type (Ko 1978). Both mating type hormones have been isolated and characterized (Qi et al. 2005; Ojika et al. 2011) and mapping experiments using experimental crosses have identified a single locus controlling mating type in *P. capsici, P. infestans*, and *P. parasitica* (Fabritius and Judelson 1997; Lamour et al. 2012; Carlson et al. 2017). Recently, a genome-wide association study was conducted to identify the mating type locus of another oomycete, the grapevine downy mildew pathogen *Plasmopara viticola* (Dussert et al. 2020). Researchers working on different oomycete pathogens have hypothesized that mating type inheritance is analogous to sex determination in an XY system, where, in the case of *P. capsici* for example, A1 isolates are homozygous (i.e., XX) and A2 isolates heterozygous (i.e., XY) at the mating type locus (Fabritius and Judelson 1997; Carlson et al. 2017; Dussert et al. 2020). Nevertheless, the exact gene or genes conferring mating type remain unknown in all oomycetes.

Once a sexual population of *P. capsici* is established in a field, the eradication of the pathogen is highly unlikely and control strategies must be implemented to manage disease in future years. In addition to cultural practices designed to promote soil drainage and thereby deny

a suitable environment for *P. capsici*, fungicides are one of the most effective means that growers rely on to control Phytophthora blight (Hausbeck and Lamour 2004). Phenylamide fungicides in particular, first the racemic metalaxyl and later its active enantiomer mefenoxam, have been used extensively since the 1970s due to their systemic activity in plants and high toxicity against many oomycete species via inhibition of ribosomal RNA (rRNA) synthesis (Davidse et al. 1983; Wollgiehn et al. 1984; Erwin and Ribeiro 1998). Shortly after these fungicides were first deployed, however, resistance emerged in populations of several important oomycete plant pathogens (Gisi and Sierotzki 2008). Isolates of *P. capsici* insensitive to mefenoxam were first reported in 1997 in New Jersey, North Carolina, and Michigan (Lamour and Hausbeck 2000; Parra and Ristaino 2001), and have since been found in many additional states, including NY (Keinath 2007; Wang et al. 2009, Dunn et al. 2010). As with mating type, the genes involved in mefenoxam insensitivity in oomycetes are largely unknown.

Once thought by many researchers to be haploid in their vegetative state, as are true fungi, cytological evidence in the 1960s and 70s established oomycetes as diploid with meiosis occurring in the gametangia immediately prior to fertilization of the oogonium (Sansome 1961; Sansome and Brasiere 1973). In recent years, data generated by next-generation sequencing technologies have been increasingly used not only for traditional population genetic analyses, but also for estimating ploidy levels of samples (Farrer et al. 2013; Zhu et al. 2016). As a result, researchers have identified polyploid *Phytophthora* isolates with three or more copies of each chromosome (Yoshida et al. 2013), as well as aneuploid individuals with a high degree of chromosomal copy number variation within a single genome (Barchenger et al. 2017; Shrestha et al. 2017). Nevertheless, there is still little known about the extent and distribution of chromosomal copy number aberrations within *P. capsici* field populations.

Since 2006, our lab has collected hundreds of isolates of *P. capsici* from vegetable-growing regions of NY State. We set out to leverage this collection in combination with isolates from an additional six states to improve our understanding of patterns of genomic variation in *P. capsici* and to discover loci associated with traits of epidemiological importance. To accomplish this, we genotyped over two hundred isolates from our culture collection with genotyping-by-sequencing (GBS) and assayed them for their mating type and mefenoxam sensitivity. The specific objectives of this study were to i) characterize the pathogen population structure in NY and compare findings with expectations based on previous inferences about pathogen dispersal and survival (Dunn et al. 2010), ii) determine the extent of chromosomal copy number variation among isolates of *P. capsici* collected from the field, and iii) conduct a genome-wide association study (GWAS) to identify loci involved in the genetic control of mating type and mefenoxam sensitivity.

MATERIALS AND METHODS

Isolate collection, phenotypic assays, and DNA extraction. Isolates described in this study were either recently collected in NY in 2017 or 2018 (*n*=157), obtained from stored cultures isolated from NY sites prior to 2017 (*n*=85), or received from out-of-state collaborators (*n*=10; Table 2.1). NY pathogen samples from 2017 and 2018 were isolated from plant parts of several different species with Phytophthora blight symptoms collected at farms and one supermarket (Table S2.1). Small pieces of surface-disinfected tissue were plated on PARPH medium (Jeffers and Martin 1986) except for samples with evident sporulation, in which case sporangia were directly transferred to the surface of PARPH Petri plates. Plates were then incubated at room temperature for one to two weeks before transferring a plug from the edge of

the growing colonies to new PARPH plates. These plates were sealed with Parafilm (Bemis, Neenah, WI, USA) and stored at room temperature in the dark until used to transfer plugs for isolation of single-zoospore cultures.

New York isolates collected prior to 2017, including nine described in previous publications (Dunn et al. 2010; Parada-Rojas and Quesada-Ocampo 2018; Table S2.1), were obtained from long-term storage tubes containing sterile water and 3-4 hemp seeds. Cultures of these isolates were started by plating a sample of the contents of the storage tubes onto PARPH plates. Cultures of non-NY isolates, including one previously described (12889; Foster and Hausbeck 2009), were received from collaborators and transferred to PARPH plates. All isolates in this study were verified as *P. capsici* by performing PCR with species-specific primers (Dunn et al., 2010) and confirming the presence of a band of the correct size via gel electrophoresis.

Single-zoospore isolates were obtained using a protocol similar to that described by Lamour and Hausbeck (2000). Isolates were induced to sporulate by plating on unclarified V8 agar and incubating under 14h daily fluorescent lighting for 7-14 days. Sporangia were then transferred with a sterile pipette tip to 1.5 mL microcentrifuge tubes containing 1 mL sterile water and incubated at room temperature for 45 min to promote zoospore release. Zoospore suspensions were serially diluted and 100 µl aliquots of 1:10, 1:100, and 1:1000 dilutions were spread-plated on water agar plates. After incubating at room temperature for approximately 16h, a stereo microscope was used to identify single germinating zoospores and transfer them to PARPH plates. Single-zoospore cultures were obtained for all but six isolates, which either featured poor colony re-growth (IMK328, FL29, 568OH) or inadvertently had DNA extracted prior to single-zoosporing (1070_3, 14_51, 2014_21).

Mating type and mefenoxam sensitivity assays were performed as described previously

(Dunn et al. 2010). Briefly, for mating type determination, isolates were co-cultured on unclarified V8 agar plates with NY isolates of known mating type (A1: 0664-1 and A2: 06180-4) (Dunn et al. 2014). After incubating plates in the dark for 7-14 days, mating type was ascertained by confirming the presence or absence of oospores in the media using a stereo microscope. For a subset of isolates, consisting of 45 of the 2013 Ontario #1 isolates and 7 isolates from 2006-07 previously characterized by Dunn et al. (2010), mating type was determined at two distinct time points, both prior to entering and after removal from long term storage. When discordant, the mating type reported and used for analysis was the mating type determined at the time point tissue was collected for DNA extraction (corresponding to prior to long term storage for the 2013 Ontario #1 isolates and after removal from long term storage for the 2006-07 isolates).

Mefenoxam sensitivity was determined by transferring 10mm plugs from the edge of growing colonies on PARPH to unclarified V8 media amended with 5 μg/ml or 100 μg/ml mefenoxam (Ridomil Gold EC; Syngenta AG, Basel, Switzerland). After incubating plates in the dark for 3 days, colony diameters were measured and used to calculate percentage relative growth (RG) compared to control plates without mefenoxam added. These assays were repeated twice for each isolate and mean RG values are reported. In order to report a single descriptive summary statistic per isolate, isolates were classified as sensitive (<40% RG on 5 μg/ml mefenoxam), intermediately sensitive (>40% RG on 5 μg/ml mefenoxam but <40% RG on 100 μg /ml mefenoxam), or resistant (>40% RG on 100 μg/ml mefenoxam) as in Silvar et al. (2006).

Mycelia collection and DNA extraction were performed as previously described (Carlson et al. 2017). Plates containing 10% clarified V8 broth were inoculated with three plugs from the edge of an actively growing culture and incubated in the dark for 4-5 days. Approximately 100 mg of mycelia was then vacuum-filtered, collected into 2 ml microcentrifuge tubes containing

two zinc-plated steel BBs (Daisy, Rogers, Arkansas, USA), and stored at -80°C prior to DNA extraction. DNA was extracted using the DNeasy Plant Mini Kit (Qiagen, Valencia, CA, USA) according to the manufacturer's instructions, except a TissueLyser (Qiagen, Valencia, CA, USA) was used to disrupt mycelia and DNA was eluted into ultrapure water instead of AE buffer.

Genotyping, SNP quality control, and clone correction. DNA samples were sent to one of two facilities to prepare and sequence 96-plex GBS libraries digested with *Ape*KI, which had been previously determined to be a suitable restriction enzyme for simultaneously discovering and scoring genome-wide SNPs in *P. capsici*. Libraries for samples from the Ontario #1 field site from 2013 were prepared in 2015 at the Institute for Genomic Diversity at Cornell University and sequenced on an Illumina Hiseq2500 generating single-end 100 bp reads. Libraries for remaining samples were prepared in 2019 at the University of Wisconsin-Madison Biotechnology Center and sequenced on an Illumina NovaSeq6000 generating paired-end 150 bp reads. Replicate samples of isolate 0664-1 were included in order to assess technical variation in genotype calls between GBS plates.

Genotypes were called with the TASSEL GBSv2 pipeline (Glaubitz et al. 2014) using default parameters. To ensure that the same fragments were sequenced for all samples, only the forward reads were used for samples that were paired-end sequenced. Alignment of unique tags to the *P. capsici* reference genome (Lamour et al. 2012) and mitochondrial genome (provided by Martin, F., USDA-ARS) assemblies was performed with the Burrows-Wheeler algorithm bwa-aln (bwa version 0.7.17) with default parameters (Li and Durbin, 2009). Genotype calls were output in variant call format (VCF) and filtered initially for several criteria using VCFtools version 0.1.17 (Danecek et al. 2011). Indels and SNPs with >2 alleles were removed, as were individuals with greater than 60% missing data. SNPs that met the following criteria were then

retained: 1) mean read depth >8 and <50; 2) >50% call rate; and 3) minor allele frequency (MAF) >0.01. Genotypes supported by fewer than 5 reads were set to missing. This SNP set was used for clonal group identification and determination of chromosomal copy numbers.

To identify clonal groups, pairwise identity-by-state (IBS), defined as the proportion of alleles shared at non-missing sites, was calculated among all isolates. We selected 95% as a threshold for declaring two isolates as clones, in order to account for an expected genotyping error rate of ~3% (Carlson et al. 2017), which was consistent with the error rate between technical replicates included among our samples. For all groups of isolates with pairwise IBS that surpassed this threshold, the isolate with the least missing data was retained to create a clone-corrected dataset, which was then further filtered to retain only SNPs with MAF >0.05 and call rate >80%. SNPs that were heterozygous in >80% of isolates were also removed, in order to remove likely artifacts of alignment errors. This clone-corrected SNP set was used for all population genetics and GWAS analyses.

All analyses, unless otherwise specified, were performed using custom R scripts (R Core Team 2019; https://github.com/gmv23/pcap-gwas). Deviations from a 1:1 mating type ratio among the clone-corrected isolate set for each site were tested using an exact binomial test with the R function *binom.test* at α=0.05. The percentage of variation in RG on mefenoxam-amended media attributed to differences between clonal lineages was calculated from the variance components of a mixed linear model predicting RG, with a random effect for clonal lineage and a fixed intercept term. Models were fit using the *mixed.solve* function in the R package rrBLUP (Endelman 2011).

Population structure. A principal component analysis (PCA) was conducted using the pcaMethods R package (Stacklies et al. 2007) on the unit-variance scaled and centered genotype

matrix, and using the *nipals* method to account for missing data. The neighbor-joining tree was created in SplitsTree version 4.14.8 (Huson 1998), using the uncorrected "P" method to estimate the distance matrix, and plotted using the R package ape (Paradis et al. 2004). Values of pairwise F_{ST} between fields, as measured by Weir and Cockerham's estimator of F_{ST} (Weir and Cockerham 1984), were calculated with the R package StAMPP (Pembleton et al. 2013).

Chromosomal copy number determination. Because there is currently no chromosome-level genome sequence for *P. capsici*, we assigned a total of 97,145 SNPs to the 18 linkage groups of the genetic map provided in Lamour et al. (2012). We then used allele balances at heterozygous sites, defined as the number of reads of the major allele divided by the total number of reads, to identify putative linkage groups with more than 2 copies present in a given isolate, following methods similar to those of Farrer et al. (2013). To minimize variation in allele balances caused by low read depths, we only calculated allele balances at sites supported by 12 reads. For each isolate, SNP allele balances on linkage groups with 30 or more heterozygous SNPs were divided into bins of 47-53% (as expected for a chromosome with 2 copies) and 30-36% or 63-69% (as expected for a chromosome with 3 copies). We did not attempt to explicitly identify linkage groups that were present in four or more copies because of the ambiguity in expected allele balances (for example, an allele balance of 0.50 could indicate a copy number of either 2 or 4). Bootstrap analysis was performed 1000 times over sites and linkage groups were assigned copy number designations if they had over 95% bootstrap support for featuring predominantly disomic or trisomic allele balances.

Read depth variation across all sites was then used to confirm linkage group copy number designations for putative aneuploid isolates. For each of these isolates, the number of sites on each linkage group was balanced by downsampling to the number of sites on the linkage group

featuring the fewest non-missing SNPs. We then performed an ANOVA to determine if site read depth varied across linkage groups and Tukey's HSD to conduct pairwise comparisons across all linkage groups for a given isolate. Putative trisomic linkage groups only retained their trisomic designation if they featured an average read depth significantly different from all putative disomic linkage groups for that isolate at a family-wide confidence level of 0.05. Fisher's exact test, using the R function *fisher.test*, was performed to test for significant enrichment for both trisomy across linkage groups and aneuploidy across clonal lineages.

Linkage disequilibrium calculation and genome-wide association study. Pairwise linkage disequilibrium (LD), as measured by r^2 (Hill and Robertson 1968), was estimated between all SNPs within 500 kb of each other using the software program PopLDDecay version 3.40 (Zhang et al. 2019). Because the RG phenotype on both 5 μg/ml and 100 μg/ml mefenoxam-amended media had a non-normal distribution, mefenoxam sensitivity was converted into a binary trait for the purpose of a better fitting model in GWAS (i.e. improved control of Type I error rate). A relatively low threshold, >10% RG on 5 μg/ml mefenoxam, was used to classify an isolate as resistant, in order to separate isolates that were almost entirely unable to grow on mefenoxam-amended media from those that grew to any extent. We did not use the RG on 100 μg/ml mefenoxam phenotype as it was highly correlated ($r = 0.95$) with RG on 5 μg/ml mefenoxam.

A genome-wide association study for each phenotype was conducted using logistic regression models implemented in the R package GENESIS (Gogarten et al. 2019). All missing genotype calls were conservatively imputed with the mean value prior to conducting association tests. The Akaike information criterion (Sakamoto et al. 1986) was used to compare the fit of different generalized linear mixed models that included up to four PCs as covariates (to control

for population structure) and a random polygenic isolate effect with a covariance structure defined by a kinship matrix (to control for unequal relatedness). The kinship matrix was estimated from the genotypic data using the *A.mat* function in rrBLUP (Endelman 2011). In the mating type GWAS, we fit a generalized linear model for each SNP that only included a fixed intercept term, as PCs were not selected for inclusion in the model and the random isolate effect (i.e., kinship) was negligible. For mefenoxam sensitivity, SNPs were tested for association in a generalized mixed linear model that included an intercept term, the first three PCs retained as fixed effects, and a random isolate effect. SNPs with a Bonferonni-adjusted *P*-value <0.05 were considered significant. Manhattan and Q-Q plots were created using the R package qqman (Turner 2014).

We used protein-to-protein blast (blastp) to find reciprocal best hits between *P. capsici* and *Plasmopara viticola*, with the aim of identifying presumable homologs between genes within the *P. capsici* mating type region reported in this study and that reported by Dussert et al. (2020) for *P. viticola*. Although Dussert et al. list a total of 40 genes in the *P. viticola* mating type region, we only used the 38 that are annotated in the published *P. viticola* reference genome (Dussert et al. 2019). The complete set of predicted protein sequences of the two oomycete species were aligned against each other using BLASTP+ with default parameters, including a minimum E-value of 10 to save hits (Camacho et al. 2009). A custom python script was then used to identify reciprocal best hits on the basis of E-value.

Data availability. Fastq files containing the raw, demultiplexed GBS reads were deposited in the National Center of Biotechnology Information Sequence Read Archive (BioProject accession number PRJNA616021). Metadata on all isolates, including collection years and locations as well as mating type and mefenoxam sensitivity phenotypes, are provided

in Table S2.1. Filtered VCF files for both the non-clone corrected and clone corrected isolate sets are available at CyVerse (http://datacommons.cyverse.org/browse/iplant/home/shared/GoreLab/dataFromPubs/Vogel_PcapGWAS_2020). Scripts used for analysis are available on Github (https://github.com/gmv23/pcap-gwas).

RESULTS

Isolate collection. Between 2007 and 2018, 242 axenic *P. capsici* cultures were isolated from symptomatic plant samples collected at 22 field sites and a supermarket (Tompkins #1) in NY State (Figure 2.1). Geographic areas were represented disproportionately and were sampled in different years, with almost all of the Capital District isolates, for example, collected in 2007. The number of isolates collected from each site also varied considerably, with eleven sites each contributing 1 isolate and another site, Ontario #1, contributing 141 isolates (Table 2.1). Ontario #1 was the only site where samples were collected in two different years, with 70 isolates sampled in 2013 and 71 sampled in 2017.

Isolates were found to belong to both mating types, with a total of 115 A1 and 127 A2 isolates collected (Table 2.1). A subset of the isolates were assayed for mating type twice, both shortly after collection and after re-culturing from long-term storage tubes, up to 13 years later. Of the 52 isolates assayed twice, 13 showed evidence of a mating type switch (Table S2.1). In all 13 of these cases, the mating type was A1 prior to storage and A2 upon re-culture.

Isolates that were intermediately sensitive or resistant to mefenoxam were identified in 12 of the 23 sites across the state (Table 2.1). Among the seven of these sites where multiple isolates were collected, Erie #2 featured the greatest proportion of intermediately sensitive or resistant isolates (94%).

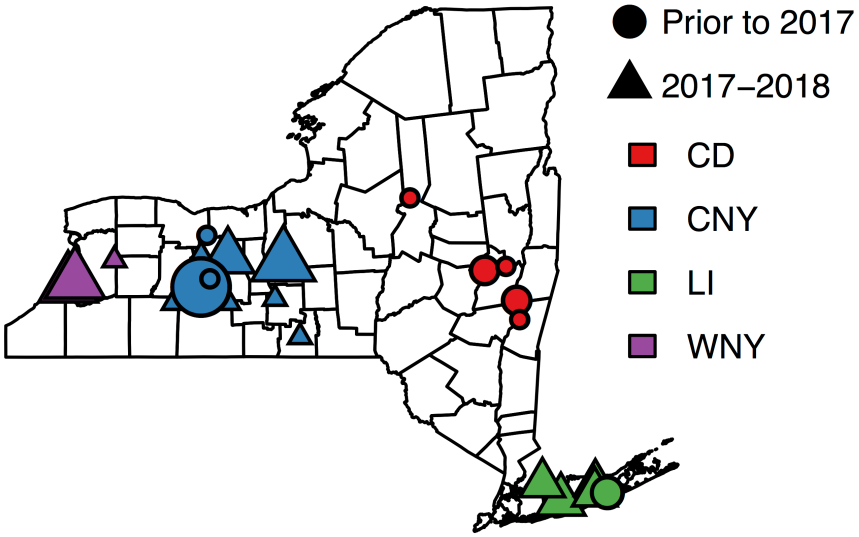

Figure 2.1: Map of NY sites where isolates were sampled. Points were randomly assigned a location within the counties where sites were located, with point size indicative of the number of isolates collected per site. One site in Ontario county was sampled twice, in both 2013 and 2017. CD = Capital District, CNY = Central New York, LI = Long Island, WNY = Western New York.

Table 2.1: Number of isolates, unique genotypes, and counts of each mating type and mefenoxam sensitivity class per site.

				Mating type counts		Mefenoxam sensitivity counts			
Field	Region[a]	Year	Isolates	A1	A2	S[b]	IS[b]	R[b]	Unique Genotypes
Columbia #1	CD	2014	1	0	1	1	0	0	1
Herkimer #1	CD	2007	1	1	0	0	1	0	1
Rensselaer #1	CD	2007	2	1	1	1	0	1	2
Schenectady #1	CD	2007	2	2	0	1	1	0	2
Schenectady #2	CD	2007	1	1	0	0	0	1	1
Cayuga #1	CNY	2017	24	9	15	20	3	1	10
Monroe #1	CNY	2006	1	1	0	1	0	0	1
Ontario #1	CNY	2013	70	34	36	44[d]	1[d]	0[d]	17

Ontario #1	CNY	2017	71	34	37	65	4	2	42
Ontario #2	CNY	2018	9	0	9	8	1	0	2
Ontario #3	CNY	2006	1	0	1	1	0	0	1
Tioga #1	CNY	2018	1	0	1	1	0	0	1
Tompkins #1	CNY	2018	1	1	0	1	0	0	1
Suffolk #1	LI	2018	6	1	5	6	0	0	6
Suffolk #2	LI	2018	4	1	3	4	0	0	2
Suffolk #3	LI	2018	4	2	2	1	0	3	2
Suffolk #4	LI	2018	3	3	0	2	0	1	3
Suffolk #5	LI	2007	3	1	2	3	0	0	3
Erie #1	WNY	2017	17	10	7	9	1	7	8
Erie #2	WNY	2017	16	10	6	1	6	9	9

Erie #3	WNY	2018	1	1	0	0	0	1	1
Non NY[c]	NA	NA	10	5	5	8	1	1	10
NY unknown	NA	NA	3	2	1	3	0	0	3
Total	NA	NA	252	120	132	181	19	27	129

[a] CD = Capital District, CNY = Central New York, LI = Long Island, WNY = Western New York.

[b] S = mefenoxam sensitive, IS = mefenoxam intermediately sensitive, R = mefenoxam resistant.

[c] Non-NY isolates were received from California (*n*=2), Florida (*n*=1), Michigan (*n*=1), New Mexico (*n*=1), Ohio (*n*=1), and South Carolina (*n*=4).

[d] Mefenoxam sensitivity counts for Ontario #1 isolates in 2013 are incomplete due to the loss of some cultures in storage prior to performing sensitivity assays.

Genotyping and clonality. The 242 NY isolates and 10 isolates from other states (CA, FL, MI, NM, OH, and SC) were genotyped using GBS. From a total of 363,044 SNPs discovered, initial filtering criteria resulted in a dataset of 107,569 filtered SNPs called on 245 isolates, after removing 7 samples with high missing data. This SNP set, featuring a mean SNP read depth with a median of 17.4 calculated across sites and a median of 18.9 calculated across samples, was used to calculate pairwise IBS among isolates in order to identify isolates clonally derived from a common ancestor. Whereas the median IBS between all pairs of samples was 0.741, pairwise IBS between technical replicates of isolate 0664-1 (including samples sequenced by different facilities) ranged between 0.980 and 0.987. To account for genotyping error, we therefore used a 95% IBS threshold for declaring two isolates as clones. The 245 isolates were resolved into 129 unique genotypes (Table 2.1), 41 of which featured multiple isolates and are hereafter referred to as clonal lineages. A total of 157 isolates belonged to one of these clonal lineages, with a median clonal lineage size of three isolates, and the largest clonal lineage consisting of 17 isolates from Ontario #1 in 2013. The proportion of isolates that were genetically unique in each site varied, with Ontario #1 in 2013 (17 unique genotypes out of 70 isolates) and Ontario #2 in 2018 (2 out of 9) featuring the least genotypically diverse samples.

Each clonal lineage was private to a particular site, and in the case of Ontario #1, none of the clonal lineages identified in 2013 appeared again in 2017. Isolates belonging to the same clonal lineage were largely consistent in terms of mating type and mefenoxam sensitivity. Out of the 41 clonal lineages, only one – consisting of one A1 and two A2 isolates from Ontario #1 in 2013 – featured isolates of opposite mating type. Seven clonal lineages contained isolates with discordant mefenoxam sensitivity classifications, but these only featured a mixture of resistant and intermediately sensitive isolates (4 clonal lineages) or intermediately sensitive and sensitive

isolates (3 clonal lineages). Among all isolates belonging to one of the 41 clonal lineages, 96.1% and 91.7% of the variation in RG on 5 μg/ml and 100 μg/ml mefenoxam, respectively, was attributed to differences between lineages.

A representative isolate was sampled from each clonal lineage to generate a clone-corrected data set consisting of 129 isolates. Using the clone-corrected isolate set, none of the site-years featured a ratio of mating types that differed significantly from 1:1, consistent with the neutral expectation for a sexually reproducing pathogen.

Population structure. In order to visualize genetic relationships among the isolates, we conducted a PCA and created an unrooted NJ tree using a high-confidence set of 64,124 SNPs (Figure 2.2). Principal component 1, explaining 15.61% of the variance in the SNP genotype data, mainly separated the 59 isolates from Ontario #1 from the remaining isolates (Figure 2.2A). Principal component 2 accounted for 4.5% of the variance explained and differentiated Western NY isolates from the 10 isolates sampled from Cayuga #1.

In the NJ tree, isolates from the same site were largely, but not exclusively, monophyletic (Figure 2.2B). Exceptions included isolates from 3 of the 5 Long Island sites, as well as the Erie #1 and Suffolk #5 populations, each of which featured a single isolate appearing in a distinct clade. The outlier isolate from Erie #1, collected in 2017, appeared closely related to an isolate sampled from a distinct site in Erie county in 2018 (Erie #3). Sites from the same region grouped together in several cases, such as with Erie #1 and Erie #2 in Western NY and 4 of the 5 Long Island sites. However, isolates from different sites in the Capital District did not cluster together on the tree and Tompkins #1 was clearly separated from the remaining Central NY sites. Non-NY isolates were sorted into several different clades, with even isolates from the same state, such as the 4 isolates from South Carolina, clustering separately. In both the PCA and the NJ tree, no

differentiation was observed between the 2013 and 2017 populations from Ontario #1.

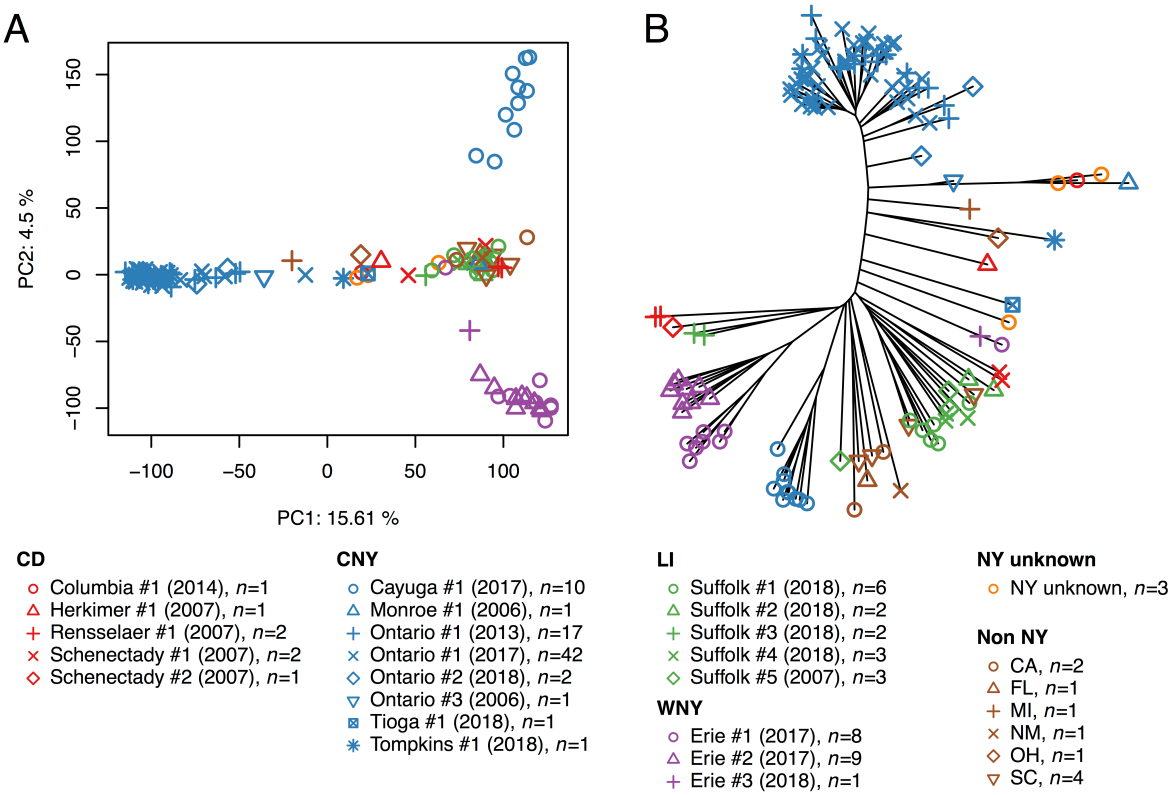

Figure 2.2: Population structure of the clone-corrected isolate set. A) Principal component analysis plot showing principal components 1 and 2 calculated from 64,630 SNPs scored on 129 genetically unique isolates. B) Unrooted neighbor-joining tree of the 129 isolates. In both plots, point color reflects geographic region and point shape reflects site within geographic region.

Table 2.2. Estimates of Weir and Cockerham's F_{ST} between sites featuring more than 5 isolates after clone-correction.

	Number isolates	Cayuga #1 (2017)	Erie #1 (2017)	Erie #2 (2017)	Ontario #1 (2013, 2017)[a]	Suffolk #1 (2018)
Cayuga #1 (2017)	10	-	0.20	0.22	0.31	0.18
Erie #1 (2017)	8	-	-	0.10	0.30	0.14
Erie #2 (2017)	9	-	-	-	0.30	0.16
Ontario #1 (2013, 2017)	59	-	-	-	-	0.26
Suffolk #1 (2018)	6	-	-	-	-	-

[a] Ontario #1 populations from 2013 and 2017 were collapsed into one population.

To quantify differentiation between individual sites, we calculated pairwise F_{ST} for the 5 fields featuring >5 isolates after clone-correction (Table 2.2). Ontario #1 isolates from 2013 and 2017 were considered jointly as one population due to their genetic similarity

(F_{ST}=0.001). Values of F_{ST} ranged from a moderate differentiation of 0.10 (Erie #1 vs Erie #2) to a very strong differentiation of 0.31 (Cayuga #1 vs Ontario #1).

Chromosomal copy number variation. Allele balances at heterozygous SNPs and intra-genome variation in read depth were used to infer copy numbers for the 18 linkage groups in each of the 245 isolates with filtered genotype data (Figure 2.3; Table S2.2). For a majority of the isolates (n = 222), we were unable to assign a copy number to certain linkage groups because they either contained too few heterozygous markers or showed ambiguous signal in their allele balances or read depths (Figure S2.1). This noisy signal was likely caused, for the most part, by low average read depth, since individual mean read depth and the number of linkage groups assigned a copy number per isolate were highly correlated (r = 0.79). Across isolates, the median number of linkage groups assigned a copy number was 13.

In total, 31 isolates were aneuploid, having between 1 to 4 trisomic linkage groups. Linkage groups featuring allele balances suggestive of trisomy mostly featured higher read depths than putative diploid linkage groups, except for four isolates (FL29, 17EH33C, 1070_3, and A2_6_1) where trisomic linkage groups featured lower than average read depth, suggesting a possible tetraploid or higher base ploidy level. Two additional isolates, 17EH20A and 17EH21C, were triploid for all of their linkage groups whose copy number we could determine (13 and 16 linkage groups for 17EH20A and 17EH21C, respectively). Although these two isolates were the exclusive representatives of a particular clonal lineage, patterns of aneuploidy were not consistent within clonal lineages for the remainder of the isolates. In fact, among the 10 clonal lineages featuring at least one aneuploid isolate, all trisomic linkage groups were private to individual isolates. There was no significant enrichment for aneuploidy in any of these 10 clonal lineages compared to the rest (Fisher's exact test P-value=0.35).

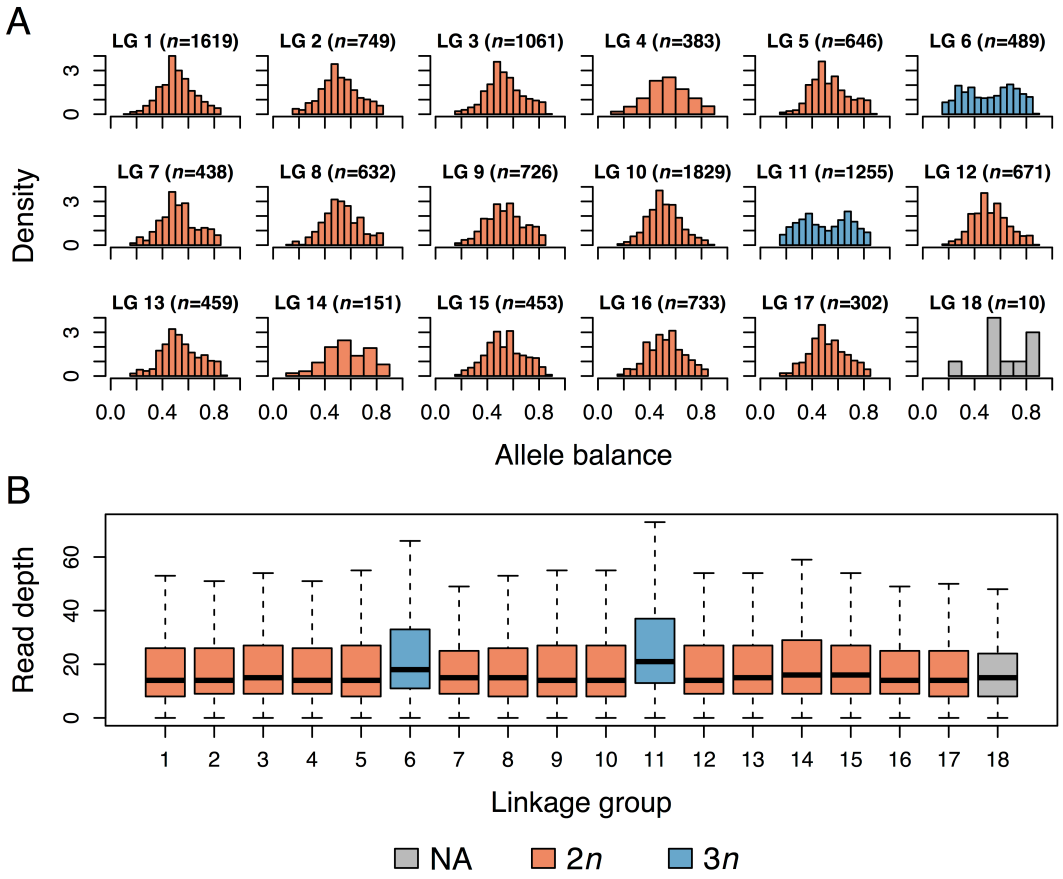

Figure 2.3: Example of ploidy level determination by linkage group in isolate 13EH38A. A) Distribution of allele balances within the 18 linkage groups of isolate 13EH38A. Number of heterozygous markers (*n*) is reported for each linkage group. B) Boxplot of SNP read depths per linkage group in isolate 13EH38A. The number of SNPs on each linkage group was down-sampled to the number on the linkage group having the fewest SNPs.

All linkage groups appeared trisomic in at least one isolate. Considering only linkage groups assigned a copy number designation, Fisher's exact test showed a significant enrichment for trisomies in certain linkage groups compared to others (P=0.01), with linkage groups 6 and 17 displaying the highest rates of trisomy, appearing trisomic in 7 and 8% of isolates, compared

to a linkage group average of 3% (Table 2.3).

Table 2.3: Distribution of copy number counts for each linkage group (LG) across 245 isolates[a].

Linkage group	2*n*	3*n*	Unknown	NA	Proportion 3*n*
1	214	2	27	2	0.01
2	174	3	65	3	0.02
3	179	3	60	3	0.02
4	156	3	82	4	0.02
5	185	3	54	3	0.02
6	138	11	91	5	0.07
7	101	2	138	4	0.02
8	191	4	47	3	0.02
9	168	2	72	3	0.01
10	208	3	31	3	0.01
11	186	4	52	3	0.02
12	161	4	77	3	0.02
13	152	3	87	3	0.02

14	130	2	108	5	0.02
15	130	4	107	4	0.03
16	178	4	60	3	0.02
17	131	11	99	4	0.08
18	57	3	110	75	0.05
Sum	2839	71	1367	133	NA

[a] Reported are the number of isolates in which a particular LG showed strong statistical support for the presence of 2 copies ('2*n*') or three copies ('3*n*'), as well as the number of isolates where that linkage group showed ambiguous signal ('Unknown') or featured too few heterozygous markers for analysis ('NA'). The proportion of trisomic isolates per linkage group is also reported among isolates where that linkage group was assigned a copy number ('Proportion 3*n*').

Linkage disequilibrium decay and genome-wide association studies. We used phenotypes and genotypes from the clone-corrected isolate set and conducted GWAS to identify loci associated with mating type and mefenoxam sensitivity. First, we plotted LD between pairwise SNPs as a function of distance, finding that genome-wide LD decayed rapidly to $r^2 <$ 0.10 by ~12 Kb, and plateaued at $r^2 = 0.04$ by ~400 Kb (Figure S2.2). We therefore focused on the region within ±400 Kb of peak SNPs identified in GWAS for candidate gene searches.

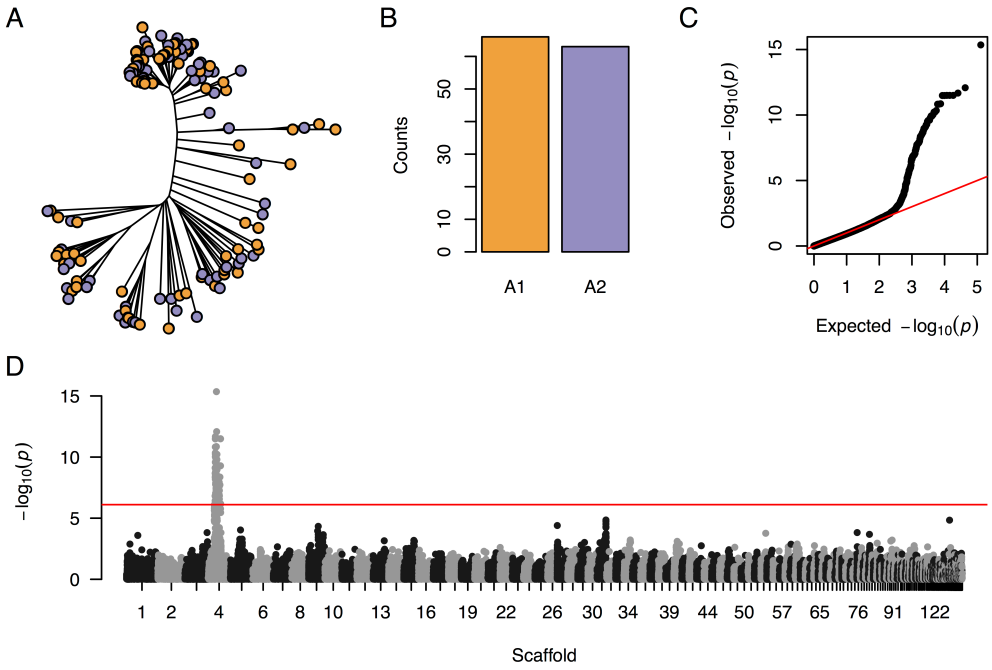

Figure 2.4: GWAS results for mating type. A) Neighbor-joining tree with point colors representing mating type where A1=orange and A2=purple. B) Counts of A1 and A2 isolates among the clone-corrected isolate set. C) Q-Q plot of *P*-values from logistic regression GWAS for mating type, using a population of 129 isolates scored for 64,630 SNPs. D) Manhattan plot showing SNP *P*-values across the genome from logistic regression GWAS for mating type.

Mating type showed no relationship with population structure, as it was not associated with any of the first four PCs (t-test P=0.60, 0.70, 0.90, 0.60 for PCs 1-4, respectively; Figure 2.4A). In addition, both mating types were represented approximately equally among the clone-corrected isolate set (n_{A1}=66; n_{A2}=63; Figure 2.4B). A logistic regression GWAS for mating type revealed one peak on scaffold 4 containing 70 SNPs with significant *P*-values (Figures 2.4C and 2.4D). The 70 significant SNPs spanned an approximately 426 Kb region (between SNPs S4_447285 and S4_873767; Figure S2.3) containing 139 annotated genes, with the peak SNP

(S4_579765; P=4.3 × 10^{-16}) located in an intron of a gene encoding a putative protein kinase (*fgenesh1_pg.PHYCAscaffold_4_#_142*). Among the 70 significant mating type-associated SNPs, A1 isolates were predominantly homozygous, with a median frequency of 0.94 for homozygous genotype calls. A2 isolates, on the other hand, were predominantly heterozygous at these sites, with a median frequency of 0.70 for heterozygous genotype calls.

A total of 290 genes were annotated within ±400 Kb of the peak SNP. Candidate genes were difficult to identify given the unknown molecular mechanism of mating type determination. We used blastp to determine if any of these 290 genes were possible homologs with any of the 38 genes annotated in the recently mapped mating type determining region of *Plasmopara viticola* (Dussert et al. 2020). Of the 290 *P. capsici* genes, 199 had a reciprocal best hit in *P. viticola*, which were found on 12 different scaffolds, none of them co-localized with the reported GWAS signal for mating type. Likewise, of the 38 *P. viticola* genes, 24 had a reciprocal best hit in *P. capsici*, which were found on four separate scaffolds, none of them scaffold 4, where the GWAS signal we identified for *P. capsici* was located.

We next decided to investigate genotype discrepancies between isolates of the clonal lineage which featured one A1 (13EH26A) and two A2 (13EH05A and 13EH76A) isolates. While 13EH26A showed a genome-wide rate of discordant genotype calls between 13EH05A and 13EH76A of 4.3 and 4.7%, respectively, the discordant call rate was 36.7 and 36.5% in the 426 Kb area spanned by significant mating type-associated SNPs. Considering only the 70 significant SNPs, the discordant call rate was 100% and 97.7%. At 38 of the 42 significant SNPs without any missing genotype calls in these three isolates, 13EH05A and 13EH76A were both heterozygous and 13EH05A was homozygous. In addition to the mating type region on scaffold 4, 13EH26A also showed a higher rate of discordant genotype calls with 13EH05A and

13EH76A on scaffolds 34 and 40 (Figure S2.4), which immediately proceed the mating type region on the *P. capsici* genetic map (Lamour et. al. 2012). Collectively, these results suggest that a loss of heterozygosity event in a large chromosomal region containing the mating type locus induced a switch from A2 to A1 in isolate 13EH05A. Since the read depth of SNPs in 13EH05A in the mating type region (mean 23.1) did not differ from the genome-wide SNP read depth (mean 22.6), it appears that this loss of heterozygosity event was conferred in a copy-neutral manner.

In contrast to mating type, mefenoxam sensitivity was more strongly confounded with population structure, showing a significant association with PC 1 (P=5.9 × 10^{-6}) and PC 3 (P=4.2 × 10^{-3}). Intermediately sensitive and resistant isolates were especially prevalent in populations from WNY sites, and rare among the 59 isolates from Ontario #1 (Figure 2.5A). In addition, different phenotypic classes were disproportionately represented, with the majority of clone-corrected isolates classified as sensitive (Figure 2.5B). We used 10% RG on 5 μg/ml mefenoxam-amended media as a threshold to classify isolates as one of 34 resistant 'cases' or 91 sensitive 'controls' and conducted a logistic regression GWAS controlling for population structure and unequal relatedness. We identified one signal spanning approximately 59 Kb on scaffold 62 (between markers S62_139120 and S62_198531; Figure S2.4) that contained 6 significantly associated SNPs (Figures 2.5C and 2.5D). The peak SNP (S62_186715; P=1.1 × 10^{-7}) was located in an exon of a gene (*gw1.62.46.1*) annotated as a dynein. The entirety of scaffold 62 was contained within the 400 Kb flanking the peak SNP and featured 100 annotated genes, including several with a plausible role in mefenoxam insensitivity, such as a homolog of the yeast ribosome synthesis factor Rrp5, located within 20 Kb of the peak SNP (Table S2.3).

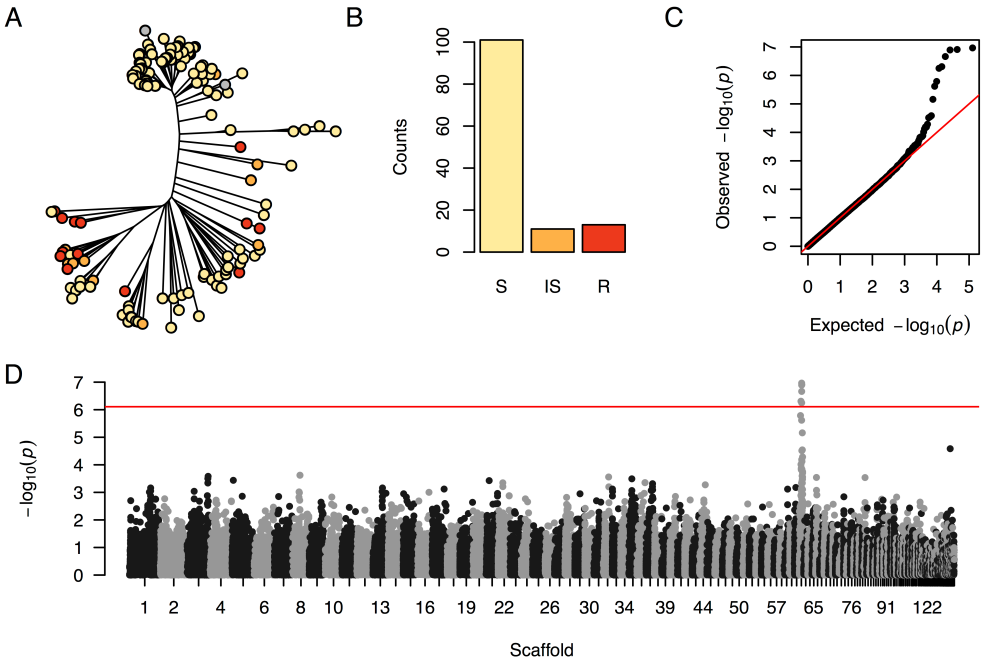

Figure 2.5: GWAS results for mefenoxam sensitivity. A) Neighbor-joining tree with point colors indicative of mefenoxam sensitivity. S = sensitive (yellow), IS = intermediately sensitive (orange), R = resistant (red). B) Counts of S, IS, and R isolates among the clone-corrected isolate set. C) Q-Q plot of *P*-values from logistic regression GWAS controlling for population structure and unequal relatedness. GWAS was conducted using a population of 125 isolates scored for 64,630 SNPs. D) Manhattan plot showing SNP *P*-values across the genome from logistic regression GWAS for mefenoxam sensitivity.

The allele associated with insensitivity at the peak SNP, S62_186715, showed an approximately additive effect on RG on both 5 µg/ml and 100 µg/ml mefenoxam (Figure 2.6). The insensitivite allele, with a frequency of 0.28 among all isolates, was found in isolates from 11 NY sites and in one SC isolate. Eight isolates, representing five different field sites in four NY regions, were homozygous for the insensitive allele. Several isolates were outliers in terms

of their sensitivity response as predicted by the genotype of SNP S62_186715, including one isolate from Erie #1 that was homozygous for the sensitive allele yet showed >95% RG on 5 µg/ml mefenoxam and >75% RG on 100 µg/ml mefenoxam, as well as an isolate from Suffolk #5 that was homozygous for the insensitive allele yet did not grow on either 5 µg/ml or 100 µg/ml mefenoxam.

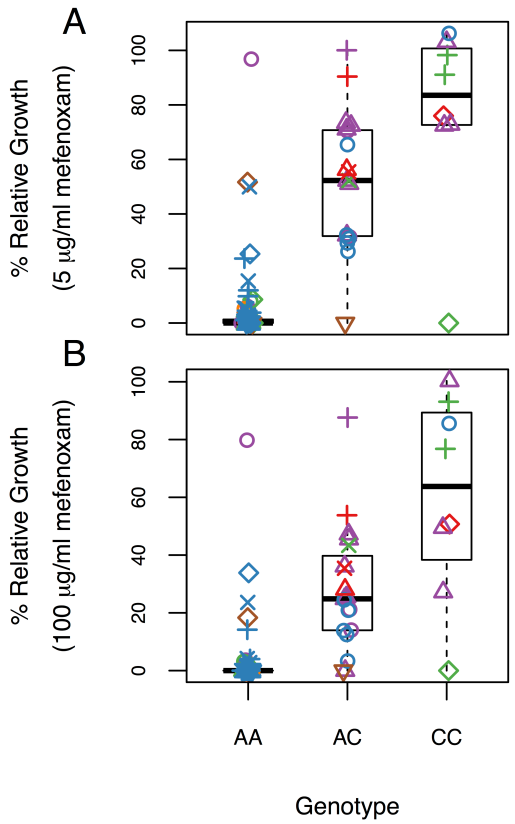

Figure 2.6. Boxplot showing the effect of the genotype at the peak SNP for mefenoxam insensitivity (S62_186715) on RG on amended media. Point colors and shapes are as in Figure 2.2. A) Effect of S62_186715 genotype on RG on 5 µg/ml mefenoxam. B) Effect of S62_186715 genotype on RG on 100 µg/ml mefenoxam.

DISCUSSION

The 252 *P. capsici* cultures characterized in this study were isolated from symptomatic plant samples obtained through several means – whether collected during field visits or received from extension agents for purposes of disease diagnostics. We genotyped this collection of isolates at 107,569 SNP loci, corresponding to one SNP on average every ~600 bp. We were able to leverage this dataset to investigate not only issues of regional importance, namely those related to the pathogen's population structure patterns in NY, but also questions of global significance, having to do with the genetic control of mating type and mefenoxam sensitivity, both epidemiologically important phenotypes in many oomycete pathogens, and the extent to which field isolates vary in terms of their chromosomal copy numbers.

Population structure and clonality. Visualizing relationships among the clone-corrected isolates with PCA and a NJ-tree (Figure 2.2) showed, for the most part, pathogen populations from different farms clustering separately. Similarly, estimates of pairwise F_{ST} between the five fields that featured a sufficient number of samples after clone-correction showed moderate to strong genetic differentiation between sites. Even isolates from farms in close geographic proximity, such as Erie #1 and Erie #2, separated into distinct, although related, clades in the NJ-tree and featured moderate levels of genetic differentiation between them. These results agree with previous hypotheses that limited gene flow occurs between *P. capsici* populations on different farms (Lamour and Hausbeck 2001; Dunn et. al. 2010).

Nevertheless, we found some examples that deviated from this overall trend. Isolates from 3 of the 5 Long Island farms did not separate into distinct clades in the NJ-tree, suggesting higher gene flow between the sampled fields in this region. We also identified two isolates, one each from Erie #1 and Suffolk #5, that did not cluster with other isolates from their respective

sites. It is possible that these outlier isolates represent independent introductions of inoculum to their fields compared to the rest of the isolates from those sites.

As expected based on our current understanding of *P. capsici* epidemiology (Lamour and Hausbeck 2001; Lamour and Hausbeck 2003; Dunn et al. 2010), we found evidence for a mixed mode of reproduction in pathogen populations in NY fields. Over half of the isolates that we surveyed belonged to a clonal lineage consisting of multiple sampled isolates, reflecting the influence of asexual reproduction within single seasons and fields. Two fields, Ontario #1 (2013) and Ontario #2 (2018), featured a particularly small number of genetically unique isolates compared to the total number of isolates sampled from those fields (Table 2.1). Interestingly, within a few months prior to sample collection, both of these fields experienced flooding events followed by their first outbreak of Phytophthora blight. One possible explanation for their low observed genotypic diversity is that the inoculum, likely introduced to these fields via floodwater, consisted of a small number of founding pathogen genotypes. Alternatively, the environmental conditions in the fields after flooding, highly conducive to asexual reproduction, could have amplified the ability of certain clonal lineages to rapidly spread and predominate in these fields, either due to random chance or because of a fitness advantage of those genotypes.

Isolates from Ontario #1 were sampled again in 2017, at the end of a season in which the field was planted for the first time since 2013 to a Phytophthora-susceptible crop and subsequently suffered another disease outbreak. The 2017 isolates, which were genetically undifferentiated from the 2013 isolates (F_{ST}=0.001; Figure 2.2), were more genotypically diverse, with 59% of isolates representing unique genotypes compared to 24% in 2013. Given that the primary inoculum for the 2017 outbreak was most likely oospores formed during the 2013 outbreak, these results show how a potentially small inoculum founder event followed by sexual

reproduction can lead to the development of a persistent bank of genotypically diverse oospores in the soil. This phenomenon has been previously demonstrated in both natural populations (Lamour and Hausbeck 2003) and experimentally inoculated research fields (Dunn et al. 2014; Carlson et al. 2017).

It is unknown when *P. capsici* inoculum first arrived in vegetable-growing areas of NY, nor where it originated from, or how many times it was independently introduced. Our population structure analyses did not show a clear relationship between NY isolates and those from any particular other state (Figure 2.2), although our non-NY sample size (n=10) was too modest to directly address this question. However, other studies have also shown only moderate differentiation between *P. capsici* populations from most U.S. states (Quesada Ocampo et al. 2011; Parada-Rojas and Quesada-Ocampo 2018), suggesting perhaps a recent common origin of inoculum for most states or frequent movement of inoculum between distant locations in the U.S. Our data, interpreted in conjunction with other studies (Lamour and Hausbeck 2000; Lamour and Hausbeck 2001; Lamour and Hausbeck 2002; Dunn et al. 2010; Jones et al. 2014) and reports from farmers, are consistent with a model of disease spread where local dispersal of inoculum, perhaps largely via run-off from fields and flooding events, leads to long-lasting sexual populations on newly infected fields that become genetically differentiated from neighboring populations due to a founder effect and subsequent genetic drift. Longer-distance movement of inoculum, mediated by transport of infested soil or infected plant-material, may also occur, as evidenced by our observation of several field populations with little relatedness to other populations in the same region (e.g. Cayuga #1).

Two observations from our collection of isolates – that A1 and A2 isolates were represented proportionally in all sites after clone correction, and that clonal lineages were

entirely unique to individual sites and years – reflect the epidemiological importance of sexual reproduction in allowing inoculum to overwinter. While obligate sexual reproduction appears to be the case in NY and other U.S. regions (Lamour and Hausbeck 2000, 2003), locations in South America and East Asia, including regions of China with temperate climates that should prohibit overwintering of asexual inoculum, have reported asexual lineages of *P. capsici* that persist over many years and over large geographic regions (Hurtado-Gonzalez et al. 2008; Hu et al. 2013). It is unknown what environmental and/or genetic factors account for the stark differences in the pathogen population structure between the U.S. and these other countries.

Chromosomal copy number variation. By analyzing patterns of variation in read counts across the genome, we identified some isolates with clear evidence of aneuploidy (Figure 2.3), as well as others with much more difficult-to-interpret signal (Figure S2.1). We therefore decided to implement conservative thresholds for declaring a linkage group trisomic, relying on significance testing (whether parametric or bootstrap-based) with two independent sources of information, allele balances at heterozygous sites and total read depth at all SNPs. Low average read depth, causing noisy allele balance histograms, was likely responsible for many of the linkage groups with ambiguous support for an allele balance mode at either 0.5 or 0.33/0.66, as evidenced by the high correlation between individual read depth and the percentage of linkage groups assigned a copy number assignations in each isolate. However, it is also possible that linkage groups in some isolates showed noisy allele balance histograms for one of several biological reasons, whether due to possessing an even higher copy number than 3, having intra-chromosomal copy number variation, or because DNA was extracted from a heterogenous population of nuclei varying in copy number for that linkage group. We therefore may have underestimated the true extent of aneuploidy in our collection of isolates, and future efforts with

higher sequencing depth are necessary to expand upon our research. It is also worth mentioning that some of the linkage groups we declared trisomic may actually have been present in greater than 3 copies, as higher-copy number linkage groups could feature allele balance patterns consistent with our definition of trisomy (for example, the tail of an allele balance peak at 0.75, as would be expected for a triplex tetraploid genotype, could cause a greater number of SNPs to have an allele balance closer to 0.66 than 0.50). Finally, our analyses do not rule out heterokaryosis (the presence of multiple distinct nuclei within a single cell), which was recently shown in the oomycete plant pathogen *Bremia lactucae* to result in similar allele balance distributions to those that we found (Fletcher et al. 2019). However, whereas *B. lactucae* produces multinucleate sporangia that germinate directly, we have observed *Phytophthora capsici* sporangia to almost exclusively germinate indirectly from mononucleate zoospores (data not shown), making heterokaryosis unlikely.

We found 33 isolates, representing 13% of the isolates we genotyped, that were either aneuploids or genome-wide polyploids. Other studies have reported both widespread polyploidy (Daggett et al. 1995) and aneuploidy (Barchenger et al. 2017; Shrestha et al. 2017) in isolates of *P. capsici* and other *Phytophthora* species. However, the number of isolates we genotyped and our detailed analyses allowed us to make several novel findings. First, we found a slight, but significant, enrichment for trisomy in certain linkage groups compared to others. It is unclear if this is due to chromosome size, since the physical size of the *P. capsici* chromosomes is unknown, or has to do with the presence of adaptive genes on certain linkage groups that confer a fitness advantage when present in higher copy number. Second, analyzing patterns of aneuploidy and polyploidy within clonal lineages showed evidence for a meiotic origin of polyploidy, as the only two genome-wide polyploids we found were the exclusive members of

the same clonal lineage, and a mitotic origin of aneuploidy, since trisomic linkage groups were not shared in any cases between isolates of the same clonal lineage. Spontaneous chromosomal loss and duplication in *Phytophthora* species has previously been identified during vegetative growth and asexual reproduction (Kasuga et al. 2016; Hu et al. 2020), supporting aneuploidy arising mitotically. In our study, differences in aneuploidy within isolates of the same clonal lineage, which presumably originated from a single oospore germinating the same year as sample collection, suggest that chromosomal copy number variation arises rapidly. However, we cannot separate chromosomal duplications that occurred in the field from those that occurred in culture. Future efforts sequencing pathogen DNA directly from field samples would be necessary to understand the rate at which aneuploidy arises and under what conditions.

Aneuploidy is known to be either lethal or causative of severe development defects in many higher organisms (Siegel and Amon 2012). Nevertheless, under selective conditions, experimental evolution studies have shown that aneuploid yeast strains often have higher fitness than euploids (Sunshine et al. 2015). Indeed, in the Sudden Oak Death pathogen *Phytophthora ramorum*, aneuploid isolates with phenotypic alterations are consistently selected for after passage through certain hosts (Kasuga et al. 2016). Because of the small number of isolates in our collection having aneuploidy for any given linkage group, we were not able to robustly associate chromosomal copy number changes with either of the traits we phenotyped. However, we hypothesize that spontaneous chromosomal loss and duplication leads to phenotypic variation, even within clonal lineages of *P. capsici*, that are subject to selection. It is unclear, however, if selection for certain aneuploidies persist beyond a single year, given that *P. capsici* undergoes obligate sexual reproduction in order to overwinter in the United States and the ability of aneuploid isolates to undergo meiosis and form viable gametes is unknown.

Genetic basis of mating type and mefenoxam sensitivity. To our knowledge, our study represents the first GWAS conducted in *Phytophthora capsici*, and one of few ever conducted in a plant-pathogenic oomycete (Ayala-Usma et al. 2019; Dussert et al. 2020). LD decayed rapidly, to r^2 <0.10 by approximately 12 Kb, almost identical to the rate reported in a population of *P. infestans* (Ayala-Usma et al. 2019), and comparable to rates reported in three plant-pathogenic fungi: *Parastagonospora nodoroum, Zymoseptoria tritici*, and *Pyrenophora teres* (Gao et al. 2016; Hartmann et al. 2017; Anke et al. 2019). Background levels of LD (r^2=0.04), however, were only reached at approximately 400 Kb, indicating the need for a fairly large candidate gene search space in GWAS.

We expected mating type to be easy to map via GWAS, since it is known to have a simple genetic architecture, represented a binary phenotype with both classes evenly distributed in our population, and was unassociated with population structure (Figure 2.4). Indeed, we found strong statistical support for a single mating type locus on scaffold 4 (Figure 2.4; Figure S2.3), the same region identified in previous studies (Lamour et al. 2012; Carlson et al. 2017).

Previous evidence from experimental crosses supports a genetic model where mating type inheritance behaves as in an XY sex determination system, where, in the case of *P. capsici*, A2 isolates are the heterozygous (i.e., XY) type and A1 isolates are the homozygous type (i.e., XX; Fabritius and Judelson 1997; Carlson et al. 2017). Our results are consistent with this hypothesis, as A1 isolates were predominantly homozygous and A2 isolates predominantly heterozygous at the 70 SNPs significantly associated with mating type. Other researchers have observed the *P. capsici* A2 mating type to be unstable (Hu et al. 2013, 2020), with evidence suggesting that mitotic loss of heterozygosity in the mating type region causes A2 isolates to switch mating type (Lamour et al. 2012). While we did not identify any A2 isolates that became

self-fertile, a phenomenon that was recently reported (Hu et al. 2020), we did observe 13 A2 isolates that converted to A1 at an undetermined point over a period of several years. In addition, we identified mating type discrepancies within a single clonal lineage, consisting of one A1 and two A2 isolates. While the three isolates were genetically identical across most of the genome, the A1 isolate featured a high rate of discordant genotype calls compared to the A2 isolates at the mating type locus and linked genomic regions (Figure S2.4), consistent with a loss of heterozygosity event in this isolate resulting in the conversion of the A2-determining haplotype. Because read depths were not halved in the mating type region compared to the rest of the genome, we hypothesize that this loss of heterozygosity occurred in a copy-neutral manner such as gene conversion, as opposed to via a deletion event resulting in hemizygosity. Given what appears to be the high frequency of unidirectional switching from A2 to A1, it may be possible in a future experiment to fine-map the mating type locus by tracking loss of heterozygosity breakpoints in a collection of A2 isolates that have switched mating type.

We found the identification of mating type candidate genes to be challenging, due to the large number of genes annotated within 400 Kb of the peak SNP and our lack of knowledge of the molecular mechanism behind mating type determination. Furthermore, in searching for reciprocal best hits between *P. capsici* and *Plasmopara viticola*, we were unable to identify any likely orthologs between the reported mating type regions of the two species. Presumably, the causal mating type determining gene or genes could encode any of a wide variety of proteins, such as enzymes in the metabolic pathways for α_1 or α_2, receptors involved in the recognition of α hormones, or transcription factors responsible for regulating mating type-specific expression levels. It is also possible that the causal gene or genes are not annotated in the *P. capsici* reference genome, and they may only be present on one of the two A2 haplotypes. Indeed, in *P.*

infestans, the mating type locus was shown to contain a heteromorphic region where certain cDNA clones only hybridized to one of the two mating type specific contigs (Randall et al. 2003).

Unlike mating type, mefenoxam sensitivity had never been mapped in *P. capsici* prior to thi*s* study. It also represented a more challenging phenotype to map, as it was confounded with population structure and exhibited an imbalance in the number of resistant versus sensitive isolates (Figure 2.5). Nevertheless, by fitting a generalized mixed model correcting for population structure and unequal relatedness, we detected significantly associated SNPs in a region on scaffold 62 (Figure 2.5; Figure S2.3). The allele associated with insensitivity at the peak SNP demonstrated an approximately additive effect (Figure 2.6), consistent with segregation patterns in lab crosses that support an incompletely dominant gene conferring metalaxyl or mefenoxam insensitivity in *P. capsici*, *P. infestans*, and *P. sojae* (Shattock 1988; Bhat et al. 1993; Gisi and Cohen 1996; Lamour and Hausbeck 2000). It appears likely, however, that additional loci may play a role in decreased sensitivity in some isolates, as several individuals in our collection of isolates were homozygous for the sensitive allele at the peak SNP on scaffold 62 yet showed intermediate or high mefenoxam insensitivity. Similarly, in *P. infestans*, there is evidence of multiple loci involved in insensitivity to metalaxyl (Judelson and Roberts 1999; Fabritius et al. 2007).

Researchers have long assumed that the target site of phenylamide fungicides is RNA Polymerase I (Griffith et al. 1992), since the mode of action of these chemicals in oomycetes involves inhibition of rRNA synthesis (Davidse et al. 1983; Wollgiehn et al. 1984). In *P. infestans,* however, attempts to associate mutations in subunits of RNA Polymerase I with metalaxyl or mefenoxam insensitivity have been inconclusive (Randall et al. 2014; Matson et al.

2015). In our case, we did not identify any genes in the region of the GWAS signal on scaffold 62 encoding RNA Polymerase I subunits. We did, however, identify several other plausible candidate genes (Table S2.3). One gene, located within 15 kb of the peak SNP, is a homolog of yeast protein Rrp5, which is required for processing of pre-rRNA transcripts into the cleaved molecules that form the ribosome (Venema and Tollervey 1996). If mefenoxam does interfere with the function of Rrp5, the buildup of precursor rRNA molecules in the nucleolus could cause a depletion of total rRNA as these intermediate molecules are degraded by exonucleases or as feedback mechanisms result in decreased rRNA transcription. Alternatively, the causal gene at this locus could be one of the transporters located nearby, or perhaps even RNA polymerase III subunit Rpc4, also located within 15 Kb of the peak SNP. Further investigation is required to determine which of these genes, if any, feature mutations that confer mefenoxam insensitivity in the isolates we assayed.

Conclusions. We genotyped a collection of NY *P. capsici* isolates at over 100,000 SNP markers and assayed them for their mating type and mefenoxam sensitivity. Results of population structure analyses were consistent with previous reports, showing limited gene flow between different fields and highlighting the importance of sexual reproduction in allowing inoculum to overwinter. Thirteen percent of the isolates we genotyped showed some degree of chromosomal copy number variation within their genomes, with linkage groups 6 and 17 featuring a particularly high rate of aneuploidy. Genome-wide association studies confirmed previous results mapping the mating type locus to a region on scaffold 4, and identified a novel locus associated with mefenoxam sensitivity on scaffold 62. These results provide a foundation for functional validation of candidate genes as well as molecular marker development for prediction of mating type and mefenoxam insensitivity. Furthermore, the panel of isolates we

assembled and the dense marker data we generated represent a genetic resource that can be used for mapping other important traits in *P. capsici*, such as sensitivity to additional chemicals or virulence on economically important host plants.

ACKNOWLEDGEMENTS

This research was supported by the New York State Department of Agriculture and Markets (grant number C00237GG), the USDA National Institute of Food and Agriculture Specialty Crop Research Initiative (2015-51181-24285), and HM Clause, who provided support for Summer Research Scholars at Cornell AgriTech. We would like to thank Ali Cala, Santiago Tíjaro Bulla, Kimberly D'Arcangelo, Holly Lange, Charlotte Mineo, and Carolina Puentes Silva, all of whom provided valuable technical assistance in this project. We also thank Maryn Carlson, who collected a portion of the data and provided feedback and edits on an earlier version of this manuscript, as well as Di Wu and Dan Ilut, who offered bioinformatic assistance. In addition, we are grateful to Traven Bentley, Kishor Bhattarai, Elizabeth Buck, Mary Hausbeck, Brian Hill, Shaker Kousik, Margaret McGrath, Abby Seaman, and Darcy Telenko for providing cultures of isolates characterized in this study.

REFERENCES

Anke, M., Moolhuijzen, P., Tao, Y., Mcilroy, J., Ellwood, S., Fowler, R. A., Platz, G. J., Kilian, A., and Snyman, L. 2019. Genomic regions associated with virulence in *Pyrenophora teres f. teres* identified by genome-wide association analysis and bi-parental mapping. Phytopathology doi: https://doi.org/10.1094/PHYTO-10-19-0372-R.

Ashby, S. F. 1929. Strains and taxonomy of *Phytophthora palmivora* Butler (P. *faberi* Maubl.). Trans. Br. Mycol. Soc. 14:18–38.

Ayala-Usma, D., Danies, G., Myers, K. L., Bond, M. O., Romero-Navarro, J. A., Judelson, H. S., Restrepo, S., and Fry, W. 2019. Genome-wide association study identifies SNP markers associated with mycelial growth at 15, 20 and 25 °C, mefenoxam resistance and mating type in *Phytophthora infestans*. Phytopathology doi: https://doi.org/10.1094/PHYTO-06-19-0206-R.

Babadoost, M., and Pavon, C. 2013. Survival of oospores of *Phytophthora capsici* in soil. Plant Dis. 97:1478–1483.

Barchenger, D. W., Lamour, K. H., Sheu, Z.-M., Shrestha, S., Kumar, S., Lin, S.-W., Burlakoti, R., and Bosland, P. W. 2017. Intra- and intergenomic variation of ploidy and clonality characterize *Phytophthora capsici* on *Capsicum* sp. in Taiwan. Mycol. Prog. 16:955–963.

Bhat, R. G., McBlain, B. A., and Schmitthenner, A. F. 1993. The inheritance of resistance to metalaxyl and to fluorophenylalanine in matings of homothallic *Phytophthora sojae*. Mycol. Res. 97:865–870.

Bowers, J. H., Papvizas, G.C., and Johnston, S.A. 1990. Effect of soil temperature and soil-water matric potential on the survival of *Phytophthora capsici* in natural soil. Plant Dis. 74:771.

Carlson, M. O., Gazave, E., Gore, M. A., and Smart, C. D. 2017. Temporal genetic dynamics of

an experimental, biparental field population of *Phytophthora capsici*. Front. Genet. 8:26.

Camacho, C., Coulouris, G., Avagyan, V., Ma, N., Papadopoulos, J., Bealer, K., and Madden, T. L. 2009. BLAST+: architecture and applications. BMC Bioinformatics. 10:421.

Daggett, S. S., Knighton, J. E., and Therrien, C. D. 1995. Polyploidy among isolates of *Phytophthora infestans* from eastern Germany. J. Phytopathol. 143:419–422.

Danecek, P., Auton, A., Abecasis, G., Albers, C. A., Banks, E., DePristo, M. A., Handsaker, R. E., Lunter, G., Marth, G. T., Sherry, S. T., McVean, G., and Durbin, R. 2011. The variant call format and VCFtools. Bioinformatics 27:2156–2158.

Davidse, L. C., Hofman, A. E., and Velthuis, G. C. M. 1983. Specific interference of metalaxyl with endogenous RNA polymerase activity in isolated nuclei from *Phytophthora megasperma f. sp.medicaginis*. Exp. Mycol. 7:344–361.

Dunn, A. R., Bruening, S. R., Grünwald, N. J., and Smart, C. D. 2014. Evolution of an experimental population of *Phytophthora capsici* in the field. Phytopathology 104:1107–1117.

Dunn, A. R., Milgroom, M. G., Meitz, J. C., McLeod, A., Fry, W. E., McGrath, M. T., Dillard, H. R., and Smart, C. D. 2010. Population structure and resistance to mefenoxam of *Phytophthora capsici* in New York State. Plant Dis. 94:1461–1468.

Dussert, Y., Mazet, I. D., Couture, C., Gouzy, J., Piron, M.-C., Kuchly, C., Bouchez, O., Rispe, C., Mestre, P., and Delmotte, F. 2019. A high-quality grapevine downy mildew genome assembly reveals rapidly evolving and lineage-specific putative host adaptation genes. Genome Biol. Evol. 11:954–969.

Dussert, Y., Legrand, L., Mazet, I. D., Couture, C., Piron, M.-C., Serre, R.-F., Bouchez, O., Mestre, P., Toffolatti, S. L., Giraud, T., and Delmotte, F. 2020. Identification of the first

oomycete mating-type locus sequence in the grapevine downy mildew pathogen, *Plasmopara viticola*. bioRxiv. :2020.02.26.962936

Elshire, R. J., Glaubitz, J. C., Sun, Q., Poland, J. A., Kawamoto, K., Buckler, E. S., and Mitchell, S. E. 2011. A robust, simple genotyping-by-sequencing (GBS) approach for high diversity species. PLoS ONE 6:e19379.

Endelman, J. B. 2011. Ridge regression and other kernels for genomic selection with R package rrBLUP. Plant Genome 4:250–255.

Erwin, D. C., and Ribeiro, O. K. 1998. *Phytophthora* Diseases Worldwide. The American Phytopathological Society, St Paul, Minnesota.

Fabritius, A.-L., and Judelson, H. S. 1997. Mating-type loci segregate aberrantly in *Phytophthora infestans* but normally in *Phytophthora parasitica*: implications for models of mating-type determination. Curr. Genet. 32:60–65.

Fabritius, A.-L., Shattock, R. C., and Judelson, H. S. 1997. Genetic analysis of metalaxyl insensitivity loci in *Phytophthora infestans* using linked DNA markers. Phytopathology 87:1034–1040.

Farrer, R. A., Henk, D. A., Garner, T. W. J., Balloux, F., Woodhams, D. C., and Fisher, M. C. 2013. Chromosomal copy number variation, selection and uneven rates of recombination reveal cryptic genome diversity linked to pathogenicity. PLoS Genet. 9:e1003703.

Fletcher, K., Gil, J., Bertier, L. D., Kenefick, A., Wood, K. J., Zhang, L., Reyes-Chin-Wo, S., Cavanaugh, K., Tsuchida, C., Wong, J., and Michelmore, R. 2019. Genomic signatures of heterokaryosis in the oomycete pathogen *Bremia lactucae*. Nat. Commun. 10:1–13.

Foster, J. M., and Hausbeck, M. K. 2009. Resistance of pepper to Phytophthora crown, root, and fruit rot Is affected by isolate virulence. Plant Dis. 94:24–30.

Gao, Y., Liu, Z., Faris, J. D., Richards, J., Brueggeman, R. S., Li, X., Oliver, R. P., McDonald, B. A., and Friesen, T. L. 2016. Validation of genome-wide association studies as a tool to identify virulence factors in *Parastagonospora nodorum*. Phytopathology 106:1177–1185.

Gisi, U., and Cohen, Y. 1996. Resistance to phenylamide fungicides: a case study with *Phytophthora infestans* involving mating type and race structure. Annu. Rev. Phytopathol. 34:549–572.

Gisi, U., and Sierotzki, H. 2008. Fungicide modes of action and resistance in downy mildews. Eur. J. Plant Pathol. 122:157–167.

Glaubitz, J. C., Casstevens, T. M., Lu, F., Harriman, J., Elshire, R. J., Sun, Q., and Buckler, E. S. 2014. TASSEL-GBS: a high capacity genotyping by sequencing analysis pipeline. PLoS ONE 9:e90346.

Gogarten, S. M., Sofer, T., Chen, H., Yu, C., Brody, J. A., Thornton, T. A., Rice, K. M., and Conomos, M. P. Genetic association testing using the GENESIS R/Bioconductor package. Bioinformatics 35:5346-5348.

Granke, L. L., Quesada-Ocampo, L., Lamour, K., and Hausbeck, M. K. 2012. Advances in research on *Phytophthora capsici* on vegetable crops in the United States. Plant Dis. 96:1588–1600.

Granke, L. L., Windstam, S. T., Hoch, H. C., Smart, C. D., and Hausbeck, M. K. 2009. Dispersal and movement mechanisms of *Phytophthora capsici* sporangia. Phytopathology 99:1258–1264.

Griffith, J. M., Davis, A. J., and Grant, B. R. 1992. Target sites of fungicides to control oomycetes. Pages 69–100 in: Target Sites of Fungicide Action, W. Koller, ed. CRC

Press, Boca Raton.

Hartmann, F. E., Sánchez-Vallet, A., McDonald, B. A., and Croll, D. 2017. A fungal wheat pathogen evolved host specialization by extensive chromosomal rearrangements. ISME J. 11:1189–1204.

Hausbeck, M. K., and Lamour, K. H. 2004. *Phytophthora capsici* on vegetable crops: research progress and management challenges. Plant Dis. 88:1292–1303.

Hill, W. G., and Robertson, A. 1968. Linkage disequilibrium in finite populations. Theor. Appl. Genet. 38:226–231.

Hu, J., Diao, Y., Zhou, Y., Lin, D., Bi, Y., Pang, Z., Fryxell, R. T., Liu, X., and Lamour, K. 2013. Loss of heterozygosity drives clonal diversity of *Phytophthora capsici* in China. PLoS ONE 8:e82691.

Hu, J., Shrestha, S., Zhou, Y., Mudge, J., Liu, X., and Lamour, K. 2020. Dynamic Extreme Aneuploidy (DEA) in the vegetable pathogen *Phytophthora capsici* and the potential for rapid asexual evolution. PLoS ONE 15:e0227250.

Hurtado-Gonzáles, O., Aragon-Caballero, L., Apaza-Tapia, W., Donahoo, R., and Lamour, K. 2008. Survival and spread of *Phytophthora capsici* in coastal Peru. Phytopathology 98:688–694.

Huson, D. H. 1998. SplitsTree: analyzing and visualizing evolutionary data. Bioinformatics 14:68–73.

Jeffers, S. N., and Martin, S. B. 1986. Comparison of two media selective for *Phytophthora* and *Pythium* Species. Plant Dis. 70:1038.

Jones, L. A., Worobo, R. W., and Smart, C. D. 2014. Plant-pathogenic oomycetes, *Escherichia coli* strains, and *Salmonella* spp. frequently found in surface water used for irrigation of

fruit and vegetable crops in New York State. Appl. Environ. Microbiol. 80:4814–4820.

Judelson, H. S. 1997. Expression and inheritance of sexual preference and selfing potential in *Phytophthora infestans*. Fungal Genet. Biol. 21:188–197.

Judelson, H. S., and Roberts, S. 1999. Multiple loci determining insensitivity to phenylamide fungicides in *Phytophthora infestans*. Phytopathology 89:754–760.

Kasuga, T., Bui, M., Bernhardt, E., Swiecki, T., Aram, K., Cano, L. M., Webber, J., Brasier, C., Press, C., Grünwald, N. J., Rizzo, D. M., and Garbelotto, M. 2016. Host-induced aneuploidy and phenotypic diversification in the Sudden Oak Death pathogen *Phytophthora ramorum*. BMC Genomics 17:385.

Keinath, A. P. 2007. Sensitivity of populations of *Phytophthora capsici* from South Carolina to mefenoxam, dimethomorph, zoxamide, and cymoxanil. Plant Dis. 91:743–748.

Ko, W. H. 1978. Heterothallic *Phytophthora*: evidence for hormonal regulation of sexual reproduction. Microbiology 107:15–18.

Kousik, C. S., and Keinath, A. P. 2008. First report of insensitivity to cyazofamid among isolates of *Phytophthora capsici* from the southeastern United States. Plant Dis. 92:979–979.

Lamour, K. H., and Hausbeck, M. K. 2003. Effect of crop rotation on the survival of *Phytophthora capsici* in Michigan. Plant Dis. 87:841–845.

Lamour, K. H., and Hausbeck, M. K. 2001. Investigating the spatiotemporal genetic structure of *Phytophthora capsici* in Michigan. Phytopathology 91:973–980.

Lamour, K. H., and Hausbeck, M. K. 2000. Mefenoxam insensitivity and the sexual stage of *Phytophthora capsici* in Michigan cucurbit fields. Phytopathology 90:396–400.

Lamour, K. H., Mudge, J., Gobena, D., Hurtado-Gonzales, O. P., Schmutz, J., Kuo, A., Miller, N. A., Rice, B. J., Raffaele, S., Cano, L. M., Bharti, A. K., Donahoo, R. S., Finley, S.,

Huitema, E., Hulvey, J., Platt, D., Salamov, A., Savidor, A., Sharma, R., Stam, R., Storey, D., Thines, M., Win, J., Haas, B. J., Dinwiddie, D. L., Jenkins, J., Knight, J. R., Affourtit, J. P., Han, C. S., Chertkov, O., Lindquist, E. A., Detter, C., Grigoriev, I. V., Kamoun, S., and Kingsmore, S. F. 2012. Genome sequencing and mapping reveal loss of heterozygosity as a mechanism for rapid adaptation in the vegetable pathogen *Phytophthora capsici*. Mol. Plant Microbe Interact. 25:1350–1360.

Li, H., and Durbin, R. 2009. Fast and accurate short read alignment with Burrows–Wheeler transform. Bioinformatics 25:1754–1760.

Matson, M. E. H., Small, I. M., Fry, W. E., and Judelson, H. S. 2015. Metalaxyl resistance in *Phytophthora infestans*: assessing role of RPA190 gene and diversity within clonal lineages. Phytopathology 105:1594–1600.

Ojika, M., Molli, S. D., Kanazawa, H., Yajima, A., Toda, K., Nukada, T., Mao, H., Murata, R., Asano, T., Qi, J., and Sakagami, Y. 2011. The second *Phytophthora* mating hormone defines interspecies biosynthetic crosstalk. Nat. Chem. Biol. 7:591–593.

Parada-Rojas, C. H., and Quesada-Ocampo, L. M. 2018. Analysis of microsatellites from transcriptome sequences of *Phytophthora capsici* and applications for population studies. Sci. Rep. 8:1–12.

Paradis, E., Claude, J., and Strimmer, K. 2004. APE: Analyses of Phylogenetics and Evolution in R language. Bioinformatics 20:289–290.

Parra, G., and Ristaino, J. B. 2001. Resistance to mefenoxam and metalaxyl among field isolates of *Phytophthora capsici* Causing Phytophthora blight of bell pepper. Plant Dis. 85:1069–1075.

Pembleton, L. W., Cogan, N. O. I., and Forster, J. W. 2013. StAMPP: an R package for

calculation of genetic differentiation and structure of mixed-ploidy level populations. Mol. Ecol. Resour. 13:946–952.

Qi, J., Asano, T., Jinno, M., Matsui, K., Atsumi, K., Sakagami, Y., and Ojika, M. 2005. Characterization of a *Phytophthora* mating hormone. Science 309:1828–1828.

Quesada-Ocampo, L. M., Granke, L. L., Mercier, M. R., Olsen, J., and Hausbeck, M. K. 2011. Investigating the genetic structure of *Phytophthora capsici* populations. Phytopathology 101:1061–1073.

R Core Team. 2012. R: A Langauge and Environment for Statistical Computing. R Foundation for Statistical Computing. Vienna, Austria. http://www.R-project.org/.

Randall, T. A., Ah Fong, A., and Judelson, H. S. 2003. Chromosomal heteromorphism and an apparent translocation detected using a BAC contig spanning the mating type locus of *Phytophthora infestans*. Fungal Genet. Biol. 38:75–84.

Randall, E., Young, V., Sierotzki, H., Scalliet, G., Birch, P. R. J., Cooke, D. E. L., Csukai, M., and Whisson, S. C. 2014. Sequence diversity in the large subunit of RNA polymerase I contributes to mefenoxam insensitivity in *Phytophthora infestans*. Mol. Plant Pathol. 15:664–676.

Sakamoto, Y., Ishiguro, M., and Kitagawa, G. 1986. Akaike information criterion statistics. D Reidel Publishing Company, Tokyo, Japan.

Sansome, E. 1961. Meiosis in the oogonium and antheridium of *Pythium debaryanum* Hesse. Nature 191:827–828.

Sansome, E., and Brasier, C. M. 1973. Diploidy and chromosomal structural hybridity in *Phytophthora infestans*. Nature 241:344–345.

Schlub, R. L. 1983. Epidemiology of *Phytophthora capsici* on bell pepper. J. Agric. Sci. 100:7–

11.

Shattock, R. C. 1988. Studies on the inheritance of resistance to metalaxyl in *Phytophthora infestans*. Plant Pathol. 37:4–11.

Shrestha, S. K., Miyasaka, S. C., Shintaku, M., Kelly, H., and Lamour, K. 2017. *Phytophthora colocasiae* from Vietnam, China, Hawaii and Nepal: intra- and inter-genomic variations in ploidy and a long-lived, diploid Hawaiian lineage. Mycol. Prog. 16:893–904.

Siegel, J. J., and Amon, A. 2012. New insights into the troubles of aneuploidy. Annu. Rev. Cell Dev. Biol. 28:189–214.

Silvar, C., Merino, F., and Díaz, J. 2006. Diversity of *Phytophthora capsici* in northwest Spain: analysis of virulence, metalaxyl response, and molecular characterization. Plant Dis. 90:1135–1142.

Stacklies, W., Redestig, H., Scholz, M., Walther, D., and Selbig, J. 2007. pcaMethods—a bioconductor package providing PCA methods for incomplete data. Bioinformatics 23:1164–1167.

Sunshine, A. B., Payen, C., Ong, G. T., Liachko, I., Tan, K. M., and Dunham, M. J. 2015. The fitness consequences of aneuploidy are driven by condition-dependent gene effects. PLoS Biol. 13:e1002155.

Turner, S. D. 2014. qqman: an R package for visualizing GWAS results using Q-Q and manhattan plots. bioRxiv 005165.

Venema, J., and Tollervey, D. 1996. RRP5 is required for formation of both 18S and 5.8S rRNA in yeast. EMBO J. 15:5701–5714.

Wang, Z., Langston, D. B., Csinos, A. S., Gitaitis, R. D., Walcott, R. R., and Ji, P. 2009. Development of an improved isolation approach and simple sequence repeat markers to

characterize *Phytophthora capsici* populations in irrigation ponds in southern Georgia. Appl. Environ. Microbiol. 75:5467–5473.

Weir, B. S., and Cockerham, C. C. 1984. Estimating F-statistics for the analysis of population structure. Evolution 38:1358–1370

Wollgiehn, R., Bräutigam, E., Schumann, B., and Erge, D. 1984. Effect of metalaxyl on the synthesis of RNA, DNA and protein in *Phytophthora nicotianae*. Z. Allg. Mikrobiol. 24:269–279.

Yoshida, K., Schuenemann, V. J., Cano, L. M., Pais, M., Mishra, B., Sharma, R., Lanz, C., Martin, F. N., Kamoun, S., Krause, J., Thines, M., Weigel, D., and Burbano, H. A. 2013. The rise and fall of the *Phytophthora infestans* lineage that triggered the Irish potato famine. eLife 2:e00731.

Zhang, C., Dong, S.-S., Xu, J.-Y., He, W.-M., and Yang, T.-L. 2019. PopLDdecay: a fast and effective tool for linkage disequilibrium decay analysis based on variant call format files. Bioinformatics 35:1786–1788.

Zhu, Y. O., Sherlock, G., and Petrov, D. A. 2016. Whole genome analysis of 132 clinical *Saccharomyces cerevisiae* strains reveals extensive ploidy variation. G3. 6:2421–243.

SUPPLEMENTARY MATERIAL

Table S2.1:. Metadata on all isolates characterized in this study, including their source, mating type, mefenoxam sensitivity classification, and presence in the clone-corrected dataset.

Sample	Source	Year	Host plant	Host tissue	State	County	Field	MT	Mef-enoxam sensitivity	Unique Genotype	In CC Dataset	Previous publications
17PZ01A	Darcy Telenko	2017	Pepper	NA	NY	Erie	Erie #2	A1	R	35	FALSE	NA
17PZ02A	Darcy Telenko	2017	Pepper	NA	NY	Erie	Erie #2	A1	R	35	TRUE	NA
17PZ11A	Darcy Telenko	2017	Pepper	NA	NY	Erie	Erie #2	A2	R	120	TRUE	NA
17PZ12B	Darcy Telenko	2017	Pepper	NA	NY	Erie	Erie #2	A1	R	36	FALSE	NA
17PZ13A	Darcy Telenko	2017	Pepper	NA	NY	Erie	Erie #2	A1	R	39	TRUE	NA
17PZ14A	Darcy Telenko	2017	Pepper	NA	NY	Erie	Erie #2	A1	IS	39	FALSE	NA
17PZ15A	Darcy Telenko	2017	Pepper	NA	NY	Erie	Erie #2	A1	R	NA	FALSE	NA
17PZ16A	Darcy Telenko	2017	Pepper	NA	NY	Erie	Erie #2	A1	IS	73	TRUE	NA
17PZ17A	Darcy Telenko	2017	Pepper	NA	NY	Erie	Erie #2	A1	IS	36	TRUE	NA
17PZ18A	Darcy Telenko	2017	Pepper	NA	NY	Erie	Erie #2	A2	IS	14	TRUE	NA
17PZ20B	Darcy Telenko	2017	Pepper	NA	NY	Erie	Erie #2	A2	R	14	FALSE	NA
17PZ21A	Darcy Telenko	2017	Pepper	NA	NY	Erie	Erie #2	A2	R	14	FALSE	NA
17PZ22A	Darcy Telenko	2017	Pepper	NA	NY	Erie	Erie #2	A1	R	118	TRUE	NA

17PZ23A	Darcy Telenko	2017	Pepper	NA	NY	Erie	Erie #2	A1	S	64	TRUE	NA
17PZ26A	Darcy Telenko	2017	Pepper	NA	NY	Erie	Erie #2	A2	IS	49	TRUE	NA
17PZ29A	Darcy Telenko	2017	Pepper	NA	NY	Erie	Erie #2	A2	IS	14	FALSE	NA
18RN01A	Chris Smart	2018	Pumpkin	Fruit	NY	Ontario	Ontario #2	A2	S	11	FALSE	NA
18RN02A	Chris Smart	2018	Pumpkin	Fruit	NY	Ontario	Ontario #2	A2	S	13	FALSE	NA
18RN04B	Chris Smart	2018	Eggplant	NA	NY	Ontario	Ontario #2	A2	S	13	FALSE	NA
18RN05A	Chris Smart	2018	Eggplant	NA	NY	Ontario	Ontario #2	A2	S	13	FALSE	NA
18RN06A	Chris Smart	2018	Pepper	NA	NY	Ontario	Ontario #2	A2	IS	11	FALSE	NA
18RN08A	Chris Smart	2018	Tomato	NA	NY	Ontario	Ontario #2	A2	S	13	TRUE	NA
18RN13A	Chris Smart	2018	Pumpkin	Fruit	NY	Ontario	Ontario #2	A2	S	11	FALSE	NA
18RN14A	Chris Smart	2018	Pumpkin	Fruit	NY	Ontario	Ontario #2	A2	S	11	FALSE	NA
18RN15B	Chris Smart	2018	Pumpkin	Fruit	NY	Ontario	Ontario #2	A2	S	11	TRUE	NA
18051_1A	Abby Seaman	2018	Cucumber	Fruit	NY	Tioga	Tioga #1	A2	S	103	TRUE	NA
18052A	Greg Vogel	2018	Zucchini	Fruit	NY	Tompkins	Tompkins #1	A1	S	53	TRUE	NA
18080A	Elizabeth Buck	2018	Eggplant	NA	NY	Erie	Erie #3	A1	R	59	TRUE	NA
17DH01A	Darcy Telenko	2017	Zucchini	NA	NY	Erie	Erie #1	A1	R	5	FALSE	NA
17DH02A	Darcy Telenko	2017	Zucchini	NA	NY	Erie	Erie #1	A1	R	5	FALSE	NA
17DH03A	Darcy Telenko	2017	Zucchini	NA	NY	Erie	Erie #1	A1	R	5	TRUE	NA
17DH04B	Darcy Telenko	2017	Zucchini	NA	NY	Erie	Erie #1	A2	S	17	TRUE	NA
17DH05A	Darcy	2017	Zucchini	NA	NY	Erie	Erie #1	A1	S	121	TRUE	NA

	Telenko											
17DH07A	Darcy Telenko	2017	Zucchini	NA	NY	Erie	Erie #1	A1	R	5	FALSE	NA
17DH09B	Darcy Telenko	2017	Zucchini	NA	NY	Erie	Erie #1	A2	IS	88	TRUE	NA
17DH10B	Darcy Telenko	2017	Zucchini	NA	NY	Erie	Erie #1	A1	S	75	TRUE	NA
17DH12A	Darcy Telenko	2017	Zucchini	NA	NY	Erie	Erie #1	A2	S	29	FALSE	NA
17DH14A	Darcy Telenko	2017	Zucchini	NA	NY	Erie	Erie #1	A1	R	5	FALSE	NA
17DH15A	Darcy Telenko	2017	Zucchini	NA	NY	Erie	Erie #1	A1	R	5	FALSE	NA
17DH16A	Darcy Telenko	2017	Zucchini	NA	NY	Erie	Erie #1	A1	S	123	TRUE	NA
17DH17A	Darcy Telenko	2017	Zucchini	NA	NY	Erie	Erie #1	A2	S	106	TRUE	NA
17DH18B	Darcy Telenko	2017	Zucchini	NA	NY	Erie	Erie #1	A2	S	17	FALSE	NA
17DH19B	Darcy Telenko	2017	Zucchini	NA	NY	Erie	Erie #1	A2	S	17	FALSE	NA
17DH20B	Darcy Telenko	2017	Zucchini	NA	NY	Erie	Erie #1	A2	S	29	TRUE	NA
17DH21A	Darcy Telenko	2017	Zucchini	NA	NY	Erie	Erie #1	A1	R	5	FALSE	NA
17JT01_1A	Chris Smart	2017	SummerSquash	Fruit	NY	Cayuga	Cayuga #1	A1	S	38	TRUE	NA
17JT02_1A	Chris Smart	2017	SummerSquash	Fruit	NY	Cayuga	Cayuga #1	A1	IS	38	FALSE	NA
17JT03_1A	Chris Smart	2017	SummerSquash	Fruit	NY	Cayuga	Cayuga #1	A2	S	68	TRUE	NA
17JT04_1B	Chris Smart	2017	Zucchini	Fruit	NY	Cayuga	Cayuga #1	A1	S	18	FALSE	NA
17JT05_1A	Chris Smart	2017	Zucchini	Fruit	NY	Cayuga	Cayuga #1	A1	S	18	FALSE	NA
17JT06_1A	Chris Smart	2017	SummerSquash	Fruit	NY	Cayuga	Cayuga #1	A1	S	41	FALSE	NA
17JT07_1B	Chris Smart	2017	SummerSquash	Fruit	NY	Cayuga	Cayuga #1	A1	S	18	TRUE	NA

17JT09_1B	Chris Smart	2017	Zucchini	Fruit	NY	Cayuga	Cayuga #1	A2	S	98	TRUE	NA
17JT10_1A	Chris Smart	2017	Zucchini	Fruit	NY	Cayuga	Cayuga #1	A2	S	3	FALSE	NA
17JT12_2A	Chris Smart	2017	Zucchini	Fruit	NY	Cayuga	Cayuga #1	A2	S	3	FALSE	NA
17JT13_1A	Chris Smart	2017	Zucchini	Fruit	NY	Cayuga	Cayuga #1	A2	S	3	FALSE	NA
17JT14_1A	Chris Smart	2017	Zucchini	Fruit	NY	Cayuga	Cayuga #1	A1	R	63	TRUE	NA
17JT15_1A	Chris Smart	2017	Zucchini	Fruit	NY	Cayuga	Cayuga #1	A2	S	NA	FALSE	NA
17JT16_1A	Chris Smart	2017	Zucchini	Fruit	NY	Cayuga	Cayuga #1	A2	S	30	TRUE	NA
17JT18_1B	Chris Smart	2017	Zucchini	Fruit	NY	Cayuga	Cayuga #1	A2	S	30	FALSE	NA
17JT19_1A	Chris Smart	2017	Zucchini	Fruit	NY	Cayuga	Cayuga #1	A2	S	89	TRUE	NA
17JT20_2A	Chris Smart	2017	Zucchini	Fruit	NY	Cayuga	Cayuga #1	A2	S	3	FALSE	NA
17JT21_1A	Chris Smart	2017	Zucchini	Fruit	NY	Cayuga	Cayuga #1	A2	IS	3	FALSE	NA
17JT23_1A	Chris Smart	2017	Zucchini	Fruit	NY	Cayuga	Cayuga #1	A2	S	3	FALSE	NA
17JT24_1A	Chris Smart	2017	Zucchini	Fruit	NY	Cayuga	Cayuga #1	A2	S	3	FALSE	NA
17JT25_2A	Chris Smart	2017	Zucchini	Fruit	NY	Cayuga	Cayuga #1	A2	S	3	TRUE	NA
17JT26_1A	Chris Smart	2017	SummerSquash	Fruit	NY	Cayuga	Cayuga #1	A1	IS	101	TRUE	NA
17JT27_1A	Chris Smart	2017	SummerSquash	Fruit	NY	Cayuga	Cayuga #1	A1	S	41	TRUE	NA
17JT28_1A	Chris Smart	2017	Zucchini	Fruit	NY	Cayuga	Cayuga #1	A2	S	3	FALSE	NA
17EH01C	Chris Smart	2017	Squash	Fruit	NY	Ontario	Ontario #1	A1	S	90	TRUE	NA
17EH02A	Chris Smart	2017	Squash	Fruit	NY	Ontario	Ontario #1	A2	IS	6	FALSE	NA
17EH03_1B	Chris	2017	Squash	Fruit	NY	Ontario	Ontario #1	A1	S	33	FALSE	NA

	Smart											
17EH03_2B	Chris Smart	2017	Squash	Fruit	NY	Ontario	Ontario #1	A1	S	33	TRUE	NA
17EH04C	Chris Smart	2017	Squash	Fruit	NY	Ontario	Ontario #1	A1	S	34	FALSE	NA
17EH05A	Chris Smart	2017	Squash	Fruit	NY	Ontario	Ontario #1	A2	S	125	TRUE	NA
17EH07B	Chris Smart	2017	Squash	Fruit	NY	Ontario	Ontario #1	A1	S	34	TRUE	NA
17EH08A	Chris Smart	2017	Squash	Fruit	NY	Ontario	Ontario #1	A2	S	51	TRUE	NA
17EH09C	Chris Smart	2017	Squash	Fruit	NY	Ontario	Ontario #1	A2	IS	6	FALSE	NA
17EH10A	Chris Smart	2017	Squash	Fruit	NY	Ontario	Ontario #1	A2	S	NA	FALSE	NA
17EH11B	Chris Smart	2017	Squash	Fruit	NY	Ontario	Ontario #1	A2	R	6	FALSE	NA
17EH12A	Chris Smart	2017	Squash	Fruit	NY	Ontario	Ontario #1	A1	S	40	FALSE	NA
17EH13C	Chris Smart	2017	Squash	Fruit	NY	Ontario	Ontario #1	A2	S	32	FALSE	NA
17EH14B	Chris Smart	2017	Squash	Fruit	NY	Ontario	Ontario #1	A2	S	84	TRUE	NA
17EH15_2B	Chris Smart	2017	Squash	Fruit	NY	Ontario	Ontario #1	A1	S	25	TRUE	NA
17EH16A	Chris Smart	2017	Squash	Fruit	NY	Ontario	Ontario #1	A1	S	31	TRUE	NA
17EH17B	Chris Smart	2017	Squash	Fruit	NY	Ontario	Ontario #1	A2	S	NA	FALSE	NA
17EH18B	Chris Smart	2017	Squash	Fruit	NY	Ontario	Ontario #1	A1	S	25	FALSE	NA
17EH19A	Chris Smart	2017	Squash	Fruit	NY	Ontario	Ontario #1	A1	S	31	FALSE	NA
17EH20A	Chris Smart	2017	Squash	Fruit	NY	Ontario	Ontario #1	A1	S	28	FALSE	NA
17EH21C	Chris Smart	2017	Squash	Fruit	NY	Ontario	Ontario #1	A1	S	28	TRUE	NA
17EH22B	Chris Smart	2017	Squash	Fruit	NY	Ontario	Ontario #1	A2	S	32	TRUE	NA

17EH23C	Chris Smart	2017	Squash	Fruit	NY	Ontario	Ontario #1	A2	S	99	TRUE	NA
17EH24B	Chris Smart	2017	Squash	Fruit	NY	Ontario	Ontario #1	A2	S	92	TRUE	NA
17EH25C	Chris Smart	2017	Squash	Fruit	NY	Ontario	Ontario #1	A2	S	19	FALSE	NA
17EH26A	Chris Smart	2017	Squash	Fruit	NY	Ontario	Ontario #1	A2	S	19	FALSE	NA
17EH27C	Chris Smart	2017	Squash	Fruit	NY	Ontario	Ontario #1	A2	R	6	FALSE	NA
17EH29A	Chris Smart	2017	Squash	Fruit	NY	Ontario	Ontario #1	A1	S	124	TRUE	NA
17EH30B	Chris Smart	2017	Squash	Fruit	NY	Ontario	Ontario #1	A1	S	21	TRUE	NA
17EH31A	Chris Smart	2017	Squash	Fruit	NY	Ontario	Ontario #1	A1	S	21	FALSE	NA
17EH32A	Chris Smart	2017	Squash	Fruit	NY	Ontario	Ontario #1	A1	S	40	TRUE	NA
17EH33C	Chris Smart	2017	Squash	Fruit	NY	Ontario	Ontario #1	A2	S	19	TRUE	NA
17EH34A	Chris Smart	2017	Squash	Fruit	NY	Ontario	Ontario #1	A2	IS	6	FALSE	NA
17EH35B	Chris Smart	2017	Squash	Fruit	NY	Ontario	Ontario #1	A2	S	12	FALSE	NA
17EH36A	Chris Smart	2017	Squash	Fruit	NY	Ontario	Ontario #1	A2	S	12	FALSE	NA
17EH37A	Chris Smart	2017	Squash	Fruit	NY	Ontario	Ontario #1	A1	S	26	FALSE	NA
17EH38A	Chris Smart	2017	Squash	Fruit	NY	Ontario	Ontario #1	A2	S	112	TRUE	NA
17EH39A	Chris Smart	2017	Squash	Fruit	NY	Ontario	Ontario #1	A2	S	102	TRUE	NA
17EH40A	Chris Smart	2017	Squash	Fruit	NY	Ontario	Ontario #1	A2	S	27	FALSE	NA
17EH41A	Chris Smart	2017	Squash	Fruit	NY	Ontario	Ontario #1	A2	S	12	FALSE	NA
17EH42C	Chris Smart	2017	Squash	Fruit	NY	Ontario	Ontario #1	A2	IS	6	TRUE	NA
17EH44A	Chris	2017	Squash	Fruit	NY	Ontario	Ontario #1	A2	S	27	TRUE	NA

	Smart											
17EH45C	Chris Smart	2017	Squash	Fruit	NY	Ontario	Ontario #1	A2	S	37	FALSE	NA
17EH46B	Chris Smart	2017	Squash	Fruit	NY	Ontario	Ontario #1	A2	S	66	TRUE	NA
17EH47B	Chris Smart	2017	Squash	Fruit	NY	Ontario	Ontario #1	A2	S	37	TRUE	NA
17EH48C	Chris Smart	2017	Squash	Stem	NY	Ontario	Ontario #1	A1	S	119	TRUE	NA
17EH49A	Chris Smart	2017	Squash	Stem	NY	Ontario	Ontario #1	A1	S	26	TRUE	NA
17EH51B	Chris Smart	2017	Squash	Stem	NY	Ontario	Ontario #1	A2	S	12	TRUE	NA
17EH53A	Chris Smart	2017	Squash	Fruit	NY	Ontario	Ontario #1	A1	S	91	TRUE	NA
17EH54A	Chris Smart	2017	Squash	Fruit	NY	Ontario	Ontario #1	A2	S	67	TRUE	NA
17EH55B	Chris Smart	2017	Squash	Fruit	NY	Ontario	Ontario #1	A1	S	78	TRUE	NA
17EH56B	Chris Smart	2017	Squash	Fruit	NY	Ontario	Ontario #1	A2	S	86	TRUE	NA
17EH57B	Chris Smart	2017	Squash	Fruit	NY	Ontario	Ontario #1	A2	S	115	TRUE	NA
17EH58A	Chris Smart	2017	Squash	Fruit	NY	Ontario	Ontario #1	A1	S	54	TRUE	NA
17EH60A	Chris Smart	2017	Squash	Fruit	NY	Ontario	Ontario #1	A1	S	10	FALSE	NA
17EH61A	Chris Smart	2017	Squash	Fruit	NY	Ontario	Ontario #1	A1	S	10	FALSE	NA
17EH63A	Chris Smart	2017	Squash	Fruit	NY	Ontario	Ontario #1	A1	S	NA	FALSE	NA
17EH64A	Chris Smart	2017	Squash	Fruit	NY	Ontario	Ontario #1	A2	S	94	TRUE	NA
17EH65C	Chris Smart	2017	Squash	Fruit	NY	Ontario	Ontario #1	A1	S	128	TRUE	NA
17EH66B	Chris Smart	2017	Squash	Fruit	NY	Ontario	Ontario #1	A2	S	107	TRUE	NA
17EH67A	Chris Smart	2017	Squash	Fruit	NY	Ontario	Ontario #1	A2	S	93	TRUE	NA

17EH68A	Chris Smart	2017	Squash	Fruit	NY	Ontario	Ontario #1	A1	S	10	TRUE	NA
17EH69A	Chris Smart	2017	Squash	Fruit	NY	Ontario	Ontario #1	A1	S	82	TRUE	NA
17EH70A	Chris Smart	2017	Squash	Fruit	NY	Ontario	Ontario #1	A2	S	79	TRUE	NA
17EH71A	Chris Smart	2017	Squash	Fruit	NY	Ontario	Ontario #1	A1	S	97	TRUE	NA
17EH72B	Chris Smart	2017	Squash	Fruit	NY	Ontario	Ontario #1	A2	S	62	TRUE	NA
17EH73A	Chris Smart	2017	Squash	Fruit	NY	Ontario	Ontario #1	A1	S	10	FALSE	NA
17EH74A	Chris Smart	2017	Squash	Fruit	NY	Ontario	Ontario #1	A1	S	21	FALSE	NA
17EH75A	Chris Smart	2017	Squash	Fruit	NY	Ontario	Ontario #1	A1	S	109	TRUE	NA
17EH76B	Chris Smart	2017	Squash	Fruit	NY	Ontario	Ontario #1	A1	S	10	FALSE	NA
17EH77B	Chris Smart	2017	Squash	Fruit	NY	Ontario	Ontario #1	A1	S	114	TRUE	NA
4E_6A	Meg McGrath	2018	Squash	NA	NY	Suffolk	Suffolk #1	A1	S	95	TRUE	NA
4E_5A	Meg McGrath	2018	Squash	NA	NY	Suffolk	Suffolk #1	A2	S	76	TRUE	NA
STKY2_1A	Meg McGrath	2018	Pumpkin	NA	NY	Suffolk	Suffolk #2	A2	S	20	FALSE	NA
STKY2_3A	Meg McGrath	2018	Pumpkin	NA	NY	Suffolk	Suffolk #2	A2	S	20	TRUE	NA
STKY2_4A	Meg McGrath	2018	Pumpkin	NA	NY	Suffolk	Suffolk #2	A2	S	20	FALSE	NA
AND_1C	Meg McGrath	2018	Pumpkin	NA	NY	Suffolk	Suffolk #4	A1	R	71	TRUE	NA
AND_2A	Meg McGrath	2018	Pumpkin	NA	NY	Suffolk	Suffolk #4	A1	S	61	TRUE	NA
AND_4A	Meg McGrath	2018	Pumpkin	NA	NY	Suffolk	Suffolk #4	A1	S	105	TRUE	NA
LEWT2_3A	Meg McGrath	2018	Pumpkin	NA	NY	Suffolk	Suffolk #3	A1	S	NA	FALSE	NA
LEWT3_2A	Meg	2018	Pumpkin	NA	NY	Suffolk	Suffolk #3	A2	R	65	TRUE	NA

	McGrath											
LEWT3_3A	Meg McGrath	2018	Pumpkin	NA	NY	Suffolk	Suffolk #3	A2	R	NA	FALSE	NA
LEWT3_6A	Meg McGrath	2018	Pumpkin	NA	NY	Suffolk	Suffolk #3	A1	R	74	TRUE	NA
STK_5A	Meg McGrath	2018	Pumpkin	NA	NY	Suffolk	Suffolk #2	A1	S	77	TRUE	NA
3W_2A	Meg McGrath	2018	Pumpkin	NA	NY	Suffolk	Suffolk #1	A2	S	85	TRUE	NA
3W_7A	Meg McGrath	2018	Pumpkin	NA	NY	Suffolk	Suffolk #1	A2	S	129	TRUE	NA
3W_8A	Meg McGrath	2018	Pumpkin	NA	NY	Suffolk	Suffolk #1	A2	S	69	TRUE	NA
3W_10C	Meg McGrath	2018	Pumpkin	NA	NY	Suffolk	Suffolk #1	A2	S	127	TRUE	NA
NM_6300A	Kishor Bhattarai	NA	NA	NA	NM	NA	NonNY	A2	S	126	TRUE	NA
SJV_CAA	Kishor Bhattarai	NA	NA	NA	CA	NA	NonNY	A1	S	122	TRUE	NA
IMK328	Traven Bentley	NA	NA	NA	SC	NA	NonNY	A1	S	81	TRUE	NA
RCZ_1B	Traven Bentley	NA	NA	NA	SC	NA	NonNY	A2	S	83	TRUE	NA
C15A	Traven Bentley	NA	NA	NA	SC	NA	NonNY	A1	S	56	TRUE	NA
H8C	Traven Bentley	NA	NA	NA	SC	NA	NonNY	A2	S	110	TRUE	NA
GPS1_1A	Traven Bentley	NA	NA	NA	CA	NA	NonNY	A1	S	55	TRUE	NA
FL29	Brian Hill	NA	NA	NA	FL	NA	NonNY	A2	S	80	TRUE	NA
568OH	Brian Hill	NA	NA	NA	OH	NA	NonNY	A2	IS	52	TRUE	NA
SC_6B	Amara Dunn	2007	Pumpkin	Fruit	NY	Schenectady	Schenectady #1	A1	IS	113	TRUE	NA
MMZ_6A	Amara Dunn	2007	Pumpkin	Fruit	NY	Suffolk	Suffolk #5	A1	S	116	TRUE	Dunn et al. 2010; Parada-Rojas and Quesada-

												Ocampo 2018
G_3A_4A_C5	Amara Dunn	2006	Pepper	NA	NY	Monroe	Monroe #1	A1	S	111	TRUE	Dunn et al. 2010; Parada-Rojas and Quesada-Ocampo 2018 (labeled isolate 0664-1)
MMZ_15A	Amara Dunn	2007	Pumpkin	Fruit	NY	Suffolk	Suffolk #5	A2	S	50	TRUE	NA
SC_15C	Amara Dunn	2007	Pumpkin	Fruit	NY	Schenectady	Schenectady #1	A1	S	60	TRUE	NA
0752_14	Amara Dunn	2007	Zucchini	Fruit	NY	Herkimer	Herkimer #1	A1[a]	IS	108	TRUE	Dunn et al. 2010
MMZ_23A	Amara Dunn	2007	Pumpkin	Fruit	NY	Suffolk	Suffolk #5	A2	S	72	TRUE	Dunn et al. 2010
BWS_1A	Amara Dunn	2007	Squash	Fruit	NY	Rensselaer	Rensselaer #1	A1[a]	R	87	TRUE	Dunn et al. 2010
A2_6_1	Amara Dunn	2006	Squash	Fruit	NY	Ontario	Ontario #3	A2	S	100	TRUE	Dunn et al. 2010; Parada-Rojas and Quesada-Ocampo 2018 (labeled isolate 6180)
BWS_2B	Amara Dunn	2007	Squash	Fruit	NY	Rensselaer	Rensselaer #1	A2	S	117	TRUE	NA
1070_3	NA	NA	NA	NA	NY	NA	Other NY	A2	S	70	TRUE	NA
GT_1A	Amara Dunn	2007	Tomato	Fruit	NY	Schenectady	Schenectady #2	A1	R	58	TRUE	Dunn et al. 2010
14_51	NA	NA	NA	NA	NY	NA	Other NY	A1	S	96	TRUE	NA

2014_21	Maryn Carlson	2014	Eggplant	NA	NY	Columbia	Columbia #1	A2	S	57	TRUE	NA
14_55C	NA	NA	NA	NA	NY	NA	Other NY	A1	S	48	TRUE	NA
12889MIA	Mary Hausbeck	NA	Pepper	NA	MI	NA	NonNY	A1	R	104	TRUE	Foster and Hausbeck 2009
13EH02A	Maryn Carlson	2013	Squash	NA	NY	Ontario	Ontario #1	A2	S	42	TRUE	NA
13EH03A	Maryn Carlson	2013	Squash	NA	NY	Ontario	Ontario #1	A1	S	9	FALSE	NA
13EH04A	Maryn Carlson	2013	Squash	NA	NY	Ontario	Ontario #1	A2[a]	S	15	TRUE	NA
13EH05A	Maryn Carlson	2013	Squash	NA	NY	Ontario	Ontario #1	A2[a]	S	16	TRUE	NA
13EH06A	Maryn Carlson	2013	Squash	NA	NY	Ontario	Ontario #1	A1	NA	2	FALSE	NA
13EH08A	Maryn Carlson	2013	Squash	NA	NY	Ontario	Ontario #1	A1	S	24	TRUE	NA
13EH09A	Maryn Carlson	2013	Squash	NA	NY	Ontario	Ontario #1	A2	S	7	TRUE	NA
13EH10A	Maryn Carlson	2013	Squash	NA	NY	Ontario	Ontario #1	A2	S	1	FALSE	NA
13EH11A	Maryn Carlson	2013	Squash	NA	NY	Ontario	Ontario #1	A2[a]	S	1	FALSE	NA
13EH12A	Maryn Carlson	2013	Squash	NA	NY	Ontario	Ontario #1	A2	S	7	FALSE	NA
13EH13A	Maryn Carlson	2013	Squash	NA	NY	Ontario	Ontario #1	A1	S	2	FALSE	NA
13EH14A	Maryn Carlson	2013	Squash	NA	NY	Ontario	Ontario #1	A2	S	1	FALSE	NA
13EH16A	Maryn Carlson	2013	Squash	NA	NY	Ontario	Ontario #1	A2	S	7	FALSE	NA
13EH17A	Maryn Carlson	2013	Squash	NA	NY	Ontario	Ontario #1	A2[a]	S	1	FALSE	NA
13EH19A	Maryn Carlson	2013	Squash	NA	NY	Ontario	Ontario #1	A2	S	1	TRUE	NA
13EH20A	Maryn Carlson	2013	Squash	NA	NY	Ontario	Ontario #1	A1	S	24	FALSE	NA

13EH21A	Maryn Carlson	2013	Squash	NA	NY	Ontario	Ontario #1	A1	S	4	FALSE	Parada-Rojas and Quesada-Ocampo 2018
13EH22A	Maryn Carlson	2013	Squash	NA	NY	Ontario	Ontario #1	A1	NA	4	FALSE	NA
13EH24A	Maryn Carlson	2013	Squash	NA	NY	Ontario	Ontario #1	A1	NA	44	TRUE	NA
13EH26A	Maryn Carlson	2013	Squash	NA	NY	Ontario	Ontario #1	A1	S	16	FALSE	NA
13EH27A	Maryn Carlson	2013	Squash	NA	NY	Ontario	Ontario #1	A2	NA	15	FALSE	NA
13EH28A	Maryn Carlson	2013	Squash	NA	NY	Ontario	Ontario #1	A2	S	15	FALSE	NA
13EH29A	Maryn Carlson	2013	Squash	NA	NY	Ontario	Ontario #1	A1	NA	4	FALSE	NA
13EH31A	Maryn Carlson	2013	Squash	NA	NY	Ontario	Ontario #1	A1	S	4	TRUE	NA
13EH32A	Maryn Carlson	2013	Squash	NA	NY	Ontario	Ontario #1	A1	S	9	TRUE	NA
13EH33A	Maryn Carlson	2013	Squash	NA	NY	Ontario	Ontario #1	A2	S	7	FALSE	NA
13EH34A	Maryn Carlson	2013	Squash	NA	NY	Ontario	Ontario #1	A1	S	45	TRUE	NA
13EH35A	Maryn Carlson	2013	Squash	NA	NY	Ontario	Ontario #1	A2[a]	S	8	FALSE	NA
13EH36A	Maryn Carlson	2013	Squash	NA	NY	Ontario	Ontario #1	A2	S	8	FALSE	NA
13EH37A	Maryn Carlson	2013	Squash	NA	NY	Ontario	Ontario #1	A1	S	9	FALSE	NA
13EH38A	Maryn Carlson	2013	Squash	NA	NY	Ontario	Ontario #1	A2[a]	S	1	FALSE	NA
13EH40A	Maryn Carlson	2013	Squash	NA	NY	Ontario	Ontario #1	A2[a]	S	8	TRUE	NA
13EH42A	Maryn Carlson	2013	Squash	NA	NY	Ontario	Ontario #1	A1	NA	43	TRUE	NA
13EH43A	Maryn Carlson	2013	Squash	NA	NY	Ontario	Ontario #1	A1	S	9	FALSE	NA

13EH44A	Maryn Carlson	2013	Squash	NA	NY	Ontario	Ontario #1	A2	S	1	FALSE	NA
13EH45A	Maryn Carlson	2013	Squash	NA	NY	Ontario	Ontario #1	A2	S	1	FALSE	NA
13EH46A	Maryn Carlson	2013	Squash	NA	NY	Ontario	Ontario #1	A2	IS	23	TRUE	NA
13EH47A	Maryn Carlson	2013	Squash	NA	NY	Ontario	Ontario #1	A1	S	9	FALSE	NA
13EH48A	Maryn Carlson	2013	Squash	NA	NY	Ontario	Ontario #1	A2[a]	S	1	FALSE	NA
13EH49A	Maryn Carlson	2013	Squash	NA	NY	Ontario	Ontario #1	A2	NA	1	FALSE	NA
13EH51A	Maryn Carlson	2013	Squash	NA	NY	Ontario	Ontario #1	A1	NA	47	TRUE	NA
13EH53A	Maryn Carlson	2013	Squash	NA	NY	Ontario	Ontario #1	A1	NA	2	FALSE	NA
13EH54A	Maryn Carlson	2013	Squash	NA	NY	Ontario	Ontario #1	A1	S	2	FALSE	NA
13EH55A	Maryn Carlson	2013	Squash	NA	NY	Ontario	Ontario #1	A1	S	4	FALSE	NA
13EH57A	Maryn Carlson	2013	Squash	NA	NY	Ontario	Ontario #1	A1	NA	4	FALSE	NA
13EH58A	Maryn Carlson	2013	Squash	NA	NY	Ontario	Ontario #1	A1	NA	2	FALSE	NA
13EH59A	Maryn Carlson	2013	Squash	NA	NY	Ontario	Ontario #1	A2	S	1	FALSE	NA
13EH60A	Maryn Carlson	2013	Squash	NA	NY	Ontario	Ontario #1	A2	NA	23	FALSE	NA
13EH61A	Maryn Carlson	2013	Squash	NA	NY	Ontario	Ontario #1	A1	NA	4	FALSE	NA
13EH62A	Maryn Carlson	2013	Squash	NA	NY	Ontario	Ontario #1	A1	S	2	TRUE	NA
13EH65A	Maryn Carlson	2013	Squash	NA	NY	Ontario	Ontario #1	A1	NA	22	FALSE	NA
13EH66A	Maryn Carlson	2013	Squash	NA	NY	Ontario	Ontario #1	A2	S	8	FALSE	NA
13EH67A	Maryn Carlson	2013	Squash	NA	NY	Ontario	Ontario #1	A1	NA	2	FALSE	NA
13EH68A	Maryn	2013	Squash	NA	NY	Ontario	Ontario #1	A1	NA	2	FALSE	NA

	Carlson											
13EH69A	Maryn Carlson	2013	Squash	NA	NY	Ontario	Ontario #1	A1	NA	2	FALSE	NA
13EH70A	Maryn Carlson	2013	Squash	NA	NY	Ontario	Ontario #1	A2	NA	1	FALSE	NA
13EH71A	Maryn Carlson	2013	Squash	NA	NY	Ontario	Ontario #1	A2	NA	8	FALSE	NA
13EH72A	Maryn Carlson	2013	Squash	NA	NY	Ontario	Ontario #1	A2	NA	7	FALSE	NA
13EH73A	Maryn Carlson	2013	Squash	NA	NY	Ontario	Ontario #1	A1	NA	4	FALSE	NA
13EH74A	Maryn Carlson	2013	Squash	NA	NY	Ontario	Ontario #1	A1	NA	22	TRUE	NA
13EH75A	Maryn Carlson	2013	Squash	NA	NY	Ontario	Ontario #1	A1	S	2	FALSE	NA
13EH76A	Maryn Carlson	2013	Squash	NA	NY	Ontario	Ontario #1	A2[a]	S	16	FALSE	NA
13EH77A	Maryn Carlson	2013	Squash	NA	NY	Ontario	Ontario #1	A1	NA	2	FALSE	NA
13EH79A	Maryn Carlson	2013	Squash	NA	NY	Ontario	Ontario #1	A2	S	46	TRUE	NA
13EH81A	Maryn Carlson	2013	Squash	NA	NY	Ontario	Ontario #1	A2[a]	S	1	FALSE	NA
13EH83A	Maryn Carlson	2013	Squash	NA	NY	Ontario	Ontario #1	A2	NA	1	FALSE	NA
13EH84A	Maryn Carlson	2013	Squash	NA	NY	Ontario	Ontario #1	A2	S	1	FALSE	Parada-Rojas and Quesada-Ocampo 2018
13EH85A	Maryn Carlson	2013	Squash	NA	NY	Ontario	Ontario #1	A2	NA	1	FALSE	NA
13EH86A	Maryn Carlson	2013	Squash	NA	NY	Ontario	Ontario #1	A1	S	2	FALSE	NA
13EH88A	Maryn Carlson	2013	Squash	NA	NY	Ontario	Ontario #1	A2[a]	S	1	FALSE	NA

[a] Indicates mating type at point DNA was extracted, for isolates that showed different mating types when assayed at different time points.

Table S2.2: Copy number estimates for every linkage group in every isolate[a].

	Linkage group																	
	1	2	3	4	5	6	7	8	9	10	11	12	13	14	15	16	17	18
0752_14	2n	?	2n	2n	2n	?	?	2n	2n	2n	2n	2n	2n	2n	2n	2n	3n	?
1070_3	2n	2n	2n	2n	2n	2n	?	2n	?	?	2n	2n	2n	3n	2n	2n	?	?
12889MIA	?	?	3n	?	?	?	?	2n	?	2n	?	2n	?	?	2n	?	?	?
13EH02A	2n	2n	2n	2n	2n	2n	?	2n	2n	2n	2n	2n	2n	2n	2n	2n	2n	?
13EH03A	2n	2n	2n	2n	2n	2n	2n	2n	2n	2n	2n	2n	2n	2n	2n	2n	2n	?
13EH04A	2n	?	2n	2n	2n	2n	?	2n	2n	2n	2n	2n	2n	?	2n	2n	?	?
13EH05A	2n	2n	2n	2n	2n	2n	?	2n	2n	2n	2n	2n	?	2n	2n	2n	2n	NA
13EH06A	2n	2n	2n	2n	2n	2n	2n	2n	2n	2n	2n	2n	2n	2n	2n	2n	2n	?
13EH08A	2n	2n	2n	2n	2n	2n	2n	2n	2n	2n	2n	2n	2n	2n	2n	2n	2n	?
13EH09A	2n	2n	2n	2n	2n	2n	2n	2n	2n	2n	2n	2n	2n	2n	2n	2n	2n	NA
13EH10A	2n	?	2n	2n	2n	2n	2n	2n	2n	2n	2n	2n	2n	?	2n	2n	2n	NA
13EH11A	2n	2n	2n	2n	2n	?	2n	2n	2n	2n	2n	2n	2n	?	2n	2n	2n	NA
13EH12A	2n	2n	2n	2n	2n	2n	2n	2n	2n	2n	2n	2n	2n	2n	2n	2n	2n	NA
13EH13A	2n	2n	2n	2n	2n	2n	2n	2n	2n	2n	2n	2n	2n	2n	2n	2n	2n	?
13EH14A	2n	?	?	2n	2n	?	?	2n	?	2n	2n	2n	?	?	?	2n	?	NA
13EH16A	2n	2n	2n	2n	2n	2n	2n	2n	2n	2n	2n	2n	2n	2n	2n	2n	2n	NA
13EH17A	2n	2n	2n	2n	2n	2n	2n	2n	2n	2n	2n	2n	2n	2n	2n	2n	2n	NA
13EH19A	2n	2n	2n	2n	2n	2n	2n	2n	2n	2n	2n	2n	2n	2n	2n	2n	2n	NA
13EH20A	2n	2n	2n	2n	2n	2n	2n	2n	2n	2n	2n	2n	2n	2n	2n	2n	?	2n
13EH21A	2n	2n	2n	2n	2n	2n	2n	2n	2n	2n	2n	2n	2n	2n	2n	2n	?	?
13EH22A	2n	2n	2n	2n	2n	2n	2n	2n	2n	2n	2n	2n	?	2n	2n	2n	2n	2n
13EH24A	?	2n	2n	?	2n	2n	?	?	2n	2n	?	2n	?	?	?	2n	?	NA
13EH26A	2n	2n	2n	?	2n	2n	?	2n	2n	2n	2n	2n	?	2n	?	2n	2n	NA
13EH27A	2n	2n	2n	2n	2n	2n	2n	2n	2n	2n	2n	2n	2n	2n	?	2n	?	2n

13EH28A	2n	2n	2n	2n	2n	?	?	2n	2n	2n	2n	2n	2n	?	?	2n	?	?
13EH29A	2n	2n	2n	2n	2n	2n	2n	2n	2n	2n	2n	2n	2n	2n	2n	2n	2n	NA
13EH31A	2n	2n	2n	2n	2n	2n	2n	2n	2n	2n	2n	2n	2n	2n	2n	2n	2n	?
13EH32A	2n	2n	2n	2n	2n	2n	2n	2n	2n	2n	2n	2n	2n	2n	2n	2n	2n	2n
13EH33A	2n	2n	2n	2n	2n	2n	?	2n	2n	2n	2n	2n	2n	2n	?	2n	2n	NA
13EH34A	2n	?	?	?	2n	2n	?	2n	2n	2n	2n	2n	2n	2n	?	2n	2n	NA
13EH35A	2n	2n	?	2n	2n	2n	?	?	?	2n	?	?	?	?	?	2n	?	?
13EH36A	2n	2n	2n	?	2n	2n	?	2n	2n	2n	2n	2n	2n	2n	2n	2n	2n	2n
13EH37A	2n	2n	2n	2n	2n	2n	2n	2n	2n	2n	2n	2n	2n	2n	2n	2n	2n	2n
13EH38A	2n	2n	2n	2n	2n	3n	2n	2n	2n	2n	3n	2n	2n	2n	2n	2n	2n	NA
13EH40A	2n	2n	2n	2n	2n	2n	2n	2n	2n	2n	2n	2n	2n	2n	2n	2n	2n	2n
13EH42A	2n	2n	2n	2n	2n	2n	?	2n	2n	2n	2n	2n	2n	?	2n	2n	2n	2n
13EH43A	2n	?	2n	2n	2n	2n	?	2n	2n	2n	2n	2n	?	?	2n	2n	?	?
13EH44A	2n	2n	?	?	2n	?	2n	2n	2n	2n	2n	2n	?	?	2n	2n	2n	NA
13EH45A	2n	2n	2n	2n	2n	2n	2n	2n	2n	2n	2n	2n	2n	?	2n	2n	2n	NA
13EH46A	2n	2n	2n	?	?	?	?	2n	2n	2n	?	2n	?	?	?	?	2n	?
13EH47A	2n	2n	2n	2n	2n	2n	2n	2n	2n	2n	2n	2n	2n	2n	2n	2n	2n	?
13EH48A	2n	2n	2n	2n	2n	2n	2n	2n	2n	2n	2n	2n	2n	2n	2n	2n	2n	NA
13EH49A	2n	2n	2n	2n	2n	2n	2n	2n	2n	2n	2n	2n	2n	2n	?	2n	2n	NA
13EH51A	2n	2n	2n	2n	2n	2n	2n	2n	2n	2n	2n	2n	2n	2n	2n	2n	2n	?
13EH53A	2n	2n	2n	?	2n	?	?	2n	?	2n	2n	2n	2n	2n	2n	?	?	?
13EH54A	2n	2n	2n	2n	2n	2n	?	2n	2n	2n	2n	2n	2n	2n	2n	2n	?	?
13EH55A	2n	2n	?	?	2n	2n	?	2n	2n	2n	2n	2n	?	2n	?	2n	2n	NA
13EH57A	2n	2n	2n	?	?	2n	?	2n	2n	2n	2n	2n	2n	?	2n	2n	?	?
13EH58A	2n	2n	2n	3n	2n	?	2n	2n	?	2n	2n	2n	2n	2n	2n	2n	2n	2n
13EH59A	2n	2n	2n	2n	2n	2n	2n	2n	2n	2n	2n	2n	2n	2n	2n	2n	?	NA
13EH60A	2n	2n	2n	2n	2n	2n	2n	2n	2n	2n	2n	2n	2n	?	?	2n	2n	?
13EH61A	2n	2n	2n	2n	2n	2n	2n	2n	2n	2n	2n	2n	2n	2n	2n	2n	2n	?

13EH62A	2n	2n	2n	2n	2n	2n	?	2n	2n	2n	2n	2n	2n	2n	2n	2n	2n	2n
13EH65A	2n	2n	2n	?	?	2n	?	2n	?	2n	2n	2n	2n	2n	2n	?	2n	2n
13EH66A	2n	2n	2n	2n	2n	2n	2n	2n	2n	2n	2n	2n	2n	2n	2n	2n	2n	2n
13EH67A	2n	2n	2n	2n	2n	2n	2n	2n	2n	2n	2n	2n	2n	2n	2n	2n	2n	2n
13EH68A	2n	2n	2n	2n	2n	2n	2n	2n	2n	2n	2n	2n	2n	2n	2n	2n	2n	2n
13EH69A	2n	2n	2n	2n	2n	2n	?	2n	2n	2n	2n	2n	2n	2n	2n	2n	2n	2n
13EH70A	2n	2n	2n	2n	2n	2n	?	?	2n	2n	2n	2n	2n	?	2n	?	?	NA
13EH71A	2n	?	2n	2n	2n	2n	?	2n	2n	2n	?	2n	?	?	?	2n	?	?
13EH72A	2n	2n	2n	2n	2n	2n	2n	2n	2n	2n	2n	2n	2n	2n	2n	2n	2n	NA
13EH73A	2n	2n	2n	2n	2n	2n	2n	2n	2n	2n	2n	2n	2n	2n	2n	2n	2n	?
13EH74A	2n	?	2n	2n	2n	3n	?	2n	2n	2n	2n	2n	2n	2n	?	?	2n	?
13EH75A	2n	2n	2n	2n	2n	?	2n	2n	2n	2n	2n	2n	2n	2n	2n	2n	2n	?
13EH76A	2n	2n	2n	2n	2n	2n	?	2n	?	2n	2n	2n	?	?	?	2n	?	NA
13EH77A	2n	2n	2n	2n	2n	2n	?	2n	2n	2n	2n	2n	2n	2n	2n	2n	2n	?
13EH79A	2n	2n	2n	2n	2n	2n	?	2n	2n	2n	2n	2n	2n	2n	2n	2n	2n	2n
13EH81A	2n	2n	2n	2n	?	2n	?	2n	2n	2n	2n	2n	2n	?	2n	2n	?	NA
13EH83A	2n	2n	2n	2n	2n	2n	2n	2n	2n	2n	2n	2n	2n	2n	2n	2n	2n	NA
13EH84A	2n	2n	2n	2n	2n	2n	2n	2n	2n	2n	2n	2n	?	?	2n	2n	2n	NA
13EH85A	2n	2n	2n	2n	2n	2n	2n	2n	?	2n	2n	2n	2n	?	2n	2n	2n	NA
13EH86A	2n	2n	2n	2n	2n	?	?	2n	2n	2n	2n	2n	2n	2n	2n	2n	2n	?
13EH88A	2n	2n	2n	?	2n	2n	?	2n	?	2n	2n	?	2n	?	?	2n	?	NA
14_51	2n	?	?	?	?	?	?	?	2n	2n	2n	?	?	?	?	?	?	NA
14_55C	2n	2n	2n	2n	2n	2n	2n	2n	2n	2n	2n	2n	2n	2n	2n	2n	2n	2n
17DH01A	2n	2n	2n	2n	2n	3n	2n	2n	2n	2n	2n	2n	2n	2n	2n	2n	2n	2n
17DH02A	?	?	2n	?	?	?	2n	2n	?	?	?	?	?	?	?	?	?	?
17DH03A	2n	2n	2n	?	2n	2n	2n	2n	2n	2n	2n	2n	2n	2n	2n	2n	2n	2n
17DH04B	2n	?	?	?	?	?	?	?	?	?	?	?	?	?	?	?	?	NA
17DH05A	?	2n	?	?	2n	?	?	?	?	2n	?	?	?	?	2n	2n	?	?

17DH07A	2n	2n	2n	?	2n	2n	?	2n	2n	2n	2n	2n	2n	2n	2n	2n	2n	?
17DH09B	2n	2n	2n	2n	2n	2n	2n	2n	2n	2n	2n	2n	2n	2n	2n	2n	?	2n
17DH10B	2n	2n	2n	2n	2n	2n	?	2n	2n	2n	2n	2n	2n	?	2n	2n	2n	?
17DH12A	?	?	?	?	?	?	?	?	?	2n	?	?	?	?	?	?	?	NA
17DH14A	2n	2n	2n	?	2n	?	?	2n	2n	2n	2n	2n	?	2n	2n	2n	2n	?
17DH15A	?	?	2n	?	2n	?	?	?	2n	?	?	?	?	?	?	2n	2n	?
17DH16A	2n	2n	2n	2n	2n	2n	?	2n	2n	2n	2n	2n	2n	2n	?	2n	2n	?
17DH17A	2n	?	2n	?	2n	?	2n	2n	2n	2n	2n	?	?	?	?	2n	?	?
17DH18B	?	2n	?	?	?	NA	?	?	?	?	?	?	?	?	?	?	?	NA
17DH19B	2n	2n	?	?	2n	2n	?	2n	2n	?	2n	?	?	?	?	2n	?	?
17DH20B	2n	2n	2n	2n	2n	?	2n	2n	2n	2n	2n	2n	2n	2n	?	2n	?	NA
17DH21A	2n	2n	2n	2n	2n	2n	2n	2n	2n	2n	2n	2n	2n	2n	2n	2n	3n	2n
17EH01C	2n	?	?	?	?	?	?	?	?	?	?	?	?	?	?	?	?	NA
17EH02A	2n	?	?	?	2n	?	?	2n	2n	2n	2n	2n	2n	?	?	2n	?	NA
17EH03_1B	2n	2n	2n	?	?	?	?	2n	?	2n	?	?	?	?	2n	2n	?	2n
17EH03_2B	2n	2n	2n	2n	?	2n	2n	2n	2n	2n	2n	?	2n	2n	?	2n	3n	?
17EH04C	2n	2n	?	2n	2n	2n	2n	2n	2n	2n	2n	?	2n	2n	?	2n	2n	2n
17EH05A	?	2n	?	?	?	?	?	?	?	?	?	?	?	?	?	?	?	NA
17EH07B	2n	2n	2n	2n	2n	2n	2n	2n	2n	2n	2n	2n	2n	2n	2n	2n	2n	2n
17EH08A	2n	?	?	?	?	?	?	2n	?	?	?	?	?	?	?	?	?	?
17EH09C	NA	NA	NA	NA	NA	NA	NA	NA	NA	NA	NA	NA	NA	NA	NA	NA	NA	NA
17EH11B	2n	?	?	2n	2n	?	?	?	2n	?	?	?	?	?	?	?	?	NA
17EH12A	2n	?	?	?	?	?	?	?	?	2n	2n	?	?	?	?	2n	?	NA
17EH13C	?	?	?	?	?	?	?	?	2n	?	?	?	?	?	?	?	?	NA
17EH14B	2n	2n	2n	?	?	?	?	2n	2n	2n	2n	2n	2n	2n	?	3n	?	?
17EH15_2B	2n	2n	2n	2n	2n	2n	?	?	?	2n	2n	2n	?	?	?	2n	2n	?
17EH16A	2n	2n	2n	2n	2n	2n	?	?	2n	2n	2n	2n	2n	2n	2n	2n	2n	?
17EH18B	2n	?	2n	2n	2n	2n	?	?	2n	2n	?	2n	?	?	?	?	?	?

17EH19A	2n	?	2n	2n	?	?	?	2n	2n	2n	?	?	?	?	?	?	?	3n
17EH20A	3n	3n	?	?	3n	?	3n	3n	3n	3n	3n	3n	3n	?	3n	3n	3n	?
17EH21C	3n	3n	3n	3n	?	3n	3n	3n	3n	3n	3n	3n	3n	?	3n	3n	3n	3n
17EH22B	2n	2n	2n	2n	2n	2n	?	2n	2n	2n	2n	2n	2n	2n	?	2n	2n	2n
17EH23C	2n	?	2n	?	2n	?	?	?	?	?	2n	?	?	?	2n	?	?	?
17EH24B	2n	?	?	?	?	2n	?	?	?	2n	?	?	?	?	?	?	3n	NA
17EH25C	?	3n	?	NA	?	NA	NA	3n	?	?	?	?	?	NA	NA	?	NA	NA
17EH26A	2n	?	?	?	?	?	?	?	?	?	?	?	?	?	?	?	?	NA
17EH27C	2n	?	2n	?	2n	?	?	2n	?	2n	2n	?	2n	?	?	?	?	NA
17EH29A	2n	2n	?	2n	2n	?	?	2n	2n	2n	2n	2n	2n	?	?	?	?	NA
17EH30B	2n	2n	2n	2n	2n	?	2n	2n	2n	2n	?	2n	2n	?	2n	2n	2n	2n
17EH31A	2n	2n	2n	2n	2n	2n	2n	2n	2n	2n	2n	2n	2n	2n	2n	2n	2n	?
17EH32A	2n	?	?	?	?	2n	?	?	?	2n	?	?	?	?	?	?	?	?
17EH33C	2n	2n	2n	2n	3n	2n	?	2n	2n	2n	2n	?	2n	2n	2n	2n	2n	?
17EH34A	2n	2n	2n	2n	2n	2n	2n	2n	2n	2n	2n	2n	2n	2n	?	2n	2n	NA
17EH35B	2n	2n	2n	2n	2n	?	2n	2n	2n	2n	2n	?	2n	2n	2n	2n	2n	?
17EH36A	2n	?	2n	?	?	?	?	?	2n	2n	?	?	?	?	?	?	2n	?
17EH37A	2n	?	?	?	2n	?	?	2n	2n	2n	?	2n	?	?	?	?	?	NA
17EH38A	2n	2n	2n	?	2n	?	2n	2n	2n	2n	2n	?	2n	?	2n	2n	2n	NA
17EH39A	2n	2n	2n	2n	2n	2n	2n	2n	2n	2n	2n	2n	?	?	2n	2n	2n	2n
17EH40A	2n	2n	2n	2n	2n	2n	2n	2n	2n	2n	2n	2n	2n	2n	2n	2n	2n	NA
17EH41A	2n	2n	?	2n	2n	2n	?	2n	2n	2n	?	?	2n	2n	2n	2n	2n	?
17EH42C	2n	2n	2n	2n	2n	2n	2n	2n	2n	2n	2n	2n	2n	2n	?	2n	2n	NA
17EH44A	2n	2n	2n	2n	2n	2n	2n	2n	2n	2n	2n	2n	2n	2n	2n	2n	2n	NA
17EH45C	?	?	?	2n	2n	?	?	?	2n	2n	?	?	?	?	2n	?	?	?
17EH46B	2n	2n	2n	2n	2n	2n	?	2n	?	2n	2n	2n	2n	?	2n	?	?	?
17EH47B	2n	2n	2n	2n	2n	2n	?	2n	2n	2n	2n	2n	?	2n	?	2n	?	2n
17EH48C	2n	2n	?	?	2n	?	?	2n	2n	2n	2n	2n	?	?	?	2n	2n	?

17EH49A	2n	?	2n	2n	2n	2n	2n	2n	2n	2n	2n	2n	2n	?	?	?	2n	NA
17EH51B	2n	2n	2n	2n	2n	2n	2n	2n	2n	2n	2n	2n	2n	2n	3n	2n	3n	2n
17EH53A	2n	2n	?	2n	?	2n	2n	2n	?	2n	2n	?	2n	2n	?	2n	?	NA
17EH54A	2n	2n	?	2n	2n	2n	?	2n	2n	2n	2n	2n	2n	2n	?	2n	?	?
17EH55B	2n	2n	2n	2n	2n	2n	?	2n	2n	2n	2n	?	2n	?	?	2n	2n	?
17EH56B	2n	?	?	?	?	?	?	2n	?	2n	2n	?	?	?	?	?	2n	?
17EH57B	2n	?	2n	2n	2n	?	?	2n	?	2n	?	?	?	2n	2n	2n	?	NA
17EH58A	2n	2n	2n	2n	2n	2n	2n	2n	2n	2n	2n	2n	2n	2n	2n	2n	2n	2n
17EH60A	?	?	2n	?	?	?	?	?	?	?	?	?	2n	?	?	?	?	NA
17EH61A	2n	2n	2n	2n	2n	?	?	2n	?	2n	2n	?	?	2n	?	2n	2n	NA
17EH64A	2n	?	2n	?	?	?	?	?	?	?	2n	2n	?	?	?	?	?	?
17EH65C	2n	?	2n	?	?	?	?	?	?	?	2n	?	?	?	?	3n	?	?
17EH66B	2n	2n	2n	2n	2n	2n	2n	2n	2n	2n	2n	2n	2n	?	?	?	3n	2n
17EH67A	2n	?	2n	2n	2n	?	2n	?	?	2n	2n	2n	2n	2n	?	2n	2n	NA
17EH68A	2n	2n	2n	2n	2n	2n	?	2n	?	2n	2n	2n	2n	2n	2n	2n	2n	NA
17EH69A	?	?	?	?	2n	?	?	?	?	?	2n	?	?	?	?	?	?	NA
17EH70A	NA	NA	NA	NA	NA	NA	NA	NA	NA	NA	NA	NA	NA	NA	NA	NA	NA	NA
17EH71A	2n	?	?	?	2n	?	?	2n	2n	2n	2n	?	?	?	?	?	?	2n
17EH72B	2n	2n	2n	?	2n	2n	?	2n	2n	2n	2n	2n	2n	2n	?	2n	2n	?
17EH73A	2n	2n	2n	2n	2n	2n	?	2n	?	2n	?	?	2n	?	?	?	2n	NA
17EH74A	2n	2n	2n	2n	2n	?	?	2n	2n	2n	2n	2n	2n	?	2n	2n	3n	?
17EH75A	2n	2n	2n	2n	2n	?	?	2n	?	2n	2n	?	?	2n	2n	2n	2n	2n
17EH76B	2n	2n	?	?	?	?	?	?	?	?	?	?	2n	?	?	?	?	NA
17EH77B	2n	2n	2n	?	2n	?	?	2n	?	2n	2n	?	?	?	2n	?	2n	?
17JT01_1A	2n	2n	2n	?	2n	2n	?	2n	2n	2n	2n	2n	?	?	2n	2n	?	?
17JT02_1A	2n	2n	2n	?	?	?	?	?	?	2n	2n	?	2n	?	?	2n	2n	?
17JT03_1A	2n	2n	2n	2n	2n	2n	?	?	2n	2n	2n	2n	2n	?	?	2n	2n	?
17JT04_1B	2n	2n	2n	?	2n	3n	?	2n	2n	2n	2n	2n	?	2n	2n	2n	?	2n

17JT05_1A	?	?	?	?	?	?	?	?	?	?	?	?	?	?	?	2n	?	?
17JT06_1A	2n	2n	?	2n	2n	?	?	2n	2n	2n	2n	?	?	2n	2n	2n	?	?
17JT07_1B	2n	2n	2n	2n	2n	2n	?	2n	2n	2n	2n	2n	2n	2n	2n	2n	2n	?
17JT09_1B	2n	2n	?	2n	2n	?	?	2n	?	2n	?	?	2n	2n	?	?	?	2n
17JT10_1A	2n	2n	?	?	2n	?	?	2n	?	2n	?	2n	?	?	?	2n	?	?
17JT12_2A	2n	?	2n	2n	?	?	?	2n	?	2n	2n	?	?	2n	?	2n	?	?
17JT13_1A	?	?	?	?	?	?	?	?	?	2n	?	?	?	?	?	?	?	?
17JT14_1A	2n	2n	?	2n	2n	2n	?	2n	2n	2n	2n	2n	2n	2n	2n	2n	2n	2n
17JT16_1A	2n	2n	2n	2n	?	?	2n	2n	2n	2n	2n	2n	?	2n	2n	2n	2n	NA
17JT18_1B	2n	?	2n	?	2n	?	?	2n	2n	2n	2n	?	2n	2n	2n	2n	2n	NA
17JT19_1A	2n	2n	2n	?	?	2n	?	2n	2n	2n	2n	2n	2n	2n	2n	2n	?	?
17JT20_2A	2n	2n	2n	2n	2n	2n	?	2n	?	2n	2n	2n	2n	2n	?	2n	2n	2n
17JT21_1A	2n	?	2n	2n	?	?	?	?	?	2n	2n	2n	?	?	?	?	2n	?
17JT23_1A	2n	2n	2n	2n	2n	2n	?	2n	?	2n	2n	2n	2n	?	2n	2n	?	?
17JT24_1A	2n	2n	2n	2n	2n	?	2n	2n	?	2n	2n	2n	2n	?	2n	2n	?	?
17JT25_2A	2n	2n	2n	2n	2n	?	2n	2n	?	2n	2n	2n	2n	2n	2n	2n	2n	?
17JT26_1A	?	?	2n	?	?	?	2n	2n	2n	?	?	?	?	?	?	?	?	?
17JT27_1A	2n	2n	2n	2n	2n	2n	2n	2n	2n	2n	2n	2n	2n	?	?	2n	?	2n
17JT28_1A	2n	2n	?	2n	2n	?	?	2n	?	2n	?	2n	?	2n	?	2n	2n	?
17PZ01A	?	?	?	?	?	?	?	?	?	?	?	?	?	?	?	?	?	NA
17PZ02A	2n	2n	2n	2n	2n	?	?	2n	2n	2n	2n	2n	2n	2n	2n	2n	2n	2n
17PZ11A	2n	2n	2n	2n	2n	2n	2n	2n	2n	2n	2n	2n	2n	2n	2n	2n	2n	2n
17PZ12B	2n	?	2n	2n	2n	2n	?	2n	2n	2n	2n	?	?	?	?	2n	?	?
17PZ13A	2n	2n	2n	2n	2n	2n	2n	2n	?	2n	2n	2n	2n	2n	?	2n	2n	?
17PZ14A	2n	2n	2n	2n	2n	2n	2n	2n	?	2n	2n	2n	2n	?	2n	2n	2n	2n
17PZ16A	2n	?	2n	2n	2n	2n	2n	2n	?	2n	2n	2n	2n	?	2n	2n	?	?
17PZ17A	2n	2n	2n	2n	2n	2n	?	2n	2n	2n	2n	2n	2n	?	2n	2n	2n	?
17PZ18A	2n	2n	2n	2n	2n	2n	2n	2n	2n	2n	2n	?	2n	2n	?	2n	2n	?

17PZ20B	?	?	?	?	?	?	?	2n	?	?	?	?	?	?	?	?	?	?
17PZ21A	2n	2n	2n	2n	2n	2n	2n	2n	2n	2n	2n	2n	2n	2n	2n	2n	2n	2n
17PZ22A	2n	?	?	?	?	?	?	2n	?	?	?	?	?	?	?	?	?	?
17PZ23A	2n	2n	?	?	2n	?	?	?	2n	?	?	2n	?	?	?	2n	2n	?
17PZ26A	2n	?	?	2n	2n	?	?	2n	?	2n	2n	?	?	2n	?	?	2n	?
17PZ29A	2n	2n	2n	2n	2n	?	2n	2n	2n	2n	2n	2n	2n	2n	?	2n	?	?
18051_1A	?	?	?	?	?	?	?	2n	?	?	?	?	?	NA	?	?	?	NA
18052A	2n	?	?	?	?	?	?	?	2n	2n	?	?	?	2n	?	?	?	NA
18080A	2n	2n	2n	2n	2n	2n	?	2n	2n	2n	2n	?	2n	?	2n	?	2n	?
18RN01A	2n	2n	2n	2n	2n	2n	2n	2n	2n	2n	2n	2n	2n	2n	2n	2n	2n	2n
18RN02A	?	NA	NA	NA	NA	NA	NA	NA	NA	NA	NA	NA	NA	NA	NA	NA	NA	NA
18RN04B	2n	2n	?	?	2n	2n	?	2n	2n	2n	2n	2n	2n	?	?	2n	?	?
18RN05A	?	?	?	?	?	?	?	2n	?	2n	?	?	?	?	?	?	?	?
18RN06A	2n	2n	2n	2n	2n	?	?	?	2n	2n	2n	2n	2n	?	?	?	?	?
18RN08A	2n	2n	?	2n	2n	2n	2n	2n	2n	2n	2n	2n	2n	?	?	2n	2n	2n
18RN13A	2n	2n	?	?	?	?	?	?	?	2n	?	?	?	?	?	2n	?	NA
18RN14A	?	2n	?	?	?	?	?	?	?	?	?	?	?	?	?	?	?	NA
18RN15B	2n	2n	2n	2n	2n	2n	2n	2n	2n	2n	2n	2n	2n	2n	2n	2n	2n	2n
2014_21	?	?	?	?	?	?	?	?	?	?	?	?	?	3n	?	?	?	NA
3W_10C	?	?	?	?	?	?	?	?	?	2n	2n	?	?	?	?	?	?	NA
3W_2A	2n	2n	2n	2n	2n	2n	2n	2n	2n	2n	2n	2n	2n	2n	2n	2n	2n	2n
3W_7A	2n	2n	2n	2n	2n	2n	2n	2n	2n	2n	2n	2n	2n	2n	2n	2n	2n	?
3W_8A	2n	2n	2n	2n	?	2n	?	2n	2n	2n	2n	2n	2n	2n	2n	2n	2n	2n
4E_5A	2n	?	?	2n	?	?	?	?	?	2n	2n	?	?	2n	?	?	?	?
4E_6A	2n	2n	?	?	2n	2n	2n	2n	2n	2n	2n	2n	2n	?	?	2n	?	?
568OH	2n	?	2n	?	2n	2n	?	2n	2n	2n	2n	2n	?	?	?	2n	2n	?
A2_6_1	2n	2n	2n	2n	2n	2n	2n	2n	2n	2n	2n	3n	?	2n	2n	2n	2n	?
AND_1C	2n	?	2n	?	2n	?	?	?	?	2n	?	?	?	?	2n	2n	?	?

AND_2A	2n	2n	2n	2n	2n	?	2n	2n	2n	2n	2n	2n	2n	2n	2n	2n	2n	2n
AND_4A	2n	2n	2n	2n	2n	2n	2n	2n	2n	2n	2n	2n	2n	?	2n	2n	2n	?
BWS_1A	2n	2n	2n	2n	?	3n	2n	2n	2n	2n	2n	2n	3n	2n	3n	2n	?	3n
BWS_2B	2n	?	2n	?	2n	2n	?	?	2n	2n	2n	?	2n	2n	2n	2n	?	2n
C15A	2n	2n	2n	2n	2n	2n	2n	2n	2n	2n	2n	2n	2n	2n	2n	2n	2n	2n
FL29	?	2n	2n	3n	?	2n	?	2n	2n	3n	3n	3n	?	?	2n	?	?	?
G_3A_4A_C5	2n	2n	2n	2n	2n	2n	2n	2n	2n	2n	2n	2n	2n	2n	2n	2n	?	?
GPS1_1A	2n	2n	2n	2n	2n	3n	2n	2n	2n	2n	2n	2n	2n	2n	2n	2n	2n	2n
GT_1A	2n	?	?	?	2n	?	?	2n	2n	?	2n	?	?	?	?	?	?	?
H8C	2n	2n	2n	2n	2n	2n	2n	2n	2n	2n	2n	2n	2n	2n	2n	2n	2n	?
IMK328	2n	?	2n	?	2n	3n	?	?	2n	2n	2n	?	?	2n	?	2n	2n	?
LEWT3_2A	2n	2n	2n	2n	2n	?	?	2n	2n	2n	?	2n	2n	2n	2n	2n	?	?
LEWT3_6A	?	?	?	?	?	?	?	3n	?	?	?	?	?	?	?	?	?	NA
MMZ_15A	2n	2n	2n	?	2n	3n	2n	2n	2n	2n	2n	2n	2n	2n	2n	2n	2n	?
MMZ_23A	2n	2n	2n	2n	2n	3n	2n	2n	2n	2n	2n	2n	2n	2n	?	2n	3n	2n
MMZ_6A	2n	2n	2n	2n	2n	3n	2n	2n	2n	2n	2n	2n	2n	2n	2n	2n	2n	2n
NM_6300A	2n	2n	2n	2n	2n	2n	2n	2n	2n	2n	2n	2n	2n	2n	2n	2n	?	?
RCZ_1B	2n	2n	2n	2n	2n	2n	?	2n	?	2n	2n	2n	2n	?	?	2n	2n	?
SC_15C	2n	2n	2n	?	2n	2n	2n	2n	2n	2n	2n	?	2n	2n	2n	2n	3n	?
SC_6B	?	?	3n	?	3n	?	?	?	?	?	?	?	?	?	?	?	?	NA
SJV_CAA	2n	2n	2n	2n	2n	2n	?	2n	2n	2n	2n	?	2n	2n	2n	2n	2n	2n
STK_5A	2n	2n	2n	2n	2n	2n	2n	2n	2n	2n	2n	2n	2n	2n	2n	2n	2n	2n
STKY2_1A	2n	2n	2n	2n	2n	2n	2n	2n	2n	2n	2n	2n	2n	2n	2n	2n	2n	2n
STKY2_3A	2n	2n	2n	2n	2n	2n	2n	2n	2n	2n	2n	2n	2n	2n	2n	2n	2n	2n
STKY2_4A	2n	2n	2n	2n	2n	2n	2n	2n	2n	2n	2n	2n	2n	2n	2n	2n	2n	?

[a] 2*n* = statistical support for presence of 2 copies, 3*n* = statistical support for presence of 3 copies, ? = ambiguous copy number designation, NA = insufficient heterozygous markers on the linkage group for analysis

Table S2.3. Curated list of candidate genes, along with their KOG and IPR annotations, within the range of linkage disequilibrium (LD) decay of peak SNP associated with mefenoxam insensitivity.

Gene ID	Protein ID	ORF start position (bp)	ORF stop position (bp)	Distance to peak SNP (bp)[a]	KOG annotation	IPR annotation
fgenesh1_pg.PHYCAscaffold_62_#_1	20330	22463	26716	-164252	Pleiotropic drug resistance proteins (PDR1-15), ABC superfamily	ABC transporter-like;ABC transporter-like;CDR ABC transporter;AAA+ ATPase, core;ABC transporter-like
fgenesh1_pg.PHYCAscaffold_62_#_8	20337	110345	108642	-76370	NA	Biopterin transport-related protein BT1;MFS general substrate transporter
estExt2_fgenesh1_pm.C_PHYCAscaffold_620005	530348	114899	119014	-71816	Pleiotropic drug resistance proteins (PDR1-15), ABC superfamily	ABC transporter-like;ABC transporter-like;ABC-2 type transporter;AAA+ ATPase, core;ABC transporter-like
e_gw1.62.86.1	126238	142989	141670	-43726	Predicted transporter	Major facilitator superfamily MFS-1;MFS general substrate transporter
e_gw1.62.160.1	126230	144559	143202	-42156	Predicted transporter	Major facilitator superfamily MFS-1;Major facilitator superfamily;MFS general substrate transporter

estExt2_fgenesh1_pg.C_PHYCAscaffold_620022	536757	175009	174164	-11706	DNA-directed RNA polymerase III subunit	RNA polymerase III Rpc4
estExt2_Genewise1Plus.C_PHYCAscaffold_620123	554474	205528	204392	18813	rRNA processing protein Rrp5	RNA-processing protein, HAT helix
e_gw1.62.85.1	126220	221210	219951	34495	Predicted transporter	Major facilitator superfamily MFS-1;Major facilitator superfamily;MFS general substrate transporter
fgenesh2_kg.PHYCAscaffold_62_#_28_#_Contig1951.1	510557	250135	249076	63420	Uncharacterized membrane protein, predicted efflux pump	Multi antimicrobial extrusion protein MatE

[a] Distance to peak SNP (bp) was calculated as the physical distance of the peak SNP position from the open reading frame (ORF) start position.

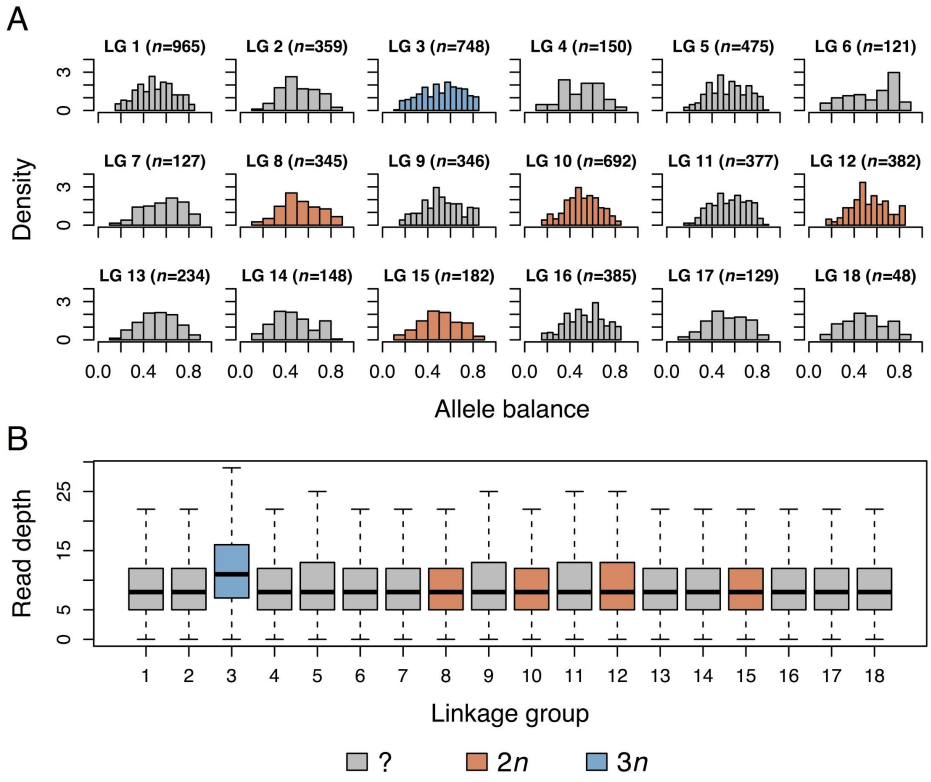

Figure S2.1: Example of ploidy level determination by linkage group in isolate 12889MIA. A) Distribution of allele balances within the 18 linkage groups of isolate 12889MIA. Number of heterozygous markers (*n*) is reported for each linkage group. B) Boxplot of SNP read depths per linkage group in isolate 12889MIA. The number of SNPs on each linkage group was down-sampled to the number on the linkage group having the fewest SNPs.

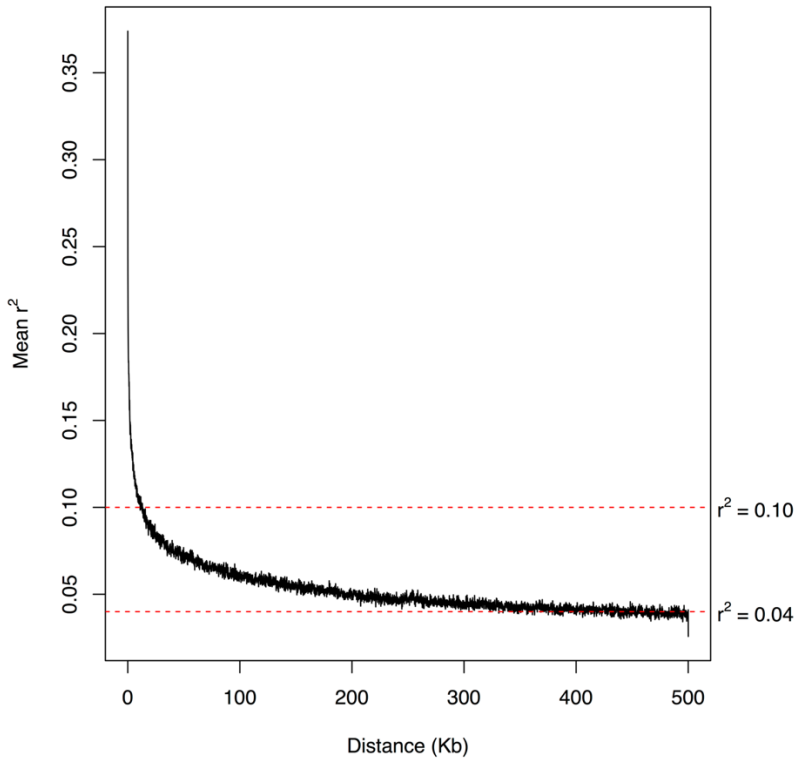

Figure S2.2: Pairwise linkage disequilibrium (r^2) between SNPs as a function of physical distance (Kb).

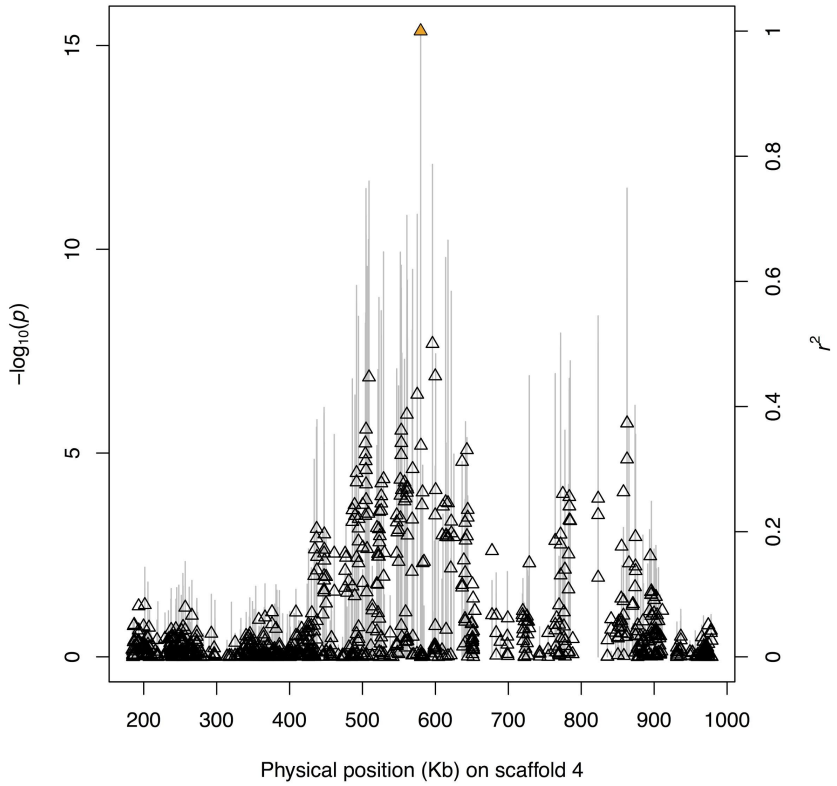

Figure S2.3: SNP *P*-values for association with mating type, represented by vertical lines, and linkage disequilibrium (r^2) with the peak SNP, represented by triangles. This plot shows the region bounded by 400 Kb on either side of the peak SNP. The orange triangle represents the peak SNP associated with mating type.

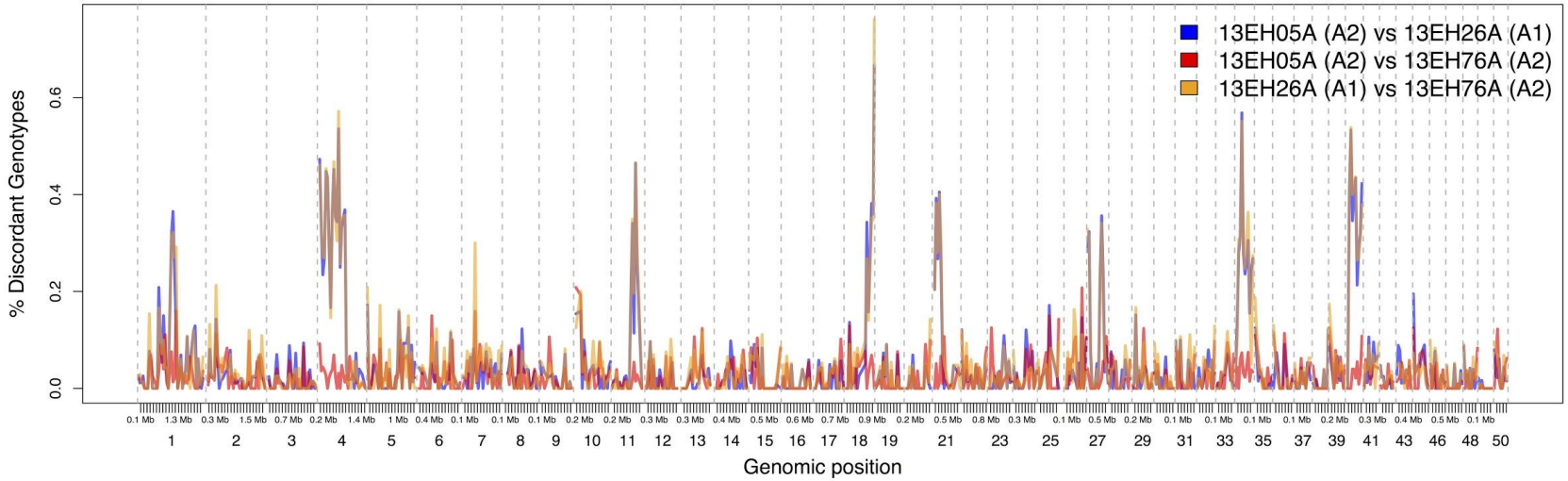

Figure S2.4: Percentage discordant genotypes in non-overlapping 50 Kb bins in pairwise comparisons between isolates 13EH05A, 13EH26A, and 13EH76A. The three isolates are members of the same clonal lineage, yet 13EH05A and 13EH76A are of the A2 mating type and 13EH26A is A1. Only the first fifty scaffolds are shown for simplicity, with scaffold 45 not included because it did not have any SNPs.

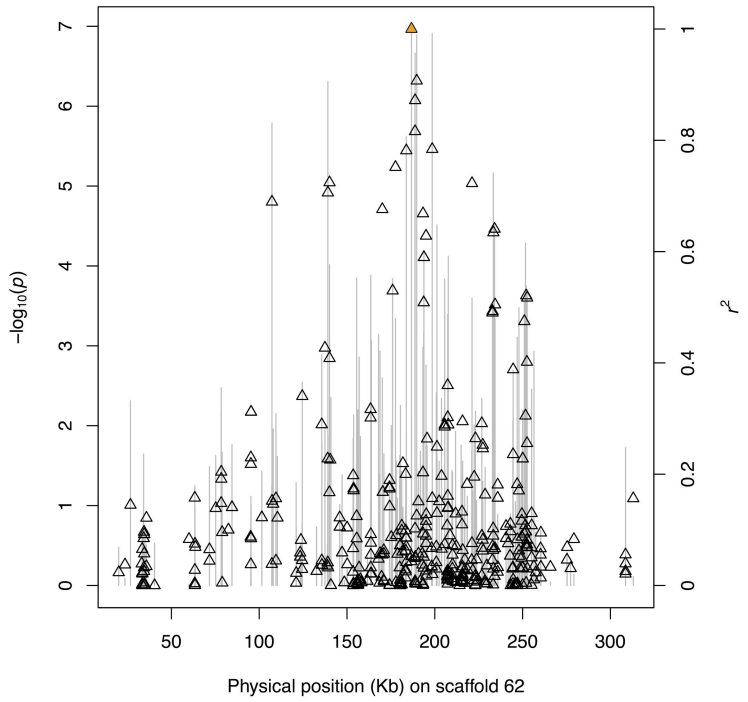

Figure S2.5: SNP *P*-values for mefenoxam insensitivity, represented by vertical lines, and linkage disequilibrium (r^2) with the peak SNP, represented by triangles, on scaffold 62. The orange triangle represents the peak SNP associated with mefenoxam insensitivity.

CHAPTER 3

GENETIC VARIATION IN *PHYTOPHTHORA CAPSICI* ASSOCIATED WITH VIRULENCE DIFFERENCES ON PEPPER

ABSTRACT

The development of pepper cultivars with durable resistance to oomycete *Phytophthora capsici* has been challenging due to differential interactions between the species that allow certain pathogen isolates to cause disease on otherwise resistant host genotypes. Currently, little is known in *P. capsici* about the genetic basis of virulence on pepper. We inoculated sixteen pepper accessions – representing commercial cultivars, sources of resistance, and host differentials – with 117 isolates of *P. capsici*, for a total of 1,866 host-pathogen combinations. With an informative subset of 8 pepper accessions and 105 pathogen isolates, we identified a significant effect of inter-species genotype-by-genotype interactions on disease outcomes, although these interactions were quantitative rather than qualitative in scale. Isolates from different pathogen subpopulations, as determined by a multivariate analysis of their genotypes at over 60,000 single-nucleotide polymorphism (SNP) loci, were not differentiated in terms of their absolute virulence levels on most individual pepper accessions. However, pathogen subpopulations did differ in terms of their relative virulence levels on certain pepper genotypes compared to others. A genome-wide association study resulted in the identification of one SNP, located inside a gene encoding a putative RXLR effector protein on *P. capsici* scaffold 39, that was significantly associated with virulence on all eight pepper accessions. However, we failed to identify any SNPs that were significantly associated with virulence on only a subset of host genotypes, consistent with the hypothesis that host specialization in *P. capsici* is controlled by

many genes of small effect.

INTRODUCTION

Populations of plant pathogens show both quantitative and qualitative variation in the disease caused by individual isolates on host plants. Qualitative differences in a pathogen's ability to cause disease, or its pathogenicity, are often the result of interactions between plant resistance (R) genes and pathogen avirulence (AVR) genes. In the classic gene-for-gene model, alleles at each of a single R and AVR gene interact to determine the presence or absence of disease (Flor 1955). On the other hand, virulence, or aggressiveness, is commonly defined as the quantitative extent of disease caused by a pathogen (Sacristán and García-Arenal 2008). Variation in virulence – and its counterpart in plants, quantitative disease resistance – is thought to be under polygenic control, governed by many genes of small effect (Pariaud et al. 2009; Nelson et al. 2018). Although it was once proposed that virulence and quantitative disease resistance were broad-spectrum in their effects (Van der Plank 1968), numerous examples of quantitative interactions between host and pathogen have since been described (Parlevliet 1976; Andrivon et al. 2007; Salvaudon et al. 2007). Recent genetic mapping and association studies in both plant and pathogen populations have identified pathogen virulence loci whose effects are conditional on host genotype (Hartmann et al. 2017; Meile et al. 2018; Stewart et al. 2018; Soltis et al. 2019), and conversely, quantitative disease resistance loci in plants whose effects are conditional on pathogen isolate (Qi et al. 1999; Zenbayashi-Sawata et al. 2005; Corwin et al. 2016; Wang et al. 2018). Nevertheless, the genetic basis of quantitative host-pathogen interactions remains poorly understood in many pathosystems.

Phytophthora capsici is a highly destructive, oomycete pathogen that causes root, crown,

and fruit rots on pepper (*Capsicum annuum*) and several other economically important host species in the Solanaceae, Cucurbitaceae, and Fabaceae families (Granke et al. 2012). As a hemibiotroph, *P. capsici* infects plants without initially causing noticeable disease symptoms, before rapidly transitioning to a necrotrophic phase of disease associated with substantial tissue death (Lamour et al. 2011). The early, biotrophic stage of disease caused by *P. capsici* is believed to be facilitated by the secretion of hundreds of small proteins known as effectors that suppress plant defense responses or play additional roles in virulence (Schornack et al. 2009; Jupe et al. 2013). Two families of effectors have been characterized in oomycetes: RXLRs (Morgan and Kamoun 2007) and CRNs (Torto et al. 2003), which are represented, respectively, by 573 and 84 predicted genes in the *P. capsici* genome (Jupe et al. 2013; Stam et al. 2013b). Virulence roles have been functionally verified for a number of these genes in *P. capsici* (Stam et al. 2013a; Mafurah et al. 2015; Fan et al. 2018; Chen et al. 2019; Li et al. 2019a, 2019b; Li et al. 2020).

The genetics of resistance to *P. capsici* in pepper have been characterized extensively. Several sources of resistance have been described, including Mexican serrano Criollos de Morelos 334 (CM 334; Guerrero-Moreno and Laborde 1980); Indian hot pepper Perennial (Lefebvre and Palloix 1996), and Central American hot pepper PI 201234 (Kimble and Grogan 1960). These accessions, and perhaps others, have been used commercially to breed resistant cultivars representing several different market classes of pepper. Mapping experiments using crosses with these sources of resistance have identified a major quantitative trait locus (QTL) on chromosome 5 of pepper that is shared by multiple resistant accessions and appears to demonstrate a consistent effect against a broad range of isolates (Thabuis et al. 2003; Ogundiwin et al. 2005; Truong et al. 2012; Mallard et al. 2013; Rehrig et al. 2014; Siddique et al. 2019). In

addition, numerous additional loci of smaller effect have been mapped that demonstrate evidence of having isolate-specific effects (Ogundiwin et al. 2005; Truong et al. 2012; Rehrig et al. 2014; Siddique et al. 2019).

As expected due to the existence of isolate-specific resistance in the host, *P. capsici* isolates vary in the extent of disease they cause on individual pepper genotypes. Certain pathogen isolates, for example, are able to overcome the resistance found in many commercial varieties (Foster and Hausbeck 2010; Parada-Rojas and Quesada-Ocampo 2019). *Phytophthora capsici* isolates have been classified into distinct physiological races using several different sets of differential host lines, including the New Mexico Recombinant Inbred Line (NMRIL) population, a set of recombinant inbred lines (RILs) derived from a cross between CM 334 and jalapeño variety Early Jalapeño (Oelke et al. 2003; Glosier et al. 2008; Sy et al. 2008; Hu et al. 2013). These experiments have resulted in race designations that are difficult to translate between populations because of the different lines used in each experiment and the large number of races identified by many researchers, who in several cases have determined that every isolate assayed in an experiment belongs to a separate race (Monroy-Barbosa and Bosland 2011; Barchenger et al. 2018; Reyes-Tena et al. 2019). Given the complexity of the interactions between pepper and *P. capsici*, and our limited understanding of the genes involved in these interactions, the standardization of race-typing protocols is a major challenge. Further knowledge of the genes underlying virulence variation in *P. capsici*, which remains largely unexplored compared to our understanding of the genetics of resistance in pepper, is needed.

Genetic studies using controlled crosses are possible in *P. capsici*, as recombinant oospores are produced readily in culture when isolates of opposite mating type are paired (Hurtado-Gonzalez and Lamour 2009). Genetic approaches have been used successfully to

determine the inheritance of traits such as fungicide sensitivity (Lamour and Hausbeck 2000) and pathogenicity on different host species (Polach and Webster 1972), but they can be challenging due to technical factors such as labor-intensive protocols for obtaining single-oospore cultures (Hurtado-Gonzalez and Lamour 2009) and biological factors such as frequent mitotic loss of heterozygosity in parental and progeny strains (Lamour et al. 2012; Carlson et al. 2017). The increased affordability of genome-wide markers obtained by next-generation sequencing have made genome-wide association studies (GWAS) an attractive alternative for exploring the genetic bases of traits in fungal and oomycete pathogens (Bartoli and Roux 2017; Plissonneau et al. 2017). Genome-wide association studies rely on historical recombination events to generate short segments of linkage disequilibrium (LD) across the genome. As a result, in pathogens that undergo frequent sexual reproduction, traits can be mapped with high resolution using natural collections of isolates from the field. Genome-wide association studies have been used to identify both qualitative and quantitative virulence loci in various fungal pathogens, including *Parastagonospora nodorum* (Gao et al. 2016), *Zymoseptoria tritici* (Hartmann et al. 2017; Zhong et al. 2017), and *Botrytis cinerea* (Soltis et al. 2019).

Recently, we used genotyping-by-sequencing (GBS) to characterize genetic variation in 245 isolates of *P. capsici*, collected largely in New York (NY) state, at over 60,000 single-nucleotide polymorphism (SNP) loci (Vogel et al. 2020). Using a subset of 129 genetically distinct (i.e. non-clonal) isolates, we found evidence for limited gene flow between pathogen subpopulations located on different farms, and discovered loci via GWAS associated with mating type and fungicide sensitivity (Vogel et al. 2020). In this project, we phenotyped 117 isolates from this genotyped panel for their virulence on each of 16 pepper accessions, with the goal of shedding light on the genetic architecture of virulence in *P. capsici* on pepper. Our

specific objectives were to: i) quantify the extent of genotype-by-genotype interactions between pepper and *P. capsici* and characterize patterns in isolate virulence profiles; ii) determine the degree of differentiation in virulence phenotypes between pathogen subpopulations collected on different farms; and iii) conduct a genome-wide association study to identify variants in *P. capsici* associated with virulence on one or multiple pepper accessions.

MATERIALS AND METHODS

Pepper accessions. Twelve pepper accessions were originally selected for inclusion in this study, and were chosen to represent either sources of disease resistance (CM334 and Perennial), lines used in previous publications as differential hosts (NMRIL-A, NMRIL-G, NMRIL-H, NMRIL-I, NMRIL-N, NMRIL-Z, and Early Jalapeño), or commercial bell pepper hybrids (Red Knight, Aristotle, and Paladin) developed for the eastern U.S., where the majority of the pathogen isolates in this study were collected. The six NMRIL lines included here were selected from the complete set of 76 NMRILs by consulting previously published data from race characterization experiments (Sy et al. 2008; Monroy-Barbosa and Bosland et al. 2011; Barchenger et al. 2018) and identifying lines whose resistance responses had high variances and low correlations between each other. The three bell pepper hybrids were chosen for their known, varying levels of overall Phytophthora root and crown rot resistance, with Red Knight highly susceptible and Aristotle and Paladin possessing low and intermediate levels of resistance, respectively (Dunn et al. 2013, 2014; Krasnow et al. 2017; Parada-Rojas and Quesada-Ocampo 2019). Of the three, Paladin is the only variety advertised as intermediately resistant by seed dealers. Because four of the NMRIL lines (NMRIL-A, NMRIL-H, NMRIL-I, and NMRIL-Z) showed complete resistance to almost all of the isolates in the first replicate of this experiment,

they were replaced in the second replicate with four additional bell pepper hybrids listed as intermediately resistant or tolerant to Phytophthora root rot in seed catalogs (Archimedes, Intruder, Revolution, and Vanguard).

Seed of commercial varieties were obtained from seed companies [Early Jalapeño: Johnny's Selected Seeds (Winslow, ME); Archimedes, Aristotle, and Red Knight: Stokes Seeds (Thorold, Ontario, CA), Paladin: Syngenta (Greensboro, NC); Intruder, Revolution, and Vanguard: Harris Seeds (Rochester, NY)]. Seed for the six NMRIL lines were obtained from Dr. Paul Bosland, seed for CM334 from Dr. Michael Mazourek, and seed for Perennial (PI 631147) from the National Plant Germplasm System (NPGS). Because of the limited quantity of seed available of these non-commercial accessions, seed was increased in a greenhouse at Cornell Agri-Tech in Geneva, NY in 2019. Three to four plants of each accession were grown in 3-gal pots and flowers were vibrated daily in order to promote self-pollination. Mature fruit from all plants within each accession were bulked and seed was extracted, washed with 10% trisodium phosphate, and dried at 24-28 °C for 1-2 days. PI 201234, obtained from the NPGS, was also grown for seed increase for inclusion in this experiment, but ultimately excluded due to morphological segregation between plants that suggested that the seed lot was highly heterogenous.

Pathogen isolates. The 129 genetically unique *P. capsici* isolates described in Vogel et al. (2020) were assayed for their degree of zoospore production and a subset of 117 isolates was identified that consistently sporulated in culture (data not shown). Two of these 117 isolates, 14-55 and 17PZ21A, were not included in the clone-corrected set described in Vogel et al., but were indirectly represented by a single-zoospore progeny in the case of 14_55 (14_55C) and by another isolate of the same clonal lineage in the case of 17PZ21A (17PZ18A). Isolates were

transferred from long-term hemp seed storage tubes (Vogel et al. 2020) to PARPH plates (Jeffers and Martin 1986) prior to conducting each replicate of disease assays. These PARPH plates were wrapped with parafilm (Beemis, Neenah, WI) and stored at room temperature until used for transferring of plugs for inoculum preparation.

Experimental design. Disease assays were conducted in greenhouses at Cornell Agri-Tech that were maintained at 29 °C day/ 23 °C night. The experiment was laid out as a split-plot design with pepper as the sub-plot treatment and isolate as the whole-plot treatment. Whole plots consisted of single 72-cell trays, with experimental units consisting of six-plant plots of peppers. Each tray, filled with soilless potting media, contained twelve plots randomly assigned one of the twelve pepper accessions and each tray was inoculated with one pathogen isolate.

Because of space and inoculum production constraints, the experiment was conducted in five batches, or incomplete blocks, per replicate. Each block contained 22-26 trays each inoculated with one of the 117 experimental isolates, in addition to one tray inoculated with water as a negative control, and three trays each inoculated with one of three check isolates. The three check isolates consisted of two isolates also represented among the 117 experimental isolates (SJV_CAA and 17EH01C) and an additional isolate (0664-1; Dunn et al. 2010). These checks were chosen for their differing degrees of overall virulence, based on preliminary data, and were included in every block in order to measure block-to-block variation in disease severity. Two complete replicates of the experiment were conducted. However, as mentioned previously, four of the twelve pepper accessions in Rep 1 were replaced with a different set of four accessions in Rep 2, resulting in eight pepper accessions with two observations (of six plants each) for each isolate and eight pepper accessions with only one observation (of six plants) for each isolate. In addition, three isolates failed to sporulate in one of two reps and were

therefore only included in one rep.

Peppers were inoculated at five weeks of age. Prior to inoculation, any cells of a tray where seed did not germinate were replaced with plants from a back-up set in order to ensure that all plots contained six plants. Plants were inoculated with a zoospore suspension that was pipetted to the potting soil surface directly adjacent to each pepper stem. Each plant was inoculated with a total of 10^5 zoospores. To prepare inoculum, isolates were plated on 15% unfiltered V8 agar and incubated at room temperature with 15 h of fluorescent lighting per day for 7, 10, or 14 days, depending on the isolate. Plates were flooded with distilled water and an L-shaped spreading rod was used to dislodge sporangia from the surface of plates, which were then collected in flasks and incubated at room temperature for 30-60 min to promote the release of zoospores. Zoospore concentrations were measured using a hemocytometer and solutions were diluted to the desired final concentration for inoculating.

Plots were rated for incidence of mortality at 4, 6, 8, 11, 13, and 15 days post inoculation (dpi). Plants were declared dead when they had fewer than two non-wilting, fully expanded leaves attached. Mortality ratings at the six time points were then used to calculate the Area Under the Disease Progress Curve (AUDPC; Shaner and Finney 1977) for each plot.

Statistical analysis of virulence experiment. The dataset was filtered to remove observations corresponding to negative controls, isolates that did not cause disease on any pepper accession, or pepper accessions on which fewer than 20% of isolates were able to kill at least one plant in both reps. The following mixed linear model was then fit:

$$Y_{ijklm} = \mu + P_i + I_j + PI_{ij} + R_k + B(R)_{kl} + T(B\times R)_{klm} + e_{ijklm} \quad (1)$$

where Y_{ijklm} are observations, μ is the intercept, P_i is the fixed effect of the *i*th pepper accession, I_j is the fixed effect of the *j*th isolate, PI_{ij} is the fixed effect of the interaction of the *i*th pepper

accession and the *j*th isolate, R_k is the fixed effect of the *k*th replicate, $B_l \sim iidN(0, \sigma_B^2)$ is the random effect of the *l*th incomplete block nested in the *k*th replicate, $T_m \sim iidN(0, \sigma_T^2)$ is the random effect of the *m*th tray nested in the l*th* block in the *k*th replicate (e.g. whole plot error term), and $e_{ijklm} \sim iidN(0, \sigma_e^2)$ is the residual error effect. This model was fit twice using different subsets of the data. First, in order to conduct significance tests of model terms, it was fit using a balanced subset of the data that featured only pepper accessions included in both replicates. Fixed effects were tested with incremental F tests using the Kenward-Roger approximation for calculation of denominator degrees of freedom (Kenward and Roger 1997). Random terms were tested using likelihood ratio tests. The model was then fit with the full dataset in order to calculate least squares means (LS means) for each isolate, pepper, and isolate × pepper combination, including for peppers on which only one replicate of each isolate was observed. These LS means were used in all downstream data analyses, such as GWAS.

In addition, the data were sub-divided into separate datasets for each of the pepper accessions included in both reps, in order to calculate broad-sense heritability (H^2) for virulence on these peppers. The following model was fit for each pepper-specific dataset:

$$Y_{ijk} = \mu + R_i + I_j + B(R)_{ik} + e_{ijk} \quad (2)$$

where Y_{ijk} are observations, μ is the intercept, R_i is the fixed effect of the *i*th replicate, $I_j \sim iidN(0, \sigma_I^2)$ is the random effect of the *j*th isolate, $B_k \sim iidN(0, \sigma_B^2)$ is the random effect of the *k*th incomplete block nested in the *i*th replicate, and $e_{ijk} \sim iidN(0, \sigma_e^2)$ is the residual error effect. Broad-sense heritabilities, calculated on an entry-mean basis, were then estimated using the following formula:

$$H^2 = \frac{\sigma_I^2}{\sigma_I^2 + \frac{\sigma_e^2}{r}} \quad (3)$$

where *r* is the harmonic mean of the number of observations per isolate on a given pepper.

Models were fit using the ASReml-R v 4 package (Butler et al. 2009). LS means were calculated using the *predict()* function. Heritabilities for virulence and their associated standard errors were calculated using the *vpredict()* function.

Virulence stability, or the relationship between the disease caused by individual isolates on a pepper and the average disease severity of that pepper, was assessed by using the following model, originally conceived for the analysis of genotype × environment interactions in crop varieties (Finlay and Wilkinson 1963; Eberhart and Russell 1966):

$$Y_{ij} = \mu_i + \beta_i P_j + e_{ij} \quad (4)$$

where Y_{ij} are LS means for AUDPC for the *i*th isolate on the *j*th pepper, μ_i is an intercept for the *i*th isolate, $\beta_i$is the regression coefficient (i.e. slope) for the *i*th isolate denoting its response to an increase in the overall susceptibility of its pepper host, P_j are AUDPC LS means for the *j*th pepper, averaged across isolates, and e_{ij} is the residual error associated with the *i*th isolate and the *j*th pepper. Three parameters from this model were used to interpret the extent of virulence stability for each isolate: μ_i, the intercept, and β_i, the slope, as in Finlay and Wilkinson (1963), as well as the mean squared error (MSE), as in Eberhart and Russell (1966). These models were fit using the lm() function in R.

Genotype data. The clone-corrected genotyping-by-sequencing SNP dataset from Vogel et al. (2020) was subset to include only those isolates that were phenotyped in this experiment and pathogenic on at least one pepper accession. This SNP set was then filtered to remove sites with minor allele frequency < 0.05. Genotypes for isolates 14_55C and 17PZ18A were assigned to the phenotypic records for isolates 14_55 and 17PZ21A, respectively. For all downstream analyses that required complete genotype data, such as GWAS and principal components

analysis, missing genotype calls were imputed with the mean allele dosage for that marker.

Association between population structure and virulence. Principal component (PC) analysis of both genotypic and phenotypic data (i.e. LS means for isolate × pepper interactions) was performed using the R function *prcomp()*, using centered and unit variance-scaled variables with mean-imputed missing data. The number of genotypic PCs selected for inclusion in analysis was determined by visually identifying the "elbow" in a PCA scree plot. Similarly, to choose the optimal number of clusters for k-means clustering of the genotypic PCA, the k-means algorithm was run with values for the number of clusters ranging from 2 to 10 and the "elbow" was identified in a plot of total within-cluster sum of squares as a function of the number of clusters. Analysis of variance, using the R functions *lm()* and *anova()*, was used to test the association between genetic cluster assignment and both phenotypic PCs and AUDPC LS means on individual peppers. *P*-values were Bonferroni-adjusted within families of related tests.

Genome-wide association study. Virulence traits used as responses in GWAS included across-pepper virulence (LS means for the isolate main effect), pepper accession-specific virulence (LS means for isolate × pepper combinations), and PCs 2-4 of the matrix of isolate × pepper LS means. Because of the non-normal distributions of virulence traits, phenotypes were log-transformed if the transformation resulted in a more normal distribution, as indicated by the Shapiro-Wilk test of normality statistic, implemented in the R function *shapiro.test()*. Prior to log-transformation, a constant was added to the phenotype to make the minimum value equal to 1. A model testing procedure was performed to identify the most appropriate covariates to include in GWAS to control for inflated Type I error caused by population structure. For each phenotype, null models (i.e. models that did not test individual SNP effects) were fit for each phenotype with up to the first four principal components of the marker matrix as fixed effects

and both with and without a random effect for isolate with a covariance structure defined by a genomic relationship matrix (GRM). The GRM was estimated using the *A.mat()* function in the R package rrBLUP (Endelman 2011). The model with the lowest value of the Akaike information criterion (Sakamoto et al. 1986) was then used for GWAS. Markers were declared significantly associated with a trait if they surpassed a 10% False Discovery Rate (FDR) threshold, as identified after using the R function *p.adjust()* to adjust raw *P*-values. Model testing and GWAS were performed using the GENESIS R package (Gogarten et al. 2019). The R package qqman was used to create Manhattan and Q-Q plots (Turner 2014).

Effector gene annotation. To identify the positions of putative effector genes in the *P. capsici* genome, the 573 gene sequences used in an effector target enrichment sequencing project (Thilliez et al. 2018) were aligned against the *P. capsici* reference genome (Lamour et al. 2012) using blastn (Camacho et al. 2009).

RESULTS

Host-isolate interactions in pepper-*P. capsici* pathosystem. Seedlings of sixteen pepper accessions were inoculated in a greenhouse experiment with each of 117 genetically distinct isolates of *P. capsici*, for a total of 2,784 measurements of mortality-based AUDPC, representing 1,866 distinct host × isolate combinations. Of the 117 isolates, 12 failed to cause disease on a single pepper accession in either replicate of the experiment. These non-pathogenic isolates were disproportionately represented by a single field population (Ontario #1) from 2013 that was maintained in long-term storage for longer than the majority of the isolates in this experiment, and the 12 isolates were subsequently excluded from analysis. Of the sixteen pepper accessions, eight were completely resistant to over 80% of the remaining isolates (FigureS3.1).

These accessions – comprised of resistant landrace CM334, hybrid bell pepper Intruder, and the six NMRIL differential lines – were excluded from analysis as well, leaving a dataset consisting of 105 isolates and eight pepper accessions: landrace Perennial, open-pollinated variety Early Jalapeño, and six hybrid bell peppers (Archimedes, Aristotle, Paladin, Red Knight, Revolution, and Vanguard).

Table 3.1: Test statistics and *P*-values associated with fixed effects in model testing the effects of isolate, pepper accession, and their interaction on AUDPC.

	Df	Denominator DF	F statistic	*P*-value
Isolate	107	119.5	11.07	2.5×10^{-32}
Pepper	4	516	851.3	1.3×10^{-225}
Isolate × Pepper	428	516	3.98	4.5×10^{-49}
Rep	1	7	0.66	0.44

Mixed linear models were fit to estimate the effects of pepper, pathogen isolate, and pepper-isolate interaction on AUDPC. Analysis of variance in a balanced dataset that excluded three pepper accessions (Archimedes, Revolution, and Vanguard, each included in a single replicate) revealed highly significant effects for pepper accession ($P = 2.5 \times 10^{-32}$), *P. capsici* isolate ($P = 1.3 \times 10^{-225}$), and their interaction ($P = 4.5 \times 10^{-49}$) (Table 3.1). Of the experimental design terms included in the model, block ($P = 4.7 \times 10^{-7}$) and tray ($P = 1.5 \times 10^{-12}$) had significant effects on AUDPC, whereas replicate ($P = 0.44$) did not (Table 3.1; Table 3.2). Block and tray collectively accounted for 36.03% of the variance explained by random terms in the

model.

Model-adjusted AUDPC means (i.e. least squares means) were estimated for each isolate-pepper combination using a linear model fit with the whole dataset, including the three pepper accessions included in only one replicate. Broad-sense heritability estimates for isolate virulence, as estimated in nested models fit separately for each pepper, were moderate to high, ranging from 0.72 in the case of Early Jalapeño to 0.93 in the case of Red Knight (Table 3.3), indicating that AUDPC phenotypes were largely consistent between experimental replicates. Virulence, as reflected by AUDPC LS mean, was non-normally distributed on each of the eight pepper accessions (Figure 3.1). On Red Knight, which was on average the most susceptible of the eight peppers with a median AUDPC of 52.8 (Table 3.3), virulence had a bimodal distribution, with the majority of isolates able to cause high levels of disease but a smaller, yet substantial, subset of isolates causing low plant mortality. On the remaining pepper accessions, virulence distributions had a mode closer to zero, although they featured heavy right tails, especially in the case of Aristotle, which was almost uniformly distributed. Early Jalapeño, Paladin, and Archimedes were the most resistant peppers overall (median AUDPCs of 2.55, 2.02, and 3.27, respectively), and while still they still featured skewed AUDPC distributions, they had less dense right tails, with only a small number of outlier isolates able to cause high levels of disease. Hierarchical clustering of peppers in terms of similarity in their resistance levels to the 105 isolates showed that accessions did not group based on their market class or improvement status, as hot pepper landrace Perennial clustered with bell pepper hybrids Aristotle, Revolution and Vanguard, and similarly, Early Jalapeño clustered with bell pepper hybrids Paladin and Archimedes (Figure 3.1).

Table 3.2: Variances explained by random effects and their test statistics and *P*-values in model testing the effects of isolate, pepper, and their interaction on AUDPC.

	Variance	Variance as percent of total (%)	LRT[a] statistic	*P*-value
Block	18.09	16.4	25.39	4.7×10^{-7}
Tray	21.65	19.63	50.07	1.5×10^{-12}
Error	70.53	63.96	NA	NA

[a] Likelihood ratio test

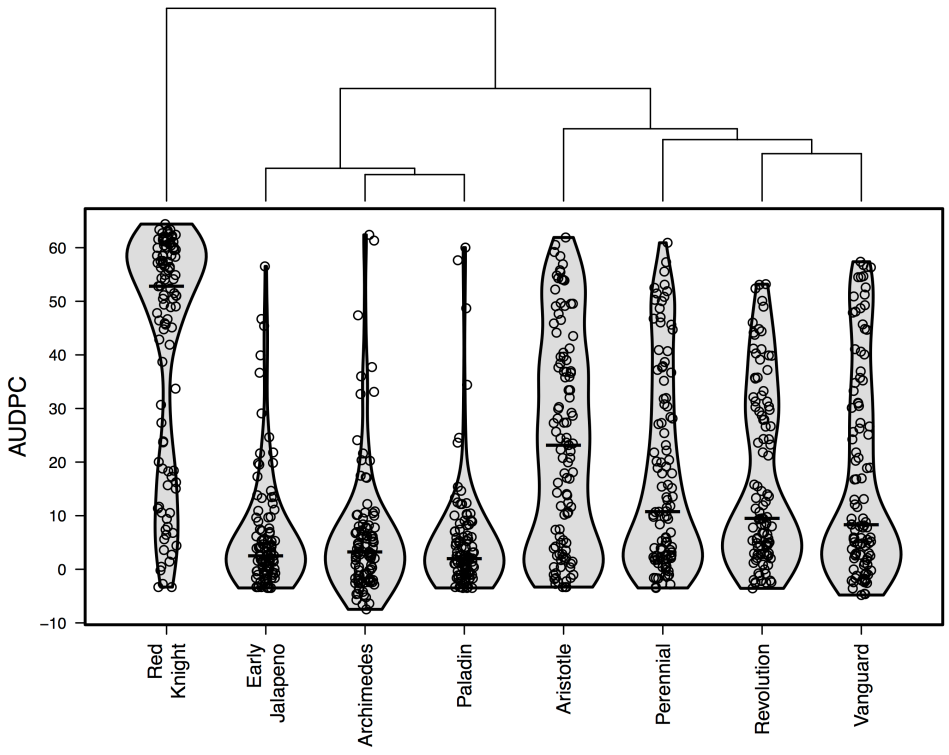

Figure 3.1. Distributions of AUDPC LS means among 105 isolates on each of 8 pepper accessions. Dendrogram created by hierarchical clustering of peppers based on the Euclidian distance between their AUDPC for each isolate.

Table 3.3: Medians and broad-sense heritabilities for AUDPC on each pepper accession.

Pepper	Median AUDPC	H^{2} [a]	SE[a]
Archimedes	3.27	NA	NA
Aristotle	23.18	0.85	0.03
Early Jalapeño	2.55	0.72	0.05
Paladin	2.02	0.81	0.04
Perennial	10.74	0.78	0.04
Red Knight	52.8	0.93	0.01
Revolution	9.49	NA	NA
Vanguard	8.34	NA	NA

[a] Heritabilities and standard errors are not shown for pepper accessions only included in one replicate.

Visualization of the virulence profiles of the 105 isolates on each pepper revealed a diversity of phenotypic patterns (Figure 3.2). In general, individual isolates tended to cause higher disease on peppers that were more susceptible on average. However, many exceptions were observed where peppers differed in rank in terms of their susceptibility to individual isolates compared to their overall susceptibility across isolates.

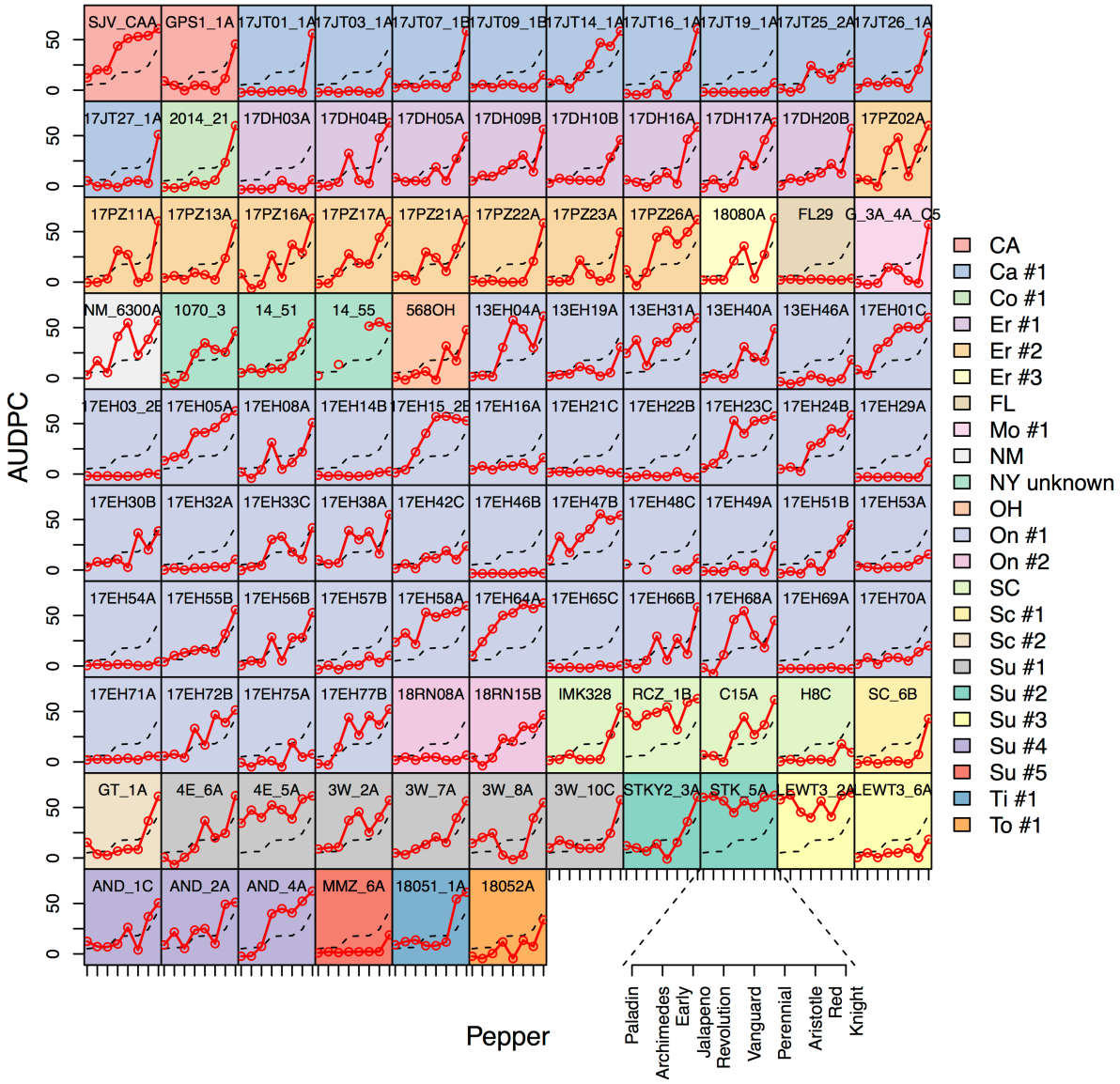

Figure 3.2: Isolate virulence profiles. Each subplot shows the AUDPC LS mean for a particular isolate on each of 8 pepper accessions in red. The black dashed line signifies the mean AUDPC for pepper, averaged across isolates. Each background color refers to a distinct field site, or state if collected outside NY. CA=California; Ca=Cayuga County, NY; Co=Columbia County, NY; Er=Erie County, NY; FL=Florida; Mo=Monroe County, NY; NM=New Mexico; OH=Ohio; On=Ontario County, NY; SC=South Carolina; Sc=Schenectady County, NY; Su=Suffolk County, NY; Ti=Tioga County, NY; To=Tompkins County, NY.

We explored the relationship between individual isolate virulence profiles and average pepper susceptibility levels by regressing the AUDPC associated with each isolate pepper combination on the average AUDPC for pepper, akin to Finlay-Wilkinson analysis, a technique used for characterizing the yield stability of crop varieties in different environments (Figure 3.3). Isolates fell into one of several categories based on their regression slopes and intercepts (Figure 3.3A-B). The majority of regression lines had a low intercept and a slope between 1 and 1.5, corresponding to isolates with average or higher than average virulence on more susceptible peppers and average or lower than average virulence on more resistant peppers. Another subset of regression lines had both intercept and slope close to 0, reflecting isolates with consistently low virulence across all of the pepper accessions in the experiment. Finally, the regression lines for four isolates (LEWT3_2A, STK_5A, RCZ_1B, and 4E_5A) had a low slope but a high intercept. These were the only isolates observed to be highly virulent on all eight pepper accessions.

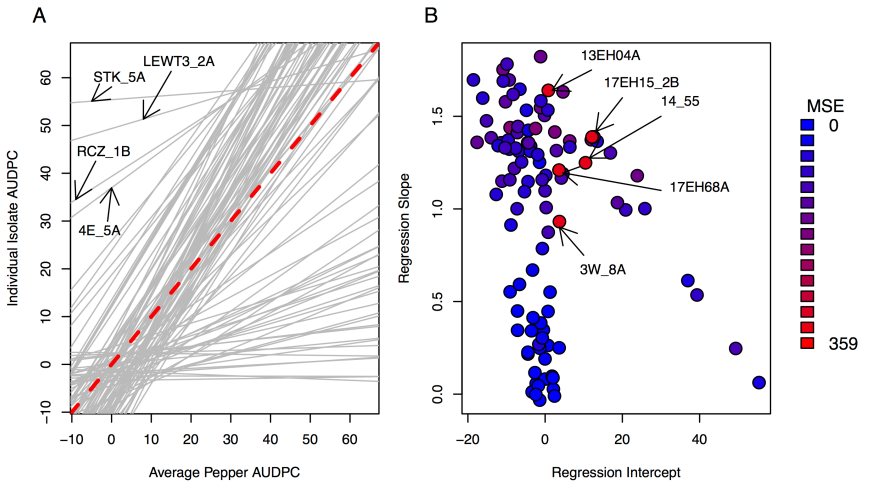

Figure 3.3: Finlay-Wilkinson regression of individual isolate AUDPCs on pepper mean AUDPCs. A) Finlay-Wilkinson regression line. Red, dashed line has intercept of 0 and slope of 1, and represents a hypothetical isolate with average AUDPC on every pepper. B) Finlay-

Wilkinson regression intercepts vs slope, colored by MSE.

The majority of regressions featured low MSE, suggesting that for most isolates, the level of disease caused on a particular pepper could be predicted accurately by the average disease severity of that pepper (Figure 3.3B). However, several MSE outliers (13EH04A, 17EH15_2B, 14_55, 17EH68A, 3W_8A) were noticeable, corresponding to isolates whose virulence on particular peppers deviated from average in unpredictable ways. For example, 3W_8A caused higher than average AUDPC on both the most susceptible (Red Knight and Aristotle) and resistant (Paladin, Archimedes, and Early Jalapeño) peppers, yet caused lower than average AUDPC on intermediately resistant peppers Revolution, Vanguard, and Perennial. 13EH04A, on the other hand, demonstrated the opposite pattern, causing higher than average AUDPC on intermediately resistant peppers but average AUDPC on the rest.

Association between pathogen population structure and virulence. Little consistency in virulence profiles was visually apparent among isolates that originated from the same field site (Figure 3.2). For example, of the four isolates demonstrating high virulence across all eight pepper accessions, three originated from Suffolk County. However, these were each sampled on a different farm, each of which also contributed isolates with virulence patterns more typical of the rest of the isolates in this experiment.

To further assess the relationship between the population structure of the isolate panel and their virulence levels on the eight pepper accessions, we compared PCAs of both genotypic data, using a dataset of 63,475 genome-wide SNP markers typed on the 105 isolates, and phenotypic data, using the isolate × pepper AUDPC LS means. K-means clustering of scores on the first four principal components of the genotype matrix, which collectively accounted for

26.02% of the variance in the genetic data, sorted the isolates into five clusters (Figure S3.2; Figure 3.4), three of which exclusively represented single counties in New York [Cluster 2: field sites Ontario #1 and #2 (Ontario County, central NY); Cluster 3: Erie #1, #2, and #4 (Erie County, western NY); Cluster 5: Cayuga #1 (Cayuga County, central NY)] (Table S3.1).

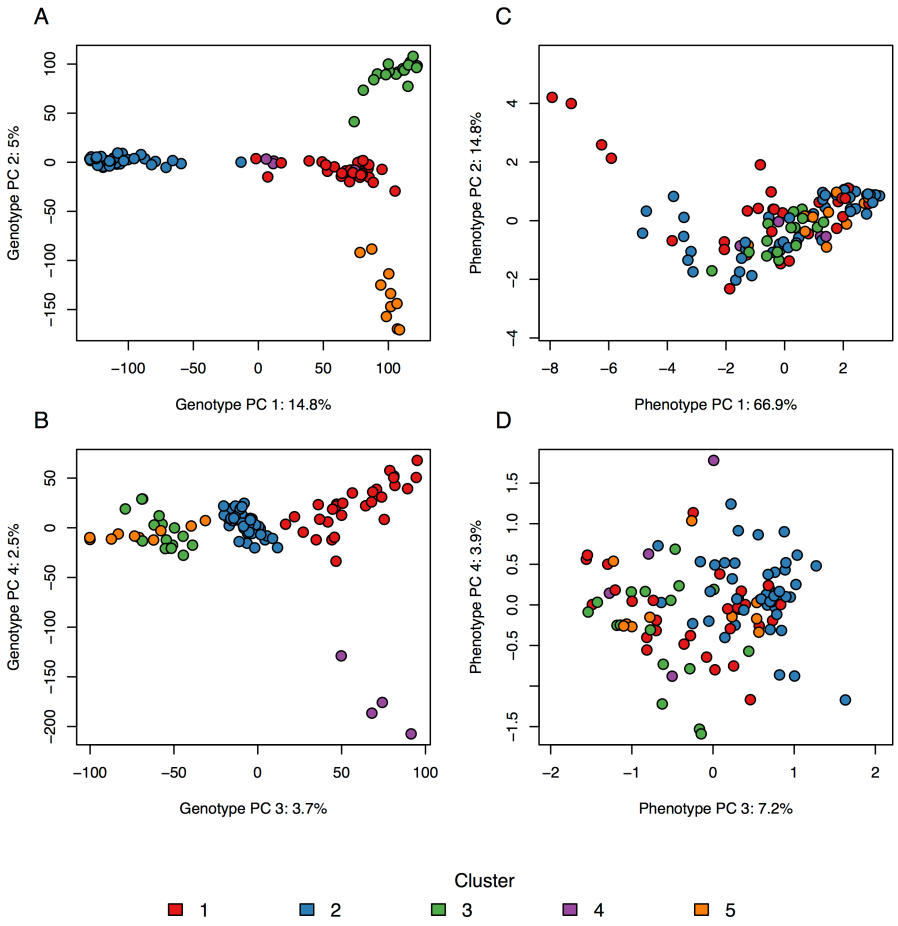

Figure 3.4: Principal component analysis plots for A-B) 63,475 single-nucleotide markers and C-D) AUDPC estimates on eight pepper accessions, for 105 *P. capsici* isolates. Panes A and C show PC 1 vs PC 2 and panes B and D show PC2 vs PC3 for their respective PCAs. Isolates are colored by genetic cluster, identified by k-means clustering using the four genotype PCs.

Clear clustering was not evident in the phenotypic PCA (Figure 3.4C-D). Phenotypic PC

1, which explained 66.9% of the variance in the disease data, separated isolates based on their overall virulence, as indicated by its almost perfect correlation with the LS mean for the main effect of isolate (r = -0.99). Phenotypic PC 2 explained 14.8% of the variance and appeared to reflect the responsiveness of isolates to changes in average pepper susceptibility, as suggested by its high correlation with Finlay-Wilkinson slope (r = -0.75). Phenotypic PCs 3 and 4 represented combinations of variables that were more difficult to interpret. However, the direction and magnitude of the loadings of individual pepper accessions on these PCs suggested that PC 3 largely measured virulence on Red Knight and Aristotle in relation to virulence on Perennial, Revolution, and Vanguard, whereas PC 4 measured virulence on Perennial and Aristotle in relation to virulence on Revolution and Vanguard (Figure S3.3).

Genetic cluster was not significantly associated with either phenotypic PC 1 or 2 (P = 0.30 and 0.12, respectively), indicating that neither overall virulence levels nor Finlay-Wilkinson slopes differed between pathogen subpopulations. However, cluster assignment was significantly associated with phenotypic PCs 3 and 4 ($P = 5.17 \times 10^{-10}$ and 0.04, respectively). Phenotypic PC 3 appeared to mainly differentiate cluster 2 isolates from isolates in clusters 3 and 4, whereas phenotypic PC 4 differentiated isolates in cluster 3 from clusters 2 and 4 (Figure 3.4). We also tested for associations between genetic cluster and virulence levels on individual peppers, finding that only virulence on Red Knight was significantly different between clusters ($P = 5.47 \times 10^{-4}$).

Genome-wide association studies for host-specific virulence. Genome-wide association studies were conducted for overall virulence averaged across pepper accession, pepper-specific virulence on each of the eight accessions retained in the dataset, and phenotypic PCs 2 to 4 (excluding PC 1 due to its high correlation with overall virulence). Traits were log-

transformed as needed, and because of the varying degree of association between population structure and each virulence trait, a model-testing procedure was used to determine the most appropriate covariates to control for false positive associations due to structure in each GWAS (Table S3.2).

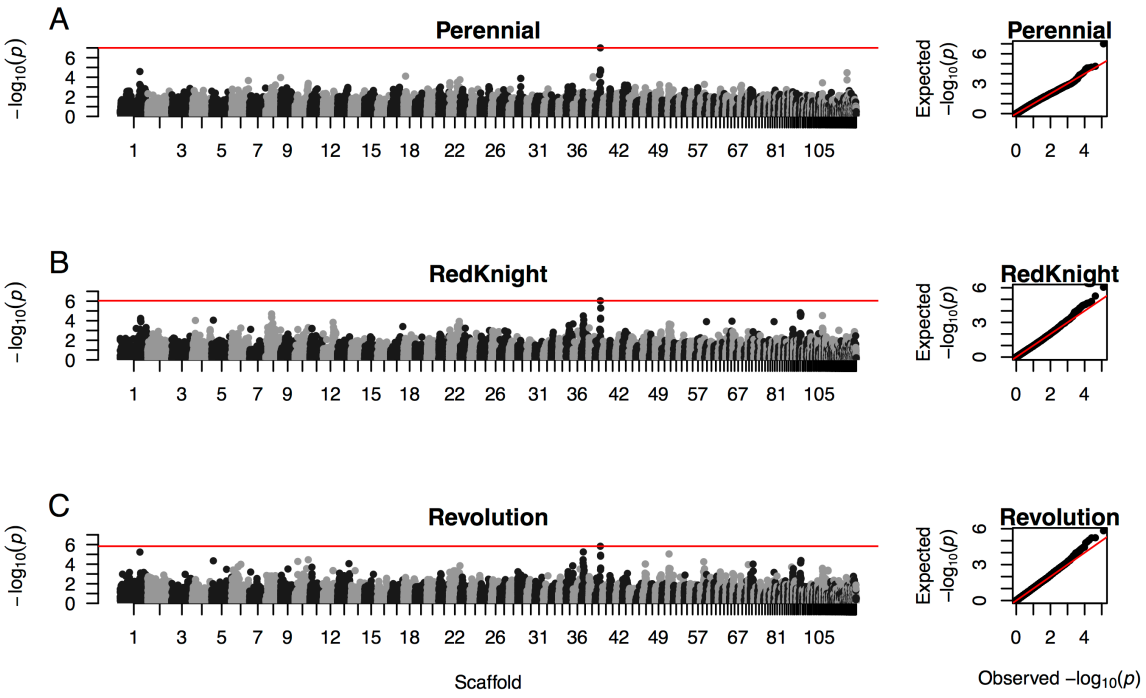

Figure 3.5: Manhattan and Q-Q plots showing *P*-values from genome-wide association studies for virulence on each of A) Perennial, B) Red Knight, and C) Revolution.

Across the nine traits, a single significant marker (39_405015, at bp 405,015 on scaffold 39) was identified, surpassing a 10% FDR threshold for association with virulence on Perennial ($P = 1.00 \times 10^{-7}$), Red Knight ($P = 9.07 \times 10^{-7}$), and Revolution ($P = 1.47 \times 10^{-6}$) (Figure 3.5). Although this SNP failed to surpass significance thresholds for the remaining traits (Figure S3.4), it was the single most significantly associated marker for virulence on Aristotle; among the 1% most significant SNPs for virulence on Early Jalapeño, Paladin, Vanguard; and among

the top 5% most significant SNPs for virulence on Archimedes. It was also among the top 1% most significant SNPs for association with overall virulence and among the top 5% most significant SNPs for association with phenotypic PCs 2 and 3. Phenotypic PC 4, however, was not associated with this marker ($P = 0.61$). Variance among isolates in the non-transformed AUDPC levels on individual peppers explained by SNP 39_405015 ranged from 5%, in the case of Archimedes, to 21%, in the case of Aristotle (Table S3.3). Isolates with the minor allele at this SNP, which had a frequency of 0.15, caused less disease on average on all eight pepper accessions, with the allelic effect of the minor allele on AUDPC ranging from -6.12 in the case of Paladin to -23.76 in the case of Red Knight (Figure S3.5; Table S3.3).

SNP 39_405015 was located inside a gene (*fgenesh1_pg.PHYCAscaffold_39_#_56*) that lacked any functional annotation in the *P. capsici* reference genome. Although it was not annotated with a signal peptide, it appeared to be in a cluster of genes encoding putative secreted proteins, with 7 genes annotated with signal peptides within a 40 Kb region surrounding the SNP. Because the *P. capsici* reference genome does not contain annotations for putative effector proteins, we referred to a published list of putative *P. capsici* effectors (Thilliez et al. 2018) and identified their coordinates in the genome. The coordinates of one of the RXLR-type effectors in this list overlapped *fgenesh1_pg.PHYCAscaffold_39_#_56*, sharing the same ending position in the reference genome but extending its start position by 348 base pairs. While *fgenesh1_pg.PHYCAscaffold_39_#_56* is a promising candidate for the causal gene associated with virulence variation at this locus, several other SNPs, spanning a region of approximately 77 Kb that included 27 annotated genes, were in high LD ($r^2 > 0.5$) with SNP 39_405015 (Figure S3.6).

DISCUSSION

Genotype-genotype interactions between pepper and *P. capsici* have been of interest to pepper breeders and pathologists for many years (Barchenger et al. 2018). However, while the genetic control of disease resistance has been studied extensively in pepper (Thabuis et al. 2003; Ogundiwin et al. 2005; Truong et al. 2012; Mallard et al. 2013; Rehrig et al. 2014; Siddique et al. 2019), little is known about the genetic variation in *P. capsici* associated with the ability to cause high levels of disease on distinct host genotypes. In this study, we measured the disease outcomes for 1,866 distinct combinations of 16 pepper accessions and 117 *P. capsici* isolates. By combining this phenotype data with genotypes at over 60,000 SNP loci in the *P. capsici* isolate panel, we characterized how virulence profiles vary within and between pathogen subpopulations, and identified a locus associated with virulence on multiple pepper hosts.

Interactions between pepper and *P. capsici*. Of the 16 pepper accessions inoculated in this experiment, eight were largely uninformative for differentiating isolate virulence levels, as they showed complete resistance to almost the entire isolate panel (Figure S3.1). Surprisingly, among these largely resistant accessions were the six NMRILs that have shown differential reactions to populations of *P. capsici* collected in various locations including New Mexico, Brazil, Taiwan, and Mexico (Sy et al. 2008; da Costa Ribeiro and Bosland 2012; Barchenger et al. 2018; Reyes-Tena et al. 2019). Only six isolates in our experiment (17EH03_2B, 17EH64A, 3W_2A, AND_4A, LEWT3_2A, and STK_5A) caused any disease on one or more of these NMRILs in both phenotypic replicates. Similarly, Hu et al. (2013) failed to observe any disease on eight NMRILs that they inoculated with 42 *P. capsici* isolates collected in China. These results suggest that avirulence genes that are polymorphic in other geographic populations of *P. capsici* may be largely fixed among the predominantly New York isolates characterized here and

the Chinese isolates characterized by Hu et al. (2013). Consequently, different sets of differential hosts may be needed to provide relevant information for distinct *P. capsici* populations.

In addition to the NMRILs, several other pepper accessions in this experiment showed unexpected responses to the 117 isolates with which they were challenged. Perennial, for example, which has been used as a resistant parent in mapping populations (Lefebvre and Palloix 1996; Thabuis et al. 2003), featured the third highest median AUDPC (Table 3.3; Figure 3.1) of the 16 pepper accessions in this experiment. Early Jalapeño, on the other hand, described by others as susceptible or possessing low levels of resistance to *P. capsici* (Rehrig et al. 2014), performed similarly to accessions known to have intermediate or high levels of resistance (Table 3.3; Figure 3.1). The high level of resistance of Early Jalapeño to the isolates in our panel also agrees with the unexpectedly consistent resistance levels of the NMRILs, as Early Jalapeño is one of the parents of the NMRIL population in addition to highly resistant landrace CM 334. It is interesting to note that while broad-sense heritabilities for virulence were high on all eight of the pepper accessions retained in our dataset, they were lowest on Early Jalapeño and Perennial (0.72 and 0.78, respectively), meaning that a relatively larger proportion of the variance in disease observed on these peppers could not be attributed to genetic variation among isolates. One possibility is that these two accessions, which were the only non-hybrid cultivars of the eight accessions retained for analysis, were partially heterogenous and segregating for disease resistance, which has been observed frequently within NPGS accessions, for example (Davis et al. 2007; Grumet and Colle 2017).

The unexpected reactions of certain pepper accessions – especially Early Jalapeño, Perennial, and the six NMRILs – in our experiment may reflect regional differences in *P. capsici* populations that have implications on resistance breeding for different geographic areas. Because

our pathogen panel was composed almost entirely of isolates from New York (108 of 117 isolates), we were unable to directly compare virulence levels between *P. capsici* populations from different geographical regions of the United States. However, we suspect that certain sources of resistance may be effective against isolates from certain geographic areas but not others, given the discrepancies between the resistance that we observed in accessions like Early Jalapeño, in comparison with reports from others.

Significant genotype-genotype interactions were observed between the eight pepper accessions and 105 *P. capsici* isolates included in our analysis (Table 3.1). However, 66.9% of the variance in the disease caused by the isolates on the eight accessions (PC 1 of the phenotypic PCA; Figure 3.4) could be largely explained by the isolate main effect, or the average virulence level of each isolate. An additional 14.8% of the phenotypic variance was strongly associated with the Finlay-Wilkinson regression slope for each isolate, which measures the rate of increase in disease caused by an isolate on peppers that are more susceptible on average. These results indicate that most of the variation in disease observed in our experiment could be predicted by three parameters: the average virulence of isolate, the average resistance of pepper accession, and the rate at which an isolate's virulence increases with average pepper susceptibility. Although several isolates featured virulence profiles that showed poor linear relationships with average pepper susceptibility (MSE outliers in Figure 3.3), there was little evidence of clear, qualitative crossover interactions, as would be expected in a gene-for-gene system where interactions between R and AVR alleles resulted in the complete presence or absence of disease for a given isolate-pepper accession combination. For example, while we observed several isolates that were able to cause high levels of disease on the mostly resistant bell pepper hybrids Paladin and Archimedes, these isolates were also among the most virulent on the other 6 pepper

accessions. In the classic gene-for-gene model, mutations in an AVR gene that enable a pathogen isolate to infect a host with a matching R gene would not also confer increased virulence on separate hosts without that R gene.

However, consistent with the identification in pepper of minor-effect resistance QTL with isolate-specific effects (Ogundiwin et al. 2005; Truong et al. 2012; Rehrig et al. 2014; Siddique et al. 2019), we found evidence in our dataset of smaller, quantitative genotype-genotype interactions. Phenotypic PC 3, for example, appeared to differentiate isolates in terms of their virulence on intermediately resistant peppers Revolution, Vanguard, and Perennial in relation to their virulence on susceptible cultivars Red Knight and Aristotle (Figure 3.4; Figure S3.3). The isolates with the most negative scores along PC 3 (3W_8A, 18051_1A, 17DH16A) caused lower than average disease on the intermediately resistant peppers, but higher than average disease on Red Knight and Aristotle, whereas the isolates with the highest scores (17EH68A, 17EH15_2B, 17EH64A) caused either equivalent levels of disease on the five accessions or even higher disease on Revolution, Vanguard, and Perennial compared to Red Knight and Aristotle (Figure 3.2). Phenotypic PC 4 differentiated between the intermediately resistant pepper accessions, separating isolates with high virulence on Perennial compared to Vanguard and Revolution (e.g. 568OH and 17EH30B) from those with high virulence on Vanguard and Revolution compared to Perennial (e.g. 17PZ11A and 17PZ02A). Although PCs 3 and 4 collectively explained a relatively small portion of the variance in the data (11.1%), the phenotypic patterns they reflect suggest that the isolates we characterized were polymorphic for virulence loci with minor effects on specific host accessions, in particular Vanguard, Revolution, and Perennial.

Variation in virulence within and between subpopulations. Evidence for differences in either overall virulence or host specialization between pathogen subpopulations was mixed.

The 105 *P. capsici* isolates clearly separated into five genetic clusters that were strongly associated with sampling location in New York (Figure 3.4A-B; Figure S3.2; Table S3.1). However, overall virulence did not significantly differ between clusters and of the eight pepper accessions, only virulence on highly susceptible Red Knight was significantly different between clusters after accounting for multiple test correction. Interestingly, however, there was strong evidence of differentiation between genetic clusters for phenotypic PCs 3 and 4 (Figure 3.4), indicating that subpopulations varied in terms of their relative virulence levels on particular combinations of pepper accessions, even if they did not vary in their absolute virulence levels on those peppers. For example, given an isolate from Erie County (genetic cluster 3) and an isolate from Ontario County (genetic cluster 2) with identical virulence on Red Knight, the Ontario County isolate would be more likely to have higher virulence on Vanguard, Revolution, and Perennial (Figure 3.2). However, without controlling for Red Knight, there was no difference between these counties for absolute virulence levels on Vanguard, Revolution, or Perennial.

Variation between genetic clusters in terms of virulence on Red Knight was largely driven by the inclusion of low-virulence isolates in clusters 1, 2, and 4, but not 3 and 4. Within clusters 1, 2, and 4, and even within individual field sites in those clusters, virulence on Red Knight, the most susceptible accession on average in this experiment, was highly variable. For example, a dramatic example of within-field variation could be observed in the Suffolk County #5 site, where only two isolates were sampled -– LEWT3_2A, among the most virulent isolates on all eight pepper accessions, and LEWT3_6A, which was avirulent or caused low levels of disease on the eight accessions (Figure 3.2). It is unclear what evolutionary forces would promote the maintenance of high variation for virulence within single, isolated subpopulations, although a similar phenomenon has been observed in fungal pathogen *Zymoseptoria tritici* (Dutta

et al. 2020). One possibility is that diversifying selection acts to favor both highly virulent isolates with increased fitness on healthy hosts as well as less virulent, more saprophytic isolates that are preferentially able to colonize dead tissue, as shown in fungal barley pathogen *Rynchosporium secalis* (Abang et al. 2006).

It is also possible, considering the wide host range of *P. capsici* and the diverse crops grown on most vegetable farms where it is found in New York, that there are tradeoffs in virulence on different host species, with certain genetic variants having opposing effects on fitness depending on the plant host. In this scenario, selection would favor different sets of alleles depending on the crop planted to a field in a given year, but fluctuating selection due to crop rotation as well as the presence of a bank of oospores in the soil, which germinate asynchronously and have been shown to act as a reservoir of genetic diversity (Carlson et al. 2017), would maintain genetic variation in a population for virulence on different crops. It is interesting to note that most of the isolates in our study were sampled from squash or pumpkin, with Erie County #2 the only field site where isolates were sampled from a pepper crop. Erie County #2 was also one of only two sites (excluding sites with <3 isolates) where every isolate was observed to cause high disease on Red Knight, consistent with the hypothesis that within-year selection acts to favor isolates virulent on that particular host crop. In contrast, isolates collected in 2017 from Ontario #1, a site that experienced two consecutive disease epidemics on pumpkin crops and had reportedly never been planted to pepper since inoculum was introduced to the site, were divided almost 50:50 in terms of those with high and low virulence on Red Knight. However, evidence of host species specialization in *P. capsici* is inconclusive. Although some studies have suggested a relationship in *P. capsici* between host of origin and virulence on a particular host species (Ristaino 1990; Lee et al. 2001), other studies have found no evidence of

a link (Enzenbacher and Hausbeck 2012; Yin et al. 2012). Segregation ratios in inheritance studies conducted by Polach and Webster (1972) suggested the existence of genes controlling pathogenicity on different hosts, but little further research has been conducted on the genetic control of host species specialization in *P. capsici*.

Genome-wide association study results. We identified only one SNP (39_405015) associated with virulence, surpassing significance thresholds for virulence on Red Knight, Perennial, and Revolution, but demonstrating a consistent effect on virulence on all eight pepper accessions. This SNP also showed an effect on phenotypic PC 2 (Finlay-Wilkinson slope) and PC 3 (virulence on Red Knight and Aristotle in relation to virulence on Perennial, Revolution, and Vanguard), which can be explained by the fact that isolates with the minor allele at this SNP tended to have flat virulence profiles, causing low disease across all eight pepper accessions. This SNP appeared to be located in a cluster of genes encoding putative secreted proteins and was inside a gene, *fgenesh1_pg.PHYCAscaffold_39_#_56*, annotated by Jupe et al. (2013) as an RXLR-type effector. Expression of *fgenesh1_pg.PHYCAscaffold_39_#_56* has been detected *in vitro* in low amounts in mycelia, zoospores, and germinating cysts (Chen et al. 2013), although it was not detected during infection of tomato (Jupe et al. 2013). If this is the causal gene associated with the GWAS signal, the low-virulence allele could result in lower disease due to either the recognition of its gene product by the host or by a loss-of-function mutation that prevents the effector from performing its defense suppression activity. Either way, the universally negative effect of the minor allele on virulence on all eight pepper accessions in this experiment, including highly susceptible Red Knight, suggests that selection would act strongly against this allele. However, it may confer a fitness advantage on other host species or even other pepper genotypes not included in this experiment. Functional characterization of this gene is

necessary to understand how it is associated with variation in virulence on pepper, and what, if any, fitness advantages are conferred by the allele conferring low virulence on pepper.

One of the goals of this experiment was to determine if the genetic architecture of virulence in *P. capsici* varied with different host pepper genotypes. However, we were unable to fully answer this question as we were unable to detect any significant associations beside 39_405015. The presence of significant genotype-by-genotype interactions indicates that there must be loci in *P. capsici* with differential effects on virulence for different pepper hosts. It is possible, however, that our experiment lacked sufficient statistical power to detect these variants. Our sample size of 105 individuals is low for GWAS, although similar sample sizes have been used successfully for mapping quantitative virulence loci in fungal species *Zymoseptoria tritici* (Hartmann et al. 2017). Other studies have reported highly polygenic architectures for virulence in several fungal species (Hartmann et al. 2017; Soltis et al. 2019). Our inability to detect more variants associated with increased disease, despite the high broad-sense heritabilities estimated for virulence, suggests that virulence in *P. capsici* may also be controlled by many genes of small effect. Alternatively, the high mutation rates reported for avirulence genes in other species (Daverdin et al. 2012) could lead to multiple resistance mutations at the same loci in our population, making them undetectable via GWAS due to their arising on independent haplotypes.

Conclusions. We identified significant evidence for genotype-genotype interactions in the pepper-*P. capsici* pathosystem. However, the magnitude of these interactions were quantitative rather than qualitative, and most of the variation in the virulence profiles of 105 isolates could be explained by their average virulence across host genotypes. Consistent with the quantitative nature of these interactions, we were unable to detect any SNPs significantly associated with differential virulence, suggestive of many genes of small effect playing a role in

host specialization to the eight pepper retained in our analysis. However, we identified a SNP on scaffold 39 of *P. capsici* where the minor allele was significantly associated with less severe disease on all eight of the pepper accessions included in our analysis. It is unclear why variation at this locus would be preserved in *P. capsici*, although we speculate that the allele conferring lower virulence on pepper may confer a fitness advantage on different host species or in a different stage of the *P. capsici* lifecycle. Further work is required to validate and characterize the effect of this naturally occurring variant associated with decreased virulence on pepper.

ACKNOWLEDGEMENTS

Colin Day, Garrett Giles, Taylere Hermann, Nicholas King, Holly Lange and Carolina Puentes Silva all made this project possible by providing valuable technical assistance. We would also like to thank Kelly Robbins, Christopher Hernandez, and Ryokei Tanaka for support with statistical analysis. Seed of the non-commercial pepper accessions used in this experiment was kindly provided by Dr. Paul Bosland, Dr. Michael Mazourek, and the USDA ARS Plant Genetics Resources Conservation Unit in Griffin, GA. Funding for this project was provided in part by a grant from the New York Department of Agriculture and Markets.

REFERENCES

Abang, M. M., Baum, M., Ceccarelli, S., Grando, S., Linde, C. C., Yahyaoui, A., Zhan, J., and McDonald, B. A. 2006. Differential selection on *Rhynchosporium secalis* during parasitic and saprophytic phases in the barley scald disease cycle. Phytopathology. 96:1214–1222.

Andrivon, D., Pilet, F., Montarry, J., Hafidi, M., Corbière, R., Achbani, E. H., Pellé, R., and Ellissèche, D. 2007. Adaptation of *Phytophthora infestans* to partial resistance in potato: evidence from French and Moroccan populations. Phytopathology. 97:338–343.

Barchenger, D. W., Lamour, K. H., and Bosland, P. W. 2018a. Challenges and strategies for breeding resistance in *Capsicum annuum* to the multifarious pathogen, *Phytophthora capsici*. Front. Plant Sci. 9

Barchenger, D. W., Sheu, Z.-M., Kumar, S., Lin, S.-W., Burlakoti, R. R., and Bosland, P. W. 2018b. Race characterization of Phytophthora Root Rot on *Capsicum* in Taiwan as a basis for anticipatory resistance breeding. Phytopathology®. 108:964–971.

Bartoli, C., and Roux, F. 2017. Genome-wide association studies in plant pathosystems: toward an ecological genomics approach. Front Plant Sci. 8:763.

Butler, D. G., Cullis, B. R., Gilmour, A. R., and Gogel, B. J. 2009. ASReml-R reference manual.

Camacho, C., Coulouris, G., Avagyan, V., Ma, N., Papadopoulos, J., Bealer, K., and Madden, T. L. 2009. BLAST+: architecture and applications. BMC Bioinformatics. 10:421.

Carlson, M. O., Gazave, E., Gore, M. A., and Smart, C. D. 2017. Temporal genetic dynamics of an experimental, biparental field population of *Phytophthora capsici*. Front. Genet. 8.

Chen, X.-R., Xing, Y.-P., Li, Y.-P., Tong, Y.-H., and Xu, J.-Y. 2013. RNA-Seq reveals infection-related gene expression changes in *Phytophthora capsici*. PLOS ONE. 8:e74588.

Chen, X.-R., Zhang, Y., Li, H.-Y., Zhang, Z.-H., Sheng, G.-L., Li, Y.-P., Xing, Y.-P., Huang, S.-X., Tao, H., Kuan, T., Zhai, Y., and Ma, W. 2019. The RXLR effector PcAvh1 is required for full virulence of *Phytophthora capsici*. Mol. Plant Microbe Interact. 32:986–1000.

Corwin, J. A., Copeland, D., Feusier, J., Subedy, A., Eshbaugh, R., Palmer, C., Maloof, J., and Kliebenstein, D. J. 2016. The quantitative basis of the *Arabidopsis* innate immune system to endemic pathogens depends on pathogen genetics. PLOS Genetics. 12:e1005789.

Daverdin, G., Rouxel, T., Gout, L., Aubertot, J.-N., Fudal, I., Meyer, M., Parlange, F., Carpezat, J., and Balesdent, M.-H. 2012. Genome structure and reproductive behaviour influence the evolutionary potential of a fungal phytopathogen. PLOS Pathogens. 8:e1003020.

Davis, A. R., Levi, A., Tetteh, A., Wehner, T., Russo, V., and Pitrat, M. 2007. Evaluation of watermelon and related species for resistance to race 1W powdery mildew. J. Am. Soc. Hortic. Sci. 132:790–795.

Dunn, A. R., Lange, H. W., and Smart, C. D. 2014. Evaluation of commercial bell pepper cultivars for resistance to Phytophthora Blight (*Phytophthora capsici*). Plant Health Prog. 15:19–24.

Dunn, A. R., Milgroom, M. G., Meitz, J. C., McLeod, A., Fry, W. E., McGrath, M. T., Dillard, H. R., and Smart, C. D. 2010. Population structure and resistance to mefenoxam of *Phytophthora capsici* in New York state. Plant Dis. 94:1461–1468.

Dunn, A. R., Wyatt, L. E., Mazourek, M., Reiners, S., and Smart, C. D. 2013. Performance and tolerance to Phytophthora Blight of bell pepper varieties. HortTechnology. 23:382–390.

Dutta, A., Croll, D., McDonald, B. A., and Barrett, L. G. 2020. Maintenance of variation in virulence and reproduction in populations of an agricultural plant pathogen. Evolutionary

Applications. 00:1-13.

Eberhart, S. A., and Russell, W. A. 1966. Stability parameters for comparing varieties 1. Crop Sci. 6:36-40.

Endelman, J. B. 2011. Ridge regression and other kernels for genomic selection with R package rrBLUP. Plant Genome. 4:250–255.

Enzenbacher, T. B., and Hausbeck, M. K. 2012. An evaluation of cucurbits for susceptibility to Cucurbitaceous and Solanaceous *Phytophthora capsici* isolates. Plant Dis. 96:1404–1414.

Fan, G., Yang, Y., Li, T., Lu, W., Du, Y., Qiang, X., Wen, Q., and Shan, W. 2018. A *Phytophthora capsici* RXLR effector targets and inhibits a plant PPIase to suppress endoplasmic reticulum-mediated immunity. Mol. Plant. 11:1067–1083.

Finlay, K. W., and Wilkinson, G. N. 1963. The analysis of adaptation in a plant-breeding programme. Aust. J. Agric. Res. 14:742–754.

Flor, H. H. Host-parasite interaction in flax rust–its genetics and other implications. Phytopathology. 45:680–685.

Foster, J. M., and Hausbeck, M. K. 2009. Resistance of pepper to Phytophthora crown, root, and fruit rot is affected by isolate virulence. Plant Dis. 94:24–30.

Gao, Y., Liu, Z., Faris, J. D., Richards, J., Brueggeman, R. S., Li, X., Oliver, R. P., McDonald, B. A., and Friesen, T. L. 2016. Validation of genome-wide association studies as a tool to identify virulence factors in *Parastagonospora nodorum*. Phytopathology. 106:1177–1185.

Glosier, B. R., Ogundiwin, E. A., Sidhu, G. S., Sischo, D. R., and Prince, J. P. 2008. A differential series of pepper (*Capsicum annuum*) lines delineates fourteen physiological races of *Phytophthora capsici*. Euphytica. 162:23–30.

Gogarten, S. M., Sofer, T., Chen, H., Yu, C., Brody, J. A., Thornton, T. A., Rice, K. M., and Conomos, M. P. 2019. Genetic association testing using the GENESIS R/Bioconductor package. Bioinformatics.

Granke, L. L., Quesada-Ocampo, L., Lamour, K., and Hausbeck, M. K. 2012. Advances in research on *Phytophthora capsici* on vegetable crops in the United States. Plant Dis. 96:1588–1600.

Grumet, R., and Colle, M. 2017. Cucumber (*Cucumis sativus*) breeding line with young fruit resistance to infection by *Phytophthora capsici*. HortScience. 52:922–924.

Hartmann, F. E., Sánchez-Vallet, A., McDonald, B. A., and Croll, D. 2017. A fungal wheat pathogen evolved host specialization by extensive chromosomal rearrangements. ISME J. 11:1189–1204.

Hu, J., Pang, Z., Bi, Y., Shao, J., Diao, Y., Guo, J., Liu, Y., Lv, H., Lamour, K., and Liu, X. 2013. Genetically diverse long-lived clonal lineages of *Phytophthora capsici* from pepper in Gansu, China. Phytopathology. 103:920–926.

Hurtado-Gonzales, O. P., and Lamour, K. H. 2009. Evidence for inbreeding and apomixis in close crosses of *Phytophthora capsici*. Plant Pathol. 58:715–722.

Jeffers, S. N., and Martin, S. B. 1986. Comparison of two media selective for *Phytophthora* and *Pythium* species. Plant Dis. 70:1038.

Jupe, J., Stam, R., Howden, A. J., Morris, J. A., Zhang, R., Hedley, P. E., and Huitema, E. 2013. *Phytophthora capsici* -tomato interaction features dramatic shifts in gene expression associated with a hemi-biotrophic lifestyle. Genome Biol. 14:1–18.

Kenward, M. G., and Roger, J. H. 1997. Small sample inference for fixed effects from restricted maximum likelihood. Biometrics. 53:983–997.

Krasnow, C. S., Wyenandt, A. A., Kline, W. L., Carey, J. B., and Hausbeck, M. K. 2017. Evaluation of pepper root rot resistance in an integrated Phytophthora Blight management program. HortTechnology. 27:408–415.

Lamour, K. H., and Hausbeck, M. K. 2000. Mefenoxam insensitivity and the sexual stage of *Phytophthora capsici* in Michigan cucurbit fields. Phytopathology. 90:396–400.

Lamour, K. H., Mudge, J., Gobena, D., Hurtado-Gonzales, O. P., Schmutz, J., Kuo, A., Miller, N. A., Rice, B. J., Raffaele, S., Cano, L. M., Bharti, A. K., Donahoo, R. S., Finley, S., Huitema, E., Hulvey, J., Platt, D., Salamov, A., Savidor, A., Sharma, R., Stam, R., Storey, D., Thines, M., Win, J., Haas, B. J., Dinwiddie, D. L., Jenkins, J., Knight, J. R., Affourtit, J. P., Han, C. S., Chertkov, O., Lindquist, E. A., Detter, C., Grigoriev, I. V., Kamoun, S., and Kingsmore, S. F. 2012a. Genome sequencing and mapping reveal loss of heterozygosity as a mechanism for rapid adaptation in the vegetable pathogen *Phytophthora capsici*. Mol. Plant Microbe Inter. 25:1350–1360

Lamour, K. H., Stam, R., Jupe, J., and Huitema, E. 2012b. The oomycete broad-host-range pathogen *Phytophthora capsici*. Mol. Plant Pathol. 13:329–337.

Lee, B. K., Kim, B. S., Chang, S. W., and Hwang, B. K. 2001. Aggressiveness to pumpkin cultivars of isolates of *Phytophthora capsici* from pumpkin and pepper. Plant Dis. 85:497–500.

Lefebvre, V., and Palloix, A. 1996. Both epistatic and additive effects of QTLs are involved in polygenic induced resistance to disease: a case study, the interaction pepper — *Phytophthora capsici* Leonian. Theor. Appl. Genet. 93:503–511.

Li, Q., Ai, G., Shen, D., Zou, F., Wang, J., Bai, T., Chen, Y., Li, S., Zhang, M., Jing, M., and Dou, D. 2019a. A *Phytophthora capsici* effector targets ACD11 binding partners that

regulate ROS-mediated defense response in *Arabidopsis*. Mol. Plant. 12:565–581.

Li, Q., Chen, Y., Wang, J., Zou, F., Jia, Y., Shen, D., Zhang, Q., Jing, M., Dou, D., and Zhang, M. 2019b. A *Phytophthora capsici* virulence effector associates with NPR1 and suppresses plant immune responses. Phytopathol. Res. 1:6.

Li, Q., Wang, J., Bai, T., Zhang, M., Jia, Y., Shen, D., Zhang, M., and Dou, D. 2020. A *Phytophthora capsici* effector suppresses plant immunity via interaction with EDS1. Mol. Plant Pathol. 21:502–511.

Mafurah, J. J., Ma, H., Zhang, M., Xu, J., He, F., Ye, T., Shen, D., Chen, Y., Rajput, N. A., and Dou, D. 2015. A virulence essential CRN effector of *Phytophthora capsici* suppresses host defense and induces cell death in plant nucleus. PLOS ONE. 10:e0127965.

Mallard, S., Cantet, M., Massire, A., Bachellez, A., Ewert, S., and Lefebvre, V. 2013. A key QTL cluster is conserved among accessions and exhibits broad-spectrum resistance to *Phytophthora capsici*: a valuable locus for pepper breeding. Mol Breed. 32:349–364.

Meile, L., Croll, D., Brunner, P. C., Plissonneau, C., Hartmann, F. E., McDonald, B. A., and Sánchez-Vallet, A. 2018. A fungal avirulence factor encoded in a highly plastic genomic region triggers partial resistance to septoria tritici blotch. New Phytol. 219:1048–1061.

Monroy-Barbosa, A., and Bosland, P. W. 2011. Identification of novel physiological races of *Phytophthora capsici* causing foliar blight using the New Mexico recombinant inbred pepper lines set as a host differential. J. Amer. Soc. Hortic. Sci. 136:205–210.

Morgan, W., and Kamoun, S. 2007. RXLR effectors of plant pathogenic oomycetes. Curr. Opin. Microbiol. 10:332–338.

Nelson, R., Wiesner-Hanks, T., Wisser, R., and Balint-Kurti, P. 2018. Navigating complexity to breed disease-resistant crops. Nat. Rev. Genet. 19:21–33.

Oelke, L. M., Bosland, P. W., and Steiner, R. 2003. Differentiation of race specific resistance to Phytophthora root rot and foliar blight in *Capsicum annuum*. J. Amer. Soc. Hortic. Sci. 128:213–218.

Ogundiwin, E. A., Berke, T. F., Massoudi, M., Black, L. L., Huestis, G., Choi, D., Lee, S., and Prince, J. P. 2005. Construction of 2 intraspecific linkage maps and identification of resistance QTLs for *Phytophthora capsici* root-rot and foliar-blight diseases of pepper (*Capsicum annuum* L.). Genome. 48:698–711.

Parada-Rojas, C. H., and Quesada-Ocampo, L. M. 2019. Characterizing sources of resistance to Phytophthora Blight of pepper caused by *Phytophthora capsici* in North Carolina. Plant Health Prog. 20:112–119.

Pariaud, B., Ravigné, V., Halkett, F., Goyeau, H., Carlier, J., and Lannou, C. 2009. Aggressiveness and its role in the adaptation of plant pathogens. Plant Pathol. 58:409–424.

Parlevliet, J. E. 1977. Evidence of differential interaction in the polygenic *Hordeum vulgare-Puccinia hordei* relation during epidemic development. Phytopathology. 67:776–778.

Plissonneau, C., Benevenuto, J., Mohd-Assaad, N., Fouché, S., Hartmann, F. E., and Croll, D. 2017. Using population and comparative genomics to understand the genetic basis of effector-driven fungal pathogen evolution. Front. Plant Sci. 8:119.

Polach, F. J., and Webster, R. K. 1972. Identification of strains and inheritance of pathogenicity in *Phytophthora capsici*. Phytopathology. 62:20-26.

Qi, X., Jiang, G., Chen, W., Niks, R. E., Stam, P., and Lindhout, P. 1999. Isolate-specific QTLs for partial resistance to *Puccinia hordei* in barley. Theor. Appl. Genet. 99:877–884.

Rehrig, W. Z., Ashrafi, H., Hill, T., Prince, J., and Deynze, A. V. 2014. CaDMR1 cosegregates

with QTL Pc5.1 for resistance to *Phytophthora capsici* in pepper (*Capsicum annuum*). Plant Genome. 7:1-12.

Reyes-Tena, A., Castro-Rocha, A., Rodríguez-Alvarado, G., Vázquez-Marrufo, G., Pedraza-Santos, M. E., Lamour, K., Larsen, J., and Fernández-Pavía, S. P. 2019. Virulence phenotypes on chili pepper for *Phytophthora capsici* isolates from Michoacán, Mexico. HortScience. 54:1526–1531.

Ribeiro, C. S. da C., and Bosland, P. W. 2012. Physiological race characterization of *Phytophthora capsici* isolates from several host plant species in Brazil using New Mexico recombinant inbred lines of *Capsicum annuum* at two inoculum levels. J. Amer. Soc. Hortic. Sci. 137:421–426.

Ristaino, J. B. 1990. Intraspecific variation among isolates of *Phytophthora capsici* from pepper and cucurbit fields in North Carolina. Phytopathology. 80:1253–1259.

Sacristán, S., and García-Arenal, F. 2008. The evolution of virulence and pathogenicity in plant pathogen populations. Mol. Plant Pathol. 9:369–384.

Sakamoto, Y., Ishiguro, M., and Kitagawa, G. 1986. *Akaike information criterion statistics*. D Reidel Publishing Company, Tokyo.

Salvaudon, L., Héraudet, V., and Shykoff, J. A. 2007. Genotype-specific interactions and the trade-off between host and parasite fitness. BMC Evol. Biol. 7:189.

Schornack, S., Huitema, E., Cano, L. M., Bozkurt, T. O., Oliva, R., Damme, M. V., Schwizer, S., Raffaele, S., Chaparro-Garcia, A., Farrer, R., Segretin, M. E., Bos, J., Haas, B. J., Zody, M. C., Nusbaum, C., Win, J., Thines, M., and Kamoun, S. 2009. Ten things to know about oomycete effectors. Mol. Plant Pathol. 10:795–803.

Shaner, G. 1977. The effect of nitrogen fertilization on the expression of slow-mildewing

resistance in Knox wheat. Phytopathology. 77:1051.

Siddique, M. I., Lee, H.-Y., Ro, N.-Y., Han, K., Venkatesh, J., Solomon, A. M., Patil, A. S., Changkwian, A., Kwon, J.-K., and Kang, B.-C. 2019. Identifying candidate genes for *Phytophthora capsici* resistance in pepper (*Capsicum annuum*) via genotyping-by-sequencing-based QTL mapping and genome-wide association study. Sci. Rep. 9:9962.

Soltis, N. E., Atwell, S., Shi, G., Fordyce, R., Gwinner, R., Gao, D., Shafi, A., and Kliebenstein, D. J. 2019. Interactions of tomato and *Botrytis cinerea* genetic diversity: parsing the contributions of host differentiation, domestication, and pathogen variation. Plant Cell. 31:502–519.

Stam, R., Howden, A. J. M., Delgado Cerezo, M., Amaro, T. M. M. M., Motion, G. B., Pham, J., and Huitema, E. 2013a. Characterization of cell death inducing *Phytophthora capsici* CRN effectors suggests diverse activities in the host nucleus. Front. Plant Sci. 4.

Stam, R., Jupe, J., Howden, A. J. M., Morris, J. A., Boevink, P. C., Hedley, P. E., and Huitema, E. 2013b. Identification and characterisation CRN effectors in *Phytophthora capsici* shows modularity and functional diversity. PLOS ONE. 8:e59517.

Stewart, E. l, Croll, D., Lendenmann, M. H., Sanchez-Vallet, A., Hartmann, F. E., Palma-Guerrero, J., Ma, X., and McDonald, B. A. 2018. Quantitative trait locus mapping reveals complex genetic architecture of quantitative virulence in the wheat *pathogen Zymoseptoria tritici*. Mol. Plant Pathol. 19:201–216.

Sy, O., Steiner, R., and Bosland, P. W. 2008. Recombinant inbred line differential identifies race-specific resistance to Phytophthora root rot in *Capsicum annuum*. Phytopathology. 98:867–870.

Thabuis, A., Palloix, A., Pflieger, S., Daubèze, A.-M., Caranta, C., and Lefebvre, V. 2003.

Comparative mapping of Phytophthora resistance loci in pepper germplasm: evidence for conserved resistance loci across Solanaceae and for a large genetic diversity. Theor. Appl. Genet. 106:1473–1485.

Thilliez, G. J. A., Armstrong, M. R., Lim, T.-Y., Baker, K., Jouet, A., Ward, B., Oosterhout, C. van, Jones, J. D. G., Huitema, E., Birch, P. R. J., and Hein, I. 2019. Pathogen enrichment sequencing (PenSeq) enables population genomic studies in oomycetes. New Phytol. 221:1634–1648.

Torto, T. A., Li, S., Styer, A., Huitema, E., Testa, A., Gow, N. A. R., van West, P., and Kamoun, S. 2003. EST mining and functional expression assays identify extracellular effector proteins from the plant pathogen *Phytophthora*. Genome Res. 13:1675–1685.

Truong, H. T. H., Kim, K. T., Kim, D. W., Kim, S., Chae, Y., Park, J. H., Oh, D. G., and Cho, M. C. 2012. Identification of isolate-specific resistance QTLs to phytophthora root rot using an intraspecific recombinant inbred line population of pepper (*Capsicum annuum*). Plant Pathol. 61:48–56.

Turner, S. D. 2014. qqman: an R package for visualizing GWAS results using Q-Q and manhattan plots. bioRxiv. :005165.

Van der Plank, J. E. 1968. *Disease resistance in plants*. Academic Press, London.

Vogel, G., Gore, M. A., and Smart, C. D. 2020. Genome-wide association study in New York *Phytophthora capsici* isolates reveals loci involved in mating type and mefenoxam sensitivity. Phytopathology. https://doi.org/10.1094/PHYTO-04-20-0112-FI.

Wang, M., Roux, F., Bartoli, C., Huard-Chauveau, C., Meyer, C., Lee, H., Roby, D., McPeek, M. S., and Bergelson, J. 2018. Two-way mixed-effects methods for joint association analysis using both host and pathogen genomes. Proc. Natl. Acad. Sci. USA. 115:E5440–E5449.

Yin, J., Jackson, K. L., Candole, B. L., Csinos, A. S., Langston, D. B., and Ji, P. 2012. Aggressiveness and diversity of *Phytophthora capsici* on vegetable crops in Georgia. Ann Appl. Biol. 160:191–200.

Zenbayashi-Sawata, K., Ashizawa, T., and Koizumi, S. 2005. Pi34-AVRPi34: a new gene-for-gene interaction for partial resistance in rice to blast caused by *Magnaporthe grisea*. J. Gen. Plant Pathol. 71:395–401.

Zhong, Z., Marcel, T. C., Hartmann, F. E., Ma, X., Plissonneau, C., Zala, M., Ducasse, A., Confais, J., Compain, J., Lapalu, N., Amselem, J., McDonald, B. A., Croll, D., and Palma-Guerrero, J. 2017. A small secreted protein in *Zymoseptoria tritici* is responsible for avirulence on wheat cultivars carrying the Stb6 resistance gene. New Phytol. 214:619–631.

SUPPLEMENTARY MATERIAL

Table S3.1: Number of isolates from each field site or state of origin assigned to each of the five genetic clusters.

Field site or state of origin[a]	Genetic cluster				
	1	2	3	4	5
CA	2	0	0	0	0
Cayuga #1 (2017)	0	0	0	0	10
Columbia #1 (2014)	0	0	0	1	0
Erie #1 (2017)	1	0	7	0	0
Erie #2 (2017)	0	0	9	0	0
Erie #3 (2018)	0	0	1	0	0
FL	1	0	0	0	0
Herkimer #1 (2007)	0	0	0	0	0
MI	0	0	0	0	0
Monroe #1 (2006)	0	0	0	1	0
NM	1	0	0	0	0
NY unknown	1	0	0	2	0
OH	1	0	0	0	0
Ontario #1 (2013)	0	5	0	0	0
Ontario #1 (2017)	0	38	0	0	0
Ontario #2 (2018)	0	2	0	0	0
Ontario #3 (2006)	0	0	0	0	0
Rensselaer #1 (2007)	0	0	0	0	0
SC	4	0	0	0	0

Schenectady #1 (2007)	1	0	0	0	0
Schenectady #2 (2007)	1	0	0	0	0
Suffolk #1 (2018)	6	0	0	0	0
Suffolk #2 (2018)	2	0	0	0	0
Suffolk #3 (2018)	2	0	0	0	0
Suffolk #4 (2018)	3	0	0	0	0
Suffolk #5 (2007)	1	0	0	0	0
Tioga #1 (2018)	1	0	0	0	0
Tompkins #1 (2018)	1	0	0	0	0

[a] CA=California; Ca=Cayuga County, NY; Co=Columbia County, NY; Er=Erie County, NY; FL=Florida; Mo=Monroe County, NY; NM=New Mexico; OH=Ohio; On=Ontario County, NY; SC=South Carolina; Sc=Schenectady County, NY; Su=Suffolk County, NY; Ti=Tioga County, NY; To=Tompkins County, NY.

Table S3.2: Transformations and covariates used in GWAS models.

Trait	Log-transformed	Covariates
Archimedes	TRUE	None
Aristotle	FALSE	PC1+PC2+PC3
EarlyJalapeno	TRUE	PC1+PC2+PC3
Paladin	TRUE	PC1+PC2+PC3+PC4
Perennial	TRUE	None
RedKnight	FALSE	PC1+PC2
Revolution	TRUE	PC1+PC2
Vanguard	TRUE	PC1+PC2
Across-pepper	FALSE	PC1+PC2+PC3
PhenoPC2	TRUE	K
PhenoPC3	FALSE	K+PC1
PhenoPC4	FALSE	PC1

Table S3.3: *P*-values, R^2 values, and allelic effect of SNP 39_405015 on each of nine traits[a].

Pepper	*P*	R^2	Allelic effect
Archimedes	0.028	0.05	-0.40
Aristotle	3.4×10^{-5}	0.21	-22.85
EarlyJalapeno	2.5×10^{-4}	0.16	-0.92
Paladin	3.1×10^{-4}	0.14	-0.83
Perennial	1.0×10^{-7}	0.27	-1.34
RedKnight	9.1×10^{-7}	0.19	-23.76
Revolution	1.5×10^{-6}	0.27	-1.25
Vanguard	2.5×10^{-3}	0.12	-0.90
Across-pepper	5.6×10^{-5}	0.19	-14.74
PhenoPC2	0.024	0.06	0.21
PhenoPC3	0.02	0.02	0.24
PhenoPC4	0.62	0.01	-0.10

[a] Models fit using non-transformed phenotypic distributions.

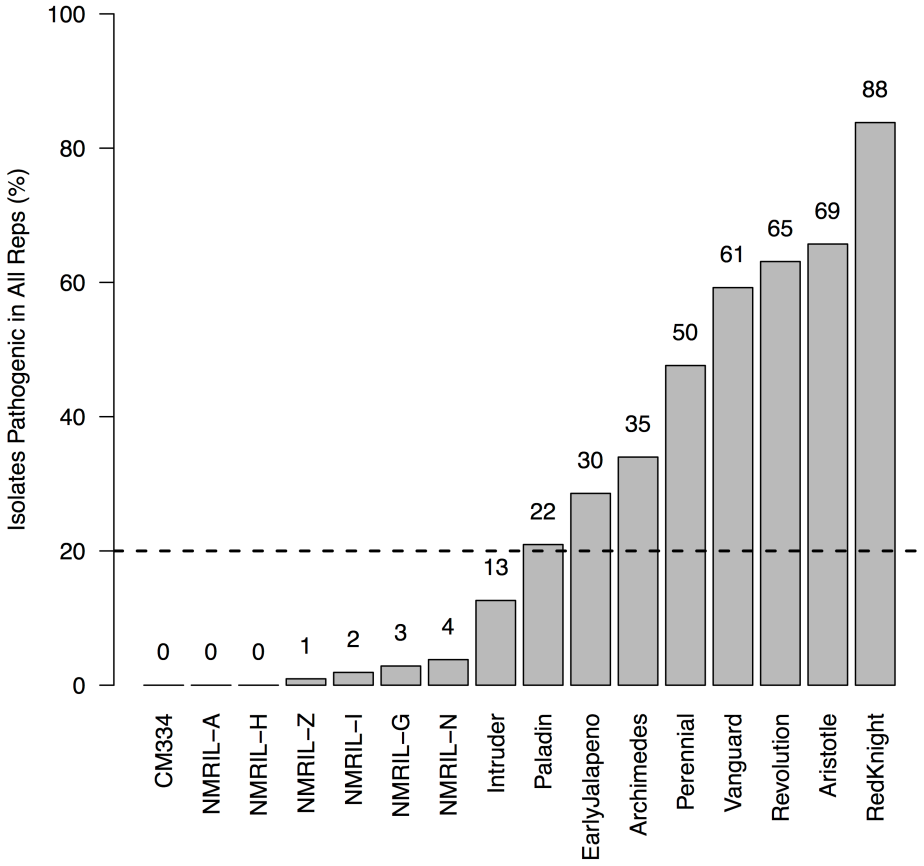

Figure S3.1: The percent of isolates that killed at least one plant in each experimental replicate for the 16 pepper accessions included in the experiment. Numbers above bars refer to the absolute number of isolates deemed pathogenic on that pepper. The dashed line at 20% denotes the cutoff used for removing non-informative pepper accessions from the dataset.

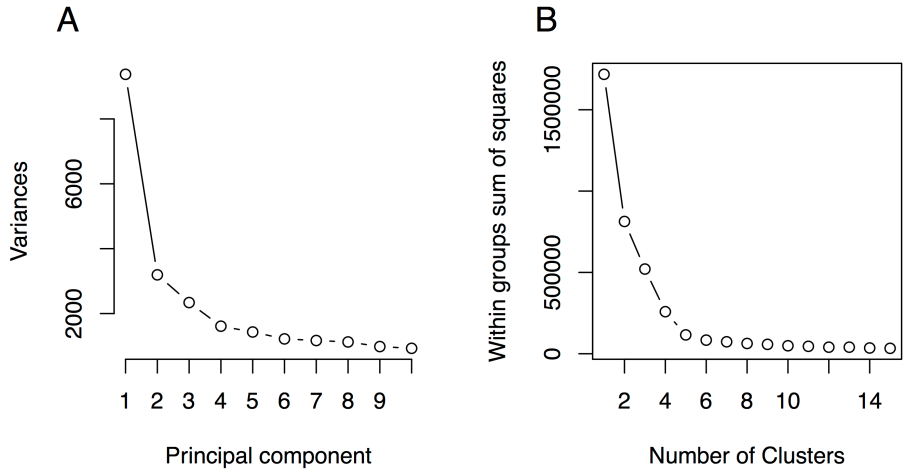

Figure S3.2: Scree plots showing A) variance explained by each principal component from the principal component analysis of the genotype matrix and B) within-groups sums of squares as a function of the number of clusters used in k-means clustering.

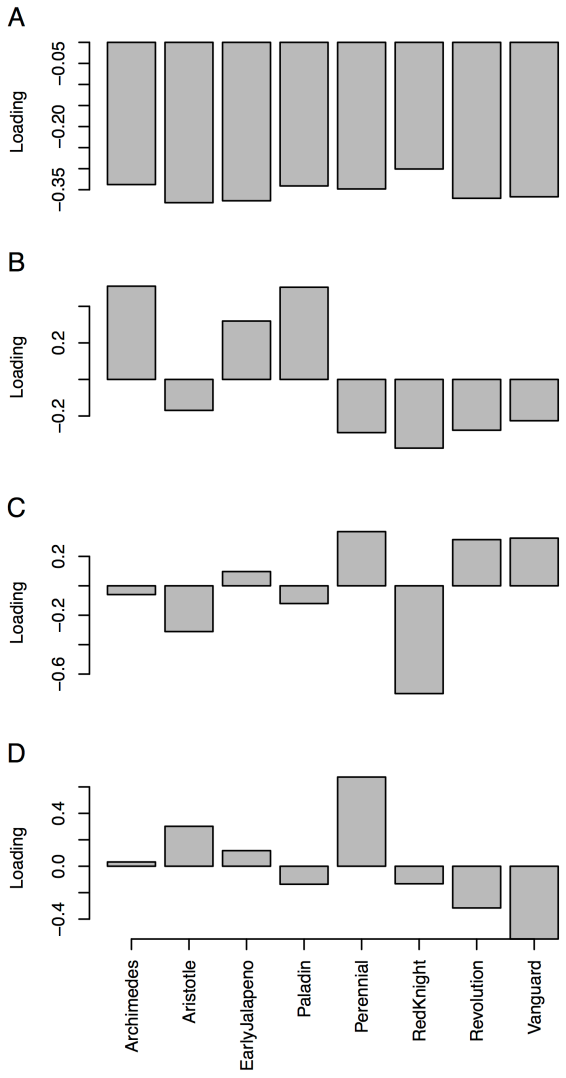

Figure S3.3: Loadings of the eight pepper accessions on principal components 1-4 (panes A-D, respectively) from the phenotype principal component analysis.

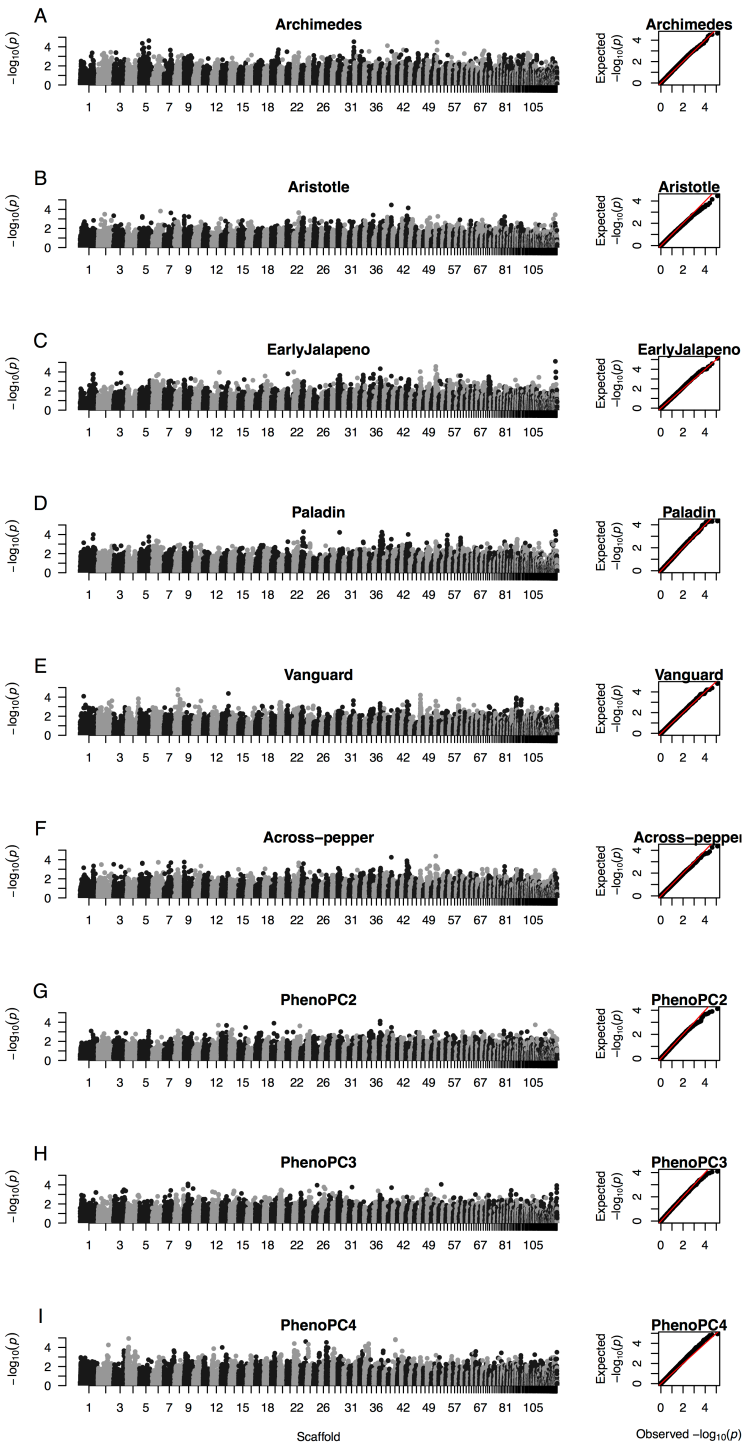

Figure S3.4: Manhattan and Q-Q plots showing *P*-values from genome-wide association studies for A) across-pepper virulence; virulence on each of B) Archimedes, C) Aristotle, D) Early Jalapeño, E) Paladin, and F) Vanguard; and association with phenotypic PCs G) 2, H) 3, and I) 4.

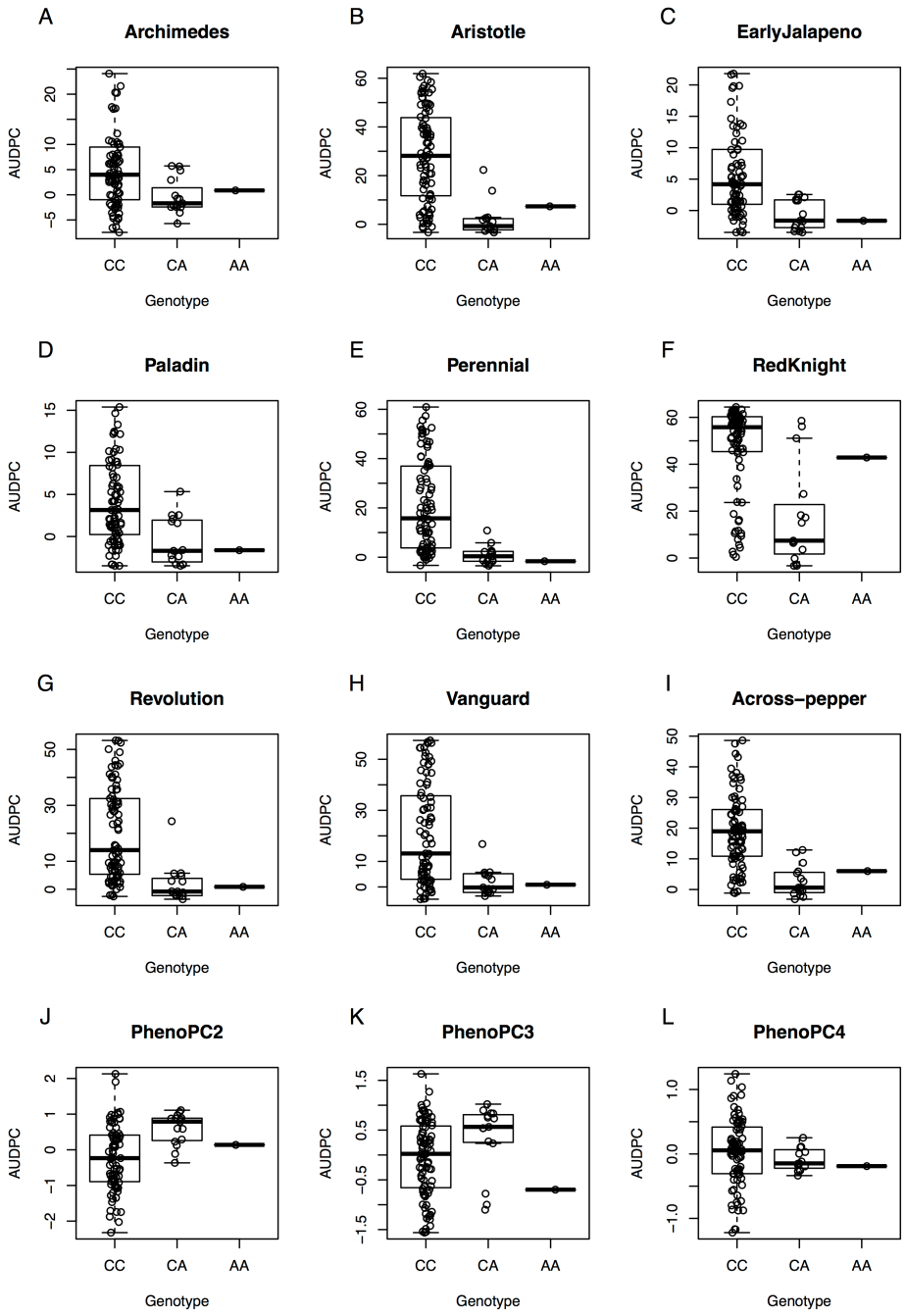

Figure S3.5: Boxplots showing the effect of genotype at SNP 39_405015 on AUDPC on each of A) Archimedes, B) Aristotle, C) Early Jalapeño, D) Paladin, E) Perennial, F) Red Knight, G) Revolution, H) Vanguard, and I) averaged across peppers, as well as the effect on phenotypic PCs J) 2, K) 3, and L) 4.

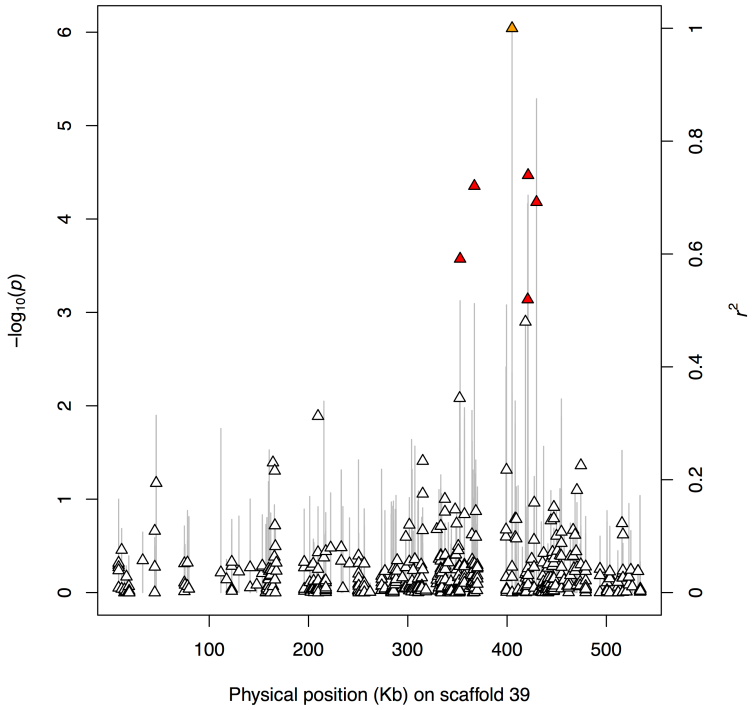

Figure S3.6: SNP *P*-values for association with virulence on Red Knight, represented by vertical lines, and linkage disequilibrium (r^2) with the peak SNP, represented by triangles, on scaffold 39. The orange triangle represents the peak SNP associated with virulence. Red triangles show SNPs with r^2 greater than 0.5 with peak SNP.

CHAPTER 4

CONCLUSIONS AND FUTURE DIRECTIONS

The goal of the research presented in this dissertation was to contribute to genetic solutions for the control of Phytophthora blight, caused by *Phytophthora capsici*, in squash and pepper. To achieve this goal, I conducted interdisciplinary projects focused on the genetics of both host and pathogen. Some of the products of this research, such as molecular markers associated with Phytophthora blight resistance in squash, are immediately applicable for practical use in disease resistance breeding. Other outcomes, such as increased understanding of the virulence phenotypes of *P. capsici* isolates from New York, can be used to inform breeding strategies as well as management recommendations for growers. The results presented in this dissertation also inspired many new questions and ideas for future research directions. In this chapter, I highlight conclusions of the projects described in this dissertation and discuss future studies that have the potential to address unresolved questions or make further progress toward the development of resistant cultivars.

Quantitative trait loci associated with partial resistance to Phytophthora blight in squash. In a population derived from a cross between a zucchini cultivar and a Cornell breeding line, we identified six quantitative trait loci (QTL) associated with Phytophthora root and crown rot resistance. Although the loci were of small effect, each explaining no more than 10% of the variance in resistance among $F_{2:3}$ families, we showed that they alone could be used to predict $F_{2:3}$ resistance levels with moderate cross-validation accuracies (0.43). Given that we only tested the effects of these loci in one population, it is unclear how useful they will be for marker-assisted selection (MAS) in different genetic backgrounds of squash. However, they can be immediately

deployed for selection within the population we used for QTL mapping. Conversion of SNPs in these QTL to a scalable marker platform, such as kASP (Kompetitive allele specific PCR), would allow large numbers of progeny to be efficiently genotyped at these loci. A greenhouse F_2 enrichment strategy combined with in-field phenotypic evaluations of marker-based selections could enable simultaneous genetic gain for Phytophthora root and crown rot resistance as well as other traits segregating in this population, including growth habit (bush vs vining); powdery mildew resistance, and fruit shape, size, and color. This MAS procedure could be performed either using remnant F_2 seeds from this population, of which there are thousands, or using the most resistant of the $F_{2:3}$ families that were generated.

However, one limitation facing the practical use of these QTL is the size of their credible intervals, which covered physical distances ranging from 1 to 7 Mb or genetic distances ranging from 8 to 36 cM. These large sizes, reflecting the considerable statistical uncertainty in the locations of causative polymorphisms underlying QTL, increase the probability of recombination events separating coupling phase linkages between causal genes and markers used in MAS. These regions could be resolved further with fine mapping in populations such as heterogenous inbred families, which allow for the isolation of individual QTL effects in a homogenous genetic background (Tuinstra et al. 1997). Alternatively, a candidate gene approach could be used to identify promising candidates for the causal genes underlying QTL. We assessed functional annotations of variants segregating in this population in addition to homology comparisons with differentially expressed melon genes but were still unable to narrow candidate gene lists to fewer than 63-144 per QTL. Expression profiling of the parents of our population in an inoculated experiment could help identify strong candidates for causative genes in QTL regions.

Population genomic characterization of New York *P. capsici* isolates and loci

associated with mating type and mefenoxam sensitivity. Consistent with results from previous research (Dunn et al. 2010), we found evidence of moderate to strong genetic differentiation between populations of *P. capsici* located on different farms in New York. This lack of gene flow between pathogen populations should reduce the rate by which adaptive mutations like fungicide resistance spread to new farms. However, insensitivity or complete resistance to mefenoxam was identified in isolates from 12 of 23 sites across the state, although no sites where multiple isolates were collected featured entirely resistant populations. These results suggest that standing genetic variation for mefenoxam insensitivity perhaps was present in the original inoculum introductions at most sites and yet, despite the high selection pressure that fungicides impose, insensitivity has not been able to rise to fixation in any of these populations. The oospore soil bank, which germinates asynchronously and acts as a reservoir of genetic variation (Carlson et al. 2017), may explain the apparent inefficiency of selection acting on fungicide insensitivity within these populations. An alternative explanation could be a pleiotropic fitness effect of a fungicide sensitivity mutation, although we observed no *in vitro* differences in growth or sporulation between fungicide sensitive and insensitive isolates.

Within-site variation for fungicide sensitivity was also beneficial for our research purposes, as it allowed us to successfully perform a genome-wide association study (GWAS) without strong confounding effects due to population structure. We found one locus strongly associated with variation for mefenoxam sensitivity. Heterozygotes at this locus showed an intermediate phenotype between homozygotes, consistent with an incompletely dominant gene conferring mefenoxam insensitivity, as identified in inheritance studies using crosses between Michigan isolates (Lamour and Hausbeck 2000). The most promising candidate gene we identified at this locus was *estExt2_Genewise1Plus.C_PHYCAscaffold_620123*, a homolog of

yeast rRNA processing protein Rrp5, located within 12 Kb of the peak SNP identified via GWAS. Mefenoxam is known to result in a depletion of rRNA in oomycetes, leading others to suggest its target site to be RNA Polymerase I (Griffith et al. 1992), although the target could just as well be a protein involved in rRNA processing such as Rrp5. A first step to confirm this hypothesis would be Sanger sequencing of the candidate gene *estExt2_Genewise1Plus.C_PHYCAscaffold_620123* in several diverse isolates representing mefenoxam sensitive, intermediately sensitive, and resistant classes, in order to identify mutations that are associated with resistance and predicted to have a functional effect on protein structure. If such mutations are identified, further characterization of Rrp5 could involve profiling its expression in resistant and sensitive isolates under both mefenoxam exposed and unexposed conditions. Finally, gene-edited strains containing knockouts or allelic swaps could be created using CRISP/Cas9, which has previously been used successfully to validate mutations in *P. capsici* associated with resistance to oxathiapiprolin (Miao et al. 2018).

We also identified a locus associated with mating type. Our results were in agreement with previous studies that localized the mating type determining region of *P. capsici* to scaffold 4 and suggested that mating type inheritance behaves as in an XY sex determination system, where A2 isolates are heterozygous and A1 homozygous at this locus (Lamour et al. 2012; Carlson et al. 2017). In contrast with mefenoxam sensitivity, we were unable to identify candidate genes for mating type determination due to the size of the genomic region showing signal in GWAS. Nevertheless, other strategies may be more successful in fine-mapping the mating type region.

One possible approach would involve exploiting spontaneous loss of heterozygosity mutations to identify mitotic breakpoints associated with mating type changes, Our sample collection included thirteen isolates that appeared to switch mating types over a period of several

years in culture, in all cases from A2 to A1. We hypothesized that mitotic loss of heterozygosity events in the mating type region caused these phenotypic changes, as had seemingly occurred in the case of another three isolates that belonged to one clonal lineage but had discordant mating types. Ten of the thirteen isolates demonstrating evidence for a mating type switch were genotyped concurrent with their first mating type assay, at which point they had an A2 phenotype. The mating type determining gene or genes must presumably be located inside a genomic interval that switched from heterozygous to homozygous in all ten of these isolates. Therefore, resequencing of these ten isolates, which now show an A1 phenotype, could delineate the mating type region by identifying loss of heterozygosity segments shared between all the isolates. In soybean pathogen *Phytopthora sojae*, loss of heterozygosity tracts were shown to be incredibly small in length – under 1 Kb on average (Chamnanpunt et al. 2001), indicating the promise for exploiting this phenomenon for mapping traits with very high resolution. However, in the case of the clonal lineage that we identified with mating type discordances, the loss of heterozygosity observed in isolate 13EH26A appeared to span over 1 Mb, suggesting perhaps a different mechanism than in *P. sojae* and less promise for high-resolution mapping of mating type genes. Nevertheless, I believe that this would be a promising approach that has potential to narrow the boundaries for the mating type region and also shed light on the size of tracts associated with mitotic loss of heterozygosity.

Implications of pepper-*P. capsici* interactions on breeding and the identification of virulence-associated loci. The presence of interactions between host and isolate genotypes has important implications for breeding strategies to achieve durable resistance. We found that interactions between pepper and *P. capsici* were quantitative in magnitude. Unlike in a classic gene-for-gene model, these interactions did not determine the complete presence or absence of

disease for a given isolate × host combination, but the relative rankings of resistance levels of pepper accessions did vary depending on the isolate with which they were inoculated. Pairwise correlations between the resistance levels of the eight pepper accessions to the 105 isolates were mostly positive (median of 0.62), suggesting that resistance to different isolates can be thought of as correlated traits, and selection for resistance to one isolate should on average result in increased resistance to another random isolate. This means that breeding programs might be successful in using one or a few isolates in testing early generation material, before evaluating the resistance of advanced lines to a wider selection of isolates, akin to how breeding programs typically expand the number of environments in which lines are evaluated as they advance through generations. Isolates should be chosen based on their known virulence profiles from other experiments, not necessarily based on their geographic origin, due to the high variability we found in variation in virulence on individual pepper accessions within pathogen subpopulations and even within individual fields.

Knowledge of the pathogen variants involved in host specialization would be useful for prediction of isolate virulence levels on particular pepper genotypes using molecular marker assays. Due to the presence of interactions between host and pathogen, we expected that GWAS would reveal associations for differential virulence in *P. capsici*, meaning virulence on some pepper accessions but not others. However, the only variant that we identified appeared to be associated with virulence on all eight pepper accessions included in our analysis. The fact that this variant was inside a putative RXLR effector gene provided biological context that supported its association with virulence. In *P. capsici*, virulence is presumably positively correlated with fitness, since the pathogen sporulates on dead tissue. Therefore, it is unclear how selection could preserve variation for a variant that confers universally lower virulence on pepper, or at least all

of the pepper accessions that we tested in this experiment. As with the candidate mefenoxam sensitivity gene *estExt2_Genewise1Plus.C_PHYCAscaffold_620123*, validation of this candidate gene is necessary. Further characterization of the gene would address questions related to its pleiotropic effects on virulence on different accessions within a host species as well as across multiple host species.

The phenotyping that was required for this experiment was extensive, taking place over a period of almost a year. It involved over 20,000 pepper seedlings and 280 independent preparations of inoculum (collectively requiring around 3,000 petri dishes). Over 20,000 phenotypic observations were taken (including all the time points that were combined for calculation of the Area Under the Disease Progress Curve). Therefore, expanding our approach in order to evaluate larger population sizes and detect potentially smaller-effect loci is unfeasible. Linkage mapping using the progeny of genetic crosses between phenotypic outliers – like STK_5A, highly virulent on all eight pepper accessions, and 17EH22B, observed to only cause minor disease on Perennial and Early Jalapeño – is one alternative approach for the genetic dissection of virulence. Compared to GWAS, this approach has the advantage of increasing rare variants to high frequency in the mapping population as well as eliminating any confounding effects of population structure. Nevertheless, genetic crosses are labor-intensive in terms of the isolation of single-oospore cultures, and would still require an extensive amount of phenotyping.

Bartouli and Roux (2017), inspired by an approach used to identify interacting variants between humans and HIV (Bartha et al. 2013), proposed a phenotyping-free association method for discovering genes involved in interactions between pathogen and host. Their idea involves sequencing matched, co-infected host-pathogen pairs from natural ecosystems and identifying genomic regions demonstrating strong inter-species linkage disequilibrium. A similar approach

could be taken in an agricultural setting by exploiting standing genetic variation in the pathogen population and manipulating the structure of the host population. This strategy would require a field with a sexual *P. capsici* population that is segregating for virulence on a host pepper genotype of interest. For example, isolates from the Suffolk County #3 site were either highly virulent or avirulent/lowly virulent on all eight pepper accessions. Assuming that this field is infested with oospores, it could be planted to a mixture of cultivars comprised of, for example, highly susceptible Red Knight and intermediately resistant Paladin. Over the course of a season, multiple isolates would be collected from each host and genotyped. Polymorphisms that influence virulence differentially on one host genotype compared to the other could then be mapped by identifying regions of allele frequency differentiation between isolates collected form Red Knight compared to Paladin. The number of isolates sampled from each host would need to be large enough to compensate for likely repeated sampling of the same genotype, as expected due to clonal reproduction. Nevertheless, this strategy has potential to identify variants associated with host specificity without conducting any labor-intensive laboratory or greenhouse disease assays, which are a major bottleneck in experiments designed to dissect the genetic basis of virulence in *P. capsici*.

REFERENCES

Bartha, I., Carlson, J. M., Brumme, C. J., McLaren, P. J., Brumme, Z. L., John, M., Haas, D. W., Martinez-Picado, J., Dalmau, J., López-Galíndez, C., Casado, C., Rauch, A., Günthard, H. F., Bernasconi, E., Vernazza, P., Klimkait, T., Yerly, S., O'Brien, S. J., Listgarten, J., Pfeifer, N., Lippert, C., Fusi, N., Kutalik, Z., Allen, T. M., Müller, V., Harrigan, P. R., Heckerman, D., Telenti, A., and Fellay, J. 2013. A genome-to-genome analysis of associations between human genetic variation, HIV-1 sequence diversity, and viral control. eLife. 2:e01123.

Bartoli, C., and Roux, F. 2017. Genome-wide association studies in plant pathosystems: toward an ecological genomics approach. Front. Plant Sci. 8:763.

Carlson, M. O., Gazave, E., Gore, M. A., and Smart, C. D. 2017. Temporal genetic dynamics of an experimental, biparental field population of *Phytophthora capsici*. Front. Genet. 8.

Chamnanpunt, J., Shan, W., and Tyler, B. M. 2001. High frequency mitotic gene conversion in genetic hybrids of the oomycete *Phytophthora sojae*. Proc. Natl. Acad. Sci. USA. 98:14530–14535.

Dunn, A. R., Milgroom, M. G., Meitz, J. C., McLeod, A., Fry, W. E., McGrath, M. T., Dillard, H. R., and Smart, C. D. 2010. Population structure and tesistance to mefenoxam of *Phytophthora capsici* in New York state. Plant Dis. 94:1461–1468.

Griffith, J. M., Davis, A. J., and Grant, B. R. 1992. Target sites of fungicides to control oomycetes. Pages 69–100 in: Target Sites of Fungicide Action, W. Koller, ed.. CRC Press, Boca Raton.

Lamour, K. H., and Hausbeck, M. K. 2000. Mefenoxam insensitivity and the sexual stage of *Phytophthora capsici* in Michigan cucurbit fields. Phytopathology. 90:396–400.

Lamour, K. H., Mudge, J., Gobena, D., Hurtado-Gonzales, O. P., Schmutz, J., Kuo, A., Miller, N. A., Rice, B. J., Raffaele, S., Cano, L. M., Bharti, A. K., Donahoo, R. S., Finley, S., Huitema, E., Hulvey, J., Platt, D., Salamov, A., Savidor, A., Sharma, R., Stam, R., Storey, D., Thines, M., Win, J., Haas, B. J., Dinwiddie, D. L., Jenkins, J., Knight, J. R., Affourtit, J. P., Han, C. S., Chertkov, O., Lindquist, E. A., Detter, C., Grigoriev, I. V., Kamoun, S., and Kingsmore, S. F. 2012. Genome sequencing and mapping reveal loss of heterozygosity as a mechanism for rapid adaptation in the vegetable pathogen *Phytophthora capsici*. Mol. Plant Microbe Interact. 25:1350–1360.

Miao, J., Chi, Y., Lin, D., Tyler, B. M., and Liu, X. 2018. Mutations in ORP1 conferring oxathiapiprolin resistance confirmed by genome editing using CRISPR/Cas9 in *Phytophthora capsici* and *P. sojae*. Phytopathology. 108:1412–1419.

Tuinstra, M. R., Ejeta, G., and Goldsbrough, P. B. 1997. Heterogeneous inbred family (HIF) analysis: a method for developing near-isogenic lines that differ at quantitative trait loci. Theor. Appl Genet. 95:1005–1011.

APPENDIX 1

PERFORMANCE AND RESISTANCE TO PHYTOPHTHORA CROWN AND ROOT ROT IN SQUASH LINES[3]

ABSTRACT

Phytophthora crown and root rot, caused by the oomycete pathogen *Phytophthora capsici*, is a devastating disease of winter squash, summer squash, and pumpkin (*Cucurbita pepo*). No currently available cultivars provide complete resistance to this disease. Three newly developed squash lines and four hybrids were evaluated in greenhouse and field experiments for their resistance to phytophthora crown and root rot as well as for their horticultural performance. The three newly developed lines ranked among the most resistant entries included in 2 years of field trials. In addition, in a separate greenhouse experiment, one of the lines was shown to display the least severe disease symptoms among a group of accessions previously reported to possess partial resistance to phytophthora crown and root. Furthermore, the resistance was observed to be robust to several isolates of *P. capsici*. However, the phytophthora-resistant lines had reduced yield relative to standard squash cultivars. These lines are useful for continued breeding efforts towards a phytophthora crown and root rot-resistant cultivar.

INTRODUCTION

Squash and pumpkin (*Cucurbita pepo*) are important crops for vegetable growers in the United States. In 2018, approximately 100,000 acres of squash and pumpkin were grown with a value of $350 million (U.S. Department of Agriculture, 2019). These crops are cultivated for

[3] LaPlant, K.E., Vogel, G., Reeves, E., Smart, C.D., and Mazourek, M. 2020. Performance and resistance to phytophthora crown and root rot in squash lines. HortTechnology. 30:608-618.
Gregory Vogel designed experiments and collected data relating to the portions of this project involving disease resistance phenotyping in the greenhouse and field. He also wrote portions of this manuscript and edited the completed draft.

food as immature fruit (summer squash) and mature fruit (winter squash and processing pumpkins), and they are also grown for fall decorations, such as jack-o'-lanterns and gourds (Paris, 2016).

Phytophthora crown and root rot, caused by the oomycete pathogen *Phytophthora capsici*, is a severe disease affecting squash and pumpkin. Originally described in 1922 after being identified on pepper (*Capsicum annum*) (Leonian, 1922), it was first reported on cucurbits (Cucurbitaceae) in 1937 (Kreutzer, 1937). Now known to infect a wide range of species, other hosts of *P. capsici* include all cucurbits, eggplant (*Solanum melongena*), tomato (*Solanum lycopersicum*), and snap bean (*Phaseolus vulgaris*) (Lamour et al., 2012; Tian and Babadoost, 2004). *Phytophthora capsici* is widespread in cucurbit production regions of the United States, and the incidence of disease has increased in recent years (Hausbeck and Lamour, 2004; Meyer and Hausbeck, 2012, 2013b). Squash and pumpkin plants can be affected by *P. capsici* during various growth stages, resulting in seedling damping off, vine and foliar blight, and fruit rot (Babadoost, 2004; Babadoost and Islam, 2003; Hausbeck and Lamour, 2004; Krasnow et al., 2014; Meyer and Hausbeck, 2013).

The presence of both mating types of *P. capsici* in a field results in sexual reproduction and the generation of thick-walled oospores capable of surviving in the soil for many years (Babadoost, 2004; Carlson et al., 2017). These oospores often serve as the primary source of inoculum, germinating after a period of dormancy and initiating the asexual cycle (Granke et al., 2012; Hausbeck and Lamour, 2004). During favorable conditions, asexual reproduction by *P. capsici* results in rapid proliferation of the pathogen, often leading to complete yield loss during severe outbreaks (Babadoost, 2000, 2004; McGrath, 2017). Runoff from infected fields may contaminate surface water sources, such as creeks, rivers, and ponds, which then transport the

pathogen long distances and lead to new epidemics (Hausbeck and Lamour, 2004; Jones et al., 2014).

Control of phytophthora crown and root rot remains a challenge for squash and pumpkin producers. Total eradication of the pathogen from an infected field is typically impossible, which has forced growers to abandon entire fields in some cases (Babadoost, 2004). Fungicides can be effective in limiting disease in squash and pumpkin, although severe crop loss can still occur despite their use when environmental conditions are favorable (Granke et al., 2012). Furthermore, insensitivity to some of the most commonly used active ingredients, such as mefenoxam and cyazofamid, has been reported in *P. capsici* populations (Dunn et al., 2010; Jackson et al., 2012), increasing the difficulty of controlling this disease chemically. Biocontrol efforts with *Trichoderma* sp. and *Bacillus* sp. have not been shown to be effective in controlling disease (Gilardi et al., 2015). Current strategies for disease mitigation include growing less susceptible cultivars, planting non-vining cultivars in raised beds with plastic mulch to limit excessive soil moisture in the root zone, employing drip irrigation to reduce pathogen movement in surface water, and improving soil drainage with subsoil tillage and drainage tiles. Cultivars with increased resistance are highly desired for improved disease management.

To date, there are no squash or pumpkin cultivars available that are completely resistant to phytophthora crown and root rot. A previous study of 115 diverse squash and pumpkin accessions found partial resistance present in several accessions, but no accessions with complete resistance were identified (Padley et al., 2008). Additionally, cultivars have been shown to vary in their degree of susceptibility (Camp et al., 2009; Enzenbacher and Hausbeck, 2012; Meyer and Hausbeck, 2012). Crookneck summer squash and acorn squash cultivars (*C. pepo* ssp. *ovifera*) are generally more susceptible to phytophthora root and crown rot than zucchini and

pumpkin cultivars (*C. pepo* ssp. *pepo*) (Krasnow et al., 2017). The range of resistance phenotypes present among squash and pumpkin accessions suggests that resistance is quantitative, controlled by many genes.

The current lack of cultivars resistant to phytophthora crown and root rot, partnered with the longevity of oospores in infested soil and the emergence of fungicide insensitivity, has resulted in severe challenges for cucurbit growers. As a result, breeding for resistance to phytophthora crown and root rot in squash and pumpkin began in 2011 at Cornell University (Ithaca, NY). Using disease assays conducted on seedlings in the greenhouse, we performed several rounds of selection to breed phytophthora-resistant (PR) lines. To determine the practical utility of these lines, we concurrently initiated several trials to evaluate the performance of these lines in a field setting and in different greenhouse experiments. In this study, we describe the development of the PR lines and the results of our evaluations, which had the following objectives: 1) evaluate the resistance of the PR lines in trials in the field and the greenhouse, 2) evaluate the horticultural performance of the PR lines, and 3) evaluate the resistance of the PR lines relative to other accessions with partial resistance and against multiple isolates of *P. capsici*.

MATERIALS AND METHODS

Development of phytophthora-resistant lines. Two squash Plant Introduction (PI) accessions, PI 615089 and PI 179269, were selected as potential sources of resistance to oomycete pathogens and then crossed to several market classes of squash and pumpkin. The F_1 progeny of these crosses were inoculated with *P. capsici* and selected for crown and root rot resistance in a field experiment, which led to the identification of a single family suitable for

further advancement and selection. The parents of this family are PI 615089 and 'Romulus', and the PR lines described herein are derived from this family. PI 615089, also known as 'Austrian Bush', is a white vegetable marrow squash, and 'Romulus' is a zucchini cultivar released from Cornell University that was briefly commercially available. This family was advanced to the F_2 generation, and the progeny were inoculated and selected for resistance in a field experiment. Cuttings were taken from the most resistant individuals of the F_2 population. Three individuals survived the initial inoculation, a hail storm, remained disease free when the cuttings were rooted in water saturated soil in bags held at 30 °C and 100% relative humidity over the aerial portions of the cuttings, and were able to be self-pollinated. Beginning with the resulting F_3 generation, selection for phytophthora crown and root rot resistance occurred in a greenhouse in every subsequent segregating generation. Seedlings were grown in 72-cell trays and inoculated with the pathogen at the second true leaf stage. Inoculation was performed as in the 2017 field disease trial, described below. After several weeks of disease and symptom progression, the most resistant plants in each generation were selected for self-pollination. Fifteen individual F_3 plants from the three $F_{2:3}$ families were selected, self-pollinated, and the most resistant individual from each of the resulting F_4 families was self-pollinated. The F_5 families were then inoculated in a replicated design, and the three most resistant families were chosen as the PR lines included in the following evaluations. No significant differences were observed among the three selected families (data not shown). Selection continued concurrently with the evaluations described herein, resulting in three F_7 PR lines. These PR lines were also crossed with 'Dunja', a zucchini cultivar, and 'Kandy Korn Plus', a small pumpkin cultivar, to produce two zucchini-type and two pumpkin-type F_1 hybrid lines. The F_1 hybrids represent our efforts to incorporate the resistance observed the PR lines into the zucchini and pumpkin market classes. The PR lines and F_1 hybrids

were evaluated in the following study.

Evaluation of phytophthora-resistant lines. Three field trials (2017 Early, 2017 Late, and 2018 field disease trials) and three greenhouse experiments were conducted to evaluate the level of resistance in the PR lines.

2017 field disease trial. The purpose of the 2017 field disease trial was to evaluate the level of resistance to phytophthora crown and root rot of the PR lines under inoculated field conditions. The 12 cultivars, accessions, and lines included in this trial are described in Table A1.1. The seed lots of the three PR squash lines evaluated in this trial are as follows: Pc-NY21 (Lot 16-10005), Pc-NY30 (Lot 16-10006), and Pc-NY32 (Lot 16-10007). The zucchini and pumpkin cultivars in this trial are representatives of their respective market classes. The accessions included in this trial are PI 615089, the source of resistance for the PR lines; PI 181761, a squash accession reported to have partial resistance (Padley et al., 2008); and PI 211996, a tropical pumpkin (*Cucurbita moschata*) accession included as a resistant check (Chavez et al., 2011).

The 2017 field disease trial was conducted at the Phytophthora Blight Farm, located at Cornell AgriTech in Geneva, NY. Two experiments were performed (2017 Early and 2017 Late field disease trials), differing in the age of the plants when first inoculated. The field used for these experiments was free of overwintering populations of *P. capsici*. The soil type at the Phytophthora Blight Farm is Odessa silt loam (Soil Survey Staff, 2020).

Table A1.1: Squash and pumpkin cultivars, breeding lines, F_1 hybrids, and accessions used in trials for evaluating resistance to phytophthora crown and root rot.

Line, cultivar, or accession	Type[z]	Source	Location	Trial[y]
'Romulus'	zu	Cornell University	Ithaca, NY	P
'Magic Lantern'	pn	Harris Seeds	Rochester, NY	FT
'Kandy Korn Plus'	pn	Holmes Seed Company	Canton, OH	FT
'Dunja'	zu	Johnny's Selected Seeds	Fairfield, ME	FT
'Spineless Beauty'[x]	zu	Harris Seeds	Rochester, NY	FT
Pc-NY21	zu	Cornell University	Ithaca, NY	FT,G2
Pc-NY30	pn	Cornell University	Ithaca, NY	FT
Pc-NY32	zu	Cornell University	Ithaca, NY	FT,G3
'Dunja' x Pc-NY21 F_1	zu	F_1 hybrid (this study)	—	FT
'Dunja' x Pc-NY32 F_1	zu	F_1 hybrid (this study)	—	FT
'Kandy Korn Plus' x Pc-NY30 F_1	pn	F_1 hybrid (this study)	—	FT
'Kandy Korn Plus' x Pc-NY32 F_1	pn	F_1 hybrid (this study)	—	FT
PI 615089	vm	Cornell University	Ithaca, NY	FT,G2

PI 181761	pn	Cornell University	Ithaca, NY	FT,G2
PI 211996[w]	bn	Cornell University	Ithaca, NY	FT
PI 169417	—	NPGS[v]	Ames, IA	G2
PI 174185	—	NPGS	Ames, IA	G2
PI 179269	—	NPGS	Ames, IA	G2
PI 209783	—	NPGS	Ames, IA	G2
PI 266925	—	NPGS	Ames, IA	G2
PI 512709	—	NPGS	Ames, IA	G2
PI 615142	—	NPGS	Ames, IA	G2

[z] Morphotypes (Type): pn = pumpkin, zu = zucchini, vm = vegetable marrow, bn = butternut.

[y] Trial in which each line was included: P = Parental breeding line only, FT = yield field trial, phytophthora crown and root rot resistance field trials, and greenhouse experiment 1, G2 = greenhouse experiment 2, G3 = greenhouse experiment 3.

[x] 'Spineless Beauty' included only in the 2018 field disease trial.

[w] PI 211996 included only in the 2017 field disease trial.

[v] National Plant Germplasm System.

Pre-emergent herbicide trifluralin was applied at a rate of 0.5 lb/acre (Triflurex HFP; Adama, Raleigh, NC) 5 d prior to transplanting. Raised beds measuring 3 ft wide by 4 inches high were formed and covered with 1.25-mil black embossed plastic mulch (Belle Terre Irrigation, Sodus, NY). As mulch was laid, 300 lb/acre 10N–4.4P–8.3K fertilizer (Phelps Supply, Phelps, NY) was applied to the beds. One drip tape line (12 inches between emitters and flow rate of 0.45 gal/min per 100 ft; Toro, Bloomington, MN) was laid underneath the mulch, slightly off center. Beds were spaced 6 ft between centers for the 2017 Early field disease trial and 10 ft between centers for the 2017 Late field disease trial.

Plants were started in a greenhouse in soilless potting media (Sunshine Mix #8; Sun Gro Horticulture, Agawam, MA) in 72-cell flats on 2 June. Seedlings were hardened off in an outdoor cold frame and transplanted to the field on 22 June. Transplants were planted in single rows with 2 ft of in-row spacing. Plants were arranged in a randomized complete block design with three replications for each of the 2017 experiments. Experimental plots were 16 ft long, containing eight plants, with 4 ft of space between adjacent plots. At the time of transplant, soluble fertilizer (Peters Excel (21N–2.2P–16.6K); JR Peters, Allentown, PA) was applied with a water wheel transplanter at an approximate rate of 1.3 g fertilizer per foot of row (2 lb fertilizer per gal water).

To control striped cucumber beetles (*Acalymma vittatum*), imidacloprid (Admire Pro; Bayer CropScience, Research Triangle Park, NC) was applied at the maximum labeled rate as a foliar spray after transplant. Plants that did not survive transplanting were replaced 1 week later. Plants were drip irrigated during the season to supplement rainfall, which totaled 3.8, 6.8, and 4.0 inches for the months of June, July, and August, respectively.

Phytophthora capsici isolate NY 0664-1 was used as a source of inoculum (Dunn et al.,

2013). Isolates were induced to sporulate by culturing on plates of 15% unfiltered V8 agar for 7-10 d with 15 h of fluorescent lighting per day. Plates were then flooded with water and sporangia dislodged with an L-shaped spreading rod. Sporangial suspensions were incubated at room temperature for 30-45 min to promote release of zoospores. After quantifying with a hemocytometer, zoospore suspensions were diluted to the desired final concentration. Five mL of zoospore suspension was applied to the base of each plant using a 4-gal diaphragm pump backpack sprayer (Solo Inc., Newport News, VA). Inoculation dates were 4 July, 11 July, and 18 July for the 2017 Early field disease trial and 19 July, 26 July, and 2 Aug. for the 2017 Late field disease trial. A concentration of 10^4 zoospores/mL was used for the first two inoculations of the 2017 Early field disease trial. All remaining inoculations of the 2017 Early and Late field disease trials were performed using a concentration of 10^5 zoospores/mL.

Plots were rated for incidence of mortality at multiple time points. Mortality was defined as total plant wilting or necrosis of all shoot tips. Ratings were recorded at 10 time points from 11 July to 25 Aug. for the 2017 Early field disease trial and seven time points from 21 July to 25 Aug. for the 2017 Late field disease trial.

2018 field disease trial. The field disease trial described above was repeated in 2018. Because no significant differences were observed between the 2017 Early and 2017 Late field disease trials, all replicates of the 2018 field disease trial were inoculated at the same time. The PR lines and hybrids included in the 2017 field disease trials were included in the 2018 field disease trial (Table A1.1). However, PI 211996 was replaced with 'Spineless Beauty', a zucchini cultivar that was previously reported to have intermediate resistance to phytophthora crown and root rot (Meyer and Hausbeck, 2012). Plants were started as in the 2017 field disease trial, except the sowing date was 12 June and transplant date was 3 July. The field was prepared with raised

beds spaced 10 ft between centers as described in the 2017 Late field disease trial, except no pre-emergent herbicide was applied. The plant spacing, fertilization, and experimental design was the same as described for 2017, except four replications were performed. Imidacloprid was applied as a transplant-water drench to control striped cucumber beetles. Plants that did not survive transplanting were replaced 1 week later to ensure all plots had eight plants. However, one plot of 'Spineless Beauty' and one plot of Pc-NY30 contained only six and seven plants, respectively, due to limited transplant availability. Plants were drip irrigated during the season to supplement rainfall, which totaled 2.7, 3.2, and 6.7 inches for the months of June, July, and August, respectively.

The plants in this experiment were inoculated with the same *P. capsici* isolate prepared in the same way as in the 2017 field disease experiment. Field inoculation occurred on 16 July using a concentration of 10^5 zoospores/mL. Plots were rated for incidence of mortality at 11 time points from 20 July to 29 Aug.

Greenhouse experiment 1. This experiment evaluated the resistance of the same set of 12 entries evaluated in the 2018 field disease experiment. The experiment was conducted in a greenhouse with the temperature maintained at 23.9/21.1 °C (day/night). Seeds were sown in the same soilless potting media as was used for transplant production in the field disease trials, in 72-cell trays using a randomized complete block design with six replications. The 72-cell trays were selected for this experiment to mimic the environmental conditions used for selection of the PR lines. Experimental units consisted of columns of six cells, with each tray serving as a block.

Inoculum was prepared as in the field experiments. Plants were each inoculated with 2.5 mL of a zoospore suspension of *P. capsici* isolate NY 0664-1 at a concentration of 10^4 zoospores/mL that was pipetted adjacent to the plant on the surface of the potting media. The

plants were inoculated at 2-3 weeks old, at the 2-true leaf stage. Mortality ratings were recorded at six time points, beginning 3 d post inoculation (DPI) and proceeding every other day.

Greenhouse experiment 2. This experiment compared the resistance of PR line Pc-NY21 to previously reported sources of partial Phytophthora root and crown rot resistance (Table A1.1). The environmental conditions for this experiment were the same as described in greenhouse experiment 1. Of the eight most resistant accessions from a previous screen of 115 diverse accessions (Padley et al., 2008), the seven with seed available from the U.S. National Plant Germplasm System were included in this experiment (Table A1.1). In addition, the source of resistance for the PR lines, PI 615089, was included, as was PI 179269, an accession identified as partially resistant in previous experiments at Cornell University. 'Dunja' was included as a susceptible check. Because this experiment occurred concurrently with the other field and greenhouse experiments, seed was limited. Therefore, a different seed lot of Pc-NY21 (Lot 17-G-014) from the previous experiments was evaluated here. This Pc-NY21 seed lot is an $F_{5:6}$ family derived from a different F_5 individual than the Pc-NY21 (Lot 16-10005) described in the field trials above. A single representative PR line was included to conserve seed, as the three PR lines are closely related. This experiment was arranged as a completely randomized design with six replications, with each experimental unit consisting of a single plant in a 4-inch square pot (Dillen, Middlefield, OH). Inoculation occurred as previously described in greenhouse experiment 1. Mortality ratings were recorded at 15 time points, beginning 3 DPI and proceeding every other day.

Greenhouse experiment 3: This experiment compared the resistance of Pc-NY32 and 'Dunja' to three different pathogen isolates. The environmental conditions for this experiment were the same as described in greenhouse experiment 1. As in greenhouse

experiment 2, a different seed lot of Pc-NY32 (Lot 17-G-009) was included in this experiment due to limited seed availability. This Pc-NY32 seed lot is an $F_{5:6}$ family derived from a different F_5 individual than the Pc-NY32 (Lot 16-10007) described in the field trials above. As before, only a single PR line was evaluated due to limited seed, so Pc-NY32 was arbitrarily chosen to represent the PR lines. California isolate SJV-CA and New Mexico isolate PCNM-6300 were used in addition to isolate NY 0664-1 in this experiment. This experiment featured a full factorial arrangement of three pathogen isolates and the two squash lines. Experimental units consisted of six adjacent plants potted individually in 4-inch pots, with experimental units arranged in a completely randomized design with three replications. Plants were inoculated as described in greenhouse experiment 1. Mortality ratings were recorded at nine time points, beginning 3 DPI and proceeding every other day.

Horticultural performance. A field trial was conducted in 2017 at the East Ithaca Research Farm of Cornell University in Ithaca, NY, to evaluate the yield and horticultural performance of the PR lines, including evaluation of percent marketability, fruit shape, and plant habit. There is no history of *P. capsici* on this farm, and the plants were not inoculated. The lines evaluated in this trial consisted of the 12 entries evaluated in both the 2017 and 2018 field disease trials (i.e. excluding 'Spineless Beauty' and PI 211996; Table A1.1). 5N–1.3P–3.3K fertilizer (Pro-Gro; North Country Organics, Bradford, VT) and blood meal (12N–0P–0K; Down To Earth Fertilizer, Eugene, OR) were banded into the field, and raised beds that were 3 ft wide and 4 inches tall were constructed, with 10-ft spacing between the centers. The beds were covered with 1-mil embossed black plastic mulch (Dubois Agrinovation, Saint-Rémi, QC, Canada), and drip tape (12 inches between emitters and flow rate of 0.45 gal/min per 100 ft; Rain-Flo Irrigation, East Earl, PA) was used for irrigation in the beds, placed slightly off center.

The soil type of the East Ithaca Research Farm is Arkport fine sandy loam (Soil Survey Staff, 2020).

Plants for the 2017 yield trial were sown in soilless potting media (Cornell Mix; Boodley and Sheldrake, 1972) in 72-cell trays on 29 May in a greenhouse. The plants were then transferred to an outdoor cold frame for 1 week for hardening off before being transplanted on 15 June. The transplants were planted into single rows with 2 ft between plants within plots. The plants were arranged in a randomized complete block design with four replications. The experimental plots consisted of eight plants, with 4 ft of space between adjacent experimental units. Plants were irrigated to supplement natural rainfall, which totaled 3.5, 5.7, 2.1, and 2.0 inches in June, July, August, and September, respectively.

Yield was measured at the East Ithaca field site beginning on 11 July. The zucchini-type lines were harvested about three times per week for 7 weeks. Fruit were harvested approximately 3 d after pollination, and categorized as marketable and unmarketable. Marketable fruit were at least 5 inches in length, straight, and blemish-free. Yield of both fruit classes were measured by total weight of fruit and total number of fruit. Total marketable fruit per plant and percent marketable yield per plant were calculated and used for subsequent analysis. On 31 July and 7 Aug., all harvested fruit were collected and the following measurements were made on individual fruit: fruit weight, fruit width at the widest point, and fruit length. Fruit shape, calculated as fruit length/fruit width, was then calculated for each fruit. The pumpkin-type lines were harvested at physiological maturity on 12 Sept. All fruit were counted and categorized as marketable or unmarketable. A fruit was considered unmarketable if large blemishes were present on its surface or if the fruit was misshapen. A random sample of ten fruit per plot, as available, were selected for additional length, width, and weight measurements. Additionally,

plant habit was determined, with each line characterized as bush type, semi-bush type, or vine type. A bush plant has a short, often upright, stem and compressed internode length. A vine type has a long stem with long internodes that creeps along the ground. A semi-bush type begins as a bush type plant with short internodes, and then the internodes of the main stem begin to elongate mid-season, transitioning to a vine type plant.

Statistics. The R statistical software (R version 3.6.2; R Foundation for Statistical Computing, Vienna, Austria) was used for all analyses. For all of the field disease trials and greenhouse experiments, disease incidence ratings were used to calculate the area under the disease progress curve (AUDPC) (Cooke et al., 2006). Pearson correlations among the entry means of the field and greenhouse disease experiments were performed using the R package "Hmisc" (Harrell Jr., 2018). Analysis of variance (ANOVA) was performed for all of the traits described above for each site and experiment, with block included as a random effect. Data from the 2017 Early and 2017 Late disease field trials were combined for analysis in a model including inoculation time and block as random effects. The package "lsmeans" (Lenth, 2016) was used to separate treatment means from all significant ANOVAs. Tukey's honestly significant difference (HSD) test (at $\alpha = 0.05$) was used to perform all pairwise comparisons and generate connecting letter diagrams. In the yield trial, lines with zucchini-type fruit were harvested multiple times, and therefore the data for the following traits were summed across all harvest dates: number of marketable fruit per plant and percent marketable fruit per plant. The sums for these traits were used for analysis.

RESULTS

Development of phytophthora-resistant lines. Inoculation and selection for

phytophthora crown and root rot resistance resulted in the identification of three PR lines with resistance derived from PI 615089. These PR lines are $F_{6:7}$ families from the following seed lots: Pc-NY21 (Lot 16-10005), Pc-NY30 (Lot 16-10006), and Pc-NY32 (Lot 16-10007). Four F_1 hybrids were included in the trials: two zucchini-type hybrids of 'Dunja' crossed to Pc-NY21 or Pc-NY32 and two pumpkin-type hybrids of 'Kandy Korn Plus' crossed to Pc-NY30 or Pc-NY32.

Evaluation of phytophthora-resistant lines. The PR lines were among the most resistant entries in all of the disease experiments. In particular, Pc-NY30 was consistently one of the most resistant lines over both years and locations (Table A1.2). Disease symptoms progressed rapidly in the susceptible lines, particularly in 'Magic Lantern'. Young plants displayed constriction of the crown, leading to wilting and plant collapse. Complete mortality in the young plant stage was observed in susceptible lines. Young plant mortality was less common in the PR lines. As the season progressed and the plants matured in the field, the disease symptoms that manifested in these lines more often consisted of death of the apical meristem.

2017 field disease trial. Data from the 2017 Early field disease trial and 2017 Late field disease trial were combined for analysis. All three PR lines were significantly more resistant than 'Magic Lantern' and 'Dunja', the susceptible pumpkin and zucchini cultivars, respectively (Table A1.2). While not previously reported to possess resistance to phytophthora crown and root rot, 'Kandy Korn Plus' was not significantly different from the PR lines, although more disease was observed on this cultivar relative to the PR lines. Less disease was observed on the two zucchini-type F_1 lines, 'Dunja' x Pc-NY21 F_1 and 'Dunja' x PcNY32 F_1, relative to 'Dunja', although they were not significantly different, and only 'Dunja' x Pc-NY21 F_1 was significantly different from its breeding line parent. The two pumpkin-type F_1 lines, 'Kandy Korn Plus' x Pc-NY30 F_1 and 'Kandy Korn Plus' x Pc-NY32 F_1, displayed a level of

resistance that was not significantly different from that of the PR lines or ‘Kandy Korn Plus’. Although not significantly more resistant, the PR lines had a lower AUDPC value relative to PI 615089, their resistant parent (Table A1.2). The PR lines were also found to be significantly more resistant than PI 181761. No significant differences were found between the PR lines and PI 211996, the resistant tropical pumpkin accession.

2018 field disease trial. The general trends in 2017 were also observed in the 2018 field disease trial (Table A1.2). All three PR lines were significantly more resistant than ‘Magic Lantern’ and ‘Dunja’. Although the three PR lines were not significantly different from one another, Pc-NY21 and Pc-NY32 had a greater AUDPC than Pc-NY30. The two zucchini-type F_1 lines continued to display intermediate resistance, although they were not significantly different from ‘Dunja’, and only ‘Dunja’ x Pc-NY32 F_1 was significantly different from its breeding line parent. The pumpkin-type F_1 lines, ‘Kandy Korn Plus’ x Pc-NY30 F_1 and ‘Kandy Korn Plus’ x Pc-NY32 F_1, were not significantly different from either of their PR line parents, Pc-NY30 and Pc-NY32, respectively. ‘Kandy Korn Plus’ was not significantly different from the PR lines in this trial, and ‘Kandy Korn Plus’ x Pc-NY32 F_1 displayed a greater AUDPC than either of the parents. In 2018, ‘Spineless Beauty’ was included in place of PI 211996 as a partially resistant zucchini check. ‘Spineless Beauty’ had a greater AUDPC than any of the PR lines, but only Pc-NY30 was significantly different.

Table A1.2: Resistance of squash and pumpkin lines to phytophthora crown and root rot. The 2017 field disease trial and the 2018 field disease trial were conducted at the Phytophthora Blight Farm at Cornell AgriTech in Geneva, NY. Resistance was measured as area under the disease progress curve (AUDPC), using disease incidence ratings taken every 2 d for greenhouse experiment 1 and approximately biweekly for the field trials.

	AUDPC[z]		
Line, cultivar, or accession	**2017 Field[y]**	**2018 Field**	**Greenhouse experiment 1**
'Magic Lantern'	37.35 a	38.78 a	9.97 a
'Dunja'	31.15 ab	35.45 a	9.86 a
'Kandy Korn Plus'	15.19 cd	12.09 de	9.11 a
'Spineless Beauty'[w]	—	29.42 abc	—
Pc-NY21	8.03 d	20.77 bcde	7.14 ab
Pc-NY30	6.03 d	8.06 e	2.94 c
Pc-NY32	13.16 cd	21.09 bcde	2.87 c
'Dunja' x Pc-NY21 F_1	20.11 bc	25.38 abcd	8.17 ab
'Dunja' x Pc-NY32 F_1	21.49 bc	27.16 abc	5.75 bc
'Kandy Korn Plus' x Pc-NY30 F_1	5.49 d	7.55 e	5.58 bc

‘Kandy Korn Plus’ x Pc-NY32 F_1	10.84 cd	26.48 abc	3.42 c
PI 615089	14.25 cd	18.86 cde	8.08 ab
PI 181761	26.91 ab	34.3 ab	8.01 ab
PI 211996[v]	4.44 d	—	—

[z] Least squares means of AUDPC.

[y] The 2017 Early disease field trial and 2018 Late disease field trial were combined for analysis.

[x] Means in the same column followed by the same letter are not significantly different at $P < 0.05$ as determined by Tukey's honestly significant difference test.

[w] The zucchini cultivar Spineless Beauty is reported to have intermediate resistance to phytophthora crown and root rot and was included in the 2018 disease field trial as a replacement for PI 211996.

[v] PI 211996 was included as a resistant check in the 2017 disease field trial

.

Greenhouse experiment 1. The disease experiments conducted in the field in 2017 and 2018 were repeated in greenhouse experiment 1 in 2018. Pc-NY30 and Pc-NY32 were the most resistant lines in the experiment and were significantly different from all of the commercial cultivars and the two partially resistant accessions. Pc-NY21, on the other hand, was not significantly different from the most susceptible entries. The resistance observed in the hybrids varied. The two hybrids with 'Kandy Korn Plus' as a parent were significantly more resistant than 'Kandy Korn Plus' and statistically similar to their breeding line parents. Of the 'Dunja' hybrids, only 'Dunja' x Pc-NY32 F_1 was significantly more resistant than 'Dunja', and both were statistically similar to their breeding line parents (Table A1.2).

The correlations among the entry means from the 2017 disease field trial, 2018 disease field trial, and greenhouse experiment 1 were calculated. Data from the 2017 Early field disease trial and 2017 Late field disease trial were combined. The two field trials were strongly and significantly correlated, with a correlation coefficient of 0.87 at $P < 0.001$. Greenhouse experiment 1 was also significantly correlated with the 2017 disease field trial, with a correlation coefficient of 0.69 ($P = 0.012$). However, greenhouse experiment 1 only had a moderate correlation with the 2018 disease field trial [r=0.48 (ns)].

Greenhouse experiment 2. In greenhouse experiment 2, PR line Pc-NY21 was ranked lowest in AUDPC among all of the partially resistant accessions and was significantly more resistant to over half of lines in the experiment (Table A1.3). PI 615089 was the second lowest ranked in AUDPC, although it was not significantly different from the majority of the entries in the experiment. The majority of the accessions displayed partial resistance, with intermediate AUDPC values compared to Pc-NY21 and the susceptible check 'Dunja.'

Table A1.3: Area under the disease progress curve (AUDPC) means from greenhouse experiment 2 for squash accessions with reported partial resistance to phytophthora crown and root rot. Disease incidence ratings were taken approximately every 2 d.

Cultivar or breeding line	AUDPC[z]	
'Dunja'	32.00	a
PI 266925	29.00	ab
PI 209783	27.00	abc
PI 169417	26.67	abc
PI 512709	26.00	abc
PI 615142	25.00	abc
PI 174185	22.42	abcd
PI 181761	16.33	abcd
PI 179269	14.08	bcd
PI 615089	11.33	cd
Pc-NY21	8.17	d

[z] Least squares mean of AUDPC.

[y] Means in the same column followed by the same letter are not significantly different at $P < 0.05$ as determined by Tukey's honestly significant difference test.

Greenhouse experiment 3. Greenhouse experiment 3 evaluated the response of two squash lines, Pc-NY32 and 'Dunja', to three geographically diverse *P. capsici* isolates. Clear, significant differences were observed between the two lines. By 12 DPI, the average incidence of mortality for all isolates on 'Dunja' was 90% or greater (Figure A1.1). No mortality was

observed on any Pc-NY32 plants, regardless of isolate. These differences due to line were highly significant ($P < 0.001$). However, there were no significant differences due to the isolate with which the two lines were inoculated ($P = 0.110$); all of the isolates caused similar levels of disease. Additionally, there was no significant line-by-isolate interaction observed ($P = 0.521$).

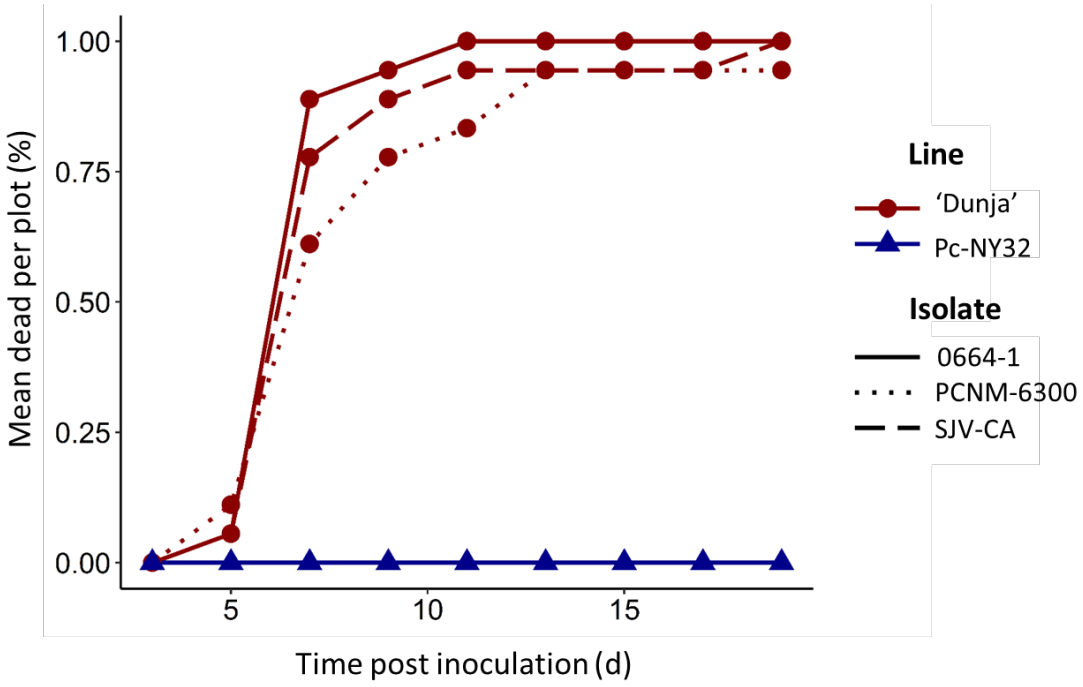

Figure A1.1: Incidence of mortality over time in greenhouse experiment 3 for phytophthora-resistant squash breeding line Pc-NY21 and susceptible zucchini cultivar 'Dunja' inoculated with three isolates of *Phytophthora capsici*.

Horticultural performance. The entries of the 2017 yield trial were divided into zucchini-type lines (Table A1.4) and pumpkin-type lines (Table A1.5). The zucchini-type lines were harvested over the course of 7 weeks, with 'Dunja' yielding the most marketable fruit and the two PR lines, Pc-NY21 and Pc-NY32, yielding the least marketable fruit over time (Figure

A1.2). The PR lines produced significantly fewer marketable fruit per plant than ‘Dunja’, as well as a significantly lower percentage of marketable fruit from the total yield (Table A1.4), whereas the F_1 lines were not significantly different from ‘Dunja’ for both traits. PI 615089 was intermediate in both its marketable yield and percent marketable fruit. Pc-NY21, as well as the F_1 lines, were not significantly different from ‘Dunja’ in fruit weight, but Pc-NY32 weighed significantly more. Only ‘Dunja’ x Pc-NY21 F_1 was not significantly different from the long, narrow fruit shape value of ‘Dunja’. All of the other lines were significantly shorter and wider than ‘Dunja’, with Pc-NY32 having the lowest length/width ratio of 2.64. ‘Dunja’ and PI 615089 were bush type lines, but the two PR lines were vine type, leading to semi-bush type F_1 lines.

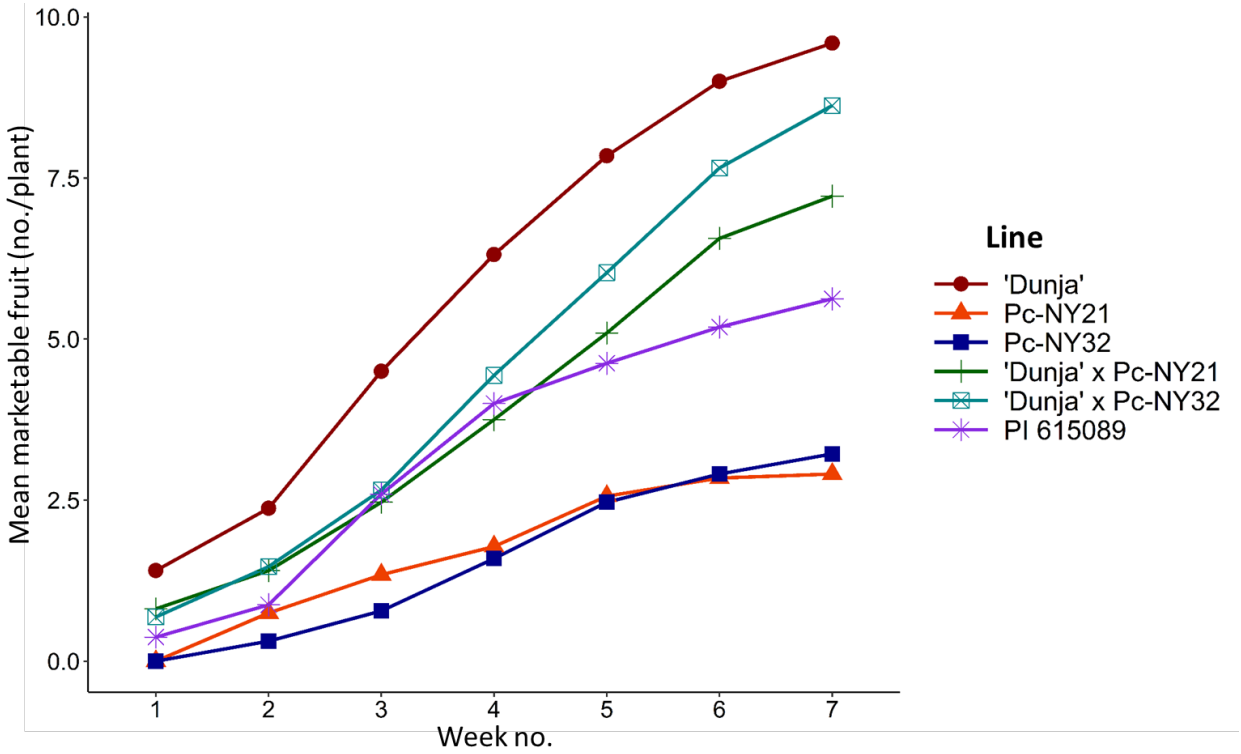

Figure A1.2: Cumulative marketable yield of zucchini-type lines over time in the 2017 yield trial at the East Ithaca Research Farm of Cornell University in Ithaca, NY. Yield is represented by the total number of marketable fruit per plant averaged across four replicates.

The pumpkin-type lines in the 2017 yield trial were harvested at physiological maturity. ‘Kandy Korn Plus’ produced significantly more marketable fruit than the other lines, with ‘Magic Lantern’, Pc-NY30, and PI 181761 producing significantly fewer fruit, approximately one per plant (Table A1.5). The F_1 lines produced an intermediate number of fruit, approximately three per plant. However, there were no significant differences among the lines in the percentage of marketable fruit produced. Fruit weight varied significantly among the lines, with ‘Magic Lantern’ producing the largest fruit by weight and ‘Kandy Korn Plus’ producing the smallest fruit. Pc-NY30, PI 181761, and the F_1 lines produced intermediate size fruit. Pc-NY30 was significantly longer and narrower than the rest of the lines. ‘Magic Lantern’ and ‘Kandy Korn Plus’ were approximately round-fruited, and PI 181761 and the F_1 lines produced intermediate, slightly elongated fruit. ‘Kandy Korn Plus’ was a bush type plant, and Pc-NY30 was a vine type plant. The F_1 lines were both semi-bush type plants, as was ‘Magic Lantern’.

Table A1.4: Yield and horticultural characteristics of zucchini-type phytophthora-resistant squash breeding lines and F_1 hybrids evaluated in the 2017 yield trial at the East Ithaca Research Farm of Cornell University in Ithaca, NY. Fruit were harvested three times per week for 7 weeks, approximately 2 or 3 d after pollination.

Cultivar or breeding line	Marketable fruit (no./plant)[z]	Marketable fruit (%)[y]	Fruit wt (g)[x]	Fruit shape[w]	Plant habit
'Dunja'	9.59 a[v]	85.03 a	272.0 b	4.25 a	Bush
'Dunja' x Pc-NY21 F_1	7.22 ab	76.41 ab	358.2 ab	4.09 a	Semi-bush
'Dunja' x Pc-NY32 F_1	8.63 a	87.39 a	413.3 ab	3.50 b	Semi-bush
Pc-NY21	2.91 b	45.27 c	376.0 ab	3.10 c	Vine
Pc-NY32	3.22 b	52.65 bc	479.5 a	2.64 d	Vine
PI 615089	5.63 ab	66.72 abc	250.9 b	3.62 b	Bush

[z] Least squares mean of the total number of marketable fruit per plant across all replicates and harvest dates.

[y] Least squares mean of the percent marketable fruit across all replicates and harvest dates.

[x] Least squares mean of individual fruit weight calculated by measuring all fruit per plot across all replicates on two harvest dates. 1 g = 0.0353 oz.

[z] Least squares mean of the total number of marketable fruit per plant across all replicates and harvest dates.

[y] Least squares mean of the percent marketable fruit across all replicates and harvest dates.

[x] Least squares mean of individual fruit weight calculated by measuring all fruit per plot across all replicates on two harvest dates. 1 g = 0.0353 oz.

[w] Least squares mean of fruit shape calculated from measurement of all fruit per plot across all replicates on two harvest dates. Fruit shape was calculated as fruit length/fruit width.

[v] Means in the same column followed by the same letter are not significantly different at $P < 0.05$ as determined by Tukey's honestly significant difference test.

Table A15: Yield and horticultural characteristics of pumpkin-type phytophthora-resistant breeding lines evaluated in the 2017 yield trial at the East Ithaca Research Farm of Cornell University in Ithaca, NY.

Cultivar or breeding line	Marketable fruit (no./plant)[z]	Marketable (%)[y]	Fruit wt (kg)[x]	Fruit shape[w]	Plant habit
'Magic Lantern'	1.06 c[v]	82.45 a	4.04 a	1.03 d	Semi-bush
'Kandy Korn Plus'	5.50 a	96.52 a	0.37 d	0.85 e	Bush
'Kandy Korn Plus' x Pc-NY30 F_1	3.25 b	95.79 a	0.85 c	1.36 c	Semi-bush
'Kandy Korn Plus' x Pc-NY32 F_1	3.09 b	96.07 a	1.13 bc	1.34 c	Semi-bush
Pc-NY30	1.19 c	85.99 a	1.26 bc	2.24 a	Vine
PI 181761	1.19 c	81.24 a	1.41 b	1.67 b	Vine

[z] Least squares mean of the number of marketable fruit per plant across all replicates.

[y] Least squares mean of the percent marketable fruit across all replicates.

[x] Least squares mean of individual fruit weight calculated from 10 fruit per plot across all replicates. 1 kg = 2.2046 lb.

[w] Least squares mean of fruit shape calculated from measurement of 10 fruit per plot across all replicates. Fruit shape was calculated as fruit length/fruit width.

[v] Means in the same column followed by the same letter are not significantly different at $P < 0.05$ as determined by Tukey's honestly significant difference test.

DISCUSSION

As phytophthora crown and root rot continues to spread and threaten cucurbit crops, development of resistant cultivars becomes an increasingly urgent goal. In this study, three squash breeding lines selected for phytophthora crown and root rot resistance were evaluated for their yield and disease resistance. The PR breeding lines displayed significantly improved resistance over the susceptible cultivars Magic Lantern and Dunja. They also exhibited increased resistance relative to PI 615089, the resistant parent of the PR lines, although these differences were not statistically significant in either year of the field trial. Although there was variability across the 2017 and 2018 field and greenhouse disease experiments, the PR lines were generally the most resistant lines in the trials. In particular, Pc-NY30 was consistently among the most resistant group of lines in all three experiments. Pc-NY21 and Pc-NY32 displayed less stable resistance, although only in greenhouse experiment 1 was the performance of one of these lines (Pc-NY21) significantly different from Pc-NY30.

The mechanisms of resistance to phytophthora crown and root rot in the PR lines remain to be elucidated. With other wilt-causing diseases of cucurbits, host resistance is associated with the inability of the pathogen to cause disruptions or occlusions in the vascular system (Main and Walker, 1971; Martyn, 1983). Histological comparisons between a phytophthora crown and root rot susceptible and partially resistant squash cultivar revealed increased hyphal colonization of crown tissue and a greater incidence of occlusions of xylem vessels in the susceptible cultivar. The partially resistant cultivar, on the other hand, featured more numerous and lignified metaxylem vessels that withstood infection to continue to provide structural support of the plant (Krasnow et al., 2017). Similar mechanisms exist in pepper, where phytophthora crown and root rot-resistant culitvars are able to prevent pathogen invasion of vascular tissue by limiting hyphal

growth to the epidermis and outermost cortical layers of roots and stems (Dunn and Smart, 2015; Kim and Kim, 2009). Preliminary microscopy studies of Pc-NY32 and 'Dunja' roots post-inoculation also showed a decreased presence of mycelia in the vascular bundles of Pc-NY32 (*data not shown*).

The variability observed in the disease resistance of the lines across environments is likely due to the hypothesized genetic complexity of resistance in squash and pumpkin and the strong influence of environmental factors on disease severity. Greenhouse experiment 1 closely mimicked the selection environment of the PR lines, and resulted in strong, significant differences between the PR lines and all of the cultivars evaluated. The field disease trials, however, represented an environment more typical of the expected growing conditions of squash in the northeastern U.S. The differences in environment, as well as the differences in the growth stage of the plants, led to significant rank changes between the field and greenhouse experiments. A previous study similarly found the phytophthora crown and root rot resistance of two squash cultivars to respond differentially to changes in growing conditions (Meyer and Hausbeck, 2012). The most dramatic change observed in this study was the increased level of field resistance displayed by 'Kandy Korn Plus'. In greenhouse experiment 1, 'Kandy Korn Plus' was as susceptible as 'Dunja' and 'Magic Lantern' when inoculated in 72-cell trays, displaying severe constriction and rot at the base of the stem that lead to rapid whole plant collapse. The PR lines displayed significantly less stem rot and mortality in greenhouse experiment 1. However, 'Kandy Korn Plus' was not significantly different from the PR lines in the field. Field conditions appeared to be more favorable for plant growth than the 72 cell trays used for the greenhouse inoculation experiment, but 'Kandy Korn Plus' displayed a pronounced differential response in the field that was not observed in the other entries of the trial. In the field, 'Dunja' and 'Magic

Lantern' rapidly developed stem rot leading to total plant collapse shortly after inoculation. As in greenhouse experiment 1, the PR lines displayed much less stem rot and rapid plant collapse upon inoculation than the susceptible lines. However, unlike greenhouse experiment 1, 'Kandy Korn Plus' also displayed reduced mortality upon inoculation. Growth architecture may have also contributed to the increased resistance observed in 'Kandy Korn Plus'. As the disease continued to progress, less mortality by whole plant collapse was observed, but mortality by necrosis of all shoot tips increased. The bush-type 'Kandy Korn Plus' plants featured multiple growing points and were therefore capable of withstanding mild disease symptoms and necrosis of several shoot tips without complete plant death. The PR lines were highly apically dominant, with many plants having a single shoot tip, and thus were more vulnerable to mortality by total shoot tip necrosis. Therefore, compared to the breeding lines, the favorable plant architecture of 'Kandy Korn Plus' at later stages of infection in the field may have compensated for its weaker resistance response at early stages of infection that made it highly susceptible in the greenhouse environment. This suggests that 'Kandy Korn Plus' may contain beneficial alleles for increased resistance to phytophthora crown and root rot, and more generally, that bush-type plants with multiple growing points, although not typical for zucchini and summer squash, could represent a desirable growth habit for phytophthora crown and root rot resistant lines. Future screening of additional cultivars may identify additional sources of partial resistance that could improve breeding efforts.

Pumpkin-type and zucchini-type F_1 hybrids were evaluated in these experiments to determine the utility of the PR lines as parents for resistant, horticulturally acceptable hybrid cultivars. In greenhouse experiment 1, the F_1 hybrids displayed intermediate resistance, not significantly different from their respective resistant parents. The hybrids also displayed

intermediate resistance in the field, although the 'Dunja' hybrids were not significantly different from 'Dunja'. The 'Kandy Korn Plus' hybrids, particularly 'Kandy Korn Plus' x Pc-NY30 F_1, displayed levels of resistance comparable to the PR lines. Overall, the disease ratings of the F_1 hybrids indicate that incorporating the PR lines as hybrid parents may provide partial resistance, although the resistance of the progeny is highly dependent on the second parent.

The entries included in greenhouse experiment 2 represent the most resistant squash and pumpkin accessions identified to date (Padley et al., 2008). Pc-NY21 was the most resistant of all entries in this study, suggesting that this line contains novel alleles or allelic combinations that are not present in the other accessions evaluated. However, the presumed quantitative basis of resistance indicates that the other partially resistant accessions likely possess beneficial alleles that may not be present in the PR lines. The resistant accessions identified by Padley et al. (2008) have since been genotyped with simple sequence repeat markers and revealed to be genetically similar to cultivars representing zucchini and pumpkin morphotypes (Michael et al., 2019). The resistance levels of the PR lines could potentially be improved by the incorporation of additional beneficial alleles from these accessions.

In the experiments described above, two different seed lots of Pc-NY21 were used, with Lot 16-10005 used for the 2017 field disease trial, 2018 field disease trial, and greenhouse experiment 1 and Lot 17-G-014 used for greenhouse experiment 2. These seed lots represent $F_{5:6}$ families derived from separate F_5 individuals. Two different seed lots were necessary due to limited seed availability because these experiments occurred concurrently with breeding efforts. In greenhouse experiment 2, Pc-NY21 (Lot 17-G-014) was highly resistant, but Lot 16-10005 was variable across the other experiments, suggesting that Lot 16-10005 was still segregating for resistance. Because these seed lots are not completely fixed for resistance, further selection and

selfing of the most resistant individuals is important to develop stable, resistant lines for further characterization.

No line-by-isolate interactions were identified in greenhouse experiment 3, suggesting that the resistance present in the PR lines may be robust to diverse isolates of *P. capsici*. *Phytophthora capsici* is a genetically diverse species, with sexual reproduction common in populations in the United States (Bowers et al., 2007; Quesada-Ocampo et al., 2011). In pepper, numerous reports support the existence of physiological races of *P. capsici* that display differential virulence patterns on different host lines (Glosier et al., 2008; Hwang et al., 1996; Monroy-Barbosa and Bosland, 2008; Oelke et al., 2003), necessitating different sources of resistance for specific isolates. In cucurbits, a previous experiment found a significant interaction effect between crop type and pathogen isolate on phytophthora crown and root rot disease severity in the greenhouse (Enzenbacher and Hausbeck, 2012), but further research is necessary to understand the extent to which differential isolate-line interactions exist in squash. PR lines with robust resistance to diverse *P. capsici* isolates are particularly desirable for the development of new resistant cultivars with broad adaptability.

The PR lines were significantly different from the commercial cultivars in almost all aspects measured in the yield trial. Pc-NY21 and Pc-NY32 yielded significantly fewer marketable fruit than 'Dunja', with a lower percentage of their fruit being marketable overall. However, the yield of the F_1 lines was not significantly different from 'Dunja', suggesting that this yield deficit can be restored by crossing with a high yielding zucchini cultivar. The fruit shape of these PR lines was also significantly shorter and wider than an ideal zucchini, which is long and cylindrical (Paris, 1996). This typical zucchini fruit shape was recovered in the F_1 lines, particularly 'Dunja' x Pc-NY21 F_1. The vining habit of the PR lines is also unacceptable for

zucchini cultivars, which have a bush growth habit by definition (Paris, 1996). The rapid recovery of acceptable yield and fruit characteristics in the F_1 lines suggest that the PR lines can produce marketable zucchini cultivars when incorporated into a breeding program, although it may be challenging to simultaneously retain all disease resistance alleles.

The pumpkin-type PR line, Pc-NY30, displayed utility as a parent for new phytophthora crown and root rot-resistant pumpkin cultivars. Although the fruit shape of this line was significantly longer than the ideal length/width ratio (approximately 1) for a typical pumpkin cultivar (Paris, 1996), the F_1 lines with 'Kandy Korn Plus' displayed a desirable fruit shape. These lines also had increased yield of highly marketable fruit. 'Kandy Korn Plus' produced many small fruit, and therefore the fruit of the F_1 lines were also small. Pairing Pc-NY30 with a larger jack-o'-lantern type pumpkin to generate a new hybrid is necessary for future production of new resistant jack-o'-lantern type pumpkins.

Phytophthora fruit rot is another disease symptom caused by *P. capsici* that is often a major limitation to cucurbit production (Babadoost, 2000, 2004; Babadoost and Zitter, 2009). Fruit rot infections can be so severe that fields are left unharvested and truckloads of fruit are rejected (Hausbeck and Lamour 2004). Fruit may become infected through contact with infested soil or when the pathogen is dispersed during rainfall or irrigation. Symptoms typically begin with a water-soaked lesion, leading to sporulation and rapid fruit collapse (McGrath, 2017). Previous studies suggest that genetic resistance to phytophthora fruit rot may be present among *Cucurbita* species (Ando et al., 2009; Krasnow et al., 2014), although age-related resistance is the most common type of fruit rot resistance (Ando et al., 2009; Krasnow and Hausbeck, 2016; Meyer and Hausbeck, 2013a). Hard-rind pumpkin cultivars with reduced susceptibility to phytophthora fruit rot are available, but relatively high incidence of disease has been reported

(McGrath and Fox, 2008), and the hard-rind trait renders the fruit unsuitable for carving into jack-o'-lanterns. Preliminary studies suggest that age-related resistance may be present in the PR lines (*data not shown*); however, observations of fruit rot in the field disease trials suggests that the PR lines do not possess sufficient levels of resistance for practical usage. Although the vining PR lines quickly spread to the soil between the rows, the semi-bush F_1 pumpkin-type lines produced the majority of their fruit on the plastic mulch. By growing lines with a semi-bush or bush growth habit on plastic mulch and raised beds, the incidence of fruit rot may be reduced by separating the fruit from infested soil (Ando and Grumet, 2006; Hausbeck and Lamour, 2004).

Conclusions. The PR lines described in this study represent a new resource for breeding phytophthora crown and root rot-resistant zucchini and pumpkin cultivars. They have demonstrated improved performance over previously identified sources of partial resistance. Additional breeding is necessary to achieve a highly marketable cultivar, but the hybrids evaluated in this study suggest that desirable phenotypes and resistance can be achieved. Phytophthora crown and root rot will continue to be a devastating disease, requiring a combined approach of cultural practices, fungicides and host resistance for adequate control. By combining the resistance found in the PR lines with alleles from other potential sources, such as PI accessions and commercial cultivars, a more complete form of resistance may be attained.

REFERENCES

Ando, K. and R. Grumet. 2006. Evaluation of altered cucumber plant architecture as a means to reduce *Phytophthora capsici* disease incidence on cucumber fruit. J. Am. Soc. Hortic. Sci. 131:491–498.

Ando, K., S. Hammar, and R. Grumet. 2009. Age-related resistance of diverse cucurbit fruit to infection by *Phytophthora capsici*. J. Amer. Soc. Hort. Sci. 134:176–182.

Babadoost, M. 2000. Outbreak of phytophthora foliar blight and fruit rot in processing pumpkin fields in Illinois. Plant Dis. 84:1345.

Babadoost, M. 2004. Phytophthora blight: A serious threat to cucurbit industries. 01 June 2020. <https://www.apsnet.org/edcenter/apsnetfeatures/Pages/PhytophthoraBlight.aspx>.

Babadoost, M. and S.Z. Islam. 2003. Fungicide seed treatment effects on seedling damping-off of pumpkin caused by *Phytophthora capsici*. Plant Dis. 87:63–68.

Babadoost, M. and T.A. Zitter. 2009. Fruit rots of pumpkin: A serious threat to the pumpkin industry. Plant Dis. 93:772–782.

Bernhardt, E.A. and R.G. Grogan. 1982. Effect of soil matric potential on the formation and indirect germination of sporangia of *Phytophthora parasitica*, *P. capsici*, and *P. cryptogea*. Phytopathology. 72:507–511.

Boodley, J.W. and R. Sheldrake, Jr. 1972. Cornell peat-lite mixes for commercial plant growing. New York College of Agr., Cornell Univ., Info. Bul. 43.

Bowers, J.H., F.N. Martin, P.W. Tooley, and E.D.M.N. Luz. 2007. Genetic and morphological diversity of temperate and tropical isolates of *Phytophthora capsici*. Phytopathology. 97:492–503.

Camp, A., H. Lange, S. Reiners, H. Dillard, and C.D. Smart. 2009. Tolerance of summer and

winter squash lines to phytophthora blight, 2008. Plant Dis. Manag. Rep. 3:V022.

Carlson, M.O., E. Gazave, M.A. Gore, and C.D. Smart. 2017. Temporal genetic dynamics of an experimental, biparental field population of *Phytophthora capsici*. Front. Genet. 8:1–19.

Chavez, D.J., E.A. Kabelka, and J.X. Chaparro. 2011. Screening of *Cucurbita moschata* Duchesne germplasm for crown rot resistance to Floridian isolates of *Phytophthora capsici* Leonian. HortScience 46:536–540.

Cooke, B.M., D.G. Jones, and B. Kaye. 2006. The epidemiology of plant diseases. 2nd ed. Springer, Dordrecht, The Netherlands.

Dunn, A.R., B.A. Fry, T.Y. Lee, K.D. Conley, V. Balaji, W.E. Fry, A. McLeod, and C.D. Smart. 2013. Transformation of *Phytophthora capsici* with genes for green and red fluorescent protein for use in visualizing plant-pathogen interactions. Australas. Plant Pathol. 42:583–593.

Dunn, A.R., M.G. Milgroom, J.C. Meitz, A. McLeod, W.E. Fry, M.T. McGrath, H.R. Dillard, and C.D. Smart. 2010. Population structure and resistance to mefenoxam of *Phytophthora capsici* in New York State. Plant Dis. 94:1461–1468.

Enzenbacher, T.B. and M.K. Hausbeck. 2012. An evaluation of cucurbits for susceptibility to cucurbitaceous and solanaceous *Phytophthora capsici* isolates. Plant Dis. 96:1404–1414.

Feng, B., P. Li, H. Wang, and X. Zhang. 2010. Functional analysis of Pcpme6 from oomycete plant pathogen *Phytophthora capsici*. Microb. Pathog. 49:23–31.

Gilardi, G., S. Demarchi, M.L. Gullino, and A. Garibaldi. 2015. Nursery treatments with non-conventional products against crown and root rot, caused by *Phytophthora capsici*, on zucchini. Phytoparasitica 43:501-508.

Glosier, B.R., E.A. Ogundiwin, G.S. Sidhu, D.R. Sischo, and J.P. Prince. 2008. A differential

series of pepper (*Capsicum annuum*) lines delineates fourteen physiological races of *Phytophthora capsici*: Physiological races of *P. capsici* in pepper. Euphytica 162:23–30.

Granke, L.L., L. Quesada-ocampo, and M.K. Hausbeck. 2012. Advances in research on *Phytophthora capsici* on vegetable crops in the United States. Plant Dis. 95:1588–1600.

Harrell Jr., F.E. 2018. Hmisc: Harrell Miscellaneous. <https://CRAN.R-project.org/package=Hmisc>.

Hausbeck, M.K. and K.H. Lamour. 2004. *Phytophthora capsici* on vegetable crops: Research progress and management challenges. Plant Dis. 88:1292–1303.

Hwang, B.K., Y.T. Kim, and C.H. Kim. 1996. Differential interactions of *Phytophthora capsici* isolates with pepper genotypes at various plant growth stages. Eur. J. Plant Pathol. 102:311–316.

Jackson, K.L., J. Yin, and P. Ji. 2012. Sensitivity of *Phytophthora capsici* on vegetable crops in Georgia to mandipropamid, dimethomorph and cyazofamid. Plant Dis. 96:1337–1342.

Jones, L.A., R.W. Worobo, and C.D. Smart. 2014. Plant-pathogenic oomycetes, *Escherichia coli* strains, and *Salmonella* spp . frequently found in surface water used for irrigation of fruit and vegetable crops in New York state. Appl. Environ. Microbiol. 80:4814–4820.

Krasnow, C.S., R. Hammerschmidt, and M.K. Hausbeck. 2017. Characteristics of resistance to phytophthora root and crown rot in *Cucurbita pepo*. Plant Dis.101:659–665.

Krasnow, C.S. and M.K. Hausbeck. 2016. Evaluation of winter squash and pumpkin cultivars for age-related resistance to *Phytophthora capsici* fruit rot. HortScience 51:1251–1255.

Krasnow, C.S., R.P. Naegele, and M.K. Hausbeck. 2014. Evaluation of fruit rot resistance in cucurbita germplasm resistant to *Phytophthora capsici* crown rot. HortScience 49:285–288.

Kreutzer, W.A. 1937. A phytophthora rot of cucumber fruit. Phytopathology 27:955.

Lamour, K.H., R. Stam, J. Jupe, and E. Huitema. 2012. The oomycete broad-host-range pathogen *Phytophthora capsici*. Mol. Plant Pathol. 13:329–337.

Leonian, L.H. 1922. Stem and fruit blight of peppers caused by *Phytophthora capsici* sp. nov. Phytopathology 12:401-408.

Li, P., B. Feng, H. Wang, P.W. Tooley, and X. Zhang. 2011. Isolation of nine *Phytophthora capsici* pectin methylesterase genes which are differentially expressed in various plant species. J. Basic Microbiol. 51:61–70.

Main, C.E. and J.C. Walker. 1971. Physiological responses of susceptible and resistant cucumber to *Erwinia tracheiphila*. Phytopathology 61:518–522.

Martyn, R.D. 1983. Susceptibility of summer squash to the watermelon wilt pathogen (*Fusarium oxysporum f. sp. niveum*). Plant Dis. 67:263–266.

McGrath, M.T. 2017. Phytophthora crown and root rot, p. 43-44. In: A.P Keinath, W.M. Wintermantel, and T.A. Zitter (eds). Compendium of cucurbit diseases and pests. 2nd ed. Am. Phytopathological Soc., Saint Paul, MN.

McGrath, M.T. and G.M. Fox. 2008. Hard-rind pumpkin cultivar evaluation for phytophthora fruit rot, 2008. Plant Dis. Manag. Reports 3:V126.

Meyer, M.D. and M.K. Hausbeck. 2013a. Age-related resistance to phytophthora fruit rot in 'Dickenson Field' processing pumpkin and 'Golden Delicious' winter squash fruit. Plant Dis. 97:446–552.

Meyer, M.D. and M.K. Hausbeck. 2012. Using cultural practices and cultivar resistance to manage phytophthora crown rot on summer squash. HortScience 47:1080–1084.

Meyer, M.D. and M.K. Hausbeck. 2013b. Using soil-applied fungicides to manage phytophthora crown and root rot on summer squash. Plant Dis. 97:107–112.

Monroy-Barbosa, A., and P.W. Bosland. 2008. Genetic analysis of phytophthora root rot race-specific resistance in chile pepper. J. Am. Soc. Hortic. Sci. 133:825–829.

Oelke, L.M., P.W. Bosland, and R. Steiner. 2003. Differentiation of race specific resistance to phytophthora root rot and foliar blight in *Capsicum annuum*. J. Am. Soc. Hortic. Sci. 128:213–218.

Padley, L.D., E.A. Kabelka, P.D. Roberts, and R. French. 2008. Evaluation of *Cucurbita pepo* accessions for crown rot resistance to isolates of *Phytophthora capsici*. HortScience 43:1996–1999.

Paris, H.S. 2016. Germplasm enhancement of *Cucurbita pepo* (pumpkin, squash, gourd: Cucurbitaceae): Progress and challenges. Euphytica 208:415–438.

Paris, H.S. 1996. Summer squash: History, diversity, and distribution. HortTechnology 6:6–13.

Quesada-Ocampo, L.M., L.L. Granke, M.R. Mercier, J. Olsen, and M.K. Hausbeck. 2011. Investigating the genetic structure of *Phytophthora capsici* populations. Phytopathology 101:1061–1073.

Soil Survey Staff. 2020. Natural Resources Conservation Service. United States Department of Agriculture. Web Soil Survey. 01 June 2020. <http://websoilsurvey.sc.egov.usda.gov/>.

Tian, D. and M. Babadoost. 2004. Host range of *Phytophthora capsici* from pumpkin and pathogenicity of isolates. Plant Dis. 88:485–489.

U.S. Department of Agriculture. 2019. Agricultural Statistics for 2018. Washington, D.C.